Investigation of the Addition of a Kinetic Bimolecular Fragment Coupling Step to the Re_2O_7-Catalyzed Transposition and Cyclization of Allylic Alcohols and Examination of the Effects of Acetonitrile

by

Shelby Marie Anderson

B.S., Grove City College, 2012

Submitted to the Graduate Faculty of the

Dietrich School of Arts and Sciences in partial fulfillment

of the requirements for the degree of

Doctor of Philosophy

University of Pittsburgh

2020

UNIVERSITY OF PITTSBURGH

DIETRICH SCHOOL OF ARTS AND SCIENCES

This dissertation was presented

by

Shelby Marie Anderson

It was defended on

November 25, 2020

and approved by

Kay Brummond, Professor, Department of Chemistry

Peng Liu, Associate Professor, Department of Chemistry

Lee McDermott, Assistant Professor, Department of Pharmaceutical Sciences

Thesis Advisor/Dissertation Director: Paul Floreancig, Professor, Department of Chemistry

Investigation of the Addition of a Kinetic Bimolecular Fragment Coupling Step to the Re_2O_7-Catalyzed Transposition and Cyclization of Allylic Alcohols and Examination of the Effects of Acetonitrile

Shelby Marie Anderson, PhD

University of Pittsburgh, 2020

The Re_2O_7-catalyzed allylic alcohol transposition, cyclization, and trapping cascade reaction developed by the Floreancig group is a synthetically versatile reaction that has been applied to the stereoselective synthesis of tetrahydropyran rings. This work expands the Re_2O_7-mediated allylic alcohol transposition reaction to include a kinetically controlled bimolecular fragment coupling reaction with weak π-silane nucleophiles to access the 2,6-*trans*-tetrahydropyran ring systems. Expansion of the fragment coupling reaction to install quaternary centers and to prepare substrates bearing pre-existing stereocenters is accomplished and gives further insight into the mechanistic details of these reactions.

Solvent effects on the reaction are analyzed, with acetonitrile providing substantial rate-enhancing effects to the reaction through stabilization of the oxocarbenium ion intermediate. Acetonitrile plays a crucial role in promoting the reaction in comparison to dichloromethane, enhancing the rate and facilitating the trapping of silane nucleophiles. This modification allows the fragment coupling reaction to be expanded to stereochemically complex products that have been previously inaccessible with Re_2O_7. Acetonitrile also provides improved stereocontrol in comparison to dichloromethane for trapping with substrates bearing a pre-existing stereocenter.

Furthermore, acetonitrile promotes equilibration to thermodynamically favored products, further illustrating its advantages.

Table of Contents

List of Tables

List of Figures

List of Schemes

Dedication

I would like to dedicate this document, and all of the work herein, to my younger sister, Anna Kathryn Anderson.

Acknowledgments

I would like to first and foremost thank my advisor, Dr. Paul Floreancig, for his mentorship and for the privilege of learning from him. I would like to thank him for his constant good ideas, helpful discussions, and support and encouragement through all the challenges I have encountered in this program.

I would like to thank the Floreancig Group members, past and present, for their camaraderie and for challenging me to become a better scientist. Thank you for inspiring me with your intellectual contributions during group meetings and for providing helpful insights and suggestions for this project.

I would like to thank my committee members, Dr. Kay Brummond, Dr. Peng Liu, and Dr. Lee McDermott for their feedback. Thank you for the time you spent reviewing my documents and for the guidance you have provided to me during my Ph.D. studies. Thank you for your excellent ideas and suggestions which have made this document stronger.

I would like to thank my parents, William and Kathryn Anderson, for their unwavering support. Thank you for teaching me to think critically from a young age and for constantly challenging me to improve myself as a student and as an individual. I would like to thank my older sister, Julia Anderson, for her constant support, friendship, and for keeping me balanced throughout my Ph.D. studies.

1.0 Molecular Complexity and Reaction Design in Organic Synthesis

The synthesis of highly complex molecules offers the opportunity for reaction design and for the study and optimization of synthetic methods. Developing new ways to achieve molecular complexity is also relevant to industrial applications. Molecular complexity is important in drug discovery in that molecules that are complex and intricate have higher selectivity profiles and are associated with less promiscuity.[1,2,3]

Whitlock analyzes molecular structures by defining them in terms of structure size and molecular complexity. Structure size is determined by the number of bonds in a molecule and molecular complexity is defined by four factors which contribute to a molecule's complexity. These factors include number of rings, unsaturations, heteroatoms, and chiral centers.[4] Bertz also contributes to this definition, stating that size, symmetry, branching, rings, multiple bonds, and heteroatoms contribute to complexity. Additionally, Bertz states that complexity increases with the type and number of these factors.[5] From the principles described in the Whitlock and Bertz analyses, a good reaction or synthetic route can be defined as one that generates molecular complexity quickly. Important practical aspects of a reaction or synthetic route include ease of purification, high overall yields, high atom economy, and cost of reagents.[6]

In designing an effective reaction method or synthetic route, reactions that generate a high level of complexity quickly from simple, easily accessible building blocks are particularly desirable. It is also advantageous if such a method or route is experimentally and operationally easy to perform.[6] In this document, we apply these principles and describe transformations catalyzed by Re_2O_7 to achieve molecules of high stereochemical complexity from simple, achiral or racemic building blocks. One of the reactions performed in this

document uses an allylic alcohol precursor and a prochiral nucleophile to form a stereochemically complex tetrahydropyran ring:

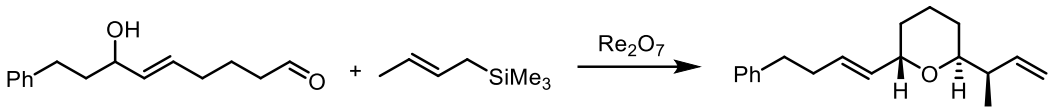

Scheme 1.1 Increase in molecular complexity in the formation of tetrahydropyran rings.

Whitlock's complexity value, *S*, is obtained by assigning a value to each complexity metric and performing the following calculation: *S* = # alicyclic rings + # nonaromatic unsaturations + # chiral centers + # heteroatoms. The alicyclic rings have a value of 4, the unsaturations have a value of 2, the chiral centers have a value of 2, and the heteroatom value is 1. Thus, the complete calculation can be described as *S* = 4(# alicyclic rings) + 2(# unsaturations) + 2(# chiral centers) + # heteroatoms.[4*] If Whitlock's calculation is used for the transformation in Scheme 1.0 above, then *S* for the allylic alcohol is 6, *S* for the crotyl trimethyl silane is 2, and *S* for the tetrahydropyran ring is 15. This calculation shows a notable increase in molecular complexity, forming both a ring and three stereocenters in one reaction from low complexity starting materials.

These reactions are also efficient and experimentally simple, with easy purification, high yields, and low catalyst loadings. Keeping the standards for molecular complexity in mind, this document expands the Re_2O_7-mediated allylic alcohol isomerization and cascade reactions to include a bimolecular fragment coupling step as shown in Scheme 1.0 providing tetrahydropyran rings of high stereochemical complexity quickly. These methods are also extended to include

[*] Sample calculation for tetrahydropyran ring product: *S* = 4(1 alicyclic ring) + 2(2 unsaturations) + 2(3 chiral centers) + 1(1 heteroatom) = 15.

building blocks containing chiral centers contributing to molecular complexity. Furthermore, the role of solvent effects on these reactions is examined, providing further insight into the mechanistic details of the Re_2O_7-catalyzed transformations and equilibrations.

1.1 Re_2O_7 in Metal-Catalyzed Rearrangements and Limitations to Regioselective and Stereoselective Synthesis

Metal-catalyzed rearrangements of allylic acetates and alcohols have been useful transformations for accessing structures containing substitution patterns that have previously not been readily obtained through classical transformations. Catalysts containing metals such as Hg(II), Pd(II), Mo(VI) and V(V) have been used for these reactions.[7,8] Specifically, mercuric trifluoroacetate and $PdCl_2(MeCN)_2$ both effectively catalyze the isomerization of allyl acetates via metal-catalyzed isomerization. In these reactions the metal species activates the alkene, enhancing its electrophilicity and catalyzing nucleophilic attack by the carbonyl oxygen.[8]

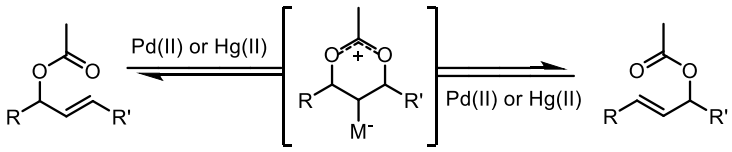

Scheme 1.2 Hg(II) and Pd(II) catalyzed isomerization of allylic acetates.[8]

Alternatively, metal-oxo catalyzed reactions are effective for directly isomerizing allylic alcohols. Molybdenum and vanadium oxo complexes have been used successfully for these reactions; however, these catalysts showed degradation in activity over time.[8,9] Rhenium centered metal-oxo catalysts are effective metals for this type of transformation with $ReO_3(OSiR_3)$ being more

resistant to reduction and degradation and catalyzing the isomerization more rapidly than the molybdenum and vanadium oxo catalysts.[9]

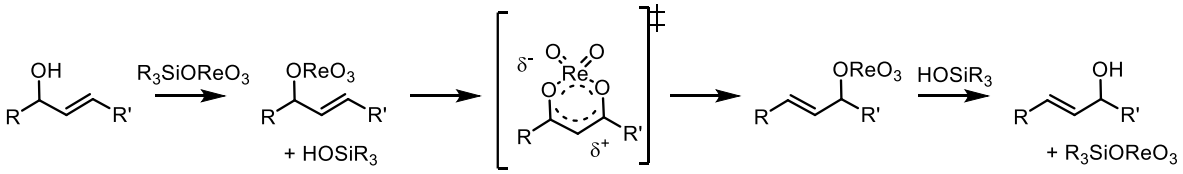

Scheme 1.3 Allylic alcohol transposition catalyzed by rhenium centered metal-oxo catalysts.[10]

Grubbs proposed two pathways that this reaction follows which are illustrated in Scheme 1.3 and 1.5. In the first pathway, the transition state mimics a six-membered transition state.

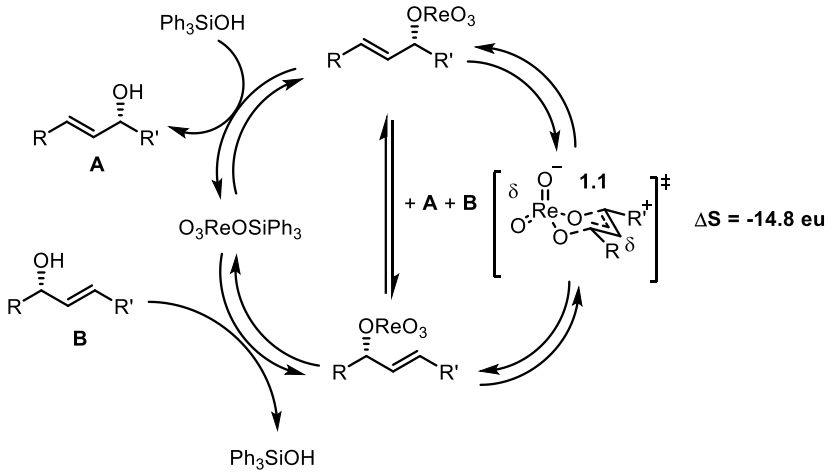

Scheme 1.4 Mechanism of Re_2O_7-catalyzed allylic alcohol transposition as proposed by Grubbs and coworkers.[10]

Kinetic studies performed by Osborn resulted in a negative activation entropy (ΔS = -14.8 eu) for transition state **1.1**, supporting the proposed reaction pathway in Scheme 1.3. A negative entropy value for this transformation indicates an ordered, cyclic transition state which proceeds through intramolecular migration of the alcohol group. A positive entropy value would suggest

greater charge separation, with the rearrangement proceeding through a more disordered ion pair intermediate rather than a cyclic six-membered transition state.[9,10] Additionally, if the reaction follows the concerted [3,3] process, chirality would be transferred to the products and the stereochemical integrity of the reaction would be maintained.[10] Indeed, for the enantiomerically pure allylic alcohol in Scheme 1.4, an enantiomerically enriched product is obtained, illustrating that this transformation can occur through a concerted process.

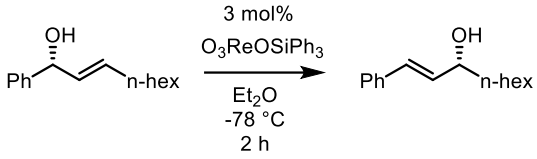

Scheme 1.5 Chirality transfer in the allylic alcohol transposition.

However, in other cases, the high polarization of the carbon-oxygen bond in **1.2** erodes the efficiency and chirality transfer of the reaction, which leads to a second pathway where a cation intermediate is formed. Formation of this intermediate results in allyl ester condensation (**1.3**), racemization (**1.4**), and dehydration **(1.5**) side products. To avoid these competitive ionization-recombination pathways, reaction and substrate design can be tailored to destabilize the allyl cation and promote the desired concerted pathway. Decreased substitution, incorporating electron withdrawing groups, and lowering the reaction temperature are all strategies which can be employed to combat the ionization-recombination pathways.[10]

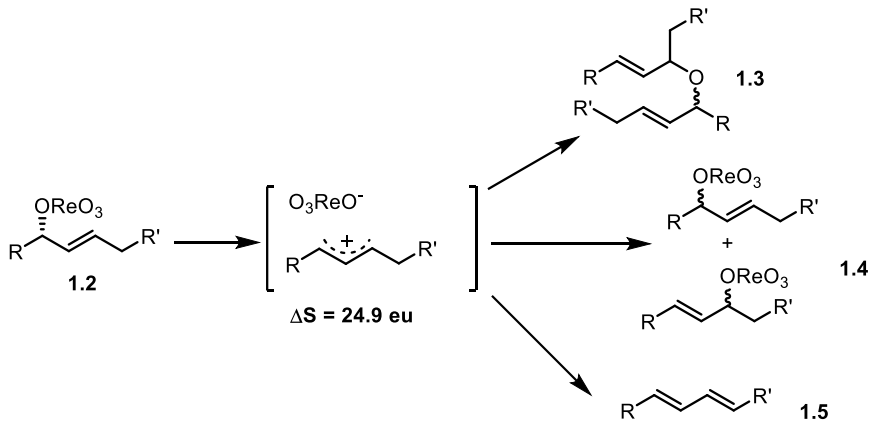

Scheme 1.6 Ionization-recombination pathway leading to allyl condensation (**1.3**), racemization (**1.4**), and dehydration (**1.5**) side products.[10]

For these transformations to be synthetically useful, it is essential to be able to control stereochemistry and regiochemistry. To evaluate the effect of different substrates on chirality transfer with $ReO_3(OSiR_3)$, Grubbs and coworkers examined these transformations with various enantiomerically pure secondary and tertiary allylic alcohols.[10]

Table 1.1 Efficiency of chirality transfer for enantiomerically pure allylic alcohols.[10]

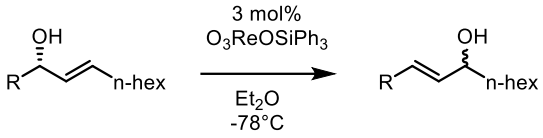

Entry	Substrate	Product	Yield (%)	ee (%)
1	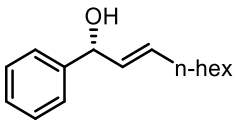 *E:Z* = 67:1 99% ee	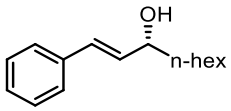	93%	81%
2	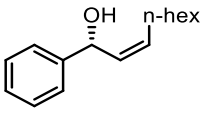 *E:Z* = 11:1 >99% ee	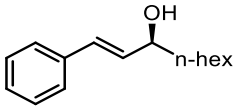	92%	72%
3	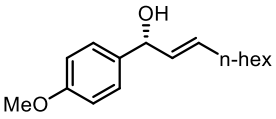 *E:Z* = 20:1 >89% ee	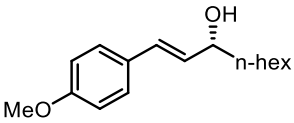	72%	1%
4	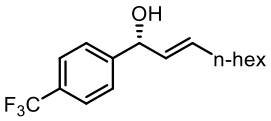 *E:Z* = 99:1 >99% ee	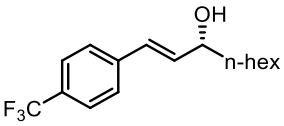	99%	95%

Although entries 1, 2 and 3 show good enantiocontrol, the addition of a methoxy group to the phenyl ring in entry 3 stabilizes the allyl cation, completely diminishing the stereochemical integrity of the reaction – resulting in an ee of 1%. The complete erosion of stereocontrol in this example limits the substrate scope and hinders its synthetic utility. Furthermore, the regiocontrol of the transposition is also limited – for example, in Scheme 1.6, secondary alcohol **1.6** is in

equilibration with primary alcohol **1.7** in a 7:3 ratio – showing only moderate regiochemical preference for **1.6**.[10]

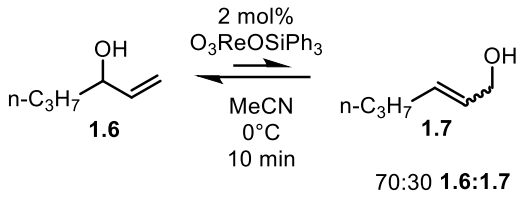

Scheme 1.7 Regioselectivity for $ReO_3(OSiR_3)$ catalyzed isomerization.[10]

The limits of stereocontrol and regiocontrol depicted above restrict the use of this method to simple substrates, diminishing its application to more complex systems such as natural products. To combat these limitations, different approaches have been developed to achieve stereo- and regiocontrol. The next section describes such approaches to these strategies and their applications to natural product total synthesis.

1.2 Re_2O_7-Catalyzed Cascade Reactions and Approaches to Regio and Stereocontrol

The Re_2O_7-catalyzed allylic alcohol transposition has been used to initiate cascade reactions to synthesize complex molecules by taking advantage of thermodynamic control or by terminating the isomerization with a trapping group. These methods have been used to produce molecules of high stereochemical integrity efficiently, inexpensively, and with good atom economy.[5,6,7] Specific strategies to achieve regio and stereocontrol include tethering the allylic

alcohol to an internal trapping group or electrophile (Scheme 1.7). Trapping groups include groups that will react or coordinate with the transposed alcohol, preventing reisomerization.

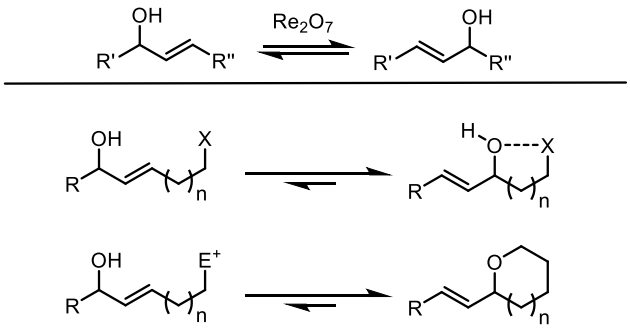

Scheme 1.8 Controlling regiochemistry of allylic alcohol transposition by trapping with an internal electrophile or coordinating group.

An example of kinetic control through the use of trapping agents to control regioselectivity is illustrated in work by Grubbs and coworkers.[10,11] To circumvent the regiocontrol issues which occur in isomerization from tertiary alcohols to primary or secondary alcohols, a silylating reagent is used to irreversibly trap the kinetically favored primary alcohol. Primary alcohols react much more rapidly than tertiary alcohols, allowing one regioisomer to be formed exclusively over the other upon protection with a silyl group. Following deprotection, the primary alcohol can be isolated as the major product.

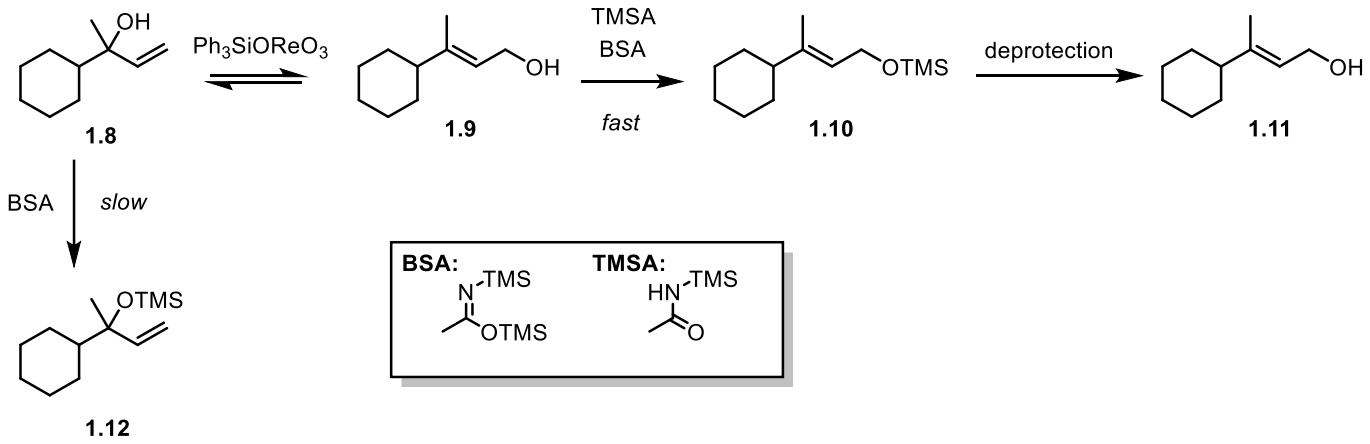

Scheme 1.9 Regiocontrol of allylic alcohol transposition by silylation of kinetically favored primary alcohol.[10,11]

As typical silylations require basic conditions and rhenium catalysts are deactivated by amine bases, careful screening of silylation conditions was required. Fortunately, a combination of 1.2 equivalents of BSA and 0.2 equivalents of its hydrolysis product, TMSA, with 2 mol% of $Ph_3SiOReO_3$ was found to successfully react with the isomerized product without deactivating the catalyst. In the rearrangement of allylic alcohol **1.13**, only 29% of the desired primary alcohol was produced with 71% of the starting material remaining. In contrast, with addition of BSA, 89% of the desired regioisomer was obtained after deprotection, making this a synthetically viable reaction.

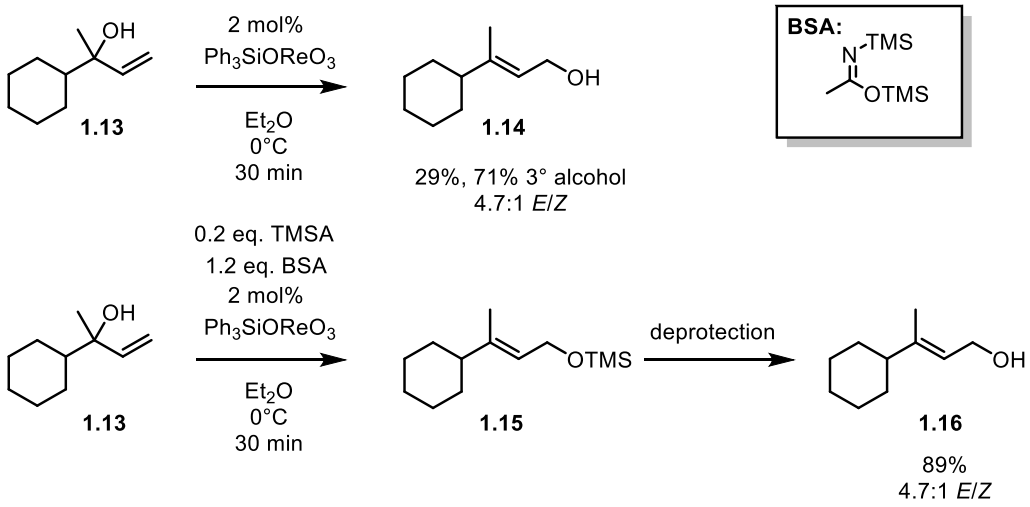

Scheme 1.10 Use of BSA to control regioselectivity of allylic alcohol isomerizations.[11]

This approach was also useful for the isomerization from tertiary alcohols to secondary alcohols. Without the addition of BSA, secondary alcohols tended to rapidly undergo various side reactions – forming primarily dehydration side products. However, in the presence of BSA, 50% of the secondary alcohol product was obtained after deprotection, further demonstrating the utility of this method in obtaining regiocontrol.[11]

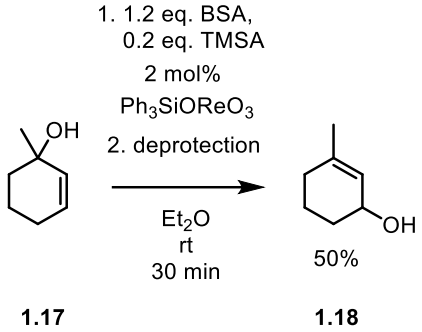

Scheme 1.11 Re_2O_7-catalyzed isomerization of tertiary allylic alcohols and trapping with BSA to obtain secondary allylic alcohols.[11]

This approach has been used effectively with Re_2O_7 instead of $Ph_3SiOReO_3$ in the synthesis of the proposed biogenetic precursor to popolohuanone E, 6'hydroxyarenarol. Following Grignard addition of vinyl magnesium bromide to **1.19**, Re_2O_7-catalyzed transposition and trapping with BSA forms protected primary alcohol **1.21** in 66% yield over two steps. Synthetic intermediate **1.21** is a crucial intermediate to forming the desired product, 6'hydroxyarenarol.[12]

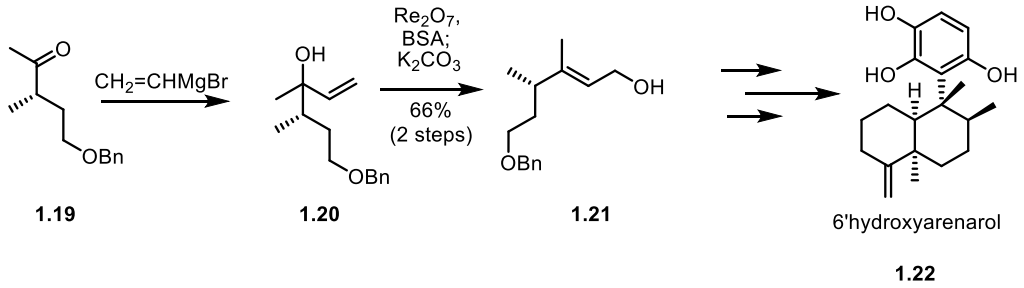

Scheme 1.12 Application of Re_2O_7-catalyzed isomerization and BSA trapping to complex molecule synthesis.[12]

Another study which uses a trapping group to favor one isomer over the other is work by Lee and coworkers.[13] This study places a boronate group in a position to trap the transposed allylic alcohol and was then successfully applied to the total synthesis of (-)-dactylolide.[13,14] The method was initially designed in order to control the regiochemistry of the allylic alcohol transposition by taking advantage of the affinity of boron for hydroxyl groups. A boronate group was installed nearby to coordinate to the alcohol, locking the transposed product in place and preventing reisomerization to **1.23**. However, rather than stalling at the transposition as expected, the transposed hydroxyl formed cyclic product **1.24** in 86% yield. Pleasingly, this cyclized product served the purpose of providing an intermediate that traps the isomerized allylic alcohol, preventing isomerization and loss of regiocontrol. Additionally, the cyclic intermediate is a suitable substrate for subsequent functionalization, in this case - Suzuki coupling to give **1.25.**[13]

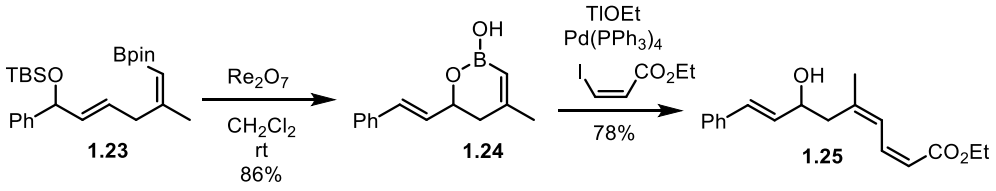

Scheme 1.13 Re_2O_7-catalyzed transposition and formation of cyclic boronic ester and Suzuki coupling.[13]

This transformation was also expanded to enantiomerically pure precursors, with cyclized products **1.27** and **1.29** obtained in good yields and stereocontrol.[13]

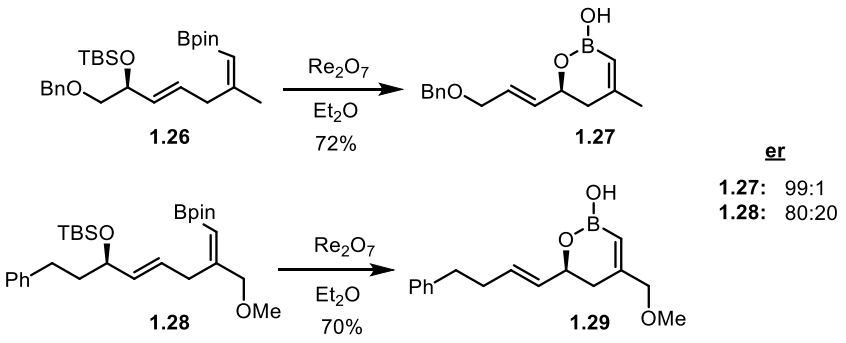

Scheme 1.14 Application of Lee's Re_2O_7 methodology to enantiomerically enriched precursors.[13]

This chemistry was used successfully in the total synthesis of (-)-dactylolide to prepare **1.30**, providing the crucial metathesis precursor five steps away from the final product (Scheme 1.14).[14] This reaction proceeded in 65% yield with excellent regio and stereocontrol, showcasing the application of the method on a more complex substrate.

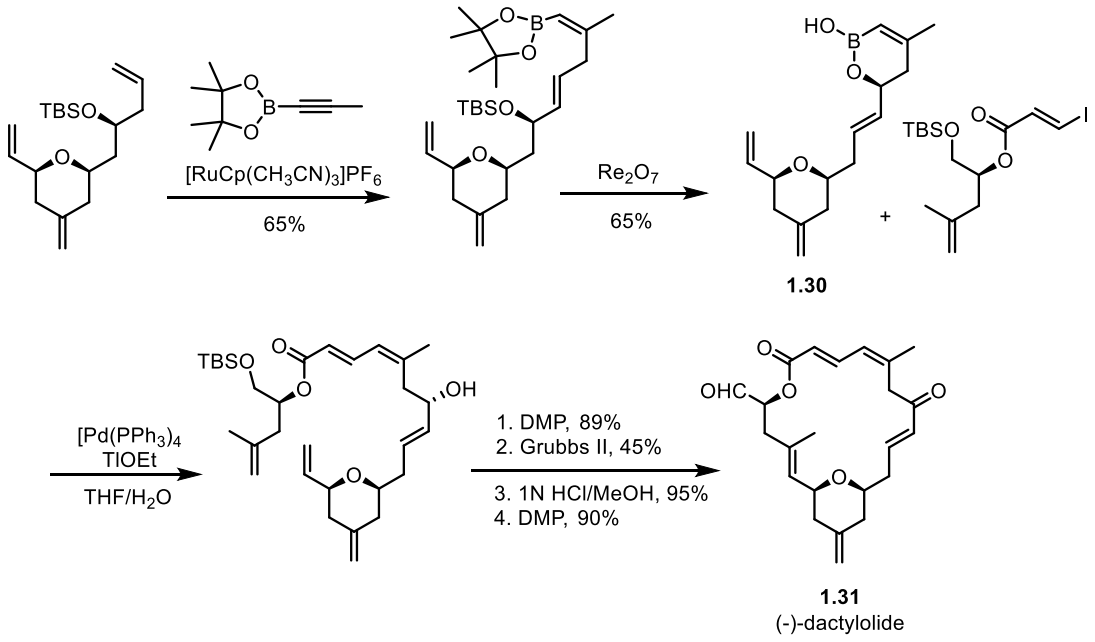

Scheme 1.15 Application of Re_2O_7-catalyzed transposition of allylic silyl ethers to the total synthesis of (-)-dactylolide.[14]

The Floreancig Group has also applied the Re_2O_7-catalyzed allylic alcohol transposition to cascade reaction design, further demonstrating its synthetic advantages. A pivotal first study which illustrates the synthetic utility of these reactions is the application of this method to the synthesis of leucascandrolide A.[15] In the following transformation, the Re_2O_7-catalyzed allylic alcohol transposition provides intermediate **1.34** which proceeds through thermodynamically driven formation of macrolactol **1.35**.

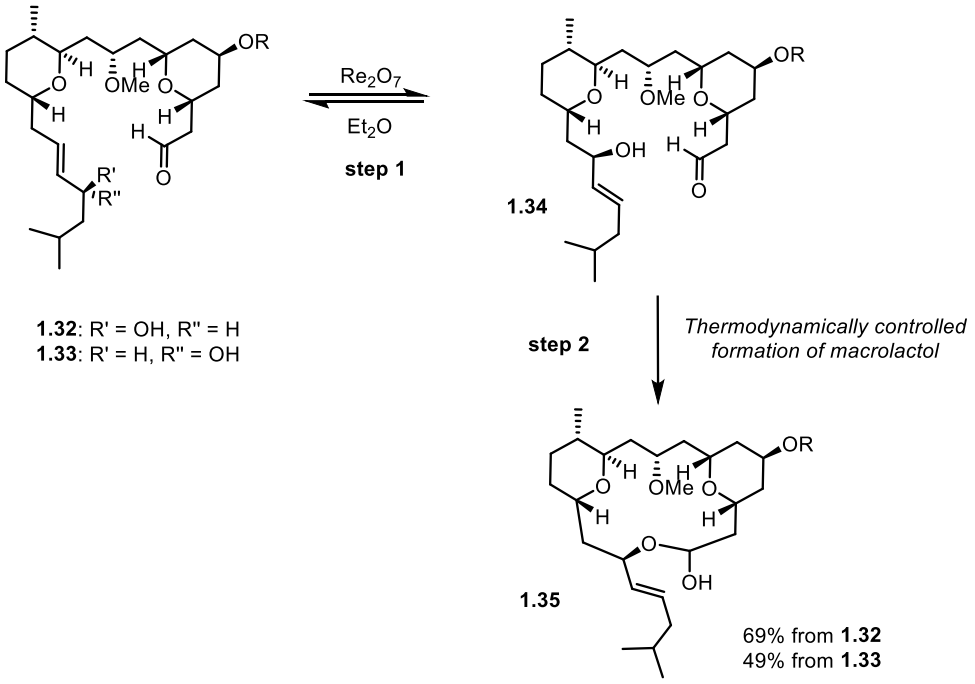

Scheme 1.16 Re_2O_7-catalyzed allylic alcohol transposition and thermodynamically controlled trapping in the formal synthesis of leucascandrolide A.[15]

Of note, allylic alcohols **1.32** and **1.33** both produce **1.35** stereoselectively from either isomer. This reaction proceeds through a reversible allylic alcohol transposition to **1.34** which then undergoes a thermodynamically controlled irreversible formation of the product, causing stereochemical control to be dictated by step **2**, regardless of the stereochemistry of the starting

allylic alcohol. Thermodynamic control is used effectively here to produce macrolactol **1.35** as one diastereomer from either precursor, eliminating the need for the preparation of stereochemically pure allylic alcohols.[15]

Another example from the Floreancig group of the role of thermodynamic equilibration in achieving stereocontrol with Re_2O_7 is illustrated in the synthesis of tetrahydropyran **1.37** (Scheme 1.16). **1.36**, synthesized in a 1:1 ratio of diastereomers, equilibrated to the thermodynamically favored 2,6-*cis* product after 5 h in CH_2Cl_2 upon exposure to Re_2O_7, providing **1.37** in excellent stereocontrol. The equilibration proceeds by Re_2O_7 ionization of **1.36** and fragmentation to an allyl cation intermediate which undergoes ring closure to form **1.37.**[16,17]

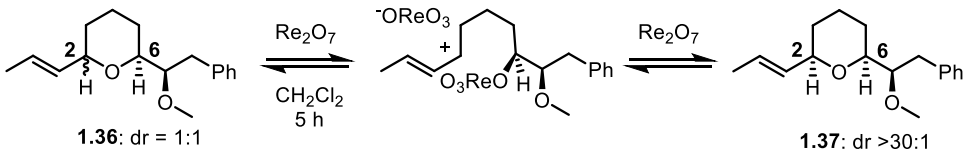

Scheme 1.17 Re_2O_7-catalyzed ionization, fragmentation, and equilibration of **1.36** to the thermodynamically favored 2,6-*cis* product.[17]

The stereocenter in **1.36** was installed by starting from allylic alcohol precursor **1.38**, in which the stereochemistry of the epoxide is relayed to the alcohol which is then protected before **1.36** is subjected to thermodynamic equilibration **(**Scheme 1.17). Interestingly, the reaction proceeded first through formation of seven membered rings **1.39** and **1.40**, which equilibrate to tetrahydropyran rings **1.41** and **1.42** upon re-exposure to Re_2O_7 (Scheme 1.17). The transformation of the oxepanyl alcohols to the thermodynamically favored tetrahydropyran rings serves as further example of Re_2O_7 mediated equilibration.

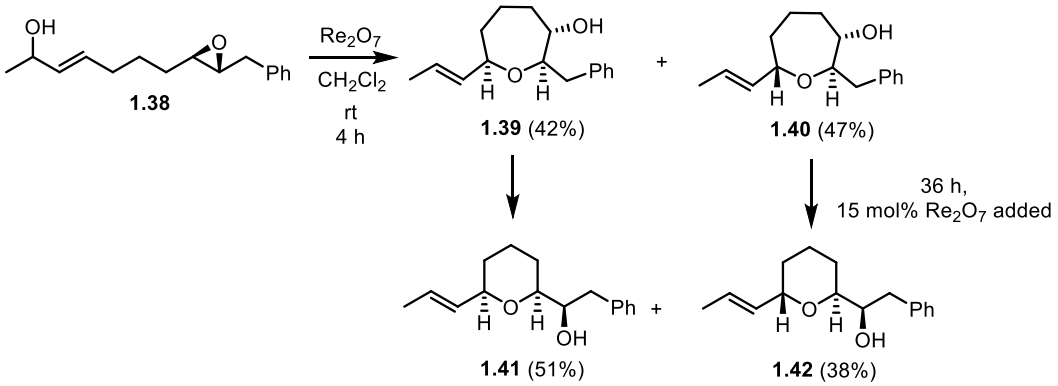

Scheme 1.18 Re_2O_7-catalyzed allylic alcohol transposition using an epoxide as a trapping agent.[16,17]

Similar to the Re_2O_7-catalyzed step in the total synthesis of leucascandrolide A, these reactions serve as an illustration of complex Re_2O_7 initiated reactions followed by Re_2O_7-mediated irreversible thermodynamic equilibration to ultimately achieve stereocontrol. These approaches illustrate the regio and stereochemical advantages of incorporating terminating agents into the Re_2O_7-catalyzed allylic alcohol transpositions and how these cascade reactions can be strategically applied to natural product total synthesis.

1.3 Methods of Synthesizing Tetrahydropyran Rings

The Re_2O_7-catalyzed allylic alcohol transposition and synthesis of tetrahydropyran rings prepares these structures with a high degree of stereochemical complexity from simple achiral precursors. In the research described in this document, tetrahydropyran rings are synthesized with nucleophile trapping through kinetic control to form a *trans* relationship at the ring juncture.

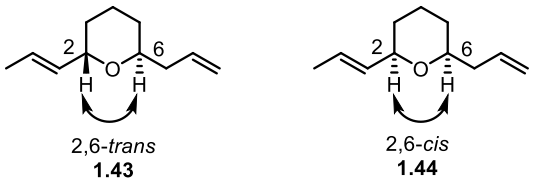

Figure 1.1 Thermodynamically favored 2,6-*cis* and thermodynamically disfavored 2,6-*trans* relationship.

As tetrahydropyran rings are common moieties in natural products, there are many ways of synthesizing these scaffolds stereoselectively. However, the products are more commonly the thermodynamically formed 2,6-*cis* rings. Simple ways of synthesizing 2,6-*trans*-tetrahydropyran rings are less frequently seen in the literature and more ways of accessing this stereochemical pattern and with increased stereochemical complexity would be appealing. In one study where rhenium catalysts are used to construct tetrahydropyran rings, $O_3ReOSiPh_3$ mediates a Prins reaction to prepare tetrahydropyran rings in good stereocontrol. However, this method forms the 2,6-*cis* tetrahydropyran rings exclusively and the scope is limited to aryl or conjugated aldehydes.[18] When aliphatic aldehydes are used, side products form from competitive 2-oxonia-Cope rearrangements.

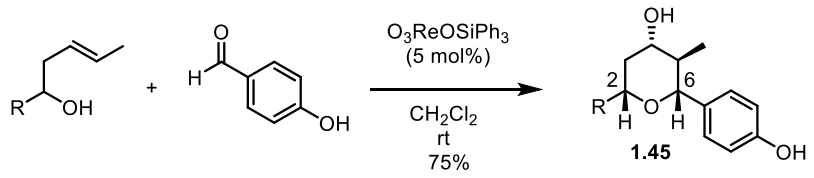

Scheme 1.19 $O_3ReOSiPh_3$ catalyzed synthesis of tetrahydropyran rings through an enantiomeric Prins reaction.[18]

The reaction proceeds via nucleophilic addition of the alcohol to the aldehyde followed by a rhenium catalyzed Prins reaction to produce a perrhenate tetrahydropyran ring which undergoes solvolysis to **1.46**.

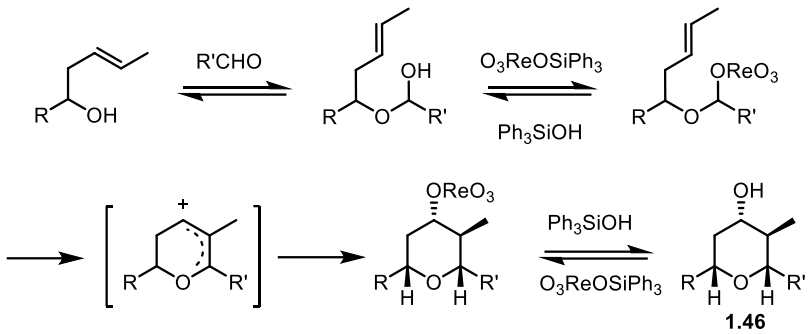

Scheme 1.20 Mechanism for the rhenium catalyzed Prins reaction.[18]

A different metal-based method of constructing tetrahydropyran rings uses a $FeCl_3$-catalyzed cyclization.[19]

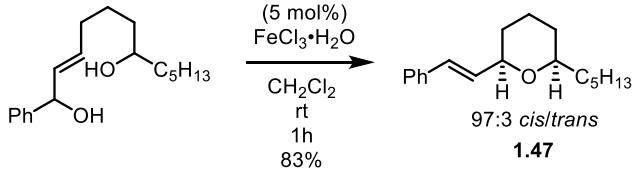

Scheme 1.21 $FeCl_3•H_2O$ catalyzed preparation of tetrahydropyran rings.[19]

This method produces 2,6-*cis*-tetrahydropyran rings in excellent yield and stereocontrol. The scope is expanded to mesityl, electron withdrawing (CO_2Me), and various alkyl groups with the corresponding products being synthesized in good yields and stereocontrol, with the *cis* product being obtained preferentially in all cases. Although this method is a facile way of synthesizing 2,6-*cis* tetrahydropyran rings, the 2,6-*trans* pattern is inaccessible under these conditions.[19]

A metal free process for synthesizing these heterocycles uses a phosphine-catalyzed isomerization. In this reaction, secondary alcohols go through an isomerization-addition reaction catalyzed with bidentate phosphine ligand 1,3-Bis(diphenylphosphino)propane (dppp) to provide the 2,6-*cis* tetrahydropyran in 84% yield.[20]

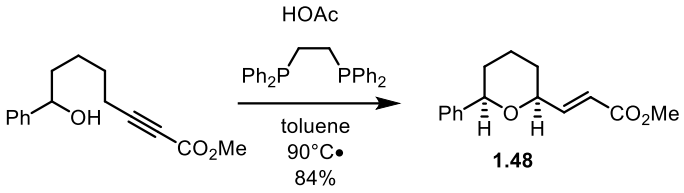

Scheme 1.22 Phosphine catalyzed formation of 2,6-*cis* tetrahydropyran rings.[20]

This cyclization proceeds through the mechanism shown below in Scheme 1.22 with addition of the phosphine ligand to the alkyne and subsequent addition of the alcohol to the allene to close the ring.[20]

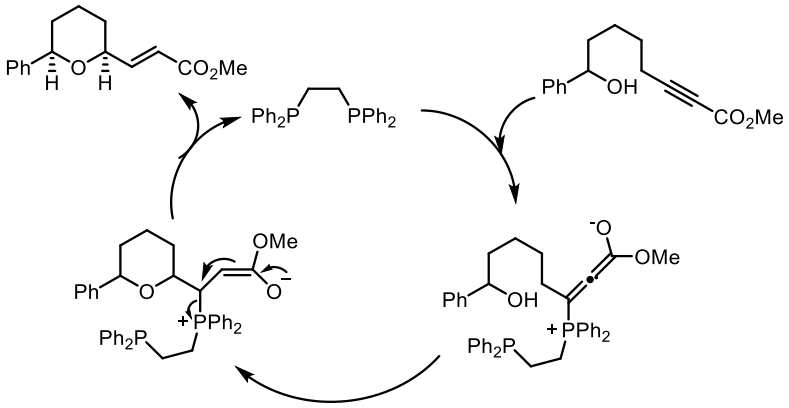

Scheme 1.23 Mechanism of the phosphine catalyzed cyclization.

While this approach is appealing in that it is mild and metal-free, it is still limited to the 2,6-*cis* product and is restricted to substrates bearing a 2-alkynoate moiety. One of the few examples of simple preparations of 2,6-*trans*-tetrahydropyran rings includes work by Semmelhack and coworkers.[21] Development of an intramolecular alkoxypalladation/carbonylation sequence from simple alcohol precursors provides tetrahydropyran rings in good yields and stereocontrol. The stereochemical outcome is determined by the alkene geometry of the starting material; the *E* olefin

produces the 2,6-*cis* product whereas the *Z* olefin produces the 2,6-*trans* product as depicted by transition state analysis in Scheme 1.23.[21]

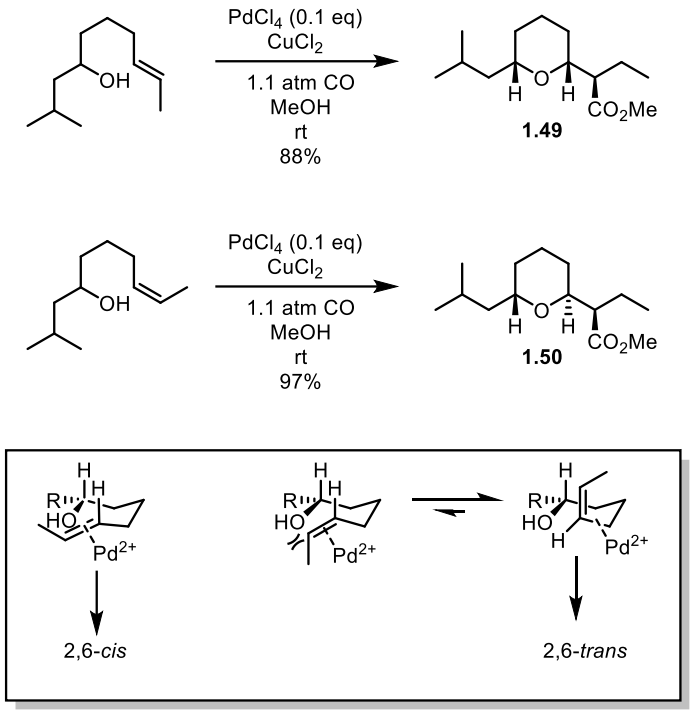

Scheme 1.24 Intramolecular alkoxypalladation/carbonylation of alkenes to synthesize 2,6-*cis* and 2,6-*trans*-tetrahydropyran rings.[21]

Although the alkoxypalladation/carbonylation of alkenes is a facile and stereoselective route to access either stereochemical pattern of 2,6 substituted tetrahydropyran rings, there is room for development of additional methods to access these structures.

1.4 Oxocarbenium Ions as Synthetic Intermediates for Stereoselective Synthesis

An elegant strategy to access 2,6-*trans*-tetrahydropyran rings exclusively involves nucleophilic addition into oxocarbenium ion intermediates. The conformation which cyclic oxocarbenium ions take allow them to serve as intermediates for approaches to stereoselective reactions. Similar to cyclohexene, six-membered oxocarbenium ions orient themselves in a half-chair conformation.[22,23]

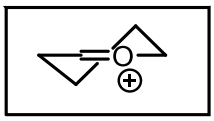

Figure 1.2 Lowest energy conformation of a six-membered cyclic oxocarbenium ion.[23]

When an alkyl stereocenter is incorporated into cyclic oxocarbenium ions, the substituent is oriented pseudoequatorially as shown below in Scheme 1.24. Nucleophilic addition in this example occurs from the bottom, approaching along an axial trajectory below the stereocenter, giving the favored chair-like conformer **1.51.** Nucleophilic addition from the top approaches above the stereocenter, giving disfavored twist boat-like conformer **1.53.**[23] Conformer **1.51** is formed preferentially, forming the tetrahydropyran product stereoselectively. Consequently, if a stereocenter is incorporated into these scaffolds, the half-chair conformation of six-membered cyclic oxocarbenium ions can be used advantageously, providing opportunities for stereocontrolled formation of tetrahydropyran rings.[22,23]

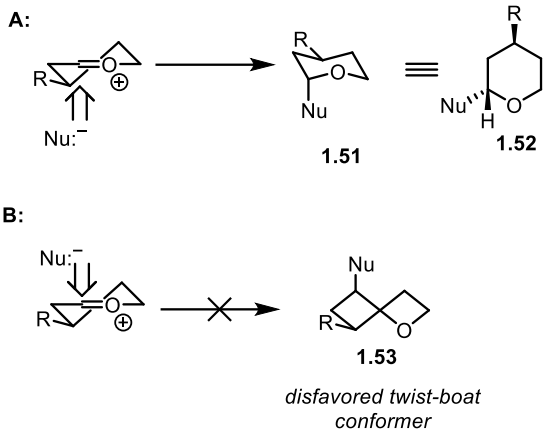

Scheme 1.25 Selective nucleophilic attack on six-membered cyclic oxocarbenium ions.[23]

The orientation of the substituent can also be dictated by steric or electronic properties, depending on the identity of the functional group. For alkyl groups, a pseudoequatorial orientation is favored, giving intermediate **1.55** (Scheme 1.25). For oxygen containing groups, e.g. hydroxyl or benzyloxy groups, a pseudo-axial orientation is favorable, giving rise to intermediate **1.56**. This orientation is favored due to the stabilization of the positively charged oxocarbenium ion by the lone pair on the electronegative heteroatom. Thus, the stereochemical outcome of these transformations can be modified by varying the properties of the functional groups.[22,23]

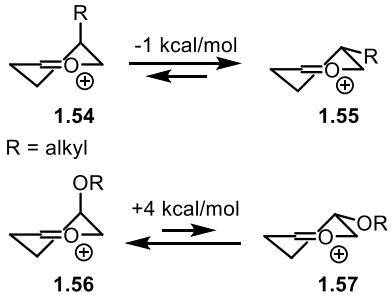

Scheme 1.26 Electronic effects of substituents on the conformation of cyclic six-membered oxocarbenium ion intermediates.[22]

An early example of nucleophilic addition into cyclic oxocarbenium ions was performed by Kishi and coworkers. In this study, it was illustrated that these transformations can be performed stereoselectively to produce 2,6-*trans* tetrahydropyran rings. p-(nitrobenzoyl) protected glycanpyranoside **1.58** was reacted with allyltrimethylsilane and BF_3•Et_2O in acetonitrile, generating a cyclic oxocarbenium ion. This intermediate undergoes nucleophilic addition from the bottom face of the oxocarbenium ion to produce the 2,6-*trans* product in 79% yield with a dr of 10:1.[24]

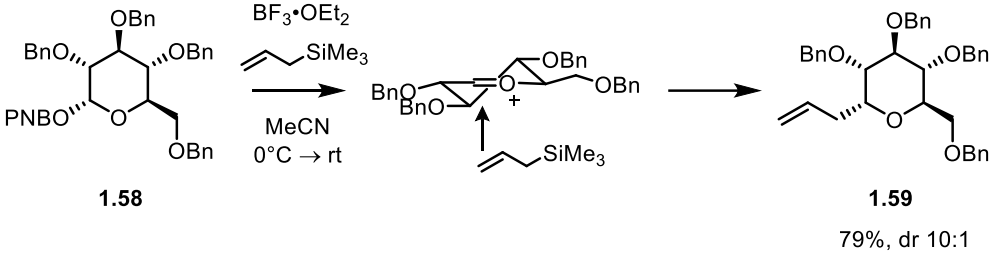

Scheme 1.27 Addition of trimethyl allylsilane to glycopyranoside **1.58**.[24]

Providing further insight into these transformations, Woerpel examined the steric and electronic effects of substituents on 3- and 4-substituted tetrahydropyran acetals. These substrates proceed from the acetal through oxocarbenium ion intermediates with nucleophilic additions of allyltrimethylsilane to provide the tetrahydropyran products. Allylsilanes add into oxocarbenium ions irreversibly and in high yield to produce kinetic products with good stereocontrol. Since this step is irreversible, the reactive conformation can be elucidated from the stereochemistry of the final products.[25] 4-Substituted substrates produced 1,4-*cis* products for substituents with alkyl functional groups and 1,4-*trans* products for substituents containing heteroatoms, both reactions proceeding with excellent stereocontrol.

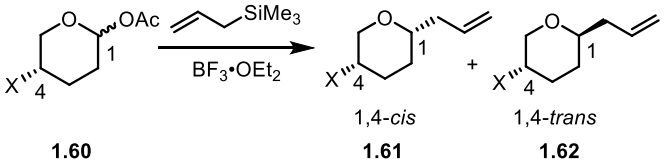

X	cis:trans	yield(%)
Me	94:6	74%
OBn	1:99	75%
CH_2Bn	93:7	77%

Scheme 1.28 Stereoselective substitution of substituted tetrahydropyran acetals.[25]

The stereochemistry of the products provides information on the reactive conformation, as illustrated in Scheme 1.28. Woerpel suggests that since the oxocarbenium ions generated in these studies are early and are reactant-like, the reactive conformation is dictated by properties that stabilize these intermediates. Therefore, the 1,4-*cis* product indicates that X is pseudo-equatorial in the reactive conformation, as is expected for alkyl substituents, and the 1,4-*trans* product indicates that X is oriented pseudo-axial, as is predicted for electronegative heteroatoms.[25]

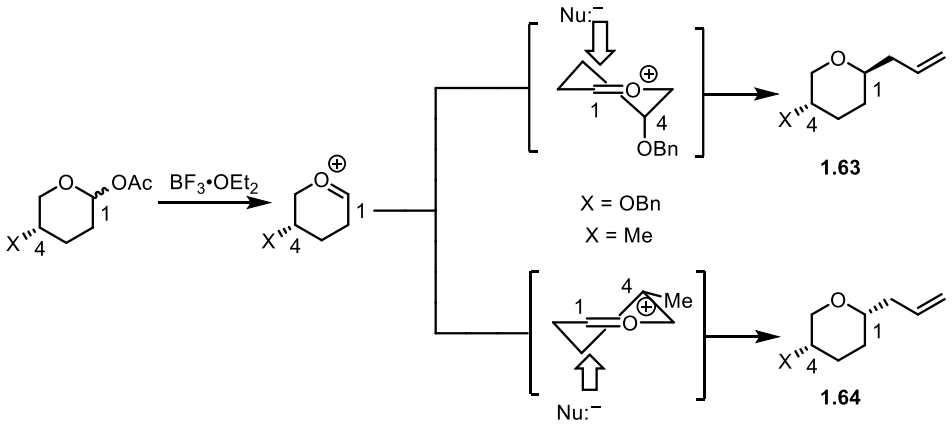

Scheme 1.29 Stereoselective transformations where the 1,4-*trans* product **1.63** is produced for X = OBn and the 1,4-*cis* product **1.64** is produced for X = Me.[25]

In an additional study, Woerpel investigated the solvent effects on these systems, providing further insight into the nucleophilic substitutions of tetrahydropyran acetals and the reactive

conformation that leads to stereocontrol in these reactions. Relationships between solvent polarity and S_N1/S_N2 specificity were observed, illustrating the importance of solvent effects in these systems. In this study, trimethylsilyl trifluoromethanesulfonate is used to promote the reactions and stabilize the oxocarbenium ion intermediate via a contact-ion pair interaction (Scheme 1.29).[26]

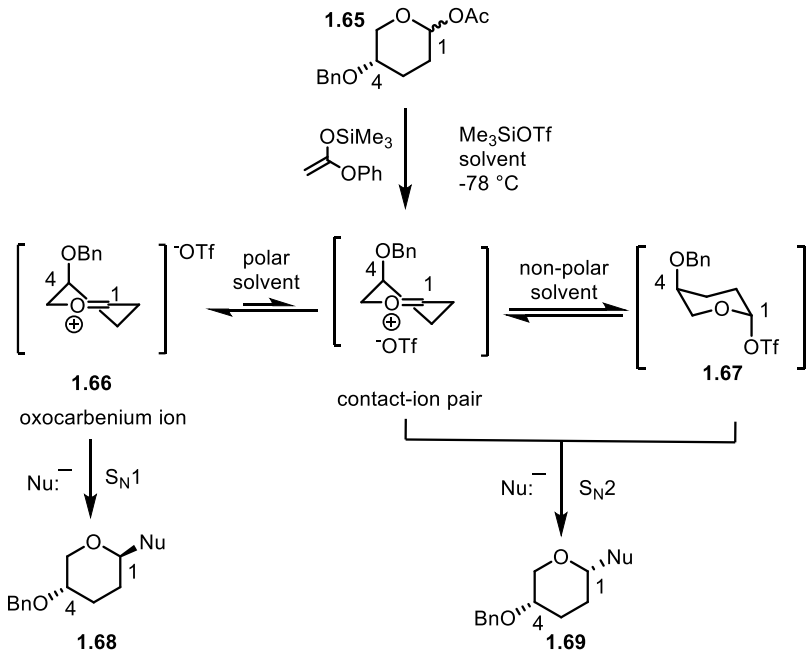

Scheme 1.30 Proposed pathways for 1,4-*trans* and 1,4-*cis* substituted tetrahydropyrans **1.68** and **1.69**.[26]

The stereochemistry of the final products in different solvents in these systems suggests **1.65** partitions between the contact ion pair intermediate and free oxocarbenium ion **1.66** to give S_N1 product **1.68**, and S_N2 product **1.69**, respectively (Scheme 1.29). It was observed that for 1,4 benzyloxy systems in polar solvents the S_N1 product is observed, proceeding through the free oxocarbenium ion and avoiding the twist-boat conformer. In the presence of non-polar solvents, the triflate anion attacks the oxocarbenium ion, then nucleophilic addition occurs through a S_N2 mechanism. Woerpel suggests that more polar solvents stabilize the oxocarbenium ion, favoring the reaction pathway through a S_N1 pathway. A sample of the solvents screened is shown in

Scheme 1.30 below on benzyloxy substituted tetrahydropyranacetal **1.70**, showing the correlation between polarity and substitution pathway.[26]

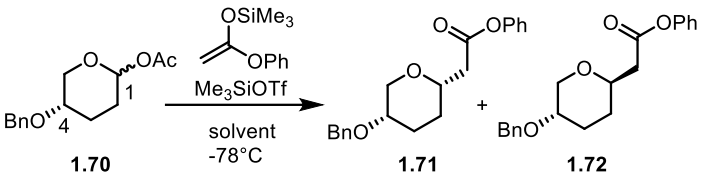

Solvent	cis:trans
EtCN	17:83
CH_2Cl_2	75:25
$Cl_2C=CHCl$	91:9

Scheme 1.31 Solvent effects on nucleophilic substitution of 1,4-benzyloxy substituted tetrahydropyran acetals.[26]

Propionitrile, a very polar solvent, gave the 1,4-*trans* product with a *cis/trans* ratio of 17:83 whereas trichloroethylene, a very nonpolar solvent, gave the 1,4-*cis* product with a *cis/trans* ratio of 91:9. The relationship between solvent polarity and stereochemical outcome in reactions which proceed through oxocarbenium ion intermediates is advantageous in that it provides further means in which these reactions can be tailored to achieve stereocontrol.[26]

Solvent effects on stereoselectivity has also been observed in glycosylation reactions. In these transformations, stereoselectivity is determined by either α or β nucleophilic attack at the anomeric center. In ethereal solvents, such as diethyl ether or 1,4-dioxane, alpha substitution is obtained whereas in polar solvents such as acetonitrile, β-D-glucosides are formed preferentially. These reactions proceed through formation of an axially oriented acetonitrilium intermediate in the α postion which then undergoes stereoselective glycosylation to form the glycoside linkage in the β position (Scheme 1.31). The polar acetonitrilium intermediate provides charge separation between O-5 and β-O-1, decreasing repulsive interactions and causing the axial substitution to be favored.[27,28]

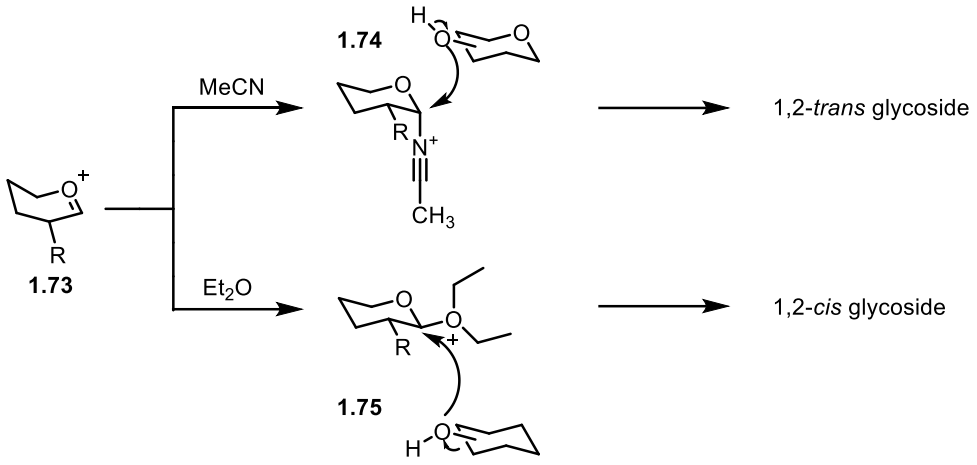

Scheme 1.32 Solvent effects on glycosylation: β-glycoside formation through an acetonitrilium intermediate.[28]

In contrast, ethereal solvents produce a β substituted intermediate (Scheme 1.31) by participation of the oxygen lone pair, causing a glycoside linkage to be formed in the thermodynamically favored α position.[27,28]

One study in which the presence of this acetonitrilium intermediate was confirmed was performed by Fraser-Reid and coworkers. In this analysis, the acetonitrilium intermediate was intercepted to form an α-amide. Formation of the α-amide was accomplished by reaction of each anomer with NBS and 2-chlorobenzoic acid in acetonitrile. **1.78** was formed in 68% and 64% yield from the β and α anomer, respectively.[29]

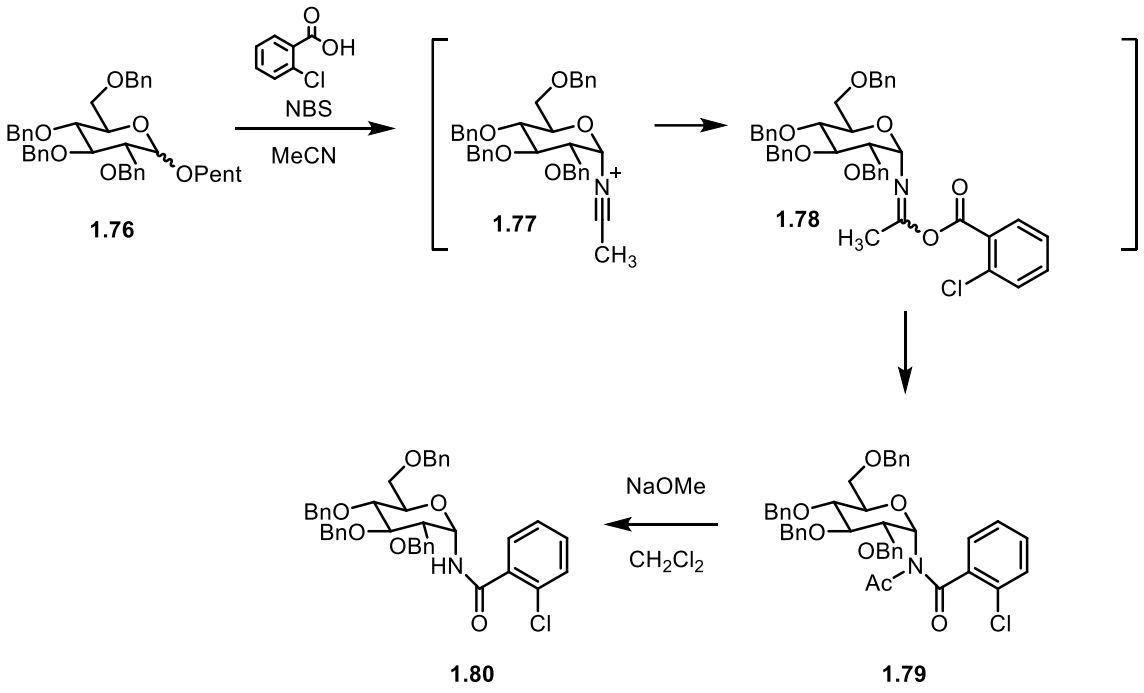

Scheme 1.33 Confirmation of an α-substituted acetonitrilium intermediate.[29]

Stereochemical configuration of the α-amide was confirmed by the downfield shifts of 3-H (δ 4.26 ppm) and 5-H (δ 4.20-4.25 ppm) indicating that the axial amido substituent is causing a deshielding effect on the respective protons. Additionally, when 1-H was irradiated via NOE difference analysis, a 15% enhancement was observed for 2-H. No enhancement occurred for 3-H or 5-H. Preparation of amide **1.80** by subjection of **1.79** to NaOMe also indicated that the α-acetonitrilium species had formed – comparison to the ^{1}H NMR spectrum of known α-amides further confirmed the stereochemistry of these products.[29] Production and confirmation of an α acetonitrilium intermediate in these transformations further illustrates the impact of solvent choice on the stereochemical outcome of substitution reactions.

2.0 Synthesis of Stereochemically Complex Tetrahydropyran Rings through Re_2O_7-Catalyzed Allylic Alcohol Isomerization and Nucleophile Trapping

The research presented in this document investigates the scope of rhenium oxide catalyzed allylic alcohol transpositions. These transformations have successfully been expanded to include fragment coupling reactions, synthesizing heterocycles of high stereochemical complexity from simple achiral building blocks. These reactions proceed through a Re_2O_7 initiated allylic alcohol transposition and cyclization with termination via stereoselective nucleophilic addition into oxocarbenium ions. The effect of acetonitrile as a solvent is examined and has a significant rate-enhancing effect on the reaction, providing access to more complex substrates. The reaction is further investigated by installing a pre-existing stereocenter into the allylic alcohol precursor. A pre-existing stereocenter dictates the stereochemistry of the trapping step and provides insight into the mechanistic details of the reaction.

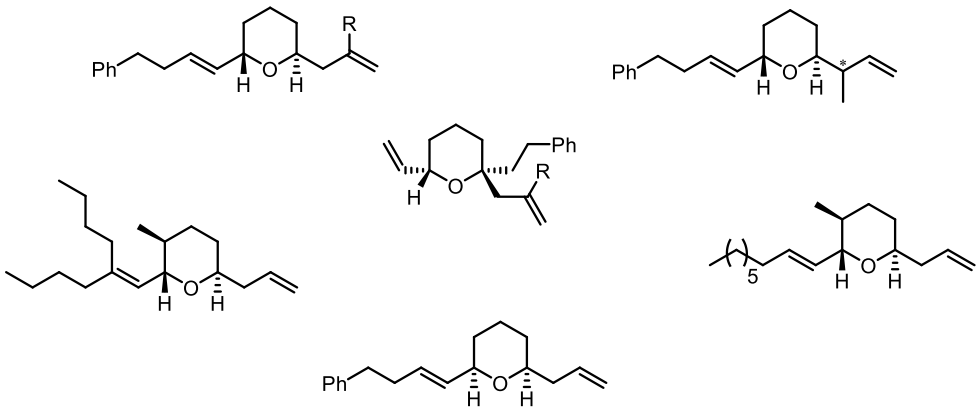

Figure 2.1 Representative scaffolds synthesized (R = H, Me).

Previously in the group, Xie applied Re_2O_7 transpositions to initiate cascade reactions to form tetrahydropyran rings with excellent stereocontrol.[30] These reactions are used to position the alcohols in a six-membered transition state, adding into a tethered electrophile to form a cyclic lactol which is ionized into an oxocarbenium ion which is then trapped with a nucleophile. These reactions proceed through the isomerization-cyclization-ionization-termination pathway depicted in Scheme 2.1.[30]

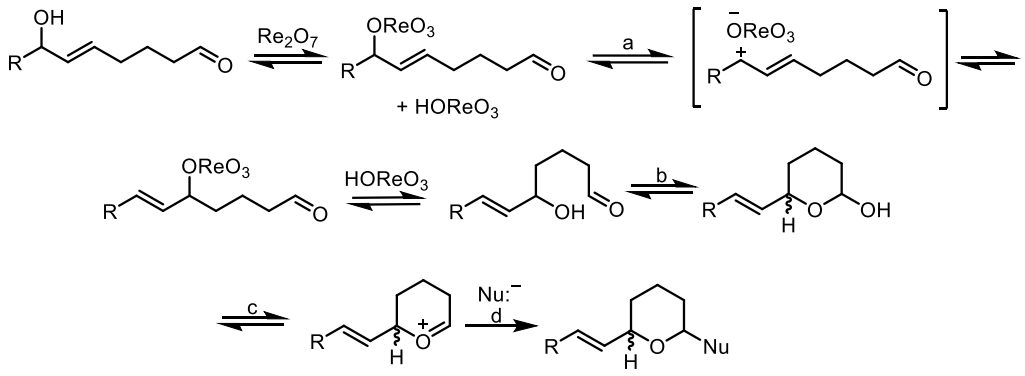

Scheme 2.1 Re_2O_7 allylic alcohol transposition-nucleophilic addition sequence. a = isomerization; b = cyclization; c = ionization and d = termination.[30]

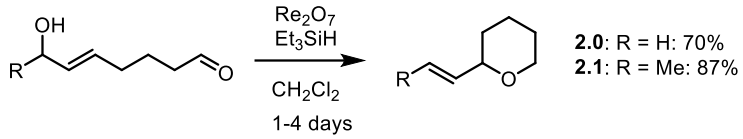

Scheme 2.2 Re_2O_7-catalyzed allylic alcohol transposition, cyclization, and reduction with Et_3SiH.[30]

Initially, Xie used Et_3SiH as the terminating agent, synthesizing tetrahydropyran rings **2.0** and **2.1** in excellent yield. Ketone precursors were also subjected to the reaction conditions to provide **2.2**

and **2.3** in good to excellent yield and with high levels of stereocontrol. The reaction proceeds via the oxocarbenium ion intermediate depicted in Scheme 2.3 with axial attack from the hydride nucleophile to give stereochemically pure 2,6-*cis* products **2.2** and **2.3**.

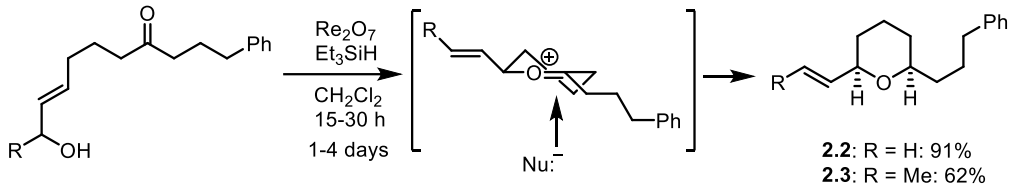

Scheme 2.3 Re_2O_7-catalyzed allylic alcohol transposition-cyclization-ionization sequence followed by termination with hydride donor Et_3SiH to yield stereochemically pure 2,6-*cis* tetrahydropyran rings.[30]

The Re_2O_7-catalyzed allylic alcohol transposition and nucleophilic addition sequence was expanded to carbon nucleophiles, including weak π-nucleophiles such as allyltrimethylsilane.[31,32] Xie prepared the cyclization precursor depicted in Scheme 2.4 to test this reaction. Although the reaction was low yielding under the standard conditions, it was discovered that addition of anion-binding sulfonamide co-catalyst $[3,5\text{-}(CF_3)_2C_6H_3NH]_2SO_2$ **2.4** greatly facilitated the reaction, providing the addition product with good conversion. This additive is theorized to bind to Re_2O_7 or $HReO_4$, enhancing the acidity and increasing the reactivity of the catalyst (Figure 2.2).[30,33,34] As the perrhenate ion is then a better leaving group, ionization is promoted, facilitating nucleophilic addition of weak π nucleophiles such as allyltrimethylsilane.

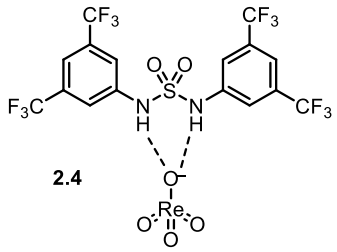

Figure 2.2 Sulfonamide co-catalyst binding to ReO_4.[30,33,34]

This reaction provided **2.5** in 83% yield and excellent stereocontrol to afford the 2,6-*trans* product.[30] Addition of allyl silane to produce a terminal alkene in the molecule is also advantageous as it provides an accessible synthetic handle that can be readily functionalized.

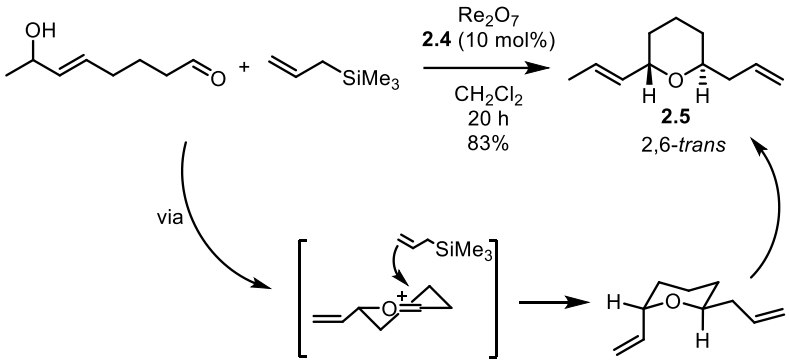

Scheme 2.4 Bimolecular fragment coupling facilitated by **2.4**. Yield determined via analysis of the crude ^{1}H NMR mixture using benzyldimethylsilane as an internal standard.[30]

The polarity of the solvent is another variable that can be modified to facilitate trapping with weak π-nucleophiles. A polar solvent should stabilize the oxocarbenium ion, increasing its concentration and reducing the activation energy required to reach this intermediate. Increased access to the oxocarbenium ion facilitates trapping, forming the fragment coupling product. It is worth noting that in contrast to Woerpel's solvent studies mentioned in Section 1.4, Scheme 1.29,

we expect our reactions to proceed through an S_N1 type mechanism regardless of solvent choice. Woerpel suggests that in nonpolar solvents, the triflate ion forms a contact-pair intermediate with the oxocarbenium ion intermediate, causing an S_N2 type mechanism to occur, inverting the stereochemistry.[26] There is much literature precedent for the formation of triflate contact ion pairs in glycosylation reactions.[35,36] In the absence of a triflate counterion, we expect the free oxocarbenium ion to exist and for the S_N1 pathway to occur regardless of solvent choice. Additionally, in our case, the perhennate ion is the leaving group rather than the acetate ion. As the perhennate ion is a better leaving group and a more stable base (pKa of $HOReO_3$ = -1.25, pKa of HOAc = 4.74), oxocarbenium ion formation should be more efficient and the S_N1 pathway should predominate.

The solvent effects can also be understood via kinetic analysis and the steady state approximation can be used to determine the overall rate expression. This approximation can be made when the first step of an intermediate-forming reaction is very slow relative to the following step. Presumably, for the Re_2O_7 reaction, oxocarbenium ion formation is the rate determining step and the subsequent step, the termination with allyltrimethylsilane, is fast relative to ionization. As transposition and cyclization are expected to be rapid, it can be assumed that the concentration of the starting material is equal to the concentration of the cyclization product, perrhenate ester **[A]** (Scheme 2.5).[37]

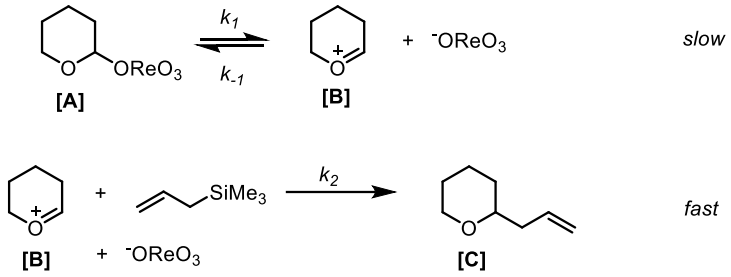

Scheme 2.5 Ionization and termination of the oxocarbenium ion intermediate.

The rate of formation of the oxocarbenium ion can then be assumed to be equal to the rate of its consumption and thus, its rate of change can be assumed to be zero (Scheme 2.6, equation 1).[37] If this is the case, then the overall rate expression can be determined for the reaction by using the oxocarbenium ion intermediate as the steady state intermediate (Scheme 2.6, equation 5).

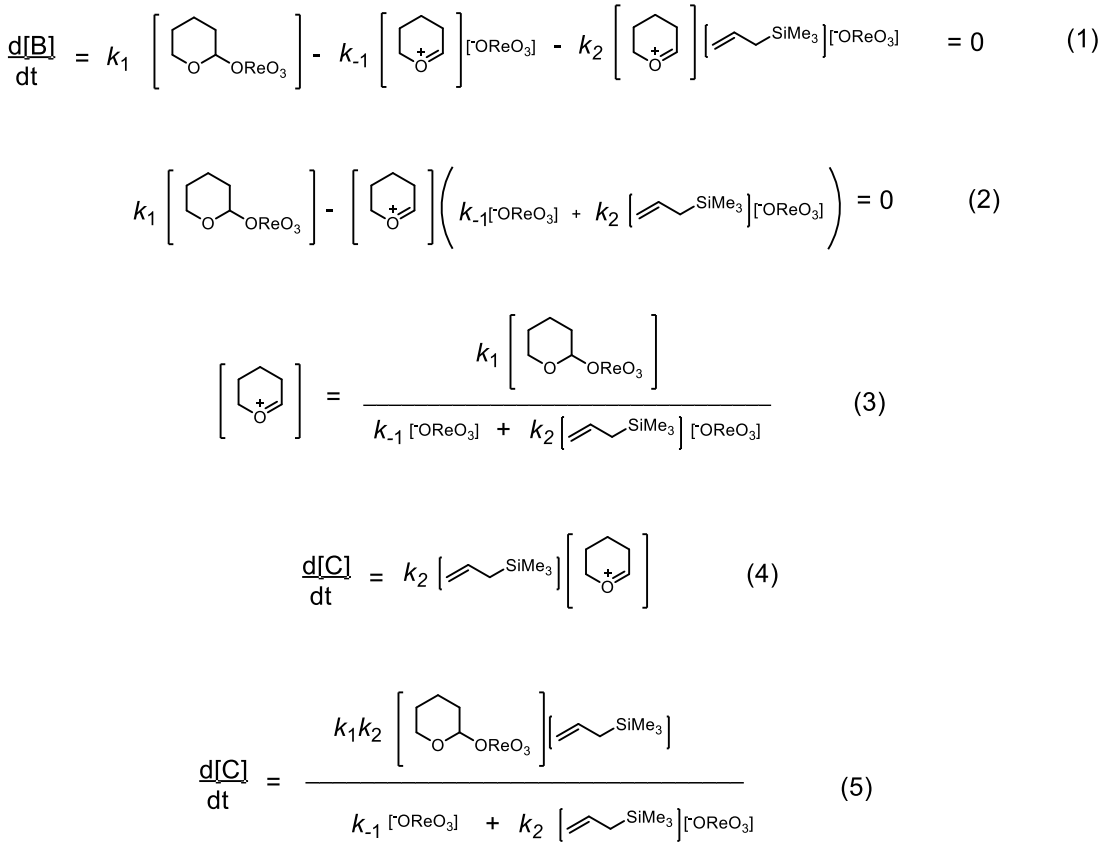

Scheme 2.6 Steady state approximation for the rate expression of the Re_2O_7 reaction.

Analysis of the rate expressions provide information about the factors that contribute to the success of the reaction. As acetonitrile stabilizes the oxocarbenium ion and decreases the activation energy required to reach it, k_1 should increase, and d[C]/dt would also increase, expediating the reaction. If the equilibrium expression in Scheme 2.5 is analyzed, the following relationship can be observed: [37a, 38]

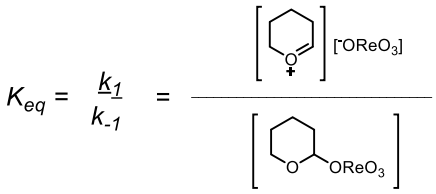

Scheme 2.7 Equilibrium expression comparing the ratio of products to reactants.

As acetonitrile stabilizes the oxocarbenium ion, the concentration of the numerator should increase relative to the concentration of the perrhenate ester in the denominator. Co-catalyst **2.4** should cause the perrhenate ion to be a better leaving group, also increasing this ratio. As this ratio is increased, k_1 is increased and d[C]/dt is increased. Additionally, equation 4 in Scheme 2.6 allows the relationship between the oxocarbenium ion and the nucleophile to be examined. As the concentration of the oxocarbenium ion is increased, the strength of the nucleophile becomes less important to the success of the reaction. Therefore, as acetonitrile stabilizes the oxocarbenium ion, weak π-nucleophiles can be successfully used as termination agents. In contrast, for stronger hydride nucleophiles such as Et_3SiH, dichloromethane is sufficient.

As mentioned in Section 1.2, thermodynamic control has been used advantageously in the Re_2O_7 cascade reactions to achieve 2,6-*cis* stereocontrol for the tetrahydropyran ring systems. This recent result in which the 2,6-*trans* product is obtained with complete stereocontrol is promising in that it allows this substitution pattern to be accessed rapidly from similar achiral precursors. Obtaining both the 2,6-*cis* and the 2,6-*trans* stereoisomers efficiently, with complete stereocontrol, and in excellent yield has applications for natural product total synthesis. Both the 2,6-*cis* and the 2,6-*trans* relationships are patterns seen in natural products containing tetrahydropyran rings [39,40,41]

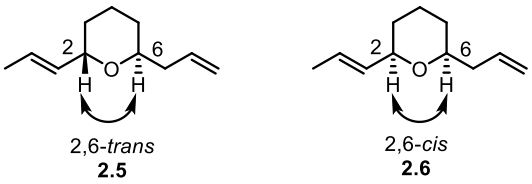

Figure 2.3 2,6-*cis* and 2,6-*trans* patterns of tetrahydropyran rings.

As the 2,6-*trans* relationship is present in natural products, achieving this stereochemical pattern through the Re_2O_7 chemistry is appealing.

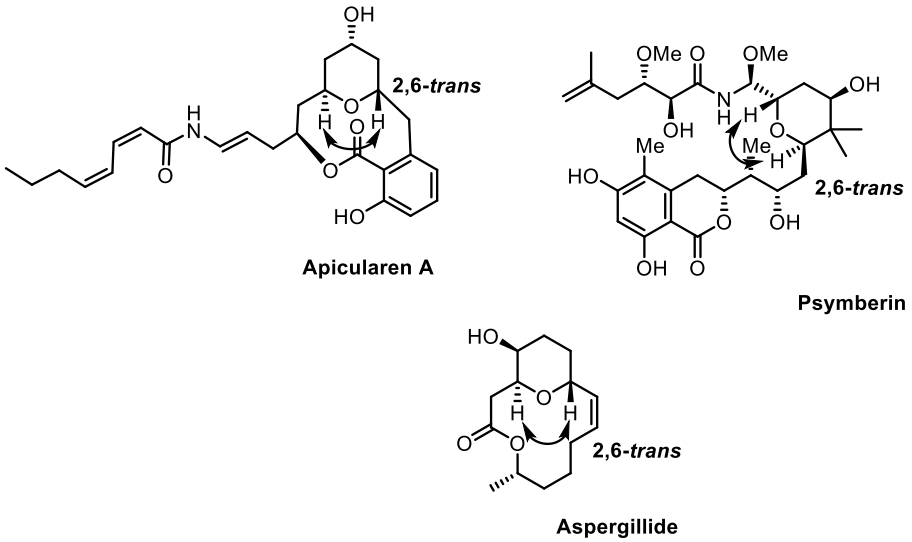

Figure 2.4 Natural products exhibiting the 2,6-*trans* relationship.

Furthermore, another pattern commonly seen in this structural motif is an additional stereocenter at carbon 7. In natural products, carbon 7 frequently bears a methyl group which orients itself *anti* to the oxygen when the side chain is oriented antiperiplanar (Figure 2.5). A *syn* pattern between the branching substituent and the oxygen is observed in natural products, albeit less frequently.[39]

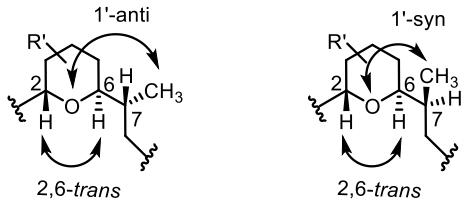

Figure 2.5 *Anti* and *syn* relationship between the branching substituent on the sidechain and the oxygen in the tetrahydropyran ring.[39]

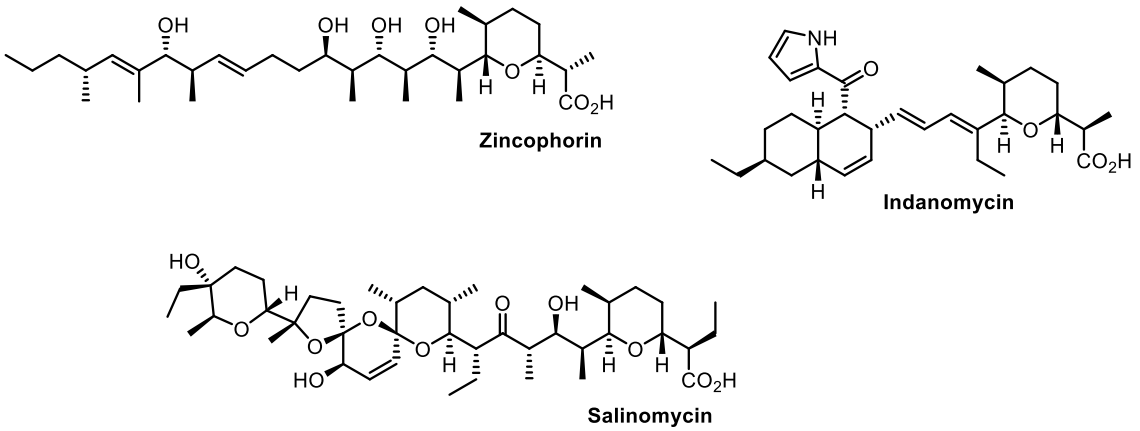

Figure 2.6 Selection of natural products exhibiting the 1′-*anti*-2,6-*trans* or 1'-*syn*-2,6-*trans* relationship.[39,42,43]

These patterns, designated by Danishefsky as the "1′-*anti*-2,6-*trans*" or "1'-*syn*-2,6-*cis*" relationship, are attractive substitution patterns for stereoselective synthesis due to their prevalence in natural products. Zincophorin, indanomycin, and salinomycin all exhibit variations of this pattern. The 1'-*anti*-2,6-*trans* pattern is seen in indanomycin and at both junctions of salinomycin. In contrast, zincophorin has both patterns – as depicted in Figure 2.6, it exhibits the *anti* pattern at the 6 position and the *syn* pattern at the 2 position.[39,42,43] The presence of a methyl group in the C_7 position is significant due to its influence on the population of conformers which can influence

biological activity.[44] Chair conformer **2.8** is preferred over **2.7** due to the presence of two equatorial substituents vs. one equatorial substituent. For **2.8**, a particular turn conformer is favored when a methyl group is present. If there is a methyl group adjacent to the tetrahydropyran ring as illustrated in Scheme 2.8, there is a *syn*-pentane interaction with the hydrogen at C_2 for two out of three 120° rotations which is relieved by formation of turn conformer **2.9**. In contrast, a hydrogen in place of the methyl group would result in only one of the rotations exhibiting a *syn*-pentane interaction.

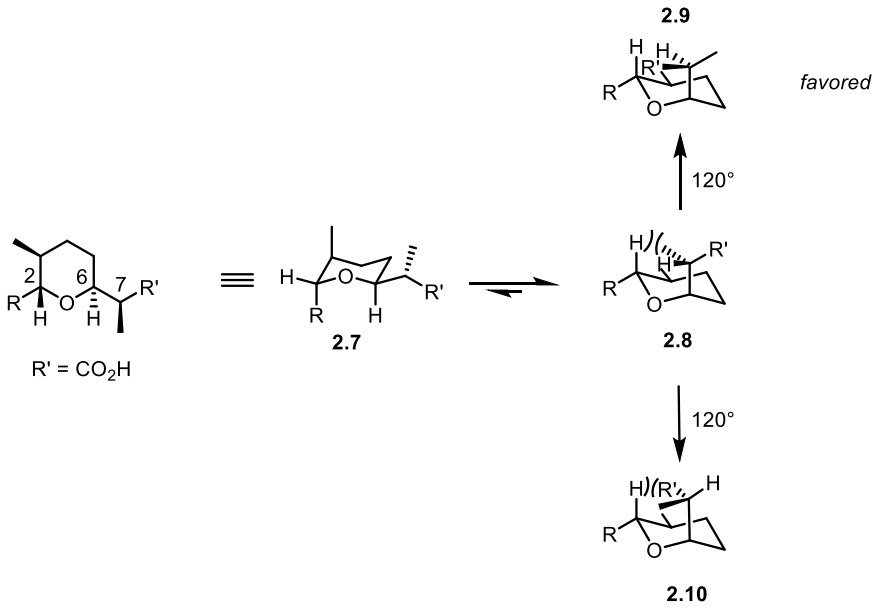

Scheme 2.8 Conformers for tetrahydropyran rings with a methyl group in the C_7 position.

This interaction causes turn conformer **2.9** to be favored as it relieves the energetic penalty associated with the *syn*-pentane interactions, influencing the population of the conformers. In regard to biological relevance, if the preferred turn conformer is representative of the binding conformation of the molecule, then the biological activity and potency of the molecule would be improved when an alkyl group is present at C_7. Exploring the incorporation of a methyl group at

this position is thus advantageous in that it has applications for improving a molecule's biological profile.

In this document, the Re_2O_7-catalyzed allylic alcohol transposition is expanded to a kinetic bimolecular fragment coupling reaction with carbon nucleophiles to achieve such transformations – accessing tetrahydropyran rings exhibiting the 2,6-*trans* pattern and installing an additional stereocenter at C_7. These transformations have been optimized to facilitate the nucleophilic trapping by enhancing the reactivity of Re_2O_7 with a sulfonamide anion binding catalyst and through stabilization of the oxocarbenium ion by acetonitrile.

2.1 Solvent Effects on Bimolecular Fragment Coupling and Kinetic vs. Thermodynamic Control

Inspired by the success of the bimolecular fragment coupling facilitated by hydrogen bonding sulfonamide co-catalyst **2.4** (Figure 2.2), we sought to further explore the reaction by examining solvent effects. As mentioned in Section 2.0, in addition to the effects of the hydrogen bonding catalyst, a polar solvent such as acetonitrile or HFIP should stabilize the oxocarbenium ion intermediate and facilitate trapping. Secondary allylic alcohol substrate **2.15** was readily synthesized for these studies in three steps. Cross metathesis of commercially available alcohol **2.13** with allylic alcohol **2.12** occurred in 41% yield to produce **2.14**. Diol **2.14** underwent selective TEMPO oxidation to produce the desired aldehyde in 62% yield.

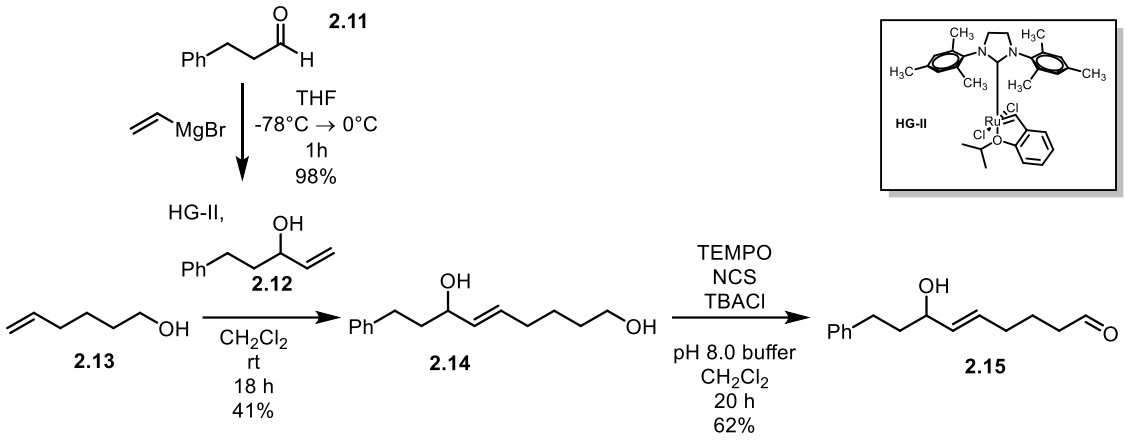

Scheme 2.9 Preparation of secondary allylic alcohol cyclization precursor **2.15**.

2.15 was subjected to Re_2O_7 in acetonitrile and we were pleased to see that it was rapidly converted to the 2,6-*trans* product in 30 minutes, obtaining the product in 79% yield with complete stereocontrol. The reaction was initiated at 0 °C to avoid dehydration and four equivalents of silane were used to avoid competitive protodesilyation of the allyltrimethylsilane. The use of acetonitrile significantly enhanced the rate of the reaction with a reaction time of 30 minutes vs. 24 h in CH_2Cl_2. Additionally, in acetonitrile no co-catalyst is needed, with a high yield being obtained despite omission of the hydrogen bonding catalyst. Furthermore, when this reaction mixture was filtered through a silica gel plug, resubjected to fresh Re_2O_7, and stirred at room temperature for 24 h, we were able to achieve full equilibration to the thermodynamically favored 2,6-*cis* product **2.17**. Analysis via COSY and NOE NMR confirmed the stereochemistry of both products.

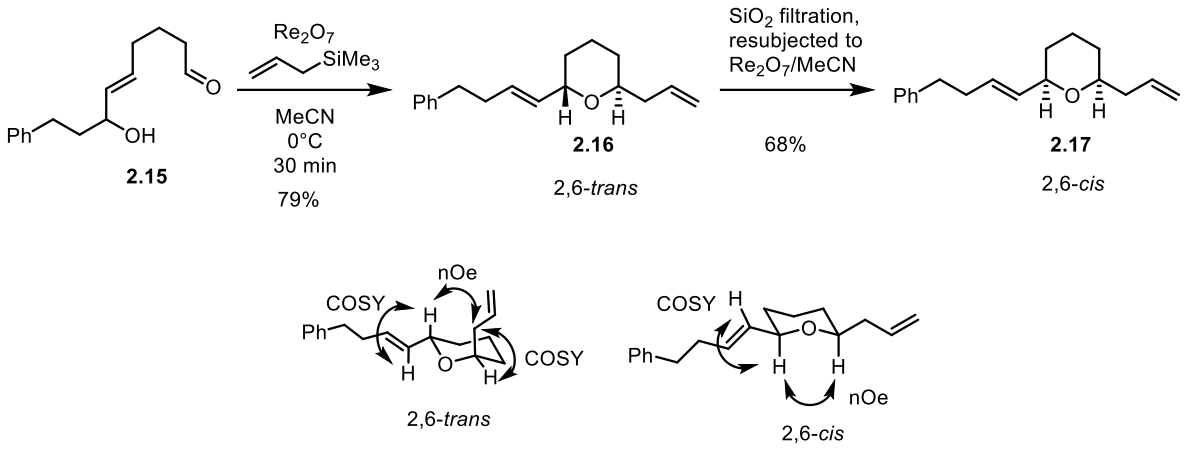

Scheme 2.10 Re_2O_7 initiated allylic alcohol transposition and cyclization to give the kinetic 2,6-*trans* product and equilibration to the thermodynamically favored 2,6-*cis* product.

Filtering the reaction mixture through silica gel was necessary for complete equilibration to **2.17**. When no filtration was performed and the reaction was warmed to room temperature and stirred overnight, the reaction stalled at a 2:1 ratio of the *trans*/*cis* product (Table 2.1). Warming the reaction to room temperature then heating to 55°C did promote faster equilibration to the *cis* product, although at the expense of the yield, resulting in 32% of the *cis* product and 23% of the *trans* product. Changing the solvent to HFIP allowed for successful conversion of the 2,6-*trans* product to the 2,6-*cis* product in 23 h without the need for silica gel filtration and resubjection. Additionally, analysis of the crude ^{1}H NMR ratio after 30 minutes in HFIP showed a 1:2 ratio of *trans*/*cis* (Table 2.1).

Table 2.1 Solvent studies on kinetic bimolecular fragment coupling with allyltrimethylsilane.

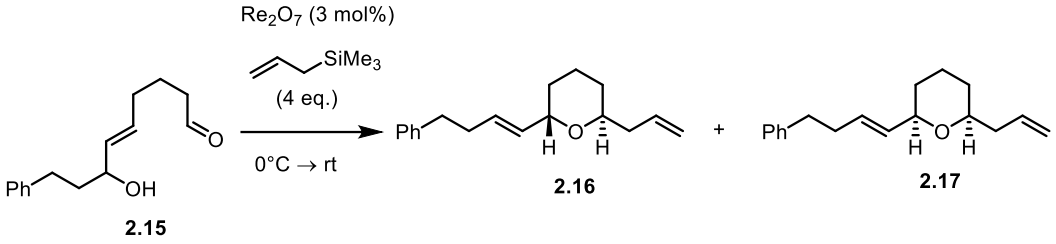

Entry	Conditions	% yield (trans/cis ratio.)[a]
1	MeCN, 30 min	79% (1:0)
2	MeCN, 19 h	(2:1)
3	MeCN, 24 h	68% (0:1)[b]
4	HFIP, 30 min	(1:2)
5	HFIP, 23 h	73% (0:1)
6	MeCN, 0°C → rt → 55°C, 3.5 h	32% *cis*, 23% *trans*

[a]ratio determined by the ratio of diastereomers as observed by ^{1}H NMR analysis of the crude mixture
[b]after filtering through SiO_2 and resubjecting to Re_2O_7/MeCN

In acetonitrile, the *cis* product is accessed through thermodynamic equilibration. In this system, a likely pathway for thermodynamic equilibration is fragmentation of kinetically formed 2,6-*trans* product **2.16** to the allyl cation intermediate, followed by stereoselective ring closure to give the 2,6-*cis* product **2.17** (Scheme 2.11).

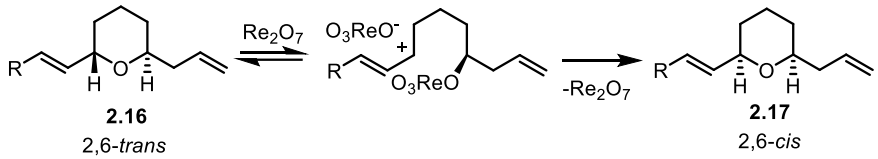

Scheme 2.11 Thermodynamic equilibration to the 2,6-*cis* product via an allyl cation intermediate.

As no *cis* product is seen when CH_2Cl_2 is the solvent, we suspect that acetonitrile facilitates this rapid isomerization by stabilizing the allyl cation intermediate, lowering the energy required for equilibration and promoting formation of the 2,6-*cis* product. If acetonitrile does provide a stabilizing effect and enhances equilibration, then using it as a co-solvent could promote faster thermodynamic equilibration for other Re_2O_7 reactions which equilibrate through allyl cation intermediates, such as **1.36** and **1.37** described in Section 1.2**.**

These results led us to further investigate the role of solvent on reaction mechanism. The exclusive formation of the 2,6-*trans*-tetrahydropyran ring in entry 1 indicates that, as expected, the reaction proceeds through an oxocarbenium intermediate and kinetically controlled nucleophile trapping. However, the 1:2 *trans*/*cis* mixture we observed in HFIP in entry 4 after only 30 minutes at 0°C suggests that the reaction may proceed through an alternative mechanism in HFIP. Previous work in the group has shown that Re_2O_7 can catalyze a dehydrative cyclization, forming both the *cis* and *trans* isomers at room temperature, with full equilibration to the *cis* product after heating.[45]

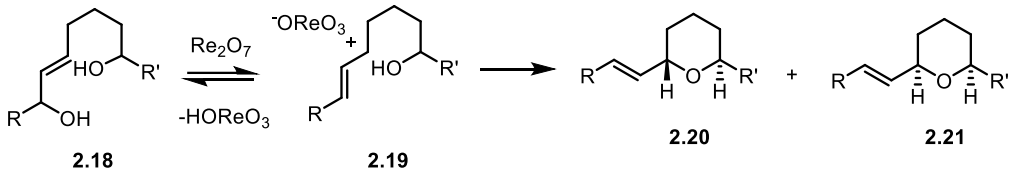

Scheme 2.12 Re_2O_7-catalyzed dehydrative coupling.

For allylic alcohol **2.22**, dehydrative cyclization could occur with Re_2O_7 acting as a Lewis acid to promote addition of allyl silane to the aldehyde. Subsequent ring closure would give a mixture of *cis* and *trans* products prior to heating.

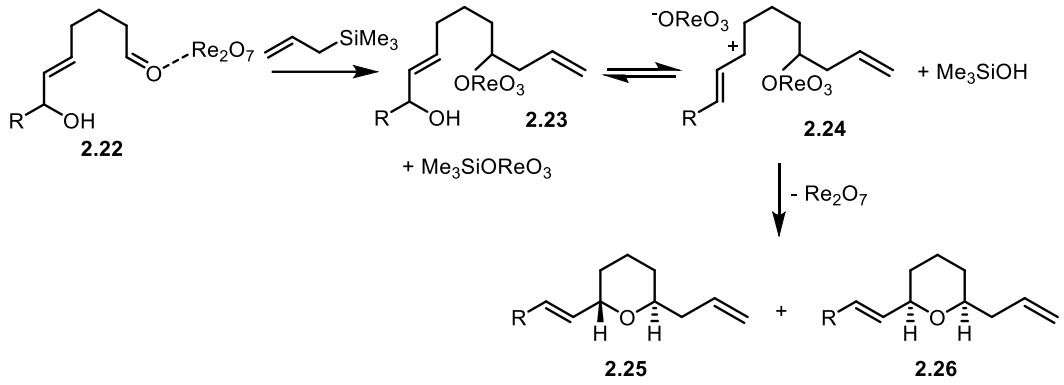

Scheme 2.13 Re_2O_7 promoted allylation and dehydrative cyclization.

To explore this possibility, we added allyltrimethylsilane to hydrocinnamaldehyde in the presence of Re_2O_7. In MeCN, we observed no allylation and obtained only recovered starting material, further confirming that the reaction proceeds through the expected mechanism in MeCN. However, in HFIP, allylation occurs after 30 minutes at 0°C with complete conversion observed after warming to room temperature and stirring for 2 h.

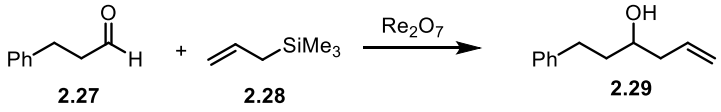

Conditions	Results
MeCN, 5 h	0% allylation
HFIP, 30 min	product formation
HFIP, 2 h	97%

Scheme 2.14 Allylation studies in acetonitrile and hexafluoroisopropanol.

As the allylation reaction is slower than the standard reaction, proceeding to completion in 2 h vs. 30 minutes, the transposition-cyclization-termination mechanism should predominate.

However, since product formation is observed after 30 minutes in the addition of allyltrimethylsilane to hydrocinnamaldehyde, this competing mechanism may also contribute to product formation, albeit to a minor extent.

The success of the reaction in acetonitrile also prompted us to try other nucleophiles. We first opted to use methallyltrimethylsilane as a nucleophile. Due to its increased substitution and higher tendency to undergo protodesilylation, it was expected that methallyltrimethylsilane might be a challenging nucleophile. The perrhenic acid generated by the transposition step (Scheme 2.15) could cause the silane to decompose before the oxocarbenium ion is reached and trapping occurs.

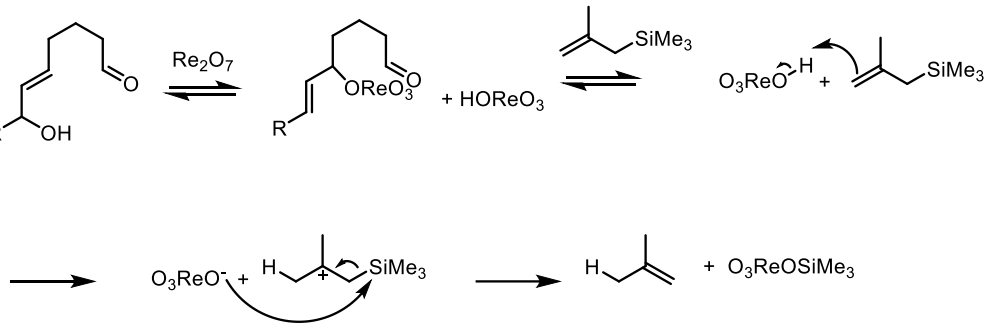

Scheme 2.15 Competitive protodesilyation of methallyltrimethylsilane with perrhenic acid.

However, with the rate-enhancing effect of acetonitrile, this reaction proceeded smoothly, providing **2.30** in good yield. Fortunately, acetonitrile's stabilizing effects on the oxocarbenium ion lowers the activation energy required to reach this intermediate and increases the rate of ionization, allowing the oxocarbenium ion to be reached faster and for trapping with methallyltrimethylsilane to occur before competitive protodesilylation with $HOReO_3$.

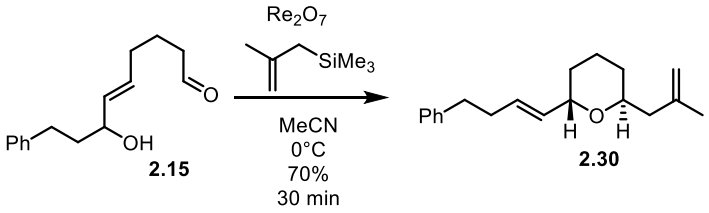

Scheme 2.16 Successful cyclization and trapping in acetonitrile using methallyltrimethylsilane.

In hopes of expanding the structural diversity of these transformations, enol ethers and cyano nucleophiles were used. Installation of nitrogen atoms would in particular expand the applications of this work and provide pharmaceutically relevant products. Unfortunately, use of these nucleophiles as trapping reagents resulted in complex product mixtures with none of the desired products observed (Table 2.2). It is likely that the enol ether is too unstable of a nucleophile and is reacting with perrhenic acid before trapping can occur successfully.

Table 2.2 Termination with diverse carbon nucleophiles.

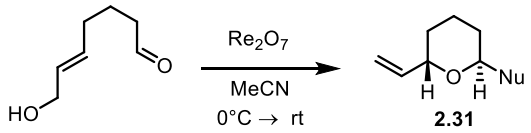

Entry	Nucleophile	Product	% yield[a]
1 (R = H)		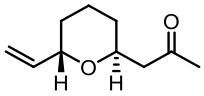	0%
2a (R = H)	TMSCN	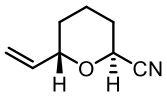	0%
2b (R = H)	NaCN		0%

[a]isolated yield

Trapping ketone **2.32** with a silyl enol ether was also attempted as the primary alcohol is less likely to undergo dehydration. However, quantitative silyl transfer onto the primary alcohol was observed.

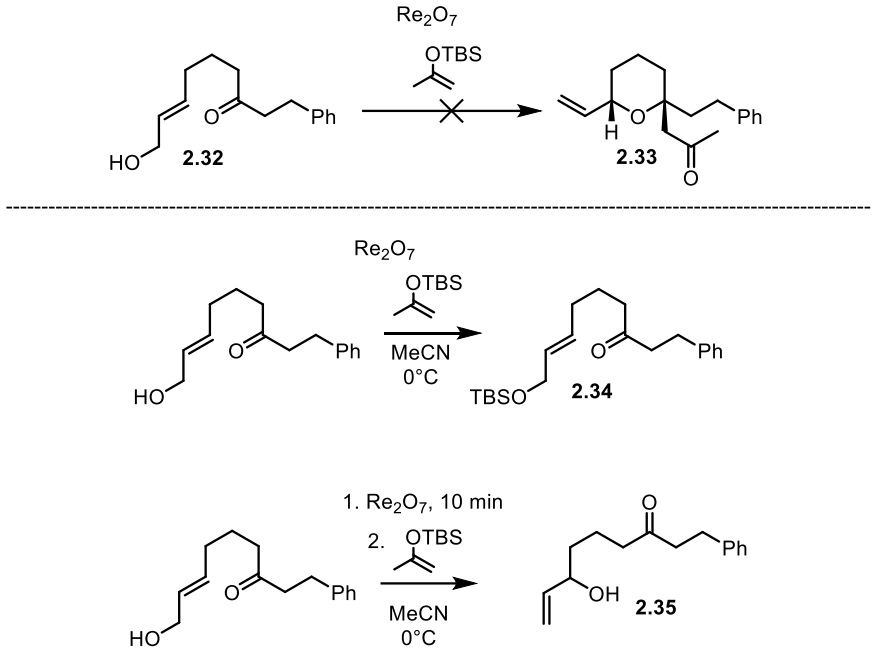

Scheme 2.17 Cyclization attempts with silyl enol ether and ketone **2.32**.

Taking note of this result, sequential addition of reagents was attempted. The typical procedure adds Re_2O_7 immediately after all other reagents have been combined. In scenario 2, Re_2O_7 was added to **2.32** in MeCN first, the reaction stirred for 10 minutes, then the enol ether was added in hopes of achieving transposition and cyclization before competitive silyl transfer occurred onto the primary alcohol. No silyl transfer was observed, but no product was obtained either, with primarily the transposed alcohol being observed by ^{1}H NMR analysis of the crude mixture, indicating that trapping is disfavored for these nucleophiles. These results are in contrast to reactions performed by Xie and coworkers where tetrahydrofuran oxocarbenium ions are

successfully trapped with enol silanes. When substrate 2.33 was subjected to the reaction conditions, trapping with enol silane **2.34** occurred in 46% yield to give a 1:1 mixture of diastereomers.[30]

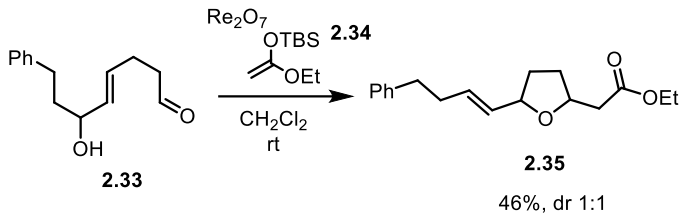

Scheme 2.18 Trapping with enol silane **2.34** to form tetrahydrofuran product **2.35**.[30]

This discrepancy is due to the propensity of tetrahydrofuran acetals to ionize more rapidly than tetrahydropyran acetals. Faster ionization would provide more access to the oxocarbenium intermediate, facilitating trapping to obtain the tetrahydrofuran products.[46,47] Although acetonitrile should stabilize the tetrahydropyran oxocarbenium ion and promote trapping, it is apparent that it's stabilizing effects are not sufficient to successfully trap enol silanes with six membered cyclic oxocarbenium ions before they undergo competitive degradation by perrhenic acid. Overall, despite efforts to vary the termination agents, the scope for fragment coupling to produce tetrahydropyran rings appears to be limited to silane nucleophiles.

2.2 Mechanistic Studies with an Isotopically Labeled Cyclization Precursor

To further probe the mechanistic pathway of this reaction, an isotopically labeled cyclization precursor was prepared. Although it is expected that the reaction proceeds through the typical mechanism as discussed in Section 2.0, Scheme 2.1, it is possible that the reaction proceeds through an alternative mechanism. Since acetonitrile stabilizes the allyl cation intermediate as seen in the equilibration studies, the reaction could also proceed through a dehydrative pathway. Scheme 2.19 depicts these pathways: pathway **A** represents the traditional expected pathway where the transposed allylic alcohol adds into the aldehyde. Alternatively, pathway **B** represents a process in which the allylic alcohol undergoes dehydration to produce an allyl cation intermediate which then undergoes nucleophilic addition by the aldehyde to produce a labeled oxocarbenium ion intermediate. This intermediate is then terminated with allyltrimethylsilane to give the isotopically labeled product. If the aldehyde is labeled isotopically, then we should be able to determine if pathway B is followed by observing if ^{18}O is incorporated into the tetrahydropyran ring.

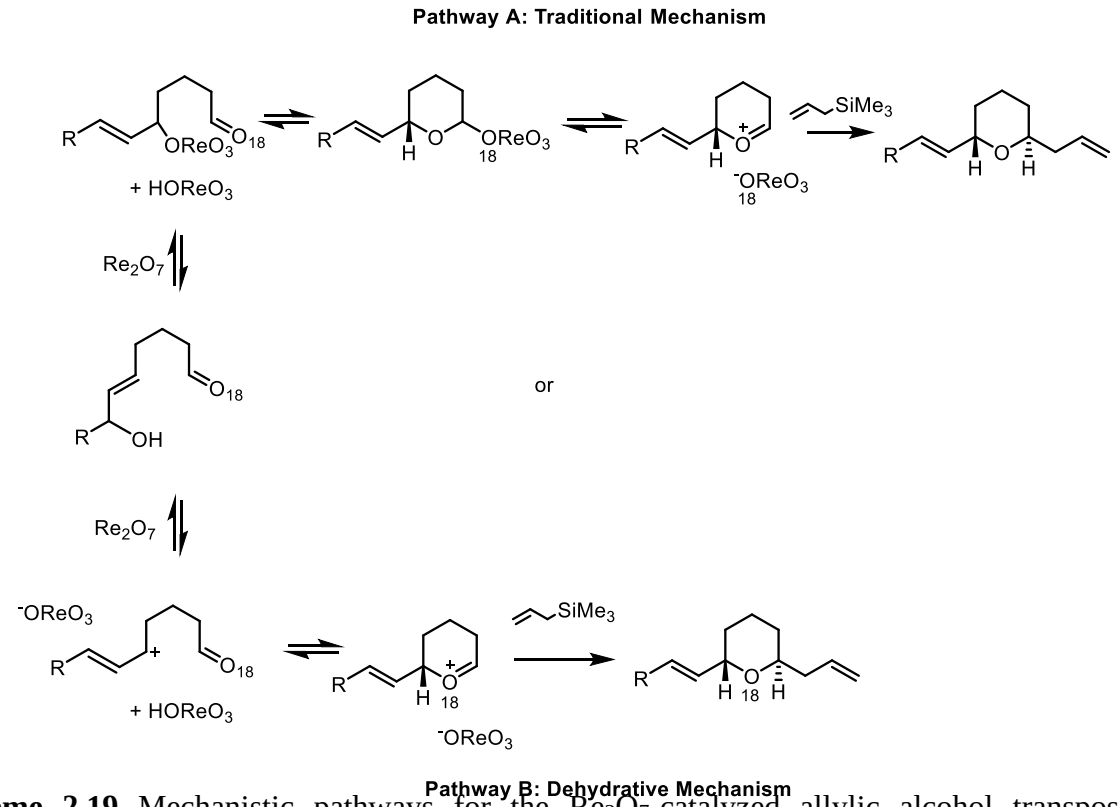

Scheme 2.19 Mechanistic pathways for the Re_2O_7-catalyzed allylic alcohol transposition, cyclization, and fragment coupling.

The isotopically labeled aldehyde was prepared by reaction of **2.36** with oxygen-18 enriched water in the presence of acidic THF.[4]

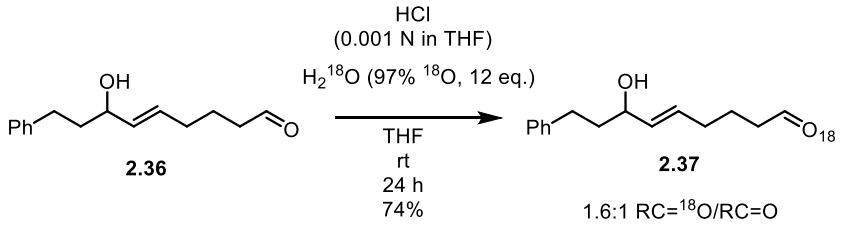

Scheme 2.20 Incorporation of ^{18}O into aldehyde cyclization precursor **2.36**.

Due to the differences in reduced masses, isotopomers exhibit different vibrational frequency values when observed by infrared spectroscopy. As is illustrated by the harmonic oscillator

approximation (Figure 2.7), a smaller value for the vibrational frequency should be observed for the carbonyl C=O stretch when the oxygen is isotopically labeled with ^{18}O.

$$\nu = \frac{1}{2\pi c}\sqrt{\frac{k}{\mu}}$$

Figure 2.7 Harmonic oscillator approximation for determination of vibrational frequency. ν = vibrational frequency, *c* = speed of light, *k* = spring constant for the bond, μ = reduced mass.

The frequency for the C=^{18}O bond typically decreases by approximately 30 cm^{-1} in comparison to the unlabeled C=O bond.[48] Indeed, upon taking an infrared spectrum of the product, a new carbonyl C=^{18}O stretch was observed at a frequency of 1687 cm^{-1} compared to 1719 cm^{-1}, indicating that the isotopically labeled oxygen had successfully been incorporated. The unlabeled C=O stretch was still observed, indicating that 100% incorporation of ^{18}O was not obtained. Assuming that the difference in dipole moments between C=O and C=^{18}O is negligible, the ratio of the two products can be approximated by comparing the intensities of the peaks.[48] The percent transmittance intensity values for the labeled and unlabeled aldehyde were 71.101% and 80.738%, respectively. Absorbance values can be calculated to be 0.148 for the labeled aldehyde and 0.093 for the unlabeled aldehyde, giving a 1.6:1 ratio of C=^{18}O: C=O, or 61% C=^{18}O.

The labeled aldehyde was subjected to the typical reaction conditions to determine which pathway the mechanism proceeds through (Scheme 2.21).

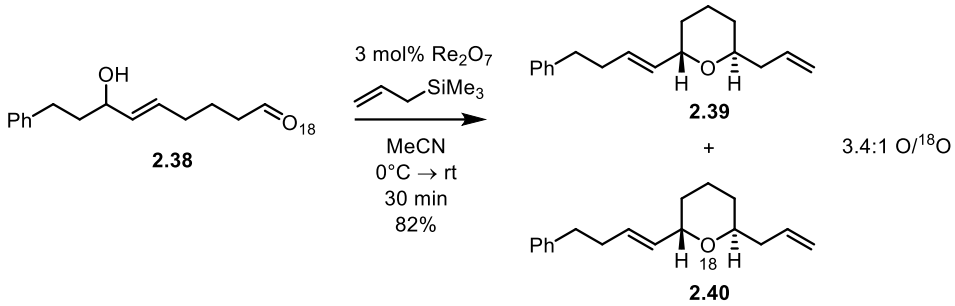

Scheme 2.21 Kinetic bimolecular fragment coupling with an isotopically labeled aldehyde precursor.

High resolution mass spectrometry analysis of the isolated product gave interesting results and provided insight into the mechanistic details of this reaction. In the mass spectrum, the unlabeled product was the major product, however, a substantial amount of the ^{18}O labeled product was also observed. The ratio of the products was determined from the intensity values of the *m/z* peaks and was found to be 3.4:1 O/^{18}O, indicating 23% ^{18}O incorporation. This result demonstrates that pathway B does occur, and that dehydration of the allylic alcohol followed by aldehyde addition into an allyl cation is a reasonable pathway for these substrates to follow. The stabilization of the allyl cation with acetonitrile would likely aid in causing some of the substrate to follow pathway B. There are multiple possibilities which can explain the decrease in ^{18}O incorporation. First, it is possible that the process occurs through a mixture of pathways, with some of the substrate proceeding through the dehydration pathway and some proceeding through the transposition pathway. Alternatively, even if 100% of the substrate undergoes the dehydration pathway, the perrhenate ion that forms from the dehydration can add into the oxocarbenium ion, which can then form the acyclic product and undergo dehydration and cyclization a second time, producing the unlabeled tetrahydropyran ring, as shown in Scheme 2.22.

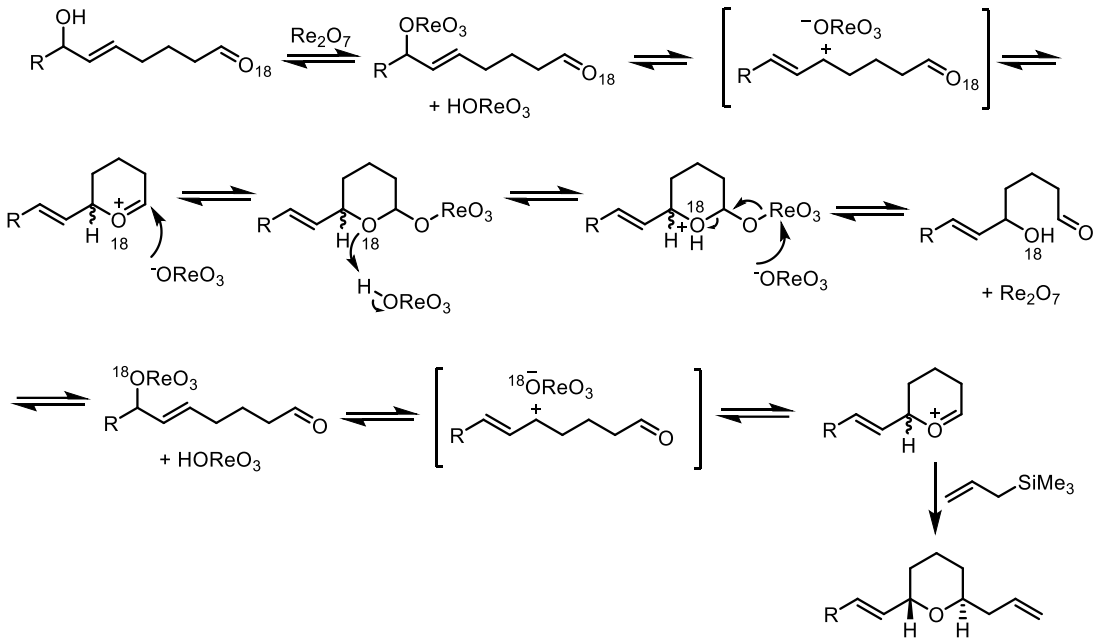

Scheme 2.22 Addition of perrhenate ion into the ^{18}O labeled aldehyde to produce the ^{16}O tetrahydropyran product through a dehydration pathway.

The mechanism depicted above in Scheme 2.22 could provide a substantial amount of the unlabeled tetrahydropyran ring, despite going through the dehydrative pathway. However, although we cannot definitively state that the process goes 100% through pathway B, the results obtained in this study provide clear evidence that the dehydrative mechanism occurs and is a viable pathway to these products.

2.3 Installation of an External Stereocenter through Addition of a Prochiral Nucleophile

The scope of these transformations was then expanded to incorporate stereocenters from the trapping agent. This strategy would allow an additional stereocenter to be installed outside of the tetrahydropyran ring by using crotyl trimethylsilane as a prochiral nucleophile (Scheme 2.23).

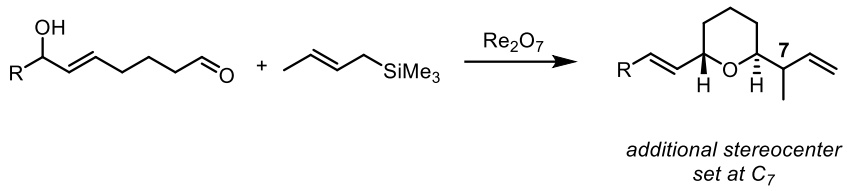

Scheme 2.23 Installation of a stereocenter at C_7.

Cyclization precursor **2.45** was synthesized via pyridinium chlorochromate oxidation of 5-hexene-1-ol to aldehyde **2.44** which was immediately subjected to cross metathesis with diol **2.42.** The *cis* alkene diol was prepared via hydrogenation of alkyne **2.41** using Lindlar's catalyst in 82% yield.

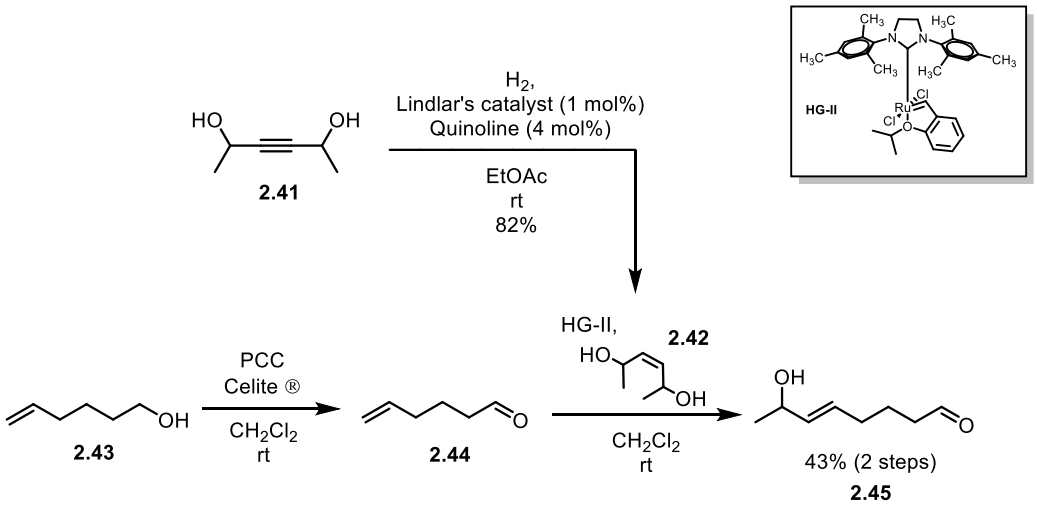

Scheme 2.24 Preparation of secondary allylic alcohol cyclization precursor **2.45**.

2.45 was initially subjected to the Re_2O_7-catalyzed allylic alcohol transposition-cyclization-ionization-termination sequence using sulfonamide co-catalyst **2.4** and crotyl trimethylsilane in CH_2Cl_2, forming stereoisomers **2.46** and **2.47**.

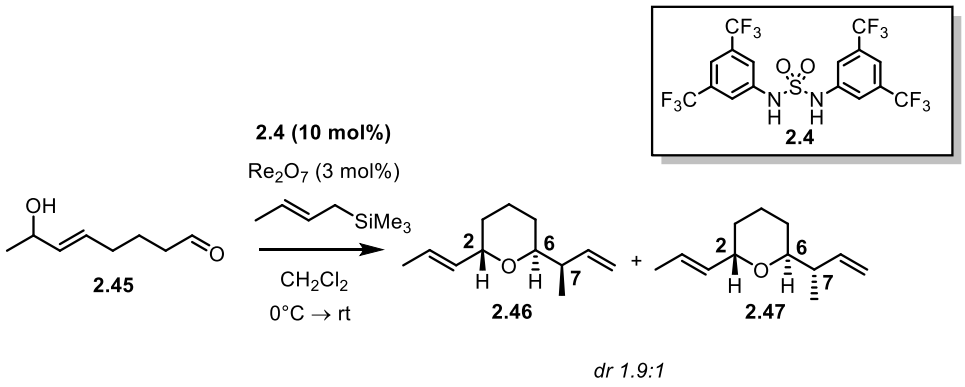

Scheme 2.25 Stereoisomers obtained from crotylation of **2.45**.

The reaction was initiated at 0°C and warming to room temperature and stirring overnight was necessary for conversion to the product. These conditions gave conversion to a mixture of the two 2,6-*trans*-tetrahydropyran isomers with a diastereomeric ratio of 1.9:1 in 24 hours as observed by analysis of the crude ^{1}H NMR mixture. Diastereomer **2.46,** exhibits Danishefsky's 1'-*anti* 2,6-*trans* substitution pattern whereas diastereomer **2.47** exhibits the 1'-*syn* 2,6-*trans* pattern (Figure 2.8). Danishefsky explores the synthesis of these patterns through a carbon-Ferrier rearrangement of glycal derivatives in which a synclinal approach vs. an antiperiplanar approach is proposed. In these studies, a synclinal approach to the oxonium bond produces the 1'-*anti* 2,6-trans pattern whereas an antiperiplanar approach produces the 1'-*syn* 2,6-trans pattern.[39]

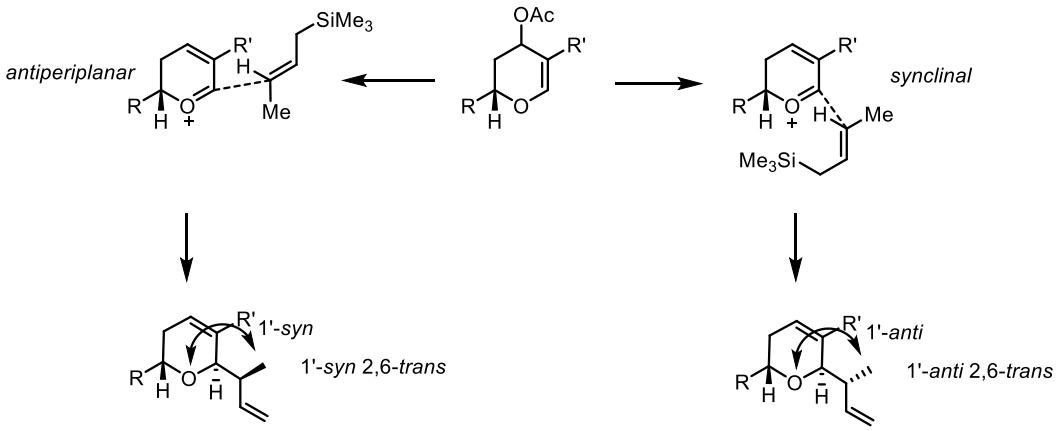

Figure 2.8 Synclinal and antiperiplanar approaches of (*E*)-crotyl trimethylsilane in the carbon-Ferrier rearrangement.

In this example, the 1'-*anti* 2,6-*trans* product was formed preferentially in a ratio of 3:1 *anti*/*syn* in 58% yield.

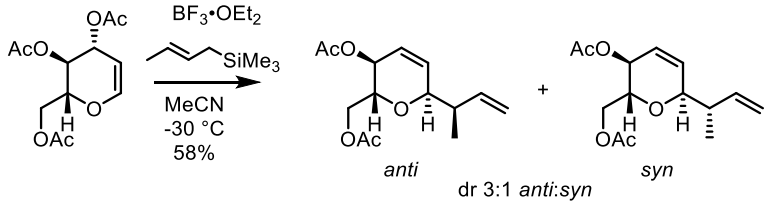

Scheme 2.26 Synthesis of a 3:1 ratio of *anti*/*syn* products via a carbon-Ferrier rearrangement.[39]

In our case, the transition state analysis is expected to be similar, suggesting two different approaches of crotyl trimethylsilane to produce the two diastereomers. For **2.46**, a plausible transition state exhibits crotyl silane approaching the oxocarbenium ion from a synclinal approach with the methyl group away from the oxonium ring to minimize gauche interactions. Nucleophilic addition should occur axially from the top face of the ring to avoid the disfavored twist-boat conformer. A plausible transition state to give the other diastereomer, **2.47,** is likely to be favored with the silane approaching antiperiplanar to the oxocarbenium ion, again with the methyl group

away from the ring. This approach would both maximize π orbital overlap and minimize gauche interactions of the methyl group with the methylene group of the oxonium ring (Figure 2.9).[39,42]

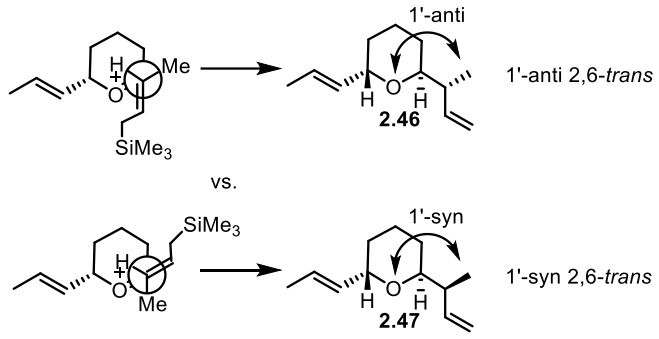

Figure 2.9 Transition state analysis for approach of crotyl trimethylsilane to tetrahydropyran oxocarbenium ions to provide the 1′-*anti*-2,6-*trans* and 1′-*syn*-2,6-*trans* substitution patterns.[39]

We predict that the synclinal approach will be favored, producing the 1'-anti 2,6-*trans* stereochemical pattern. A rationalization for the favorability of the synclinal approach is that the lone pair on the oxygen stabilizes the developing positive charge on the nucleophile. The positive charge is in closer proximity to the oxygen in the synclinal approach; therefore, this approach should be favored due to the increased stabilizing electronic effects.

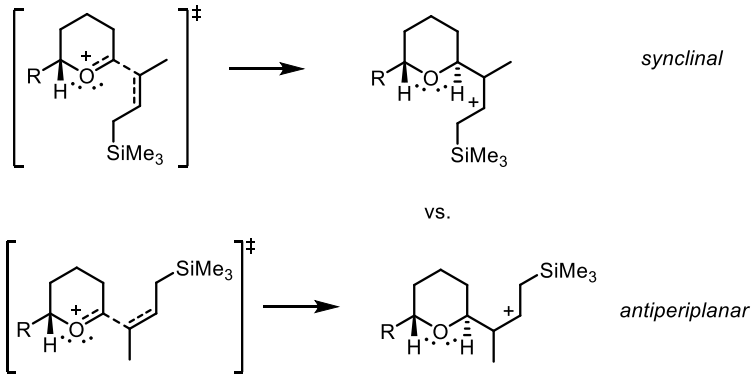

Figure 2.10 Stabilization of the developing positive charge on the nucleophile by the oxygen lone pairs of the tetrahydropyran ring.

Literature precedent suggests an additional justification for a synclinal approach based off of steric interactions. This favorability is based on previous work on a similar system performed by Hsung and coworkers in their formal synthesis of (+)-zincophorin.[49] Addition of $SnBr_4$ to the tetrahydropyran precursor removed the cyclic urea and generated a cyclic oxocarbenium ion intermediate (Scheme 2.27). In this transformation, an 80:20 ratio of the 1'-*anti* to the 1'-*syn* product was observed, indicating that a synclinal approach was favored over an antiperiplanar approach, assuming that both approaches proceed with the methyl group away from the oxonium ring.

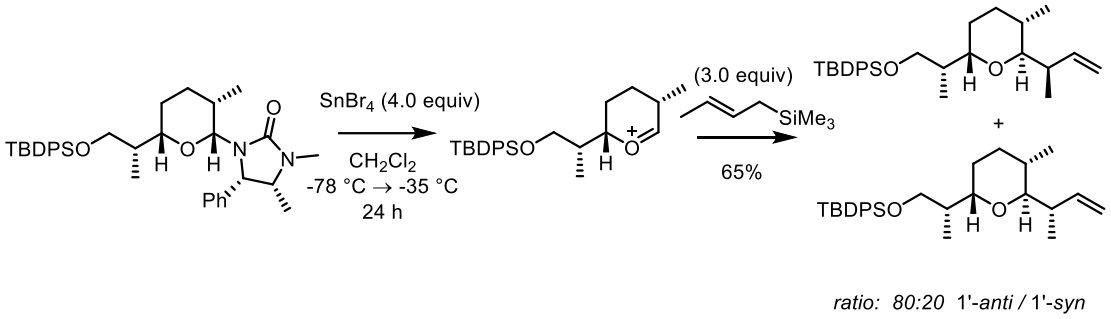

Scheme 2.27 Formation of oxocarbenium ion and crotylation.[49]

Hsung and coworkers justify the preference for the synclinal approach by comparing the severity of the gauche interactions. In comparing the two transition states, the antiperiplanar approach yields a more severe gauche interaction as the methylene group in the nucleophile should be in closer proximity to the hydrogens on the tetrahydropyran ring than the methyl group (Figure 2.11).

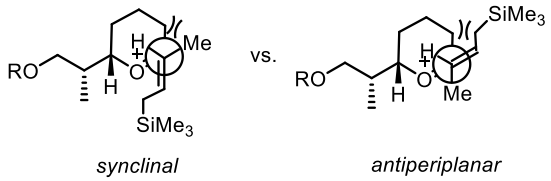

Figure 2.11 Gauche interactions for the synclinal and antiperiplanar approaches of crotyl trimethylsilane in work by Hsung and coworkers.[49]

Both the electronic effects and steric effects discussed likely contribute to the synclinal approach being favored. Furthermore, since the 1'-anti 2,6-*trans* pattern is more prevalent in natural products than the 1'-anti 2,6-*cis* pattern, the preference for the synclinal transition state would be especially appealing (Figure 2.6).[39]

Encouraged by our initial success in dichloromethane, we sought to improve the diastereoselectivity by modifying the solvent. Addition of a more polar solvent should stabilize the oxocarbenium intermediate generated, giving rise to a later transition state that more closely resembles the products. A later transition state would cause steric or electronic effects to be more prevalent as the nucleophile would be in closer proximity to the oxocarbenium ion. With an increased stabilization of the developing positive charge by the lone pairs on the oxygen and the decreased steric interactions, crotyl trimethylsilane should be more likely to approach from the favored synclinal transition state, improving the stereocontrol. In hopes of accomplishing this increase in stereocontrol, acetonitrile was added as a co-solvent. As is consistent with previous results with allyltrimethylsilane, this modification significantly enhanced the rate of the reaction, showing complete conversion after 1 h. This alteration also showed some improvement on the diastereoselectivity, with a dr of 2.3:1 in 1:2 CH_2Cl_2/MeCN (entry 2).

Table 2.3 Studies on solvent and anion binding sulfonamide catalyst effects on Re_2O_7-catalyzed bimolecular fragment coupling with crotyl trimethylsilane.

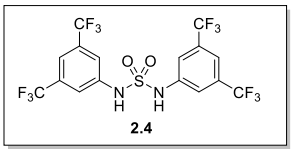

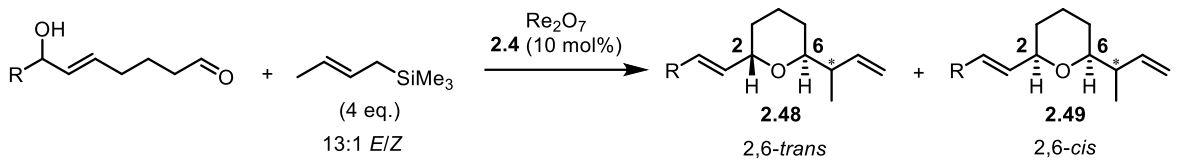

Entry	R	Conditions	C_7 d.r.[a]
1	Me	0°C → rt, CH_2Cl_2, 24 h	1.9:1
2	Me	0°C → rt, 1:2 CH_2Cl_2/MeCN, 1 h	2.3:1
3	Me	-30°C, 7:3 CH_2Cl_2/MeCN, 20 h	trace product
4[b]	Me	0°C → rt, 1:2 CH_2Cl_2/MeCN, 1 h	2.3:1
5[b]	-CH_2CH_2Ph	0°C, MeCN, 1 h	70%[c]. 2.5:1
6[b]	-CH_2CH_2Ph	0°C, HFIP, 2 h	57%[c], 1:1 trans/cis (trans dr: 1.3:1, cis dr: 1.9:1)

[a] dr determined by the ratio of diastereomers as observed by ^{1}H NMR analysis of the crude mixture
[b] co-catalyst **2.4** omitted
[c] isolated yield

To determine if the improved rate and stereocontrol were independent of co-catalyst **2.4**, the crotylation was performed in 1:2 CH_2Cl_2/MeCN with no additive present. The reaction proceeded with no change in rate or stereocontrol, indicating that the use of acetonitrile is sufficient for enhancing the rate of this reaction (entry 4). Decreasing the temperature to -30°C (entry 3) impeded the reaction with only trace amount of product observed after 20 h. Finally, performing the reaction in straight acetonitrile at 0°C gave the 2,6-*trans* product in 70% yield in 30 minutes with a slight improvement in dr of 2.5:1. We elected to use HFIP as a solvent in hopes of further adjusting the polarity and stabilizing the oxocarbenium ion intermediate. However, the use of HFIP as a solvent led to a decrease in yield and erosion of stereocontrol – with a 1:1 *trans*/*cis* ratio

observed after 2 h with a dr at C_7 of 1.3:1 for the *trans* isomer and a dr of 1.9:1 for the *cis* isomer. As discussed in Section 2.1, the prevalence of the *cis* product in HFIP may be caused by some of the reaction proceeding through the allylation-dehydration-cyclization mechanism, or it may be due to a more rapid equilibration of the *trans* product through an allyl cation intermediate. The allylation-dehydration-cyclization mechanism may also contribute to the erosion in the stereocontrol at C_7 due to the addition of allyltrimethylsilane to the acyclic precursor before the stereochemical defining step would occur in the traditional pathway. COSY and NOESY ^{1}H NMR data confirmed the stereochemistry of the products.

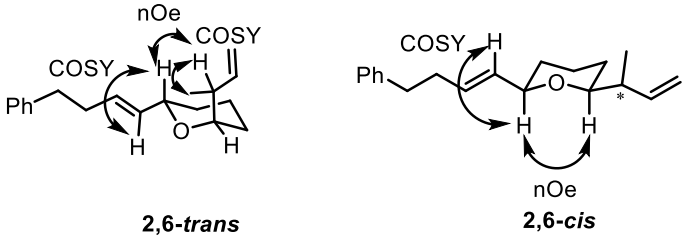

Figure 2.12 Stereochemical confirmation of the 2,6 relationship of the *cis* and *trans* crotylation products.

An additional variable that has played a critical role in these reactions in previous work in the Floreancig Group is nucleophile reactivity. Xie compared the stereocontrol of the reactions of Et_3SiH and Ph_3SiH with precursor **2.50**. This precursor undergoes the following pathway to obtain two possible diastereomers as products (Scheme 2.28).

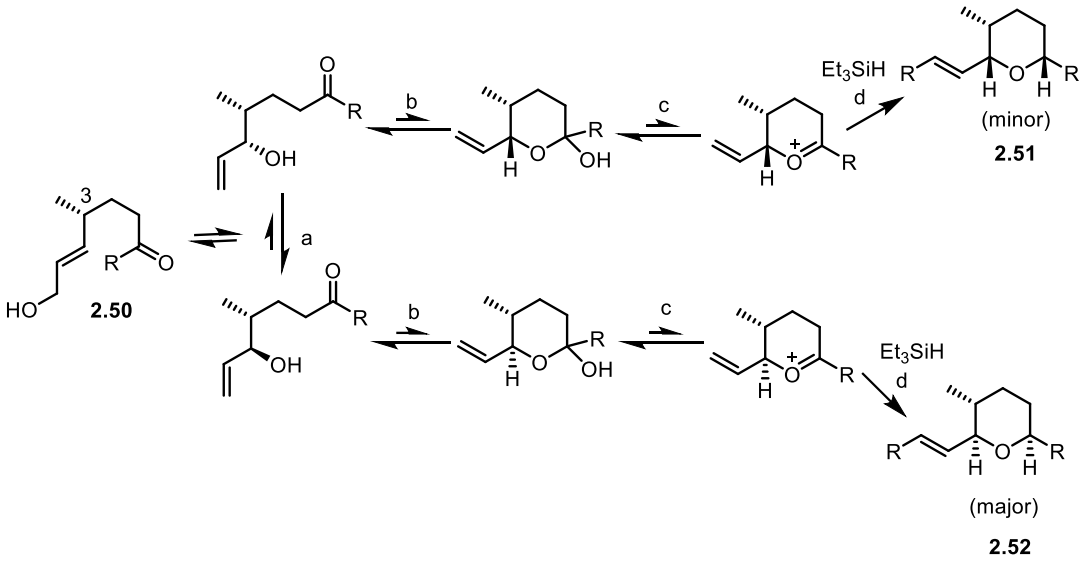

Scheme 2.28 Isomerization pathway for enantiomerically pure precursor **2.50**.[27]

Xie theorized that less reactive nucleophiles should exhibit a reduced trapping rate, allowing for better thermodynamic equilibration through the pathway in Scheme 2.28 and improving stereocontrol. Compared to Et_3SiH, Ph_3SiH is a less reactive nucleophile which should improve the stereocontrol of these reactions.[50,51] When Xie used both Et_3SiH and Ph_3SiH as trapping agents in the Re_2O_7-catalyzed cyclization of the enantiomerically pure precursor shown in Scheme 2.29, using triphenylsilane instead of triethylsilane as a hydride donor provided the product with improved stereocontrol – increasing the diastereoselectivity from 3:1 to 9:1.[30]

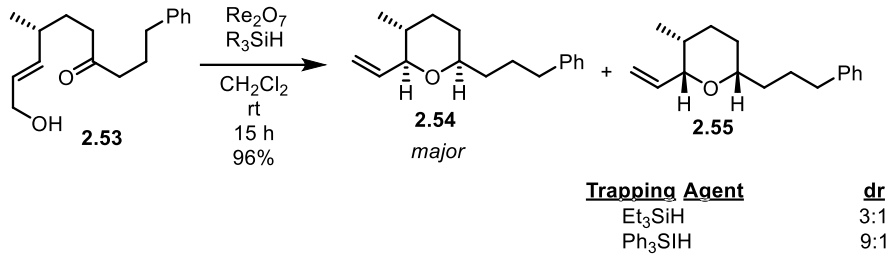

Scheme 2.29 Relationship between trapping agent reactivity and stereocontrol.[30]

We hoped that slowing down the rate of the trapping step would also improve stereocontrol when the stereocenter is incorporated from the nucleophile. A reduced trapping rate could cause the transition state to be later and more closely resemble the product, enhancing the steric and electronic effects associated the competing transition states (Figures 2.10 and 2.11). The disfavored steric interactions in the antiperiplanar transition state and the favorable electronic interactions in the synclinal transition state should cause the nucleophile to favor the synclinal approach, increasing the amount of the 1'-*anti* product formed and improving stereocontrol. In hopes of achieving this stereocontrol, **2.45** was trapped with the less reactive crotyl dimethylphenyl silane.[50,51] No change in diastereoselectivity was evident, with a ratio of 2.2:1 observed for both entries.

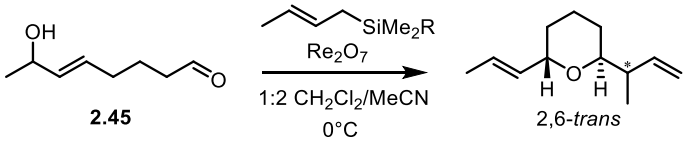

Trapping Agent	dr
R = Me	2.2:1
R = Ph	2.2:1

Scheme 2.30 Comparison of silane nucleophiles in the crotylation of **2.45**.

Although modification of nucleophile reactivity is a viable strategy to obtain stereocontrol when the stereocenter is pre-installed into the tetrahydropyran ring and thermodynamic equilibration can be established, in this case it does not have an effect on the stereocontrol of the trapping step when two different nucleophile approaches are possible. Decreasing nucleophile reactivity and slowing down the trapping step does not appear to favor the synclinal transition state as hoped.

In order to determine if the 1′-*anti*-2,6-*trans* or 1′-*syn*-2,6-*trans* product was formed preferentially, we attempted to determine the stereochemistry at the C_7 position of crotylation product **2.48** shown in Table 2.3. An initial strategy was to derivatize and crystallize the product in hopes of obtaining x-ray crystallography data. However, multiple attempts to crystallize the crotylation product and its derivative were unsuccessful. Despite functionalization with 4-bromobenzoyl chloride and 2,4-dinitrophenylhydrazine, the substrate's low polarity and tendency to exist as an oil prevented effective crystallization (Scheme 2.31)

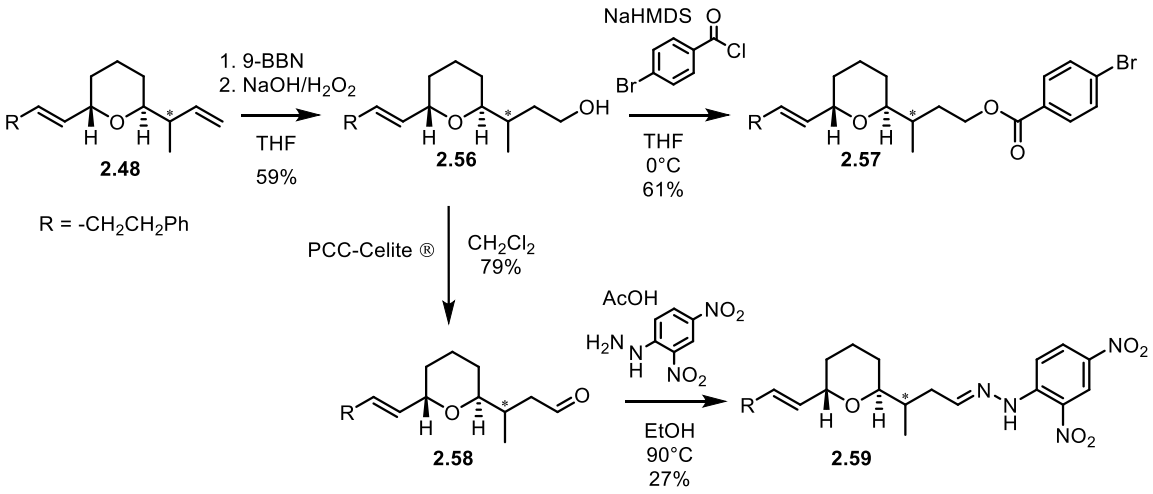

Scheme 2.31 4-bromobenzoyl and 2,4-DNP derivatization of **2.48**.

Although a crystal structure could not be obtained, we can compare the chemical shifts of the diastereomers to those reported by Hsung and coworkers, structures which were confirmed via x-ray crystallography.[49] In the ^{1}H NMR spectrum, internal vinyl proton H_a is distinct for both isomers for Hsung's products. For the 1'-*anti*-2,6-*trans* product, the peak representing H_a for the major diastereomer is at 5.84 ppm whereas the minor diastereomer peak is at 5.64 ppm. In our structures, a similar pattern is observed. H_b is from the major diastereomer, with a chemical shift of 5.90 ppm. The minor diastereomer proton peak is buried beneath the internal alkene signals; however, its general location is clearly shown via COSY NMR with a chemical shift of approximately 5.7 ppm.

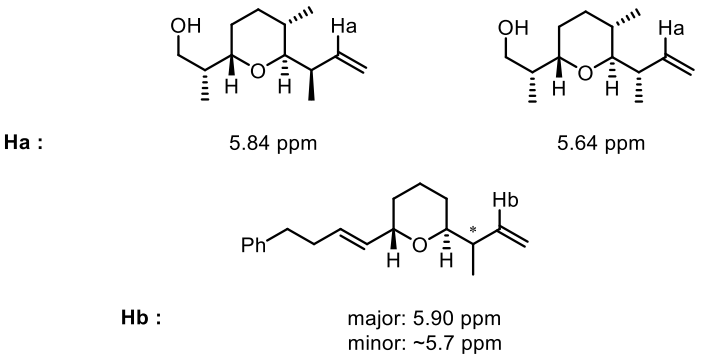

Figure 2.13 Comparison of chemical shifts between crotylation products.[49]

From this comparison the conclusion can be made that the major product from the crotylation reaction is the 1'-*anti*-2,6-*trans* product, resulting from a synclinal approach of the silane nucleophile. This result confirms earlier predictions regarding the influence of solvent choice. As the polarity of the solvent is increased, the favorable electronic effects between the oxocarbenium ion and the approaching nucleophile in the synclinal approach should also be increased. Additionally, the unfavorable steric interactions will be more prevalent and in order to be minimized, will more strongly favor the synclinal approach. These factors should lead to an

increase in stereocontrol, which was observed to a minor extent upon switching the solvent from dichloromethane to acetonitrile. Furthermore, obtaining the 1'-*anti*-2,6-*trans* product is especially appealing as this stereochemical pattern is more prevalent in natural products than the 1'-*syn*-2,6-*trans* pattern.[39]

Through this work it is illustrated that prochiral nucleophiles can be used to install external stereocenters into these substrates with modest diastereoselectivity to achieve the desirable 1'-*anti*-2,6-*trans* stereochemical pattern. The installation of the stereocenter is also advantageous as an alkyl substitution at this position has biological applications. In addition, acetonitrile significantly increased the rate of the reaction, facilitated trapping, and provided an increase in diastereoselectivity in comparison to dichloromethane.

2.4 Installation of a Quaternary Center via Re_2O_7-Catalyzed Allylic Alcohol Transposition and Bimolecular Fragment Coupling

Encouraged by the prior results, we applied these conditions to more synthetically difficult transformations. Few examples in the literature exist of synthesizing tetrahydropyran rings with quaternary centers in the **2** or **6** position. Additionally, scaffolds involving the formation of quaternary centers via nucleophilic addition into oxocarbenium ions have been previously inaccessible in good yield with Re_2O_7.[17] Cyclization precursors **2.67** and **2.68** were synthesized via Grignard addition of 5-bromo-1-pentene into hydrocinnamaldehyde followed by oxidation

with pyridinium chlorochromate, then cross metathesis with allylic alcohols **2.64 (R = H)** and **2.65 (R = Me)**.

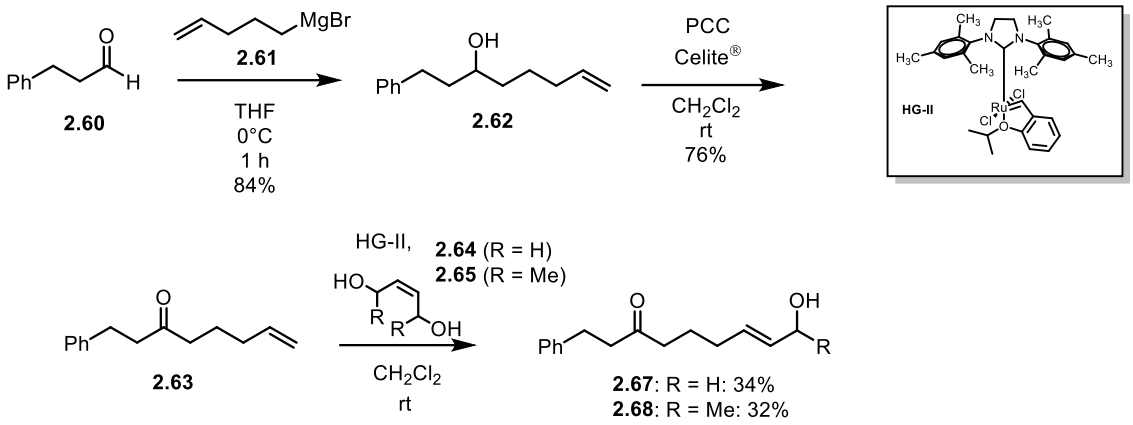

Scheme 2.32 Synthesis of ketones **2.67** and **2.68**.

Cyclization precursor **2.68** gave no product under the conditions used, regardless of solvent choice or hydrogen bonding catalyst, yielding a mixture of diene isomers via an E1 decomposition pathway when the reaction was performed in dichloromethane (entries **1a** and **2a**). In acetonitrile, the diene side products were not observed; however, no desired product was observed either when **2.68** was the cyclization precursor. A major side product for entry **3a** was observed by analysis of the crude ^{1}H NMR mixture but was unidentifiable. Entries **1a** and **2a** are consistent with previous work in the Floreancig group, suggesting that dehydration is a competitive side reaction for ketone substrates containing secondary allylic alcohols. This decomposition pathway is more likely occur for ketone substrates rather than aldehyde substrates due to the increased stability of the oxocarbenium ion generated for ketone precursors. The additional alkyl substituent for ketone precursors provides stability to the oxocarbenium ion intermediate, reducing the rate of trapping

and providing more opportunity for the decomposition pathway to occur. Additionally, the increased substitution of secondary alcohol **2.68** stabilizes the allylic cation intermediate, which also favors decomposition pathways.[10,30] This example illustrates the necessity of using primary alcohol precursors for the kinetic bimolecular coupling reaction when ketones are used as the intramolecular trapping group. Fortunately, primary alcohol **2.67** readily converted to **2.69** in acetonitrile in 90% yield in 30 minutes with excellent stereocontrol (entry **3b**). Notably, acetonitrile is crucial for the high yield of this reaction; when **2.67** was subjected to the reaction conditions in dichloromethane, only trace amounts of product was detected, with transposed alcohol **2.72** observed as the major product by analysis of the crude ^{1}H NMR mixture after 1 h. Addition of the sulfonamide co-catalyst to dichloromethane did improve the reaction but was not as influential as the solvent choice – some conversion was observed via TLC after 1 h and in hopes of achieving full conversion, the reaction was allowed to warm to room temperature and stirred for an additional 23 hours. After purification, 41% of desired product **2.69** was obtained (entry **2b**). The results for entries **2b** and **3b** suggest that enhancement of Re_2O_7 or stabilization of the oxocarbenium ion is critical for nucleophilic trapping on these substrates to occur at all, with acetonitrile stabilization of the oxocarbenium ion intermediate promoting the reaction more effectively than the effects of sulfonamide catalyst **2.4**. Additionally, it appears that in the absence of termination as seen in entry **1b**, the acyclic transposed alcohol is favored over the cyclic hemiacetal for the ketone substrates (see reaction pathway in Scheme 2.1)[10,30]

Table 2.4 Troubleshooting of cyclization and nucleophilic trapping of ketone precursors **2.52** and **2.53**.

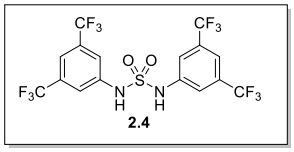

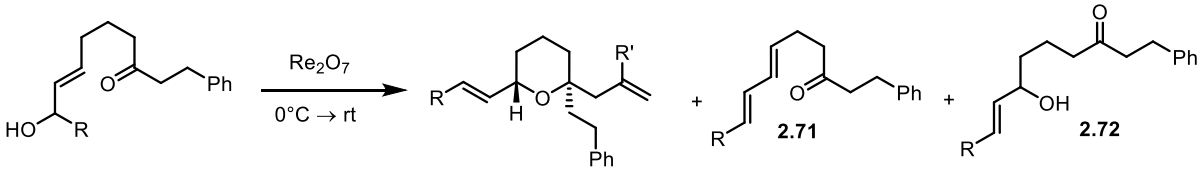

2.69: R' = H
2.70: R' = CH_3

Entry	Nucleophile	Conditions	Product	% yield[a]
1a (R = Me)		CH_2Cl_2, 1 h	2.71	major product[b]
1b (R = H)		CH_2Cl_2, 1 h	2.72	major product[b]
2a (R = Me)		CH_2Cl_2, **2.4**, 1 h	2.71	major product[b]
2b (R = H)		CH_2Cl_2, **2.4**, 24 h	2.69 (R' = H)	41%
3a (R = Me)		MeCN, 1 h	unidentifiable side product	
3b (R = H)		MeCN, 1 h	2.69 (R' = H)	90%
3c (R = H)	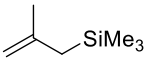	MeCN, 30 min	2.70 (R' = Me)	81%

[a]isolated yield
[b]as observed by ^{1}H NMR analysis of the crude mixture

Furthermore, methallyltrimethylsilane was successfully used as a nucleophile in this reaction, illustrating the benefits of the rate enhancing effect of acetonitrile – here two challenging fragments are coupled together in excellent yield and diastereoselectivity (entry 3c). The stereochemical outcome for both substrates was confirmed via a NOESY correlation between the tertiary and allylic hydrogens as shown below.

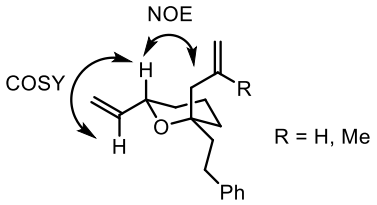

Figure 2.14 Confirmation of stereochemistry for products containing a quaternary center.

Additionally, upon allowing the reaction with methallyltrimethylsilane to warm to room temperature and stirring overnight, some isomerization was observed, with approximately 10% of the minor diastereomer present after 17 h. With this observation and our previous results for thermodynamic equilibration, we expect that this isomerization also proceeds through an allyl cation intermediate.

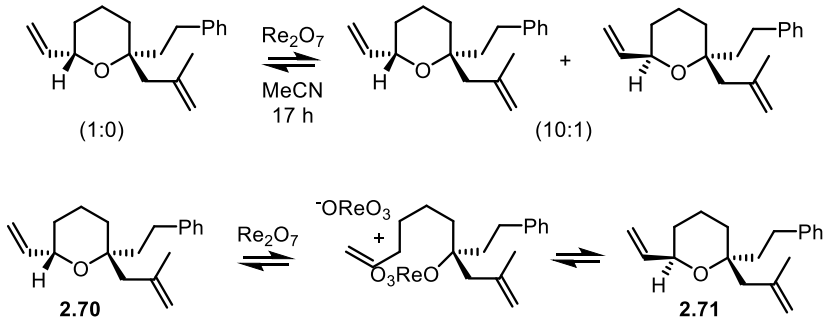

Scheme 2.33 Re_2O_7 promoted ionization of **2.70** and fragmentation to allyl cation intermediate to provide isomer **2.71.**

As little equilibration was observed for this substrate, it is expected that the terminal alkene generated from primary alcohol **2.67** provides poor stability for an allyl cation intermediate. This result further confirms the equilibration pathway. Through these experiments, stereochemically complex tetrahydropyran rings containing quaternary centers were accessed in excellent yield.

2.5 Analysis of the Effect of a Pre-Existing Stereocenter on the Reaction

It was also of interest to us to examine the effects of a pre-existing stereocenter on the diastereocontrol of the reaction. Expanding this reaction to include substrates with a stereocenter provides insight into the mechanistic details of the reaction and the installation of a stereocenter could promote the equilibration of the oxocarbenium ion intermediates to favor one isomer. Additionally, as many natural products with the 2,6-*trans* stereochemical pattern also bear stereocenters within the tetrahydropyran ring, particularly at C_3 (Figure 2.15), accessing these substrates through the Re_2O_7 chemistry is desirable. It is also of interest of us to observe the effect that a remote stereocenter has on the mechanism of the reaction.

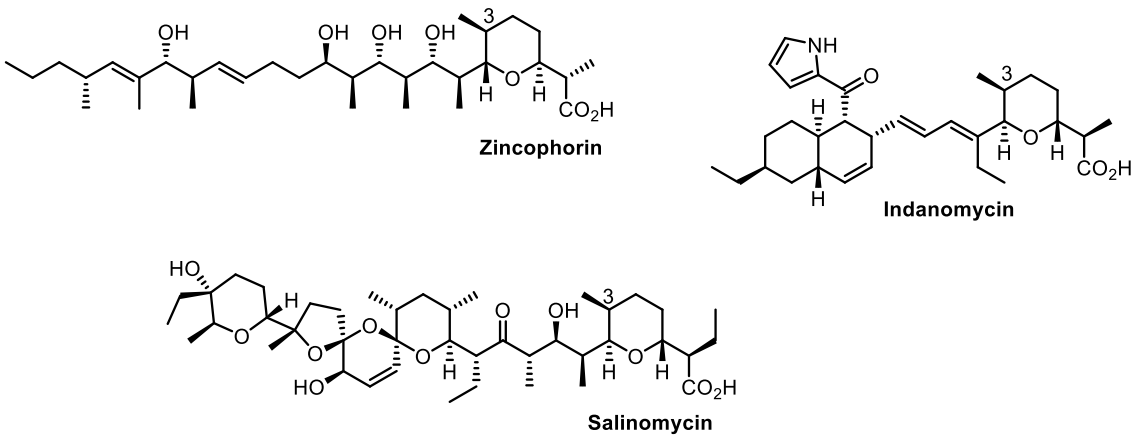

Figure 2.15 Natural products exhibiting the 2,6-*trans* pattern and bearing a stereocenter at carbon 3. [39,42,43]

The premise for this approach was based on previous results in the group on Re_2O_7-catalyzed cascade reactions and bimolecular coupling using a hydride source as a nucleophile. In this reaction, incorporation of a pre-existing stereocenter provided insight into the stereochemical pathway of the reaction. In particular, details into the relationship between the substrate structure, intramolecular trapping group, product substitution pattern, and external nucleophile were discovered. Xie determined that high stereocontrol can be achieved if the proper balance of equilibration rates and rates of oxocarbenium ion formation and trapping can be established.[30] For the cyclization precursor below**,** containing a stereocenter at position **3**, the following isomerization pathway was proposed using Et_3SiH as the hydride donor:

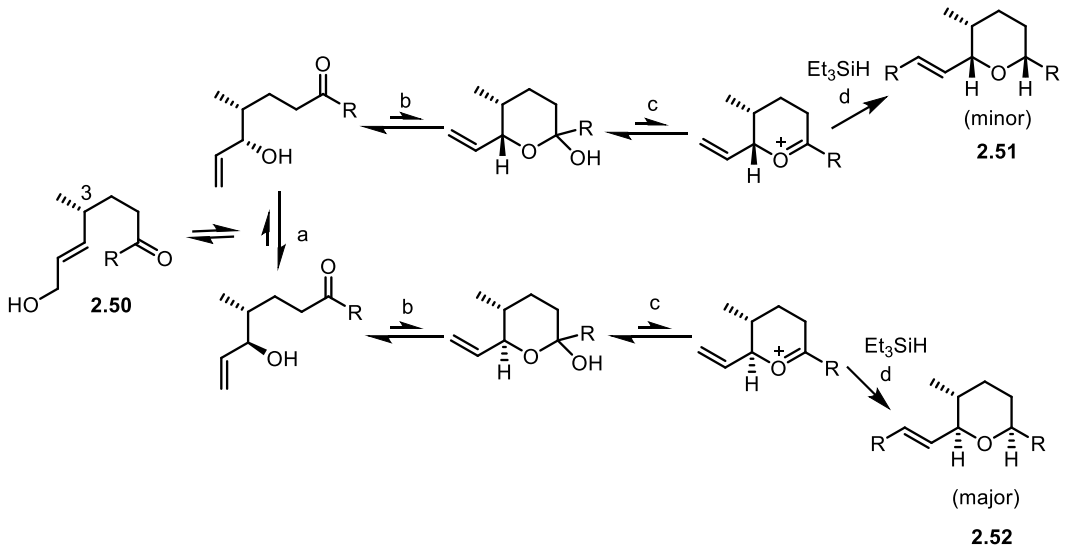

Scheme 2.34 Isomerization pathway for an enantiomerically pure allylic alcohol cyclization precursor as proposed by Xie. Pathway goes through transposition-isomerization-cyclization-ionization-termination steps.[30]

In the illustrated pathway, Xie proposed that greater stereocontrol is achieved if **a** is rapid, equilibrium **b** does not strongly favor the lactol, **c** is readily reversible, and **d** is slow. Greater stereocontrol is also achieved when the two equilibrating lactols have a large enough energy difference between their six membered chair-like structures for one to be thermodynamically favored. Of interest, for substrates **2.72** and **2.74** and Et_3SiH, it was observed that equilibration between the two acyclic allylic alcohol diastereomers through a cationic intermediate is strongly influenced by substitution at the allylic carbon. Secondary alcohol precursor **2.74** should equilibrate between the two acyclic precursors much more rapidly, leading to a higher degree of stereocontrol. As expected, **2.74** (2^o alcohol precursor), led to tetrahydropyran product **2.75** with a dr of 11:1 whereas primary alcohol precursor **2.72** led to tetrahydropyran product **2.73** with a dr of 3:1 (Scheme 2.35).

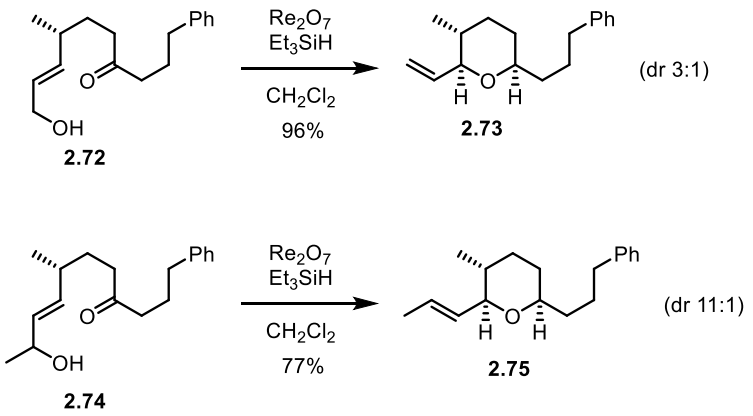

Scheme 2.35 Differences in stereocontrol with primary or secondary cyclization precursors when trapping with a hydride nucleophile as performed by Xie et al.[30]

We expected similar principles to apply when using carbon nucleophiles as the termination agents. Stabilization of the oxocarbenium ion intermediate by acetonitrile should also improve stereocontrol. To examine these principles, we prepared a substrate bearing a stereocenter in the 3 position, and a substrate containing a tertiary alcohol precursor. Substrate **2.82** bearing a stereocenter at position 3 was prepared in a convergent sequence from (+)-β-citronellene and 1-octanol (Scheme 2.36).

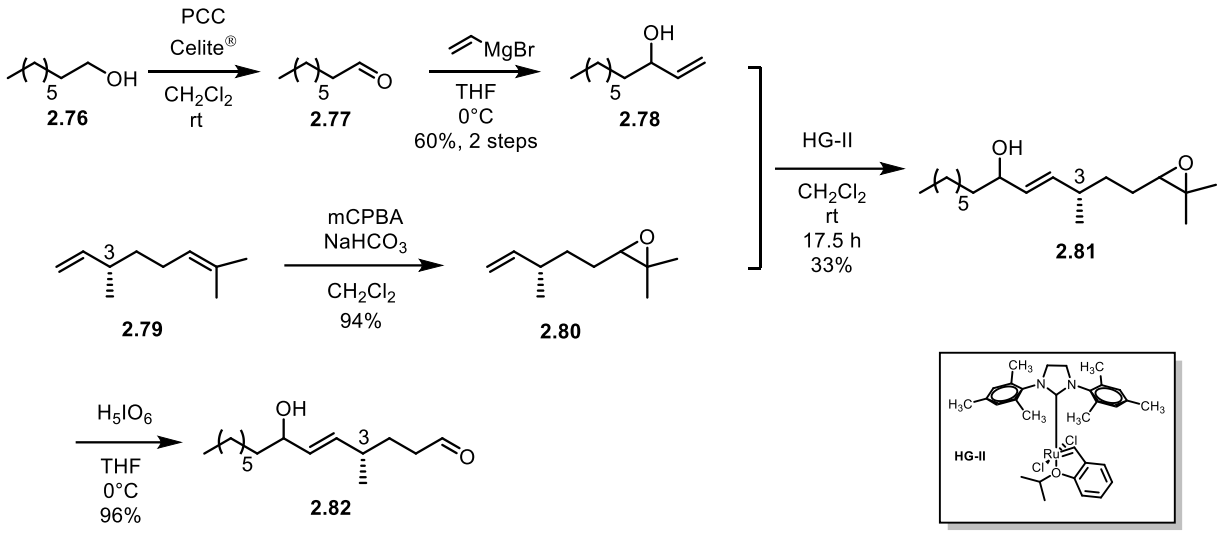

Scheme 2.36 Preparation of substrate **2.82**.

Oxidation of 1-octanol and addition of vinyl magnesium bromide provided allylic alcohol **2.78** and epoxidation of (+)-β-citronellene gave **2.80** which were coupled together via cross metathesis to give **2.81** in 33% yield. The epoxide was cleaved with periodic acid at 0°C, giving **2.82** in 96% yield. When substrate **2.82** was combined with Re_2O_7 and allyltrimethylsilane in acetonitrile at 0°C, tetrahydropyran product **2.83** was obtained in 73% yield as a 5:1 mixture of diastereomers. However, when the reaction was performed in 2:1 CH_2Cl_2/MeCN a decrease in stereocontrol was observed, with a dr of 3:1 and multiple side products observed via crude ^1H NMR analysis, indicating that acetonitrile provides improvements in diastereoselectivity and clean conversion. Stabilization of the oxocarbenium ion intermediate by acetonitrile provides more opportunity for stereochemical equilibration through the pathway depicted in Scheme 2.34, increasing the diastereoselectivity. Confirmation of the major diastereomer was achieved with NOESY analysis - allylic proton 2 showed a correlation with the protons on the methyl stereocenter

and with the allylic protons in the axial position (Scheme 2.37). The minor isomer is anticipated to be the other 2,6-*trans* diastereomer based on the predicted oxocarbenium ion intermediates. As expected, no signals that would indicate formation of the 2,6-*cis* isomer were observed in the NOESY spectrum.

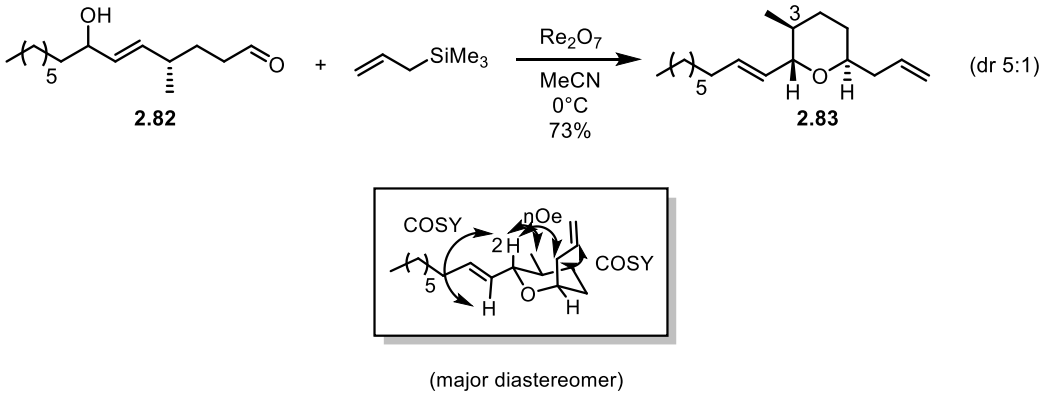

Scheme 2.37 Cyclization and stereochemical determination of tetrahydropyran cyclization product **2.69**.

Formation of diastereomer **2.83** as the major product is in agreement with the relative favorability of the two possible cyclic oxocarbenium ion intermediates generated. The preferred intermediate contains two equatorial substituents and termination proceeds via axial attack of allyltrimethylsilane from the top face of the intermediate avoiding the disfavored twist-boat conformer (Scheme 2.38). Stabilization of the oxocarbenium ion intermediates by acetonitrile promotes equilibration to the preferred intermediate, leading to better stereocontrol than seen in dichloromethane.

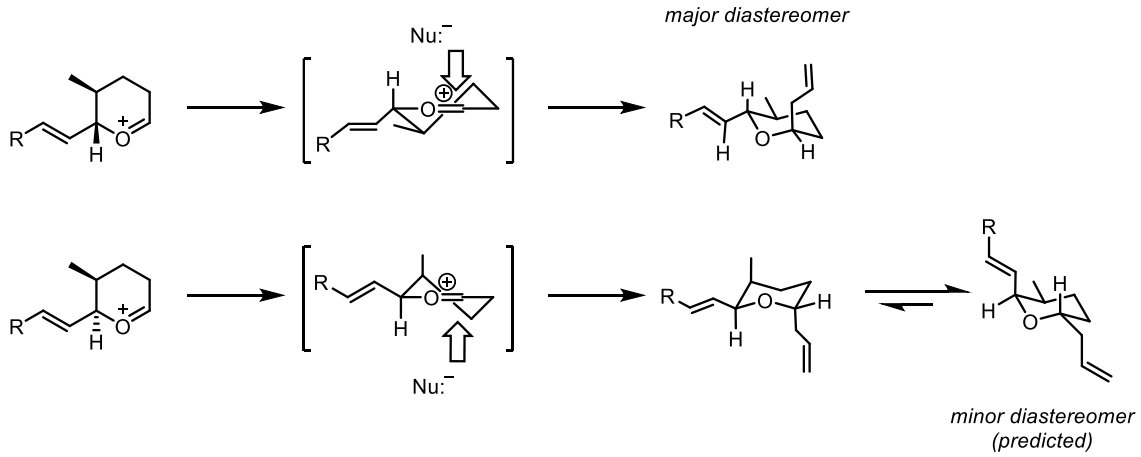

Scheme 2.38 Nucleophile trapping and stereochemical outcome for substrate **2.83**.

The successful outcome of this reaction illustrates that the use of acetonitrile can improve stereocontrol via stabilization of the oxocarbenium ion intermediate. Furthermore, preparation of a 2,6-*trans*-tetrahydropyran ring bearing a C_3 stereocenter is advantageous as this pattern is seen in many natural products, demonstrating our methods' applications to natural product synthesis.[34,39,40]

Preparation of a tertiary allylic alcohol allowed us to further examine the mechanistic details of this pathway. As mentioned previously, increased substitution at the allylic carbon should increase the rate of equilibration between the acyclic allylic alcohols and lead to a higher degree of stereocontrol (Scheme 2.34).[17,30] However, synthesis of this substrate was somewhat challenging due to the high reactivity of the allylic alcohol. Synthesis of substrate **2.91** was initially planned in six steps from (+)-β-citronellene (Scheme 2.39). However, removal of the acetal group under acidic conditions led to rapid cyclization and mixtures of side products, even when the reaction was performed at low temperatures.

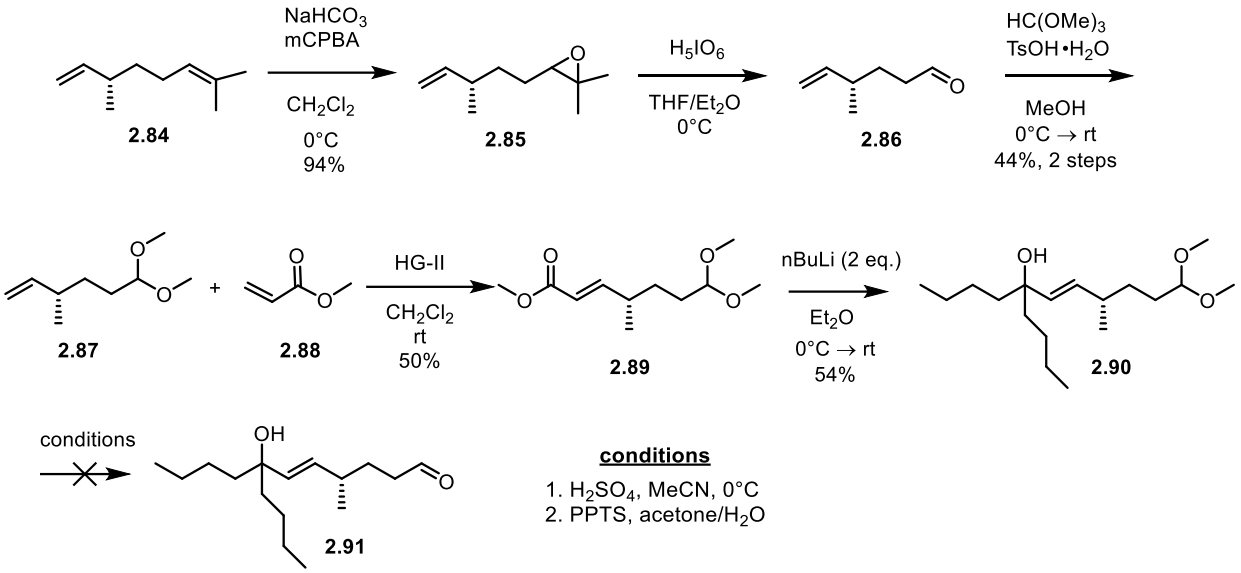

Scheme 2.39 Initial attempts at synthesizing **2.91**.

Similarly, we expected that a benzylic allylic alcohol precursor would improve the stereocontrol of the reaction; however, this substrate was also difficult to prepare due to its reactivity. Deprotection of the acetal under acidic conditions led to cyclization and methylation of the reactive benzylic allylic alcohol. Furthermore, presumably due to the reactivity of this substrate, even a selective oxidation of the primary alcohol in the presence of TEMPO and NCS provided none of the desired aldehyde precursor.

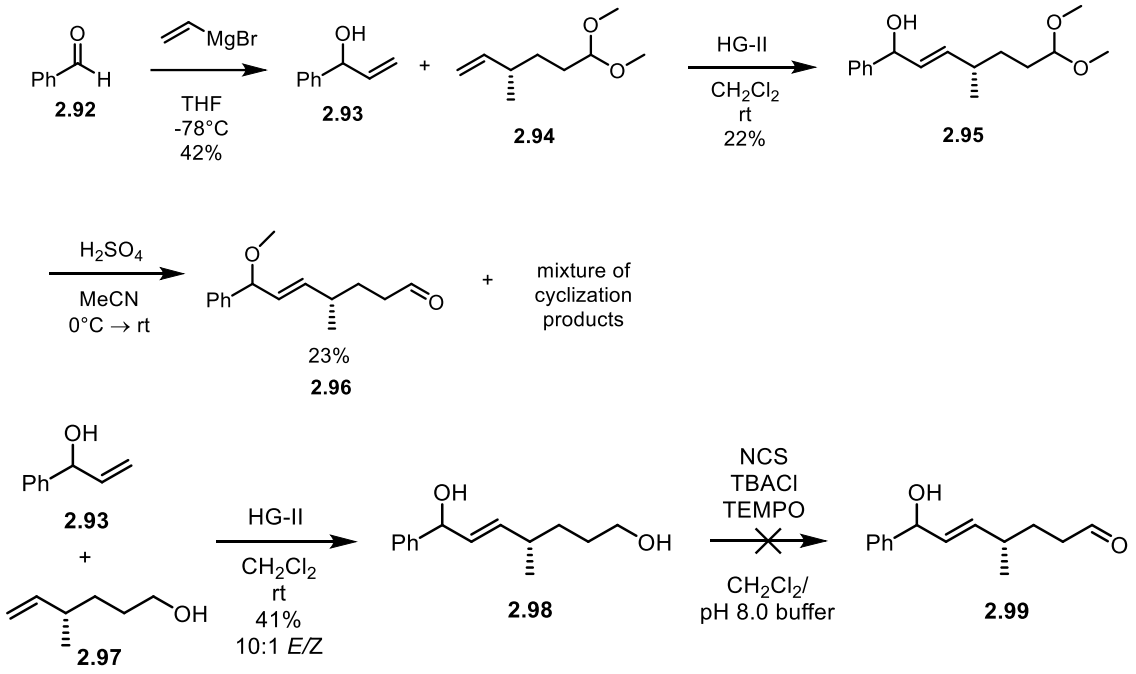

Scheme 2.40 Attempts at synthesizing **2.99**.

Fortunately, we were able to prepare the tertiary allylic alcohol precursor by avoiding acidic conditions in the last step. Preparing a primary alcohol precursor then oxidizing at the last step removed the need for acidic conditions to unmask the aldehyde, eliminating the risk of side reactions. Enantiomerically pure alcohol **3.3** was prepared in 3 steps from (+)-β-citronellene through selective epoxidation of the more electron rich alkene, cleavage with periodic acid, and sodium borohydride reduction. The low yield of 33% is due to the volatility of the aldehyde intermediate. **3.4** was prepared from alcohol **3.3** and methyl acrylate via cross metathesis in 51% yield as a 14:1 *E/Z* mixture. The primary alcohol was protected with TBSCl in 87% yield to avoid competitive oxa-michael addition in the subsequent step. The tertiary center was installed by addition of two equivalents of n-BuLi to provide **3.6** in 91% yield. TBAF deprotection provided diol **3.7** in 75% yield. Finally, Parikh-Doering oxidation at room temperature gave the desired

cyclization precursor in 55% yield, 5.1% yield in 8 steps overall (Scheme 2.41). Chromium based oxidation reagents were avoided for the oxidation step due to the propensity of tertiary allylic alcohols to rearrange in the presence of chromium (VI).[52]

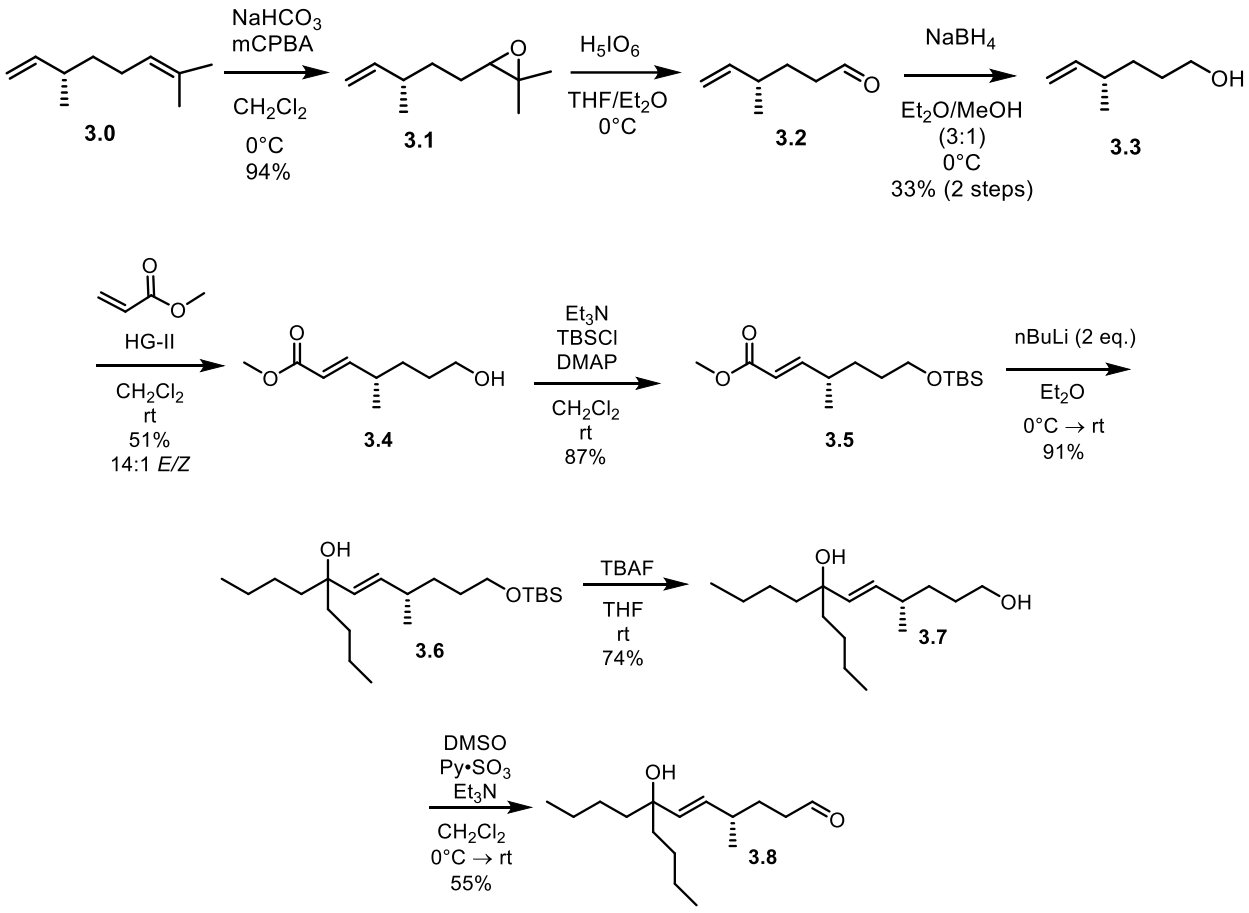

Scheme 2.41 Preparation of tertiary allylic alcohol substrate **2.92**.

Cyclization of substrate **3.8** gave interesting results. **3.8** was combined with Re_2O_7 (3 mol%, 10 mg/mL in Re_2O_7) in acetonitrile at 0°C to provide **3.9** and **3.10** in 69% yield as a 3:1 mixture. ^{1}H NMR and NOE analysis of the crude mixture indicated that, unexpectedly, the 2,6-

cis product was the major product. Upon separation of the two diastereomers, 44% of the 2,6-*cis* product and 20% of the 2,6-*trans* product was isolated. COSY and NOE analysis of the products confirmed the stereochemistry (Scheme 2.42).

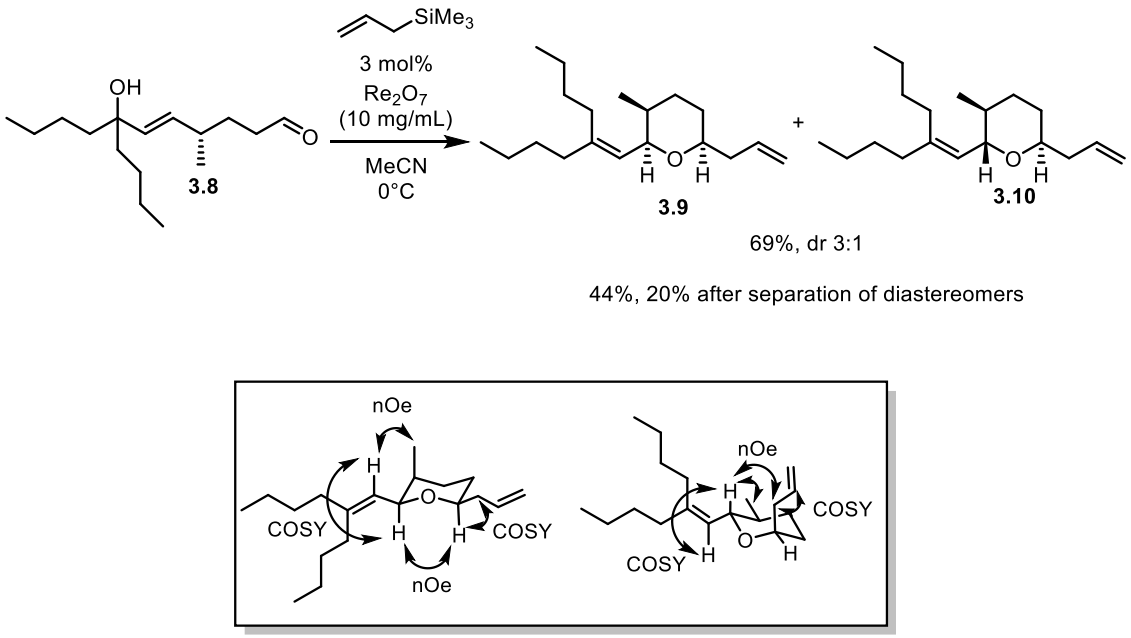

Scheme 2.42 Cyclization and stereochemical determination of **3.9** and **3.10**.

Similar to substrate **2.83** as described in Scheme 2.38, transition state analysis supports the formation of the 2,6-*trans* product observed with the COSY and NOESY spectrum. Out of the two possible oxocarbenium ions that could generate 2,6-*trans* products, **3.11** is more thermodynamically favored, with two equatorial substituents as opposed to one axial and one equatorial substituent as observed in **3.12**.

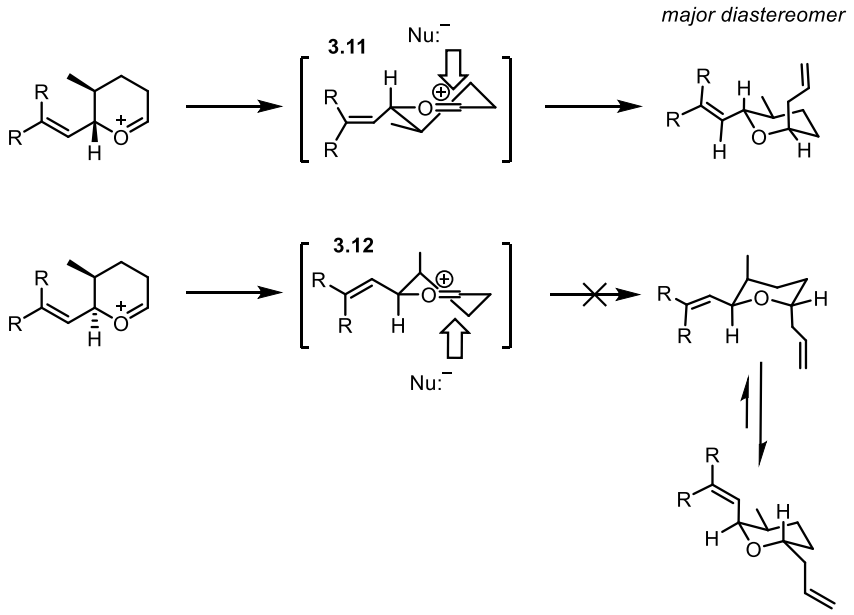

Scheme 2.43 Stereochemical rationale for formation of the major diastereomer.

The presence of the 2,6-*cis* product indicates that the increased substitution at the allylic carbon may cause the formed 2,6-*trans* product to equilibrate extremely rapidly via an allyl cation intermediate to the more thermodynamically favored *cis* product, almost as soon as termination with allyl silane has occurred (Scheme 2.44). The reaction proceeding through an allylation-dehydration-cyclization mechanism can be ruled out as this process does not occur in acetonitrile as discussed in Section 2.1.

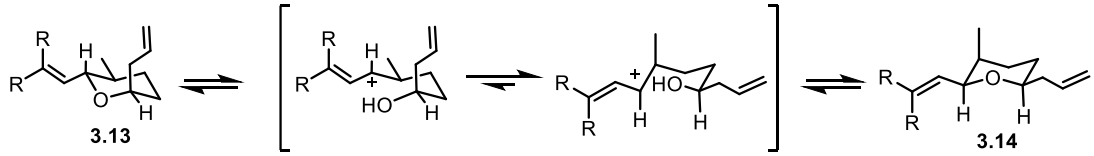

Scheme 2.44 Equilibration of **2.94** to **2.93** through a stabilized allyl cation intermediate.

Transition state analysis also further supports this pathway for formation of the 2,6-*cis* product as this diastereomer is unlikely to form from nucleophilic addition to the cyclic oxocarbenium ion due to 1,3-diaxial interactions between the allylic carbon and the approaching nucleophile. In addition, nucleophilic addition to these oxocarbenium ion intermediates is less favorable than the addition to oxocarbenium ion **3.11** in Scheme 2.45 due to the presence of one axial substituent in the oxocarbenium ion intermediate.

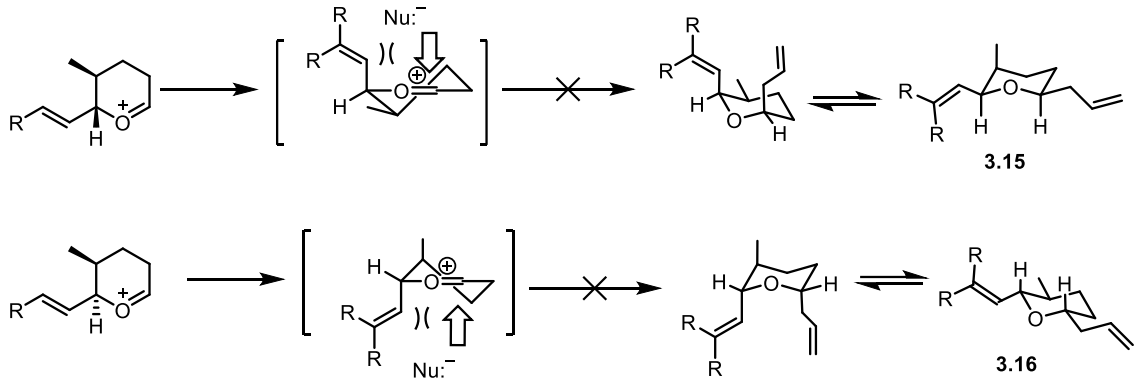

Scheme 2.45 1,3-diaxial steric interactions in formation of 2,6-*cis* products **3.15** and **3.16** through a cyclic oxocarbenium ion intermediate.

Although two isomers were obtained from this reaction, this result is in agreement with our predictions. The pre-installed stereocenter and increased substitution at the allylic carbon allowed the reaction to proceed with high levels of enantioselectivity – the 2,6-*trans* enantiomer depicted in Scheme 2.44 formed exclusively then underwent rapid equilibration to the 2,6-*cis* product. We can conclude that, in agreement with Xie's observations, the stereocontrol is due to the increased substitution at the allylic carbon and corresponding rate of equilibration of the acyclic substrates. Furthermore, analysis of the reaction mixture after only 30 seconds at 0°C shows a 3:1 mixture of the 2,6-*trans* isomer to the 2,6-*cis* isomer (Table 2.5). No further equilibration after 30 seconds

indicates that ~3:1 may be representative of the thermodynamic ratio of the diastereomers. Additional studies were performed using this substrate in hopes of obtaining one stereoisomer exclusively.

Table 2.5 Conditions screened for cyclization of tertiary allylic alcohol precursor.

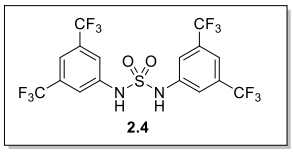

2.4

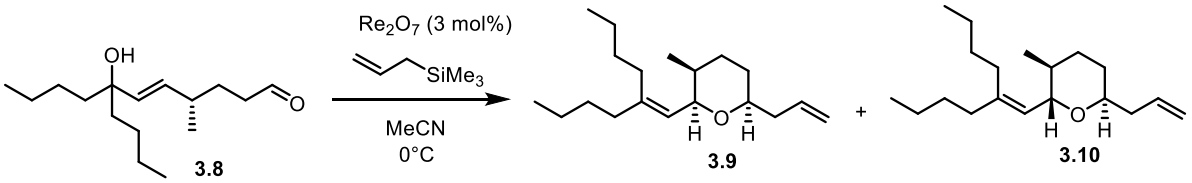

Entry	Conditions	% yield[a] (d.r.)[b]
1	MeCN, 30 min	44% **3.9**, 20% **3.10** (3:1)
2	MeCN, 30 seconds	3:1
3	MeCN, 24 h	complex mixture
4	HFIP, 30 min	complex mixture
5	**3.10** isolated, equilibrated in Re_2O_7/MeCN (rt, 24 h)	complex mixture
6	CH_2Cl_2/**2.4**, rt, 4 h	complex mixture

[a]isolated yield
[b]dr values determined by ^{1}H NMR analysis of the crude residue

Attempts were made to reduce the rate of the reaction and generate the 2,6-*trans* product exclusively by running the reaction in the less polar solvent, CH_2Cl_2. However, this modification led to the presence of multiple side products, suggesting that this pathway would not be a feasible route to stereocontrol for this substrate. Additionally, these results indicate that acetonitrile is necessary for clean conversion. We then attempted to obtain the thermodynamically favored 2,6-

cis product exclusively. In entry 3, the mixture was stirred at room temperature in acetonitrile for 24 h; however, the product degraded over time, giving a complex mixture. Presumably, at extended reaction times at room temperature, the ring opens to form the highly reactive and stabilized allyl cation which goes through many side reactions, generating a complex mixture of degradation products. When the reaction is performed in HFIP, the substrate degrades after only 30 minutes, generating a complex mixture (entry 4, Table 2.5). Additionally, when **3.10** is isolated and equilibrated in MeCN, degradation also occurs.

Intrigued by the equilibration observed in entry 1, we wondered if a different Re species, generated from the initial cyclization, could act as a catalyst for the equilibration, promoting conversion without degradation. Substrate **3.17** was first reacted with Re_2O_7 to form known tetrahydropyran **3.18**. After complete conversion was observed via TLC, 2,6-*cis* product **3.9** was added and the reaction mixture was stirred at 0°C for 4 h. Clean conversion to a 2.2:1 ratio of the *cis*/*trans* products was observed, indicating that the Re species generated from the standard reaction is enough to catalyze equilibration without resulting in degradation (Scheme 2.46). 2,6-*trans* product **3.18** did not equilibrate to its isomer, the thermodynamically favored 2,6-*cis* isomer, as the secondary allylic cation is presumably less stable than the tertiary allylic cation. This result also indicates that selectivity in equilibration can be achieved, as the tertiary allylic substrate isomerizes whereas the secondary allylic substrate does not.

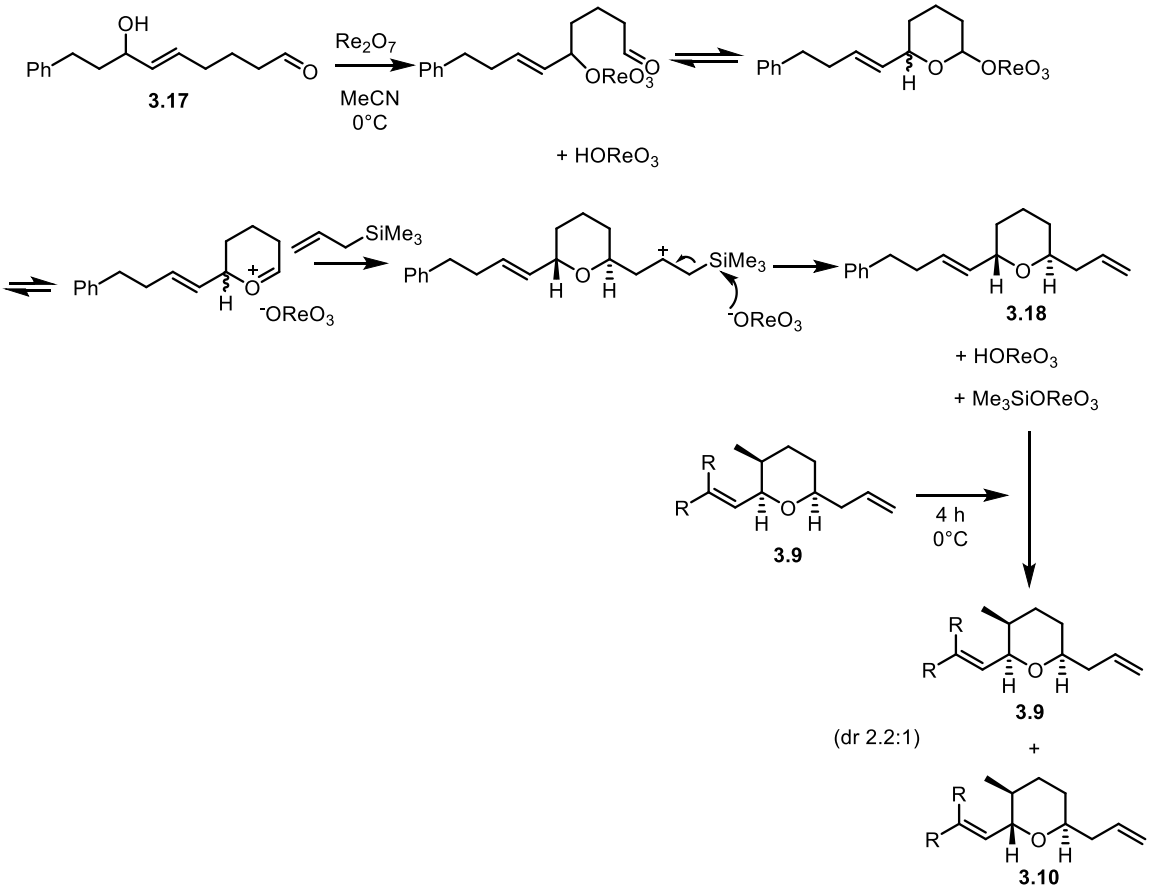

Scheme 2.46 Equilibration catalyzed by Re species generated from an initial transposition and cyclization and termination.

As $HOReO_3$ and $Me_3SiOReO_3$ are both generated from the standard Re_2O_7-catalyzed reaction (Scheme 2.34), it is expected that one of these byproducts is the catalyst that promotes the equilibration. This result illustrates that Re_2O_7 acts as a precatalyst in this transformation and that $HOReO_3$ or $Me_3SiOReO_3$ can catalyze the equilibrations through allylic cation intermediates effectively. This result has applications for future work – if an equilibration through an allylic cation intermediate is desired, $HOReO_3$ or $Me_3SiOReO_3$ could be used as mild catalysts for these transformations rather than Re_2O_7.

Analysis of the results of substrates bearing a stereocenter on the bimolecular fragment coupling reaction provides additional insight into the mechanistic details of these reaction. 2,6-

trans-tetrahydropyran rings containing a stereocenter at carbon 3 were able to be prepared in good yield in a diastereomeric mixture of 5:1 in acetonitrile vs. 3:1 in CH_2Cl_2. Increasing the substitution at the allylic carbon by synthesizing a tertiary alcohol substrate provides enantiocontrol to the reaction but increases the reactivity such that rapid equilibration to a thermodynamic ratio of products is observed after nucleophile trapping. Additionally, it was observed that initial generation of $HOReO_3$ or $Me_3SiOReO_3$ from the reaction can catalyze equilibration of 2,6-*cis* tetrahydropyran **3.9** without degradation to side products.

3.0 Conclusions

An approach to constructing molecules of high stereochemical complexity from simple, easily accessible precursors was developed. These substrates are created through a Re_2O_7-catalyzed allylic alcohol transposition, intramolecular trapping with a tethered electrophile to form a cyclic oxocarbenium ion intermediate, and a kinetically controlled bimolecular fragment coupling step. Through the experiments and analyses presented in this document we examine the stereocontrol, rate, mechanism, and effect of thermodynamic equilibration on the reaction. In our studies with allyltrimethylsilane and crotyl trimethylsilane, we discovered that nucleophilic addition into oxocarbenium ions is promoted by both the enhanced Lewis Acidity of Re_2O_7 by an anion-binding sulfonamide catalyst and the improved stabilization of the oxocarbenium ion intermediate by acetonitrile. The stabilization induced by acetonitrile enhances the overall rate of the reaction, providing many advantages to the kinetic bimolecular coupling reaction including faster reaction times, modest improvements in diastereoselectivity, promoted equilibration to thermodynamically favored products, and expansion of the scope to stereochemically complex products previously inaccessible with Re_2O_7. In broadening the scope of the reaction, tetrahydropyran rings containing a quaternary center were synthesized in excellent yield and complete stereocontrol. Substrates bearing a pre-existing stereocenter were also synthesized to expand the scope of heterocycles synthesized to motifs present in natural products and to further probe the mechanistic details of the reaction. Tetrahydropyran rings bearing a stereocenter in the 3 position were formed in a 5:1 diastereomeric ratio in acetonitrile. Increased substitution at the allylic carbon allowed the reaction to occur with enantioselectivity although it also promoted rapid equilibration to the thermodynamically favored 2,6-*cis* isomer, giving a 3:1 ratio of 2,6-*cis* to 2,6-

trans products. Separation of these products was accomplished to provide enantiomerically pure products bearing a stereocenter in the 3 position as is seen in a variety of natural products exhibiting the 2,6-*trans* pattern. Furthermore, the mechanism of these reactions was examined through an oxygen-18 labeling study. This analysis provided evidence for an alternative dehydration-addition pathway to the tetrahydropyran products, giving further insight into the mechanistic details of the reaction.

In this work, a kinetically controlled bimolecular fragment coupling reaction catalyzed by rhenium oxide was developed. A variety of stereochemically complex tetrahydropyran rings were synthesized using this method and the mechanistic details of the reaction were studied. The rate enhancing effects of acetonitrile in particular provided many opportunities for examining the scope, mechanistic details, and stereocontrol of the reaction

Appendix A : Supporting Information

General Experimentals

All commercially available reagents were used as received unless noted. All moisture sensitive reactions were performed using syringe-septum techniques under an atmosphere of dry N_2 or argon using flame-dried glassware. Deuterated chloroform ($CDCl_3$) was stored over 3 Å molecular sieves. Analytical TLC was performed on E. Merck pre-coated (25 mm) silica gel 60 F_{254} plates and visualized under UV (254 nm), or stained with p-anisaldehyde (95 mL ethanol, 3 mL conc. H_2SO_4, 2 mL acetic acid, 5 mL anisaldehyde, I_2 (silica gel and I_2), or $KMnO_4$ (1.5 g $KMnO_4$, 10 g K_2CO_3, and 1.25 mL of 10% NaOH in 200 mL of water). Reagent grade CH_2Cl_2 was distilled from CaH_2. Reagent grade tetrahydrofuran and diethyl ether were dried using an alumina column solvent drying system or distilled over Na/benzophenone. Reagent grade acetone, dichloromethane, diethyl ether, hexanes, pentane, and ethyl acetate were purchased from Fisher Scientific and used as-is for chromatography. Reagent grade or HPLC grade acetonitrile was dried over 3 Å molecular sieves and stored under an atmosphere of dry argon or distilled from CaH_2. Proton (^{1}H NMR) and carbon (^{13}C NMR) were recorded on a Bruker Avance 300, 400, 500, or 600 spectrometers at 300, 400, 500, 600 and 75, 100, 125, 150 MHz respectively. Chemical shifts are tabulated in parts per million (ppm) using the following solvent peaks as reference: ^{1}H NMR ($CDCl_3$) = 7.26 ppm, ^{13}C NMR ($CDCl_3$) = 77.16 ppm. Data is reported as follows (s = singlet; d = doublet, t = triplet, q = quartet, dd = doublet of doublets; ddd = doublet of doublet of doublets; dt = doublet of triplets; tt = triplet of triplets; m = multiplet and coupling constants (*J*) in Hertz (Hz)). Infrared spectra were collected on a Nicolet IR200 FT-IR spectrometer on NaCl plates. High and low resolution mass spectra were collected on one of the following: Q-Tof Ultima API, Micromass

UK Limited; Q-Exactive, Thermo Scientific.

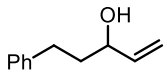

2.12

5-phenylpent-1-en-3-ol (2.12)[53]

To a solution of hydrocinnamaldehyde (5.00 g, 37.3 mmol) in THF (75 mL) was added vinylmagnesium bromide (56 mL, 1 M in THF) dropwise at -78 °C and the reaction was stirred for 30 minutes, allowed to warm to 0°C, and stirred for 1.5 h. The reaction mixture was quenched with 1N HCl (~10 mL), extracted with diethyl ether, washed with brine, dried ($MgSO_4$), and concentrated under reduced pressure to give the product as a yellow oil (6.04 g, 100%). Characterization data is consistent with literature values.

^{1}H NMR ($CDCl_3$, 400 MHz): δ = 7.35-7.22 (m, 5 H), 5.98-5.90 (m, 1 H), 5.28 (dt, 1 H, *J* = 1.6, 17.2 Hz), 5.18 (dt, 1 H, *J*= 10.4 Hz), 4.16 (q, 1 H, *J* = 6.0 Hz), 2.83-2.71 (m, 2 H), 2.33-2.29 (bs, 1 H), 1.93-1.87 (m, 2 H). ^{13}C ($CDCl_3$, 100 MHz): δ = 141.9, 141.0, 128.5 (2 C), 128.4 (2 C), 125.9, 115.0, 72.5, 38.5, 31.7.

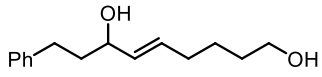

2.14

(*E*)-9-phenylnon-5-ene-1,7-diol (2.14)

To a solution of **2.13** (2.04 g, 20.3 mmol) and **2.12** (4.94 g, 30.5 mmol) in CH_2Cl_2 (78 mL) was added Hoyveda-Grubbs 2nd generation catalyst (0.074 g, 0.118 mmol) and the mixture was stirred under argon at room temperature for 18 h. The reaction mixture was concentrated under reduced pressure and purified by chromatography on SiO_2 (8-16% acetone/CH_2Cl_2) to give diol **2.14** as a brown oil (2.30 g, ~9:1 *E*/Z, 41%).

IR (ATR) 3382.6, 3026.5, 2934.6, 2859.7, 1776.0, 1705.2, 1495.9, 1454.3, 1429.7, 1350.9, 1292.2, 1182.4, 1055.6, 1030.6, 972.4, 918.0, 849.0, 817.8, 749.0, 700.0, 637.0 cm^{-1}. ^{1}H NMR ($CDCl_3$, 300 MHz) δ = 7.24-7.7.20 (m, 2 H), 7.14-7.10 (m, 3 H), 5.63-5.38 (m, 2 H), 4.37 (minor isomer, q, 0.11 H, *J* = 6.8 Hz), 4.00 (q, 1 H, *J* = 6.5 Hz), 3.55 (t, 2 H, *J* = 6.3 Hz), 2.66-2.58 (m, 2 H), 2.09 (bs, 2 H), 2.01 (q, 2 H, *J* = 7.1 Hz), 1.85-1.67 (m, 2 H), 1.56-1.46 (m, 2 H), 1.43-1.33 (m, 2 H). ^{13}C NMR ($CDCl_3$, 75 MHz): δ = 142.1, 133.2, 131.9, 128.51 (2 C), 128.42 (2 C), 125.85, 72.4, 62.6, 38.9, 32.1, 31.93, 31.86, 25.3. Minor diastereomer ^{13}C NMR: δ = 141.9, 133.9, 132.8, 132.1, 128.47 (2 C), 125.94, 71.6, 67.0, 39.1, 38.7, 31.78, 27.4, 25.9. HRMS [ESI^+] calcd for $C_{15}H_{22}O_2$ [M+H], 235.1693, found 235.1690.

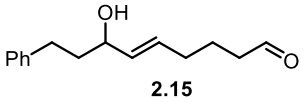

2.15

(*E*)-7-hydroxy-9-phenylnon-5-enal (2.15)[54]

To **2.14** (1.05 g, 4.48 mmol), TEMPO (0.070 g, 0.45 mmol), and TBACl (0.103 g, 0.450 mmol) in CH_2Cl_2 (90 mL) and pH 8.6 buffer (90 mL, 0.5 M $NaHCO_3$, 0.05 M K_2CO_3) was added N-chlorosuccinimide (1.08 g, 8.06 mmol) in one portion and the reaction mixture was stirred at room temperature for 20 h. The layers were separated, extracted with ethyl acetate, combined, dried ($MgSO_4$), and concentrated under reduced pressure to give the crude residue which was purified by chromatography on SiO_2 (3-9% acetone/CH_2Cl_2) to give **2.15** as an orange oil (0.643 g, ~8.1 *E*/*Z*, 62%).

IR (neat): 2920, 2862, 1978, 1952, 1719, 1453, 1275, 1261, 1029, 972, 749, 698. ^{1}H ($CDCl_3$, 500 MHz): δ = 9.80 (t, 1 H, *J* = 1.5 Hz), 7.32-7.20 (m, 5 H), 5.67-5.56 (m, 2 H), 4.11 (q, 1 H, *J* = 6.5 Hz), 2.75-2.69 (m, 2 H), 2.47 (td, 2 H, *J* = 1.5, 7.0 Hz), 2.12 (q, 2 H, *J* = 7.5 Hz), 1.91-1.82 (m, 2 H), 1.76 (q, 2 H, *J* = 7.0 Hz). ^{13}C ($CDCl_3$, 125 MHz), 202.4, 141.9, 134.1, 130.7,

128.44 (2 C), 128.40 (2 C), 72.2, 43.2, 38.8, 31.8, 31.5, 21.5. HRMS [ESI$^+$] calcd for $C_{15}H_{20}O_2$ [M+H], 232.1458, found 232.1398.

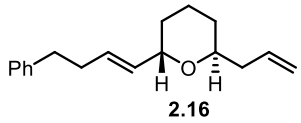

2.16

2,6-*trans*-2-allyl-6-((*E*)-4-phenylbut-1-en-1-yl)tetrahydro-2*H*-pyran (2.16)[*]

To a solution of (*E*)-7-hydroxy-9-phenylnon-5-enal (0.0500 g, 0.215 mmol) and allyltrimethylsilane (0.098 g, 0.860 mmol) in MeCN (6 mL) at 0 °C was added Re_2O_7 (0.003 g, 0.006 mmol) and the reaction was stirred for 30 minutes. The pale-yellow reaction mixture was directly filtered through a plug of SiO_2 (2"), rinsed through with CH_2Cl_2, and concentrated under reduced pressure to afford the product as a yellow oil (0.0431 g, 79%).

IR (neat) 2932.0, 2859.8, 221.6, 2032.7, 2018.3, 1977.3, 1453.6, 1031.2, 969.0, 910.7, 747.2, 697.8 cm^{-1}. ^{1}H ($CDCl_3$, 300 MHz): 7.22-7.08 (m, 5 H), 5.76-5.67 (m, 1 H), 5.65-5.44 (m, 2 H), 5.02-4.94 (m, 2 H), 4.22-4.29 (m, 1 H), 3.65-3.57 (m, 1 H), 2.66-2.60 (m, 2 H), 2.33-2.22 (m, 3 H), 2.11-2.06 (m, 1H), 1.59-1.51 (m, 1 H), 1.50-1.42 (m, 4 H), 1.24-1.18 (m, 1 H). ^{13}C ($CDCl_3$, 125 MHz) δ = 142.0, 135.4, 131.6, 131.1, 128.6 (2 C), 128.4 (2 C), 125.9, 116.6, 72.1, 70.7, 39.2, 35.8, 34.4, 30.1, 29.6, 18.7. HRMS [ESI$^+$] calcd for $C_{18}H_{24}O$ [M+H], 256.1827, found 256.1800.

[*] It is worth noting that for these transformations, some decrease in yield (~30%) occurs in months of high humidity (>60% humidity). Increasing the loading of Re_2O_7 to 20 mol%, extending reaction times to 3-5 h at room temperature, or using a pre-prepared 10 mg/mL solution of Re_2O_7 in acetonitrile appears to mitigate these humidity effects and are strategies that can be used to increase the yield during these months.

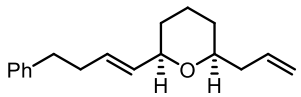

2.17

2,6-*cis*-2-allyl-6-((*E*)-4-phenylbut-1-en-1-yl)tetrahydro-2*H*-pyran (2.17)

To a solution of (*E*)-7-hydroxy-9-phenylnon-5-enal (0.040 g, 0.172 mmol) and allyltrimethylsilane (0.079 g, 0.689 mmol) in MeCN (6 mL) at 0°C was added Re_2O_7 (0.003 g, 0.006 mmol) and the reaction was allowed to warm to room temperature and stirred for 18.5 h. The dark pink reaction mixture was directly filtered through a plug of SiO_2 (2"), rinsed through with CH_2Cl_2, and concentrated under reduced pressure to afford a yellow oil. MeCN (6 mL) and fresh Re_2O_7 (0.003 g, 0.006 mmol) were added and the reaction mixture was stirred at room temperature for 20 h. The reaction mixture was directly filtered through a plug of SiO_2 (2"), rinsed through with CH_2Cl_2, and concentrated under reduced pressure to afford the product as a yellow oil (0.029 g, 68%).

IR (CH_2Cl_2): 3027.7, 2925.4, 2854.7, 1717.0, 1454.1, 1265.3, 1182.7, 1081.2, 700.4 cm^{-1}; ^1H ($CDCl_3$, 500 MHz) δ = 7.29-7.17 (m, 5 H), 5.89-5.73 (m, 1 H), 5.75-5.69 (m, 1 H), 5.56-5.52 (m, 1 H), 5.09-5.02 (m, 2 H), 3.79 (dd, 1 H, *J* = 6.0, 11.0 Hz), 3.41-3.36 (app dtd, 1 H *J* = 1.8, 6.5, 12.8 Hz), 2.70 (app t, 2 H, *J* = 7.7, 8.2 Hz), 2.39-2.32 (m, 3 H), 2.22-2.16 (m, 1 H), 1.86-1.82 (m, 1 H), 1.62-1.53 (m 2 H), 1.52-1.46 (m, 1 H), 1.33-1.26 (qd, 1 H, *J* = 4.3, 13.0 Hz), 1.22-1.14 (qd, 2 H, *J* = 3.8, 12.8 Hz). ^{13}C ($CDCl_3$, 125 MHz) δ = 142.1, 135.3, 132.1, 130.7, 128.6 (2 C), 128.4 (2 C), 125.9, 116.7, 78.4, 41.2, 35.7, 34.4, 31.9, 30.8, 29.9, 23.6. HRMS [ESI^+] calcd for $C_{18}H_{24}O$ [M+H], 256.1821, found 256.1764.

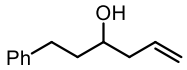

2.29

1-phenylhex-5-en-3-ol (2.29)[55]

To a solution of hydrocinnamaldehyde (0.030 g, 0.224 mmol) and allyltrimethylsilane (0.102 g, 0.894 mmol) in hexafluoroisopropanol (7.5 mL) at 0°C was added Re_2O_7 (0.003 g, 0.007 mmol) and the mixture was stirred for 15 minutes then allowed to warm to room temperature and stirred for 2 h. The mixture was quenched with pyridine (2 drops), concentrated under reduced pressure, and purified by chromatography on SiO_2 (0-3% acetone/CH_2Cl_2) to give the product as a clear oil (0.038 g, 97%). Characterization data is consistent with literature values.

^{1}H NMR ($CDCl_3$, 300 MHz) δ = 7.23-7.08 (m, 5 H), 5.81-5.67 (m, 1 H), 5.10-5.08 (m, 1 H), 5.04-5.03 (m, 1H), 3.60 (app quint, 1 H, J = 4.7, 7.3 Hz), 2.78-2.56 (m, 2 H), 2.29-2.21 (m, 1 H), 2.15-2.05 (m, 1 H), 1.75-1.67 (m, 2 H), 1.56 (bs, 1 H). ^{13}C NMR ($CDCl_3$, 75 MHz): δ = 142.2, 134.7, 128.6 (2 C), 128.5 (2 C), 126.0, 118.5, 70.1, 42.2, 38.6, 32.2.

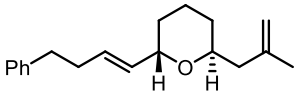

2.30

2,6-*trans*-2-(2-methylallyl)-6-(*E*-4-phenylbut-1-en-1-yl)tetrahydro-2*H*-pyran (2.30)

To a solution of (*E*)-7-hydroxy-9-phenylnon-5-enal (0.0522 g, 0.215 mmol) and methallyltrimethyl silane (0.110 g, 0.860 mmoml) in MeCN (6 mL) at 0°C was added Re_2O_7 (0.003 g, 0.006 mmol) and the reaction was stirred for 30 minutes. The pale-yellow reaction mixture was directly filtered through a plug of SiO_2 (2"), rinsed through with CH_2Cl_2, and concentrated under reduced pressure to afford the product as a yellow oil (0.041 g, 70%).

IR (CH_2Cl_2) 3038.2, 3042.1, 3027.09, 2033.7, 1717.7, 1603.3, 1496,0, 1453.7, 1376.6, 1256.4, 1195.4, 1056.1, 1041.4, 1030.4, 749.3, 700.5 cm^{-1}. ^1H NMR ($CDCl_3$, 300 MHz): δ = 7.29-7.17 (m, 5 H), 5.71-5.55 (m, 2 H), 4.75 (d, 2 H, *J* = 14.1 Hz), 4.29 (q, 1 H, *J* = 4.5 Hz), 3.85 (qd, 1 H, *J* = 3.3, 7.8 Hz), 2.71 (t, 2 H, *J* = 7.5 Hz), 2.41-2.29 (m, 3 H), 2.12 (dd, 1 H, *J* = 6.0, 13.8 Hz), 1.73 (s, 3 H), 1.67-1.53 (m, 5 H), 1.32-1.26 (m, 1H). ^{13}C ($CDCl_3$, 125 MHz) 143.1, 142.0, 131.7, 131.1, 128.6 (2 C), 128.4 (2 C), 125.9, 112.3, 72.0, 69.4, 43.0, 35.8, 34.5, 30.3, 29.7, 22.7, 18.8. HRMS [ESI^+] calcd for $C_{19}H_{27}O$ [M+H], 271.2056, found 271.2044.

tert-butyldimethyl(prop-1-en-2-yloxy)silane[56]

To a solution of triethylamine (4.37 mL, 31.3 mmol) in CH_2Cl_2 (7 mL) was added tert-butyldimethylsilyl trifluoromethanesulfonate (6.72 mL, 31.3 mmol) at 0 °C. Acetone (2.53 mL, 34.4 mmol) was added dropwise over 10 minutes and the solution was stirred at 0 °C for 1 h. The reaction mixture was poured into a mixture of hexanes and water (1:1, 10 mL). The hexanes layers were extracted, washed with brine, dried ($MgSO_4$), and concentrated under reduced pressure to give the crude residue. The pale-yellow liquid was decanted from the mixture, diluted with CH_2Cl_2, filtered through Celite ®, and concentrated under reduced pressure to give the product as a pale-yellow liquid (4.20 g, 71%). Characterization data is consistent with literature values.

^1H ($CDCl_3$, 300 MHz): 4.04 (s, 2 H), 1.77 (s, 3 H), 0.93 (s, 9 H), 0.16 (s, 6 H). ^{13}C ($CDCl_3$, 125 MHz) δ = 156.4, 91.4, 25.8 (3 C), 22.9, 18.2, -4.5 (2 C).

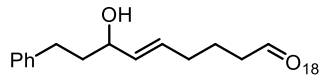

2.37

^{18}O labeled (*E*)-7-hydroxy-9-phenylnon-5-enal (2.37)[48]

A solution of 0.001 N acidic THF was prepared as follows:

0.5 mL of concentrated hydrochloric acid was added slowly to 55 mL of anhydrous THF and stirred at room temperature for 5 minutes. 2.5 mL of this solution was then added slowly to 247.5 mL of anhydrous THF and stirred at room temperature for 5 minutes.

To a solution of **2.15** in acidic THF (0.001 N HCl in THF) was added $H_2{}^{18}O$ (97%, 10 µL) and the reaction mixture was stirred at room temperature for 23 h. Anhydrous Na_2CO_3 (0.001 g) was added, the mixture was diluted with diethyl ether, and the layers were separated. The organic layer was dried ($MgSO_4$) and concentrated under reduced pressure to give the product as a yellow oil as a 1.6:1 C=^{18}O/C=O mixture of isotopomers as observed by infrared spectroscopy (0.075 g, 74%). NMR data is consistent with that of **2.15**.

IR (ATR) 3405.8, 3084.5, 3061.4, 3025.9, 2930.2, 2860.3, 2719.3, 2360.0, 1948.8, 1719.6 (C=O stretch), 1687.32 (C=O^{18}) stretch, 1602.8, 1495.7, 1454.1, 1408.3, 1385.2, 1179.0, 1097.4, 1057.0, 1030.2, 972.7, 916.2, 821.1, 748.2, 700.2, 668.4 cm^{-1}

Infrared Spectroscopy Data

Spectrum:	2-198	
Region	4000	600
Absolute Threshold	96.189	
Sensitivity	58	

Peak list	Position	668.4	Intensity	87.296	
	Position	700.22	Intensity	65.006	
	Position	748.24	Intensity	76.648	
	Position	821.14	Intensity	91.542	
	Position	916.19	Intensity	87.238	
	Position	972.70	Intensity	67.974	
	Position	1030.20	Intensity	75.702	
	Position	1056.98	Intensity	76.991	
	Position	1097.44	Intensity	81.325	
	Position	1179.00	Intensity	89.353	
	Position	1385.15	Intensity	85.527	
	Position	1408.34	Intensity	85.251	
	Position	1454.14	Intensity	73.355	
	Position	1495.65	Intensity	82.390	
	Position	1602.80	Intensity	89.451	
	Position	**1687.32**	**Intensity**	**71.101**	**C=^{18}O**
	Position	**1719.63**	**Intensity**	**80.738**	**C=O**
	Position	1948.79	Intensity	96.164	
	Position	2340.79	Intensity	93.579	
	Position	2360.03	Intensity	92.109	
	Position	2719.34	Intensity	92.689	
	Position	2860.28	Intensity	80.057	
	Position	2930.19	Intensity	70.696	
	Position	3025.90	Intensity	85.259	
	Position	3061.36	Intensity	91.032	
	Position	3084.46	Intensity	92.753	
	Position	3405.75	Intensity	79.093	

A = absorbance

T = transmittance

$A = 2\text{-}\log_{10}\%T$

$A_{C=O} = 2\text{-}\log_{10}(80.738) = 0.093$

$A_{C=O18} = 2\text{-}\log_{10}(71.101) = 0.148$ 0.148:0.093 = 1.6:1 C=^{18}O: C=O

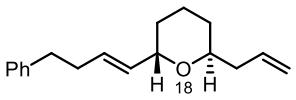

^{18}O labeled 2,6-*trans*-2-allyl-6-((*E*)-4-phenylbut-1-en-1-yl)tetrahydro-2*H*-pyran (2.40)

To **2.37** (0.010 g, 0.043 mmol) and allyltrimethylsilane (0.020 g, 0.172 mmol) in MeCN (1.4 mL) at 0°C was added Re_2O_7 (10 mg/mL in MeCN, 60 µL, 0.002 mmol) and the reaction mixture was allowed to warm to room temperature and stirred for 30 minutes. The mixture was quenched with pyridine (1 drop) and concentrated under reduced pressure to give the crude residue which was purified by chromatography on SiO_2 (CH_2Cl_2) to give the product as a yellow oil (0.009 g, 82%) as a 3.4:1 $^{16}O/^{18}O$ mixture of isotopomers as observed by HRMS. NMR data is consistent with that of **2.16**. ^{16}O product: HRMS [ESI$^+$] calcd for $C_{18}H_{25}O$ [M+H], 257.1900, found 257.1904 ^{18}O product: HRMS [ESI$^+$] calcd for $C_{18}H_{25}{}^{18}O$ [M+H], 259.1942, found 259.1949

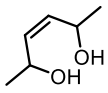

2.42

(*Z*) – Hex-3-ene-2,5-diol (2.42)[57]

To a solution of hex-3-yne-2,5-diol **(**10.0 g, 87.6 mmol) in ethyl acetate (450 mL) was added Lindlar's catalyst (0.093 g, 0.88 mmol) and quinoline (0.509 g, 3.94 mmol) and the mixture was stirred under H_2 for 4 h. The mixture was filtered through a plug of Celite®, concentrated under reduced pressure, and purified by chromatography on SiO_2 (0-40% acetone/CH_2Cl_2) to afford the product as a pale-yellow oil that solidified upon storage at -20°C (8.38 g, 82%). Characterization data is consistent with literature values.

^{1}H NMR ($CDCl_3$, 500 MHz): δ = 5.46-5.44 (m, 2 H), 4.65 (quint, 2 H, J = 6.0 Hz), 3.00-2.86 (bs, 2 H), 1.28 (d, 3 H, J = 6.0 Hz), 1.23 (d, 3 H, J = 6.5 Hz). ^{13}C NMR ($CDCl_3$, 125 MHz): δ = 134.8, 134.6, 64.5, 63.5, 24.0, 23.5.

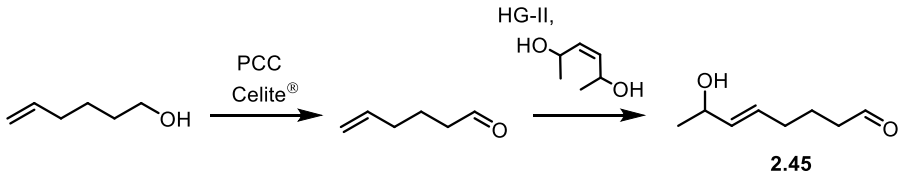

2.45

(*E*) – 7-hydroxyoct-5-enal (2.45)[30]

To a solution of hex-5-en-1-ol (2.00 g, 20.0 mmol) in CH_2Cl_2 (65 mL) was added pyridinium chlorochromate (6.47 g, 30.0 mmol) and Celite® (6.47 g) and the reaction mixture was stirred at room temperature for 6 h. The mixture was loaded directly onto a column of dry silica gel, rinsed through with CH_2Cl_2, concentrated to a volume of ~50 mL, and carried immediately onto the next step without further purification.

The crude aldehyde was diluted with CH_2Cl_2 (70 mL) and (*Z*)–hex-3-ene-2,5-diol (2.83 g, 24.5 mmol) and Hoveyda-Grubbs 2nd generation catalyst (0.020 g, 0.030 mmol) were added and the reaction was stirred for 13 h at room temperature. The solvent was removed under reduced pressure and the crude residue was purified by chromatography on SiO_2 (20-50% ethyl acetate/hexanes) to afford the product as a brown oil (1.28 g, 10:1 *E/Z*, 43% over two steps).

^{1}H NMR ($CDCl_3$, 400 MHz): δ = 9.75 (t, 1 H, J = 1.6 Hz), 5.62-5.49 (m, 2 H), 4.62-4.55 (m, *Z* isomer, 0.1 H), 4.25 (quint, 1 H, J = 6.0 Hz), 2.43 (td, 2 H, J = 1.6, 7.2 Hz), 2.06 (q, 2 H, J = 6.4 Hz), 1.71 (quint, 2 H, J = 7.2 Hz), 1.24 (d, 3 H, J = 6.4 Hz). ^{13}C NMR ($CDCl_3$, 125 MHz): δ = 202.7, 135.5, 129.5, 68.8, 43.3, 31.5, 23.5, 21.6.

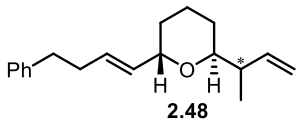

2.48

2,6-*trans*-2-(but-3-en-2-yl)-6-((*E*)-4-phenylbut-1-en-1-yl)tetrahydro-2*H*-pyran (2.48)

To a solution of (*E*)-7-hydroxy-9-phenylnon-5-enal (0.0171 g, 0.064 mmol) and crotyl trimethylsilane (13:1 *E/Z* , 0.033 g, 0.256 mmol) in MeCN (4 mL) at 0 °C was added Re_2O_7 (0.002 g, 0.004 mmol) and the reaction was stirred for 60 minutes. The yellow reaction mixture was quenched with pyridine (~2 drops) and concentrated under reduced pressure to give the crude residue which was purified by chromatography on SiO_2 (0-10% ethyl acetate/hexanes) to give the product as a yellow oil as a 2.6:1 mixture of diastereomers (0.014 g, 70%).

IR (CH_2Cl_2) 3053.8, 2930.6, 2359.8, 2306.1, 1454.4, 1421.8, 1265.3, 739.3, 704.4 cm^{-1}. ^1H ($CDCl_3$, 500 MHz):): δ = 7.36-7.24 (m, 5 H), 5.93-5.86 (m, 1 H), 5.77-5.67 (m, 2 H), 5.62-5.58 (m, 1 H), 4.41-4.40 (m, 1 H), 4.34-4.32 (m, 0.39 H, minor isomer), 3.50-3.46 (m, 1 H), 3.44-3.42 (m, 0.44 H, minor isomer), 2.81-2.75 (m, 2H), 2.48-2.43 (2 H), 2.38 (app sextet, 1 H, *J* = 7.1, 7.6 Hz), 1.80-1.73 (m, 1 H), 1.66-1.57 (m, 4H), 1.48-1.39 (m, 1 H), 1.10 (d, 1.2 H, *J* = 6.7 Hz, minor isomer), 1.04 (d, 3 H, *J* = 6.8 Hz). ^{13}C ($CDCl_3$, 125 MHz) δ = 142.0, 141.8, 141.5 (minor isomer), 131.6, 131.5 (minor isomer), 131.4 (minor isomer), 131.14, 128.6 (2 C), 128.4 (2 C), 125.9, 114.5 (minor isomer), 114.0, 74.6 (minor isomer), 74.4, 72.3, 72.0 (minor isomer), 41.6, 41.3 (minor isomer), 35.8, 34.4, 29.7 (minor isomer), 29.3, 28.0, 27.9 (minor isomer), 18.9, 18.8 (minor isomer), 16.5 (minor isomer), 16.4. HRMS [ESI^+] calcd for $C_{19}H_{27}O$ [M+H], 271.2062, found 271.2057.

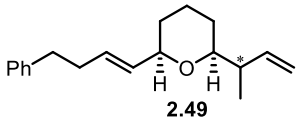

2.49

2,6-*cis*-2-(but-3-en-2-yl)-6-((*E*)-4-phenylbut-1-en-1-yl)tetrahydro-2*H*-pyran (2.49)

To a solution of (*E*)-7-hydroxy-9-phenylnon-5-enal (0.020 g, 0.086 mmol) and crotyl trimethylsilane (13:1 *E/Z* , 0.044 g, 0.344 mmol) in HFIP (3 mL) at 0 °C was added Re_2O_7 (0.001 g, 0.004 mmol) and the reaction was stirred for 2 h.. The reaction mixture was quenched with pyridine (~2 drops) and concentrated under reduced pressure to give the crude residue which was purified by chromatography on SiO_2 (0-10% diethyl ether/pentane) to give the product as a yellow oil as a mixture of 1:1 *trans*/*cis* isomers (*trans* dr 1.3:1, *cis* dr 1.9:1) (0.0133 g, 57%). To achieve equilibration and isolate the *cis* product exclusively the mixture was diluted with acetonitrile (0.3 mL), cooled to 0°C, and Re_2O_7 (0.001 g, 0.004 mmol) was added. The mixture was allowed to warm to rt and stirred for 23 h. The mixture was filtered through a pipette plug of SiO_2 (2") and concentrated under reduced pressure to give the 2,6-*cis* product (0.0121 g, 91%, dr 1.6:1).

IR (ATR): 3072.3, 3029.1, 2931.1, 2854.3, 1639.9, 1451.9, 1372.8, 1201.2, 1077.6, 1040.3, 968.1, 911.9, 832.5, 745.5, 698.5 cm^{-1}.^{1}H NMR ($CDCl_3$, 500 MHz): δ = 7.29-7.27 (m, 2 H), 7.19-7.17 (m, 3 H), 5.88 (ddd, 0.6 H, *J* = 7.3, 10.5, 17.8 Hz, major diastereomer), 5.78 (ddd, 0.4 H, *J* = 7.8, 10.4, 17.6 Hz, minor diastereomer), 5.74-5.67 (m, 1 H), 5.56-5.50 (m, 1 H), 3.76 (app dd, 1 H, *J* = 5.7, 11.2 Hz), 3.23 (ddd, 0.6 H, *J* = 1.7, 5.4, 11.3 Hz, major diastereomer), 3.12 (ddd, 0.4 H, 1.7, 7.1, 11.0 Hz, minor diastereomer), 2.69 (app t, 2 H, *J* = 7.6, 8.3 Hz), 2.36-2.30 (m, 2 H), 1.86-1.83 (m, 1 H), 1.60-1.59 (m, 2 H), 1.52-1.45 (2 H), 1.29-1.20 (m, 2 H), 1.16-1.13 (m, 0.4 H, minor diastereomer), 1.06 (d, 1 H, *J* = 6.8 Hz, minor diastereomer), 1.03 (d, 2 H, *J* = 6.9 Hz, major diastereomer). ^{13}C NMR ($CDCl_3$, 125 MHz): δ = 141.6, 141.3, 132.32, 130.01, 128.6 (2 C), 128.4 (2 C), 125.9, 114.0, 81.25, 78.31, 42.9, 35.8, 34.4, 32.1, 27.6, 23.8, 15.5.

^{13}C minor diastereomer (CDCl3, 125 MHz): 142.2, 132.28, 130.09, 114.4, 81.26, 78.27, 43.71, 32.0, 28.6, 16.4

HRMS [ESI+] calcd for $C_{19}H_{27}O$ [M+H], 271.2056, found 271.2060.

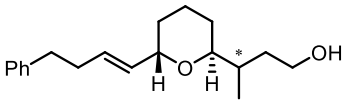

2.56

2,6-*trans*-(*E*)-3-(6-(4-phenylbut-1-en-1-yl)tetrahydro-2*H*-pyran-2-yl)-3-butan-1-ol (2.56)

To a solution of **2.48** (dr 2.6:1, 0.100 g, 0.368 mmol) in THF (0.5 mL) was added 9-BBN dimer (0.5 M in THF, 3.4 mL) and the reaction mixture was stirred at room temperature for 1 h. The reaction mixture was cooled to 0°C, and aqueous NaOH (3.0 M, 0.36 mL) and 30% H_2O_2 (0.36 mL) was added and the reaction was allowed to warm to room temperature and stirred for 80 minutes. The mixture was extracted with CH_2Cl_2, washed with brine, dried ($MgSO_4$), and concentrated under reduced pressure to give the crude residue as a yellow oil which was purified by chromatography on SiO_2 (0-5% acetone/CH_2Cl_2) to give the product as a clear oil (dr 2.6:1, 0.064 g, 59%).

IR (CH_2Cl_2): 3421.4, 2922.2, 2853.4, 1455.6, 1413.0, 1328.8, 1295.3, 1209.0, 1165.9, 1035.2, 973.7, 750.5, 699.3 cm^{-1}. ^{1}H NMR ($CDCl_3$, 400 MHz) δ = 7.29-7.27 (m, 2 H), 7.19-7.17 (m, 3 H), 5.69-5.53 (m, 1 H), 4.39-4.38 (m, 0.3 H, minor diastereomer), 4.37-4.36 (m, 1 H), 3.73-3.69 (m, 1 H), 3.58-3.57 (m, 1 H), 3.46-3.42 (m, 0.3 H, minor diastereomer), 3.32-3.27 (m, 1 H), 2.84 (bs, 1 H), 2.75-2.69 (m, 2 H), 2.42-2.36 (m, 2 H), 1.78-1.66 (m, 4 H), 1.60-1.54 (m, 7 H), 1.46-1.33 (m, 2 H), 0.90 (d, 1 H, minor diastereomer, J = 6.9 Hz), 0.87 (d, 3 H, J = 6.8 Hz). ^{13}C NMR ($CDCl_3$, 125 MHz): δ = 141.9, 132.1, 130.6, 128.7 (2 C), 128.4 (2 C), 125.9, 75.1, 72.7, 61.1, 37.1, 35.76, 35.1, 34.4, 29.1, 28.7, 18.9, 17.0. ^{13}C NMR minor diastereomer: 130.5, 74.1,

73.0, 61.4, 36.0, 35.79, 34.4, 29.8, 28.9, 26.8, 19.0, 16.0. HRMS [ESI$^+$] calcd for $C_{19}H_{29}O_2$ [M+H], 289.2162, found 289.2169.

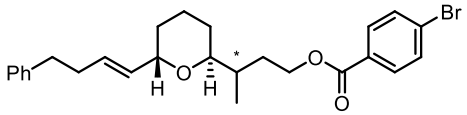

2.57

2,6-*trans*-(*E*)-3-(6-(4-phenylbut-1-en-1-yl)tetrahydro-2*H*-pyran-2-yl)butyl 4-bromobenzoate (2.57)

To a solution of **2.56** (0.030 g, 0.106 mmol) in THF (1.5 mL) at 0°C was added NaHMDS (1.0 M in THF, 0.21 mL) dropwise and the reaction mixture was stirred for 30 minutes. 4-bromobenzoyl chloride (0.046 g, 0.21 mmol) in THF (0.6 mL) was added dropwise and the reaction mixture was stirred for 2 h at 0°C. The reaction mixture was concentrated under reduced pressure and purified by chromatography on SiO_2 (0-5% ethyl acetate/hexanes) to give the product as a white solid (dr 2.6:1, 0.0298 g, 61%).

IR (CH_2Cl_2): 2931.6, 1719.2, 1590.9, 1453.2, 1398.4, 1272.4, 1173.5, 1103.3, 1069.1, 1012.2, 848.9, 757.4 cm^{-1}. ^{1}H NMR ($CDCl_3$, 500 MHz) δ =7.90 (d, 2 H, J = 8.5 Hz), 7.57 (d, 2 H, J = 8.5 Hz), 7.28-7.25 (m, 2 H), 7.18-7.16 (m, 3 H), 5.66-5.53 (m, 2 H), 4.42-4.34 (m, 2 H), 4.31 (bs, 1 H), 3.41-3.38 (m, 0.4 H, minor diastereomer), 3.33 (app t, 1 H, J = 7.4, 7.3 Hz), 2.72-2.68 (m, 2 H), 2.40-2.37 (m, 2 H), 2.12-2.05 (m, 1 H), 1.94-1.87 (m, 0.4 H, minor diastereomer), 1.78-1.68 (m, 2 H), 1.58-1.47 (5 H, 1.38-1.35 (m, 1 H), 0.97 (d, 1 H, J = 6.8 Hz, minor diastereomer), 0.92 (d, 3 H, J = 6.8 Hz). ^{13}C NMR ($CDCl_3$, 125 MHz): δ = 166.1, 141.9, 131.8 (2 C), 131.7, 131.2 (2 C), 131.1, 129.7, 128.6 (2 C), 128.4 (2 C), 128.0, 125.9, 74.7, 72.3, 64.3, 35.8, 34.4, 33.9, 31.8, 29.4, 27.8, 18.9, 15.9. ^{13}C NMR minor diastereomer: 73.8, 72.5, 64.1, 34.2, 29.9, 29.2, 19.1, 15.1.

HRMS [ESI$^+$] calcd for $C_{26}H_{32}O_3Br$ [M+H], 471.1529, found 471.1525. mp 141-147 °C (dec.)

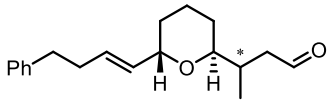

2.58

2,6-*trans*-(*E*)-3-(6-(4-phenylbut-1-en-1-yl)tetrahydro-2*H*-pyran-2-yl)butanal (2.58)

To a solution of **2.56** (0.064 g, 0.22 mmol) in CH_2Cl_2 (1 mL) was added pyridinium chlorochromate (0.067 g, 0.31 mmol) and Celite ® (0.067 g) and the reaction was stirred for 4.5 h under argon at room temperature. The reaction mixture was filtered through SiO_2, rinsed through with CH_2Cl_2, then 1% acetone/CH_2Cl_2, and concentrated under reduced pressure to give the product as a clear oil (0.049 g, 77%). IR (CH_2Cl_2): 2920.7, 2852.4, 1710.0, 1458.8, 1377.7, 1267.7, 1201.2, 1087.4, 1036.6, 969.8, 751.8, 703.0 cm^{-1}. ^{1}H NMR ($CDCl_3$, 400 MHz) δ =9.74-9.72 (m, 1 H), 7.29-7.26 (m, 2 H), 7.19-7.17 (m, 3 H), 5.63-5.44 (m, 2 H), 4.35 (bs, 0.3 H, minor diastereomer), 4.283-4.276 (m, 1 H), 3.40 (ddd, 0.3 H, minor diastereomer, J = 2.7, 4.2, 10.3 Hz), 3.23-3.18 (m, 1 H), 2.74-2.69 (m, 2 H), 2.58-1.53 (m, 1 H), 2.41-2.35 (m, 3 H), 2.21-2.12 (m, 2 H) 1.70-1.58 (m, 4 H), 1.33-1.25 (m, 1 H), 0.94 (d 1 H, minor diastereomer, J = 6.6 Hz), 0.89 (d, 3 H, J = 6.6 Hz). ^{13}C NMR ($CDCl_3$, 100 MHz): δ = 203.0, 141.9, 131.8, 130.9, 130.8, 128.7 (2 C), 128.4 (2 C), 125.9, 74.6, 72.3, 48.4, 35.8, 34.3, 33.0, 29.0, 28.5, 27.3, 18.7, 16.9. ^{13}C NMR minor diastereomer: 131.9, 130.8, 73.1, 72.6, 47.5, 32.4, 28.9, 27.3, 18.9, 15.6. HRMS [ESI$^+$] calcd for $C_{19}H_{27}O_2$ [M+H], 287.2006, found 287.2014.

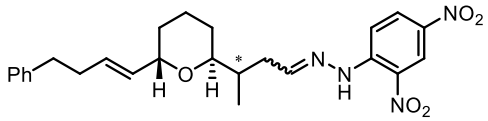

2.59

2,6-*trans*-((*E*)-1-(2,4-dinitrophenyl)-2-(3-(6-((*E*)-4-phenylbut-1-en-1-yl)tetrahydro-2*H*-pyran-2-yl)butylidene)hydrazine (2.59)

To a solution of **2.58** (0.041 g, 0.143 mmol) and 2,4-dinitrophenylhydrazine (<30% water content, 0.041 g, 0.143 mmol) in ethanol (1.5 mL) was added one drop of acetic acid and the reaction mixture was heated at 90°C for 3 h. The mixture was allowed to cool to room temperature, diluted with ethyl acetate, washed with saturated sodium bicarbonate, extracted with ethyl acetate, dried ($MgSO_4$), and concentrated under reduced pressure to give the crude residue as a dark orange solid which was purified by chromatography on SiO_2 (pre-treated with 1% Et_3N, 0-3% acetone/CH_2Cl_2) to give the product as an orange oil (0.018 g, 27%) as a mixture of *E/Z* isomers and a 1.8:1 mixture of diastereomers. IR (ATR) 3301.4, 3026.7, 2920.1, 2850.1, 1618.3, 1592.2, 1518.8, 1424.0, 1332.5, 1308.8, 1278.4, 1222.0, 1137.1, 1078.4, 1036.5, 911.7, 832.8, 743.4, 699.9 cm^{-1} ^1H NMR ($CDCl_3$, 400 MHz) δ = 11.0 (major *E/Z* isomer, bs, 0.7 H), 9.13-9.07 (m, 1 H), 8.32-8.25 (m, 1 H), 7.96-7.91 (m, 1 H), 7.55-7.49 (major *E/Z* isomer, m, 0.77 H), 7.28-7.24 (m, 2 H), 7.19-7.11 (m, 3 H), 5.67-5.50 (m, 2 H), 4.32 (major diastereomer, bs, 0.56 H), 3.32-3.24 (major diastereomer, m, 0.57 H), 2.71-2.64 (m, 2 H), 2.62-2.50 (m, 1 H), 2.39-2.30 (m, 2 H), 2.28-2.22 (m, 1 H), 1.98-1.91 (m, 1 H), 1.75-1.59 (m, 4 H), 1.47-1.25 (m, 2 H), 0.93 (d, 1.4 H, J = 6.8 Hz). ^1H NMR minor *E/Z* isomers: δ = 11.2 (bs, 0.15 H), 7.03-6.98 (m, 0.2 H), 1.02 (d, 0.2 H, J = 6.9 Hz). ^1H NMR minor diastereomers: δ = 4.39 (bs, 0.32 H), 3.48-3.44 (m, 0.32 H), 0.98 (d, 1 H, J = 6.9 Hz). ^{13}C NMR ($CDCl_3$, 100 MHz) major isomer: δ = 153.1, 152.6, 145.2, 141.8, 131.9, 130.87, 130.1, 128.60 (2 C), 128.5, 128.42 (2 C), 125.99, 123.71, 116.63, 74.6, 72.5, 36.6, 35.7,

35.6, 34.3, 29.1, 28.4, 18.8, 16.4. ^{13}C NMR minor isomers: δ = 131.94, 130.7, 130.5, 128.8, 128.62, 128.41, 125.96, 123.69, 116.59, 73.0, 72.8, 36.2, 36.0, 34.4, 28.7, 27.7, 19.0. 16.8, 15.2. HRMS [ESI$^+$] calcd for $C_{25}H_{31}O_5N_4$ [M+H], 467.2289, found 467.2288.

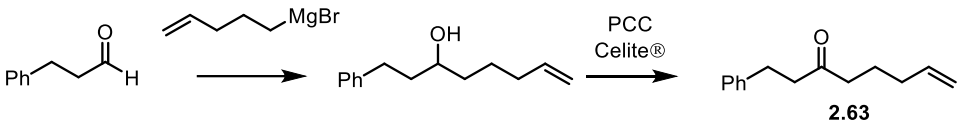

2.63

1-phenyloct-7-en-3-one (2.63)[58]

To magnesium turnings (1.15g, 47.0 mmol) in THF (5 mL) at room temperature under argon was added neat 5-bromopent-1-ene (0.500 g, 3.36 mmol) dropwise. The reaction mixture turned amber and began refluxing gently. 5-bromopent-1-ene (6.50 g, 43.6 mmol) in THF (10 mL) was added dropwise to the mixture over 15 minutes, maintaining the reaction at a gentle reflux. The mixture was allowed to cool to room temperature, then carefully transferred off the excess magnesium turnings by syringe and added dropwise to a solution of hydrocinnamaldehyde (90% pure, 5.73 g, 42.7 mmol) in THF (15 mL) at 0 °C and stirred for 1 h. The mixture was quenched with saturated ammonium chloride, extracted with diethyl ether (3x50 mL), washed with brine, dried ($MgSO_4$), filtered through a plug of SiO_2 with CH_2Cl_2, and concentrated under reduced pressure to give the product as a yellow oil (7.35 g) which was used without further purification.

To a solution of 1-phenyloct-7-en-3-ol (5.00 g, 24.5 mmol) in CH_2Cl_2 (80 mL) at 0 °C was added pyridinium chlorochromate (7.91 g, 36.7 mmol) and Celite® (7.91 g) and the reaction mixture was allowed to warm to room temperature and stirred for 20 h. The mixture was loaded directly onto a column of dry silica gel, rinsed through with CH_2Cl_2, and concentrated under reduced pressure to give the crude residue as a yellow liquid which was purified by chromatography on SiO_2 (0-10% EtOAc/hexanes) to give the product as a pale-yellow oil (3.74 g, 76%).

^{1}H NMR ($CDCl_3$, 400 MHz): δ = 7.33-7.20 (m, 5 H), 5.81-5.73 (m, 1 H), 5.06-4.98 (m, 2 H), 2.93 (app t, 2 H, J = 7.2, 8.0 Hz), 2.75 (app t, 2 H, J = 7.2, 8.0 Hz), 2.42 (app t, 2 H, J = 7.6, 7.2 Hz), 2.06 (q, 2 H, J = 7.2 Hz), 1.70 (quint, 2 H, J = 7.2 Hz). ^{13}C NMR ($CDCl_3$, 100 MHz): δ = 210.0, 141.2, 138.0, 128.5 (2 C), 128.4 (2 C), 126.1, 115.3, 44.4, 42.2, 33.1, 29.8, 22.8.

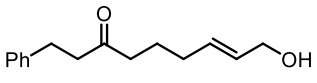

2.67

(*E*)-9-hydroxy-1-phenylnon-7-en-3-one (2.67)

To a solution of 1-phenyloct-7-en-3-one (1.40 g, 6.92 mmol) in CH_2Cl_2 (25 mL) was added *(Z)*-ethene-1,2-diol (3.00 g, 34.2 mmol) and Hoyveda-Grubbs 2nd generation catalyst (0.020 g, 0.030 mmol) and the reaction was stirred for 18 h at room temperature. The solvent was removed under reduced pressure and the crude residue was purified by chromatography on SiO_2 (10-50% ethyl acetate/hexanes) to afford the product as a brown oil (0.544 g, 34%).

IR (neat): 3404.7, 3382.6, 2928.2, 1996.7, 1979.8, 1708.0, 1495.9, 1453.0, 1407.9, 1371.4, 1088.3, 970.2, 748.8, 699.4 cm^{-1}. ^{1}H NMR ($CDCl_3$, 300 MHz): δ = 7.30-7.16 (m, 5 H), 5.64-5.61 (m, 2 H), 4.08 (bs, 2 H), 2.89 (t, 2 H, J = 7.2 Hz), 2.72 (app t, J = 7.2 Hz), 2.39 (t, 2 H, J = 7.2 Hz), 2.06-1.99 (m, 2 H), 1.71-1.59 (q, 2 H, J = 7.5 Hz), 1.28 (bs, 1 H). ^{13}C ($CDCl_3$, 100 MHz): δ = 210.1, 141.2, 132.2, 130.0, 128.6 (2 C), 128.4 (2 C), 126.2, 63.7, 44.5, 42.3, 31.6, 29.9, 23.1. HRMS [ES^{+}] calcd for $C_{15}H_{20}O_2$ [M], 232.1463, found 232.1464.

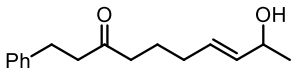

2.68

(*E*)-9-hydroxy-1-phenyldec-7-en-3-one (2.68)

To a solution of 1-phenyloct-7-en-3-one (0.384 g, 1.90 mmol) in CH_2Cl_2 (6 mL) was added (*Z*)-hex-3-ene-2,5-diol (0.264 g, 2.28 mmol) and Hoyveda-Grubbs 2nd generation catalyst (0.020

g, 0.030 mmol) and the reaction was stirred for 13 h at room temperature. The solvent was removed under reduced pressure and the crude residue was purified by chromatography on SiO_2 (10-50% ethyl acetate/hexanes) to afford the product as a brown oil (0.150 g, 32%).

IR (CH_2Cl_2) 3583.2, 3417.8, 3026.8, 2931.0, 1710.2, 1453.4, 1432.1, 1358.5, 1109.2, 699.2 cm^{-1} ^1H NMR ($CDCl_3$, 500 MHz): δ = 7.30-7.17 (m, 5 H), 5.60-5.36 (m, 2 H), 4.25 (app quint, 1 H, J = 6.0, 6.5 Hz), 2.89 (app t, 2 H, J = 7.5, 8.0 Hz), 2.72 (app t, 2 H, J = 7.5, 8.0 Hz), 2.38 (t, 2 H, J = 7.5 Hz), 2.00 (q, 2 H, J = 7.0 Hz), 1.65 (quint, 2 H, J = 7.5 Hz), 1.58 (bs, 1 H), 1.24 (d, 3 H, J = 6.5 Hz). ^{13}C ($CDCl_3$, 125 MHz): δ = 210.1, 141.3, 135.2, 130.0, 128.6 (2 C), 128.5 (2 C), 126.3, 68.9, 44.5, 42.3, 31.6, 29.9, 23.6, 23.2. HRMS [ESI^+] calcd for $C_{16}H_{23}O_2$ [M+H], 247.1693, found 247.1680.

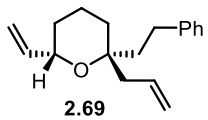

2.69

2-allyl-2-phenethyl-6-vinyltetrahydro-2*H*-pyran (2.69)

To a solution of (*E*)-9-hydroxy-1-phenylnon-7-en-3-one (0.0270 g, 0.121 mmol) and allyltrimethylsilane (0.055 g, 0.484 mmol) in MeCN (6 mL) at 0°C was added Re_2O_7 (0.003 g, 0.006 mmol) and the reaction was stirred for 30 minutes. The amber reaction mixture was directly filtered through a plug of SiO_2 (2”), rinsed through with CH_2Cl_2, and concentrated under reduced pressure to afford the product as a yellow oil (0.027 g, 90%).

IR (CH_2Cl_2): 3054.2, 3028.2, 2982.6, 2942.1, 2869.0, 2305.5, 1719.4, 1639.5, 1602.9, 1495.7, 1446.2, 1360.4, 1265.6, 1033.9, 919.6, 738.7, 703.7 cm^{-1}. ^1H NMR ($CDCl_3$, 400 MHz): δ = 7.21-7.08 (m, 5 H), 5.82-5.69 (m, 2 H), 5.19-5.14 (dt, 1 H, J = 1.6, 17.2 Hz), 5.06-4.98 (m, 3 H), 4.05-4.01 (dd, 1 H, J = 5.6, 11.6 Hz), 2.62 (t, 1 H, J = 8.8 Hz), 2.58-2.52 (dd, 1 H, J = 6.8, 14.4

Hz), 2.32-2.26 (dd, 1 H, J = 8.0, 14.4 Hz), 1.74-1.57 (m, 5 H), 1.48-1.42 (m, 3 H), 1.19-1.18 (m, 2 H). ^{13}C ($CDCl_3$, 125 MHz): δ = 143.2, 140.4, 134.2, 128.6 (2 C), 128.4 (2 C), 125.7, 117.5, 114.2, 75.1, 70.9, 42.8, 36.4, 31.9, 31.6, 31.0, 29.4, 19.4. HRMS [ESI$^+$] calcd for $C_{18}H_{24}O$ [M+H], 256.1822, found 256.1740.

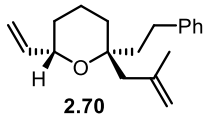

2.70

2-(2-methylallyl)-2-phenethyl-6-vinyltetrahydro-2*H*-pyran (2.70)

To a solution of (*E*)-9-hydroxy-1-phenylnon-7-en-3-one (0.0300 g, 0.129 mmol) and methallyltrimethylsilane (0.066 g, 0.517 mmol) in MeCN (5 mL) at 0°C was added Re_2O_7 (0.003 g, 0.006 mmol) and the reaction was stirred for 15 minutes. Pyridine (2 drops) was added to the amber reaction mixture and the mixture was concentrated under reduced pressure then purified by chromatography on SiO_2 (hexanes, then CH_2Cl_2) to afford the product as a yellow oil (0.0451 g, 89%).

IR (CH_2Cl_2) 3054.4, 2986.3, 2942.4, 2305.6, 1712.2, 1421.8, 1265.3, 1034.4, 896.2, 738.7, 704.7 cm^{-1}. ^{1}H NMR ($CDCl_3$, 500 MHz): δ = 7.27-7.15 (m, 5 H), 5.87-5.80 (ddd, 1 H, J = 5.5, 10.5, 17.5 Hz) 5.25-5.21 (dt, 1 H, J = 1.5, 17.5 Hz), 5.06-5.04 (dt, 1 H, J = 1.5, 10.5 Hz), 4.87 (bs, 1 H), 4.78 (bs, 1 H), 4.21-4.18 (m, 1 H), 2.80 (d, 1 H, J = 14.5 Hz), 2.71-2.66 (m, 2 H), 2.15 (d, 1 H, J = 14.5 Hz), 1.83-1.80 (m, 5 H), 1.75-1.66 (m, 3 H), 1.57-1.54 (m, 2 H), 1.31-1.26 (m, 1 H). ^{13}C ($CDCl_3$, 125 MHz) 143.2, 140.2, 136.0, 128.5 (2 C), 128.4 (2 C), 125.7, 114.4, 114.1, 75.7, 70.8, 42.6, 39.3, 33.2, 31.7, 29.8, 24.1, 19.6. HRMS [ESI$^+$] calcd for $C_{19}H_{27}O$ [M+H], 271.2056, found 271.2051.

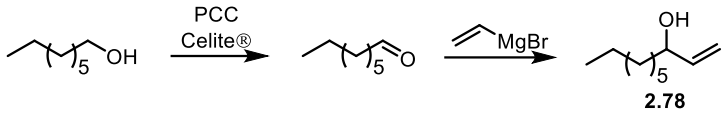

2.78

dec-1-en-3-ol[59] **(2.78)**

To a solution of 1-octanol (3.00 g, 23.0 mmol) in CH_2Cl_2 (77 mL) was added pyridinium chlorochromate (7.45 g, 34.6 mmol) and Celite® (7.45 g) and the reaction was stirred for 2.5 h under argon at room temperature. The reaction mixture was filtered through SiO_2, rinsed through with CH_2Cl_2, and concentrated under reduced pressure to give 1-octanal as a yellow liquid.

1-octanal was dissolved in THF (14 mL), cooled to 0°C, and vinylmagnesium bromide (28 mL, 1.0 M in THF) was added dropwise over 20 minutes and the reaction was stirred at 0°C under argon for 1 h, allowed to warm to room temperature, and stirred for 2.5 h. The reaction mixture was cooled to 0°C, quenched with 1 N HCl, extracted with diethyl ether (3x), dried ($MgSO_4$), filtered, and concentrated under reduced pressure to give the crude residue which was purified by chromatography on SiO_2 (0-15% ethyl acetate/hexanes) to give **2-78** as a pale-yellow oil (2.16 g, 60%). Characterization data is consistent with literature values.

^{1}H NMR ($CDCl_3$, 400 MHz): δ = 5.86 (ddd, 1 H, J = 6.2, 10.4, 16.9 Hz), 5.21 (dt, 1 H, J = 1.2, 17.2 Hz), 5.10 (dt, J = 1.2, 10.4 Hz), 4.09 (app quint., J = 5.2, 5.6, 6.0, 6.4 Hz), 1.54-1.47 (m, 3 H), 1.39-1.24 (m, 10 H), 0.89-0.86 (m, 3 H). ^{13}C ($CDCl_3$, 100 MHz): δ = 141.5, 114.7, 37.2, 31.9, 29.7, 29.4, 25.5, 22.8, 14.2.

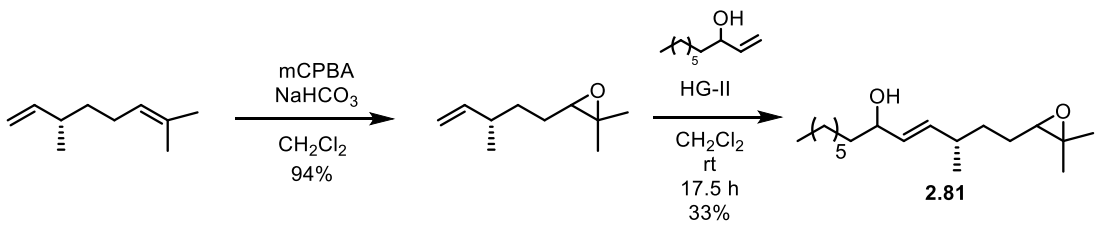

(3*R*,*E*)-1-(3,3-dimethyloxiran-2-yl)-3-methyltridec-4-en-6-ol (2.81)

To a stirred mixture of mCPBA (11.3 g, 65.6) and sodium bicarbonate (10.8 g, 129 mmol) in CH_2Cl_2 (350 mL) was added (-)-β-citronellene (7.5 g, 54.2 mmol) and the reaction mixture was stirred for 2 h. Saturated sodium bicarbonate was added and the reaction mixture was stirred for 10 minutes, then extracted with CH_2Cl_2, washed with water, dried ($MgSO_4$), filtered, and concentrated under reduced pressure to give the product as a clear liquid (7.05 g, 94%).

To a solution of **2-36** (0.533 g, 3.46 mmol) and **2-73** (0.702 g, 4.49 mmol) in CH_2Cl_2 (12 mL) was added Hoyveda-Grubbs 2nd generation catalyst (0.021, 0.034 mmol) and the mixture was stirred under argon at room temperature. Additional catalyst (0.010 g, 0.017 mmol) was added after 5.5 h and the reaction mixture was stirred for an additional 17.5 h. The reaction mixture was concentrated under reduced pressure and purified by chromatography on SiO_2 (0-4% acetone/CH_2Cl_2) to give **2-81** as a brown oil as a mixture of diastereomers (0.326 g, 33%). IR (CH_2Cl_2): 3378.6, 2922.8, 2892.8, 2823.1, 1542.6, 1440.4, 1362.3, 1310.3, 1235.7, 1108.7, 959.4 cm^{-1}. ^{1}H NMR ($CDCl_3$, 400 MHz): δ = 5.54-5.39 (m, 2 H), 4.04-4.02 (m, 1 H), 2.69 (app t, 1 H, J = 4.7, 5.6 Hz), 2.19-2.15 (m, 1 H), 1.53-1.42 (m, 7 H), 1.30-1.25 (m, 17 H), 1.01 (dd, 3 H, J = 2.5, 6.7 Hz), 0.89-0.86 (m, 3 H).^{13}C ($CDCl_3$, 100 MHz) major diastereomer: δ = 137.2, 132.1, 73.3, 64.5, 58.3, 37.6, 36.5, 33.7, 32.0, 29.7, 29.4, 26.9, 25.7, 25.0, 22.8, 20.7, 18.9, 14.2. HRMS [ESI$^+$] calcd for $C_{18}H_{35}O_2$ [M+H], 283.2632, found 283.2639.

^{13}C minor diastereomer ($CDCl_3$, 100 MHz): δ = 137.3, 137.0, 132.3, 132.2, 73.24, 73.22, 64.7, 64.6, 58.4, 37.5, 36.4, 36.3, 33.8, 33.6, 26.86, 25.63, 20.65.

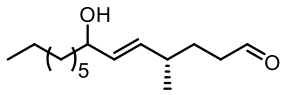

2.82

(4*R*,*E*)-7-hydroxy-4-methyltetradec-5-enal (2.82)

To a solution of **2-81** (0.180 g, 0.637 mmol) in diethyl ether (3.2 mL) was added periodic acid (0.174 g, 0.764 mmol) in THF (3 mL) at 0°C and the reaction mixture was stirred for 1 h. The reaction mixture was diluted with diethyl ether, washed with water, extracted with diethyl ether, dried ($MgSO_4$), and concentrated under reduced pressure to give the crude residue which was purified by chromatograpy on SiO_2 (0-4% acetone/CH_2Cl_2) to give the product as a yellow oil as a mixture of diastereomers (0.147 g, 96%).

IR (CH_2Cl_2) 3382.4, 2920.5, 2893.3, 2822.9, 2685.6, 1704.7, 1441.4, 1361.3, 1088.0, 993.2, 961.7 cm^{-1}. ^{1}H NMR ($CDCl_3$, 500 MHz): δ = 9.76 (t, 1 H, J = 1.6 Hz), 5.45-5.44 (m, 2 H), 4.06-4.02 (m, 1 H), 2.45-2.41 (m, 2 H), 2.19-2.12 (m, 1 H), 1.62-1.58 (m, 2 H), 1.56-1.42 (m, 3 H), 1.28-1.25 (m, 10 H), 1.02 (d, 3 H, J = 6.8 Hz), 0.88 (t, 3 H, J = 6.8 Hz). ^{13}C NMR ($CDCl_3$, 125 MHz): δ = 202.7, 136.2, 133.0, 73.1, 42.0, 37.6, 36.2, 32.0, 29.6, 29.4, 28.9, 25.6, 22.8, 20.7, 14.2. HRMS [ESI$^+$] calcd for $C_{15}H_{27}O$ [M-OH], 223.2056, found 223.2054.

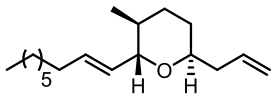

2.83

2,6-*cis*-(3*S*)-6-allyl-3-methyl-2-((*E*)-non-1-en-1-yl)tetrahydro-2*H*-pyran (2.83)

To a solution of **2.82** (0.010 g, 0.042 mmol) and allyltrimethylsilane (0.019 g, 0.166 mmol) in acetonitrile (1.4 mL) at 0°C was added Re_2O_7 (0.001 g, 0.002 mmol) and the reaction mixture

was stirred at 0°C for 30 minutes. The reaction mixture was quenched with pyridine (~2 drops), filtered through SiO_2, rinsed through with CH_2Cl_2, and concentrated under reduced pressure to give the crude residue which was purified by chromatography on SiO_2 (0-6% diethyl ether/pentane) to afford the product as a 5.4:1 mixture of diastereomers (0.008 g, 73%).

IR (CH_2Cl_2): 3040.6, 2893.2, 2822.3, 1622.8, 1440.8, 1360.8, 1047.1, 1018.2, 956.2, 900.7 cm^{-1}. ^1H NMR ($CDCl_3$, 500 MHz) δ = 5.84-5.71 (m, 1 H), 5.66-5.60 (m, 1 H), 5.44-5.40 (m, 1 H), 5.09-5.01 (m, 2 H), 4.14 (minor diastereomer, app t, 0.19 H, J = 5.8, 6.6 Hz), 3.93-3.88 (m, 1 H), 3.67 (t, 1 H, J = 7.4 Hz), 2.52-2.46 (m, 1 H), 2.29-2.23 (m, 1 H), 2.07-1.99 (m, 2 H), 1.73-1.65 (m, 2 H), 1.55-1.45 (m, 1 H), 1.40-1.33 (m, 3 H), 1.29-1.26 (m, 9 H), 0.89-0.86 (m, 6 H), 0.75 (minor diastereomer, d, 0.74 H, J = 7.0 Hz). ^{13}C NMR ($CDCl_3$, 125 MHz): δ = 135.7, 135.4, 134.3, 130.2, 124.6, 116.6, 77.7, 71.8, 69.1, 40.8, 34.3, 32.8, 32.6, 32.0, 31.4, 29.9, 29.31, 29.29, 27.5, 27.3, 26.6, 22.8, 18.4, 17.7, 14.2.

^{13}C minor diastereomer ($CDCl_3$, 125 MHz): δ = 135.4, 124.6, 69.1, 32.8, 31.4, 29.9, 27.5

HRMS [ESI^+] calcd for $C_{18}H_{33}O$ [M+H], 265.2526, found 265.2530.

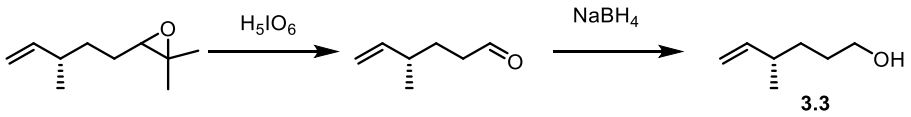

3.3

(*R*)-4-methylhex-5-en-1-ol[60] (3.3)

To epoxide **3.1 (**2.50 g, 16.2 mmol) in diethyl ether (81 mL) at 0°C was added periodic acid (4.06 g, 17.8 mmol) in THF (17 mL) dropwise and the reaction mixture was stirred for 1.5 h. Diethyl ether was added and the mixture was washed with water, saturated sodium bicarbonate, dried ($MgSO_4$), filtered, and concentrated under reduced pressure (20°C). The resulting liquid was

filtered through SiO_2, rinsed through with CH_2Cl_2, and concentrated under reduced pressure (20°C) to give the intermediate aldehyde as a yellow liquid (1.89 g).

Aldehyde **3.2** was dissolved in diethyl ether/methanol (3:1) and cooled to 0°C. Sodium borohydride was added portionwise over 5 minutes and the reaction mixture was allowed to warm to room temperature and stirred for 18 h. The mixture was cooled to 0°C, quenched with 1 N HCl, extracted with diethyl ether, washed with brine, dried ($MgSO_4$), and concentrated under reduced pressure. The crude residue was purified by chromatography on SiO_2 (10-40% diethyl ether/pentane) to give the product as a yellow liquid (0.610 g, 33% over two steps). Characterization data is consistent with literature values.

^{1}H NMR ($CDCl_3$, 300 MHz): δ = 5.69 (ddd, 1 H, J = 7.6, 10.2, 17.4 Hz), 5.00-4.90 (m, 2 H), 3.66-3.61 (m, 2 H), 2.14 (septet, 1 H, J = 7.1 Hz), 1.62-1.52 (m, 2 H), 1.43-1.31 (m, 2 H), 1.22 (bs, 1 H), 1.01 (d, 3 H, J = 6.7 Hz). ^{13}C ($CDCl_3$, 75 MHz): δ = 144.6, 112.9, 63.3, 37.8, 32.8, 30.7, 20.4.

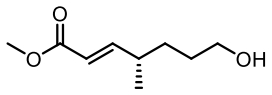

3.4

methyl (*R*,*E*)-7-hydroxy-4-methylhept-2-enoate (3.4)

To **3.3** (0.610 g, 5.25 mmol) and methyl acrylate (0.904 g, 10.5 mmol) in CH_2Cl_2 (18 mL) was added Hoyveda-Grubbs 2nd generation catalyst (0.033 g, 0.053 mmol) and the mixture was stirred at 40°C for 22 h. The reaction mixture was cooled to room temperature, concentrated under reduced pressure and purified by chromatography on SiO_2 (0-12% acetone/CH_2Cl_2) to give **3.4** as a clear liquid (0.460 g, 51%, 14:1 *E*/*Z*).

IR (ATR): 3418.7, 2937.3, 2870.7, 1718.0, 1653.2, 1437.1, 1351.4, 1270.1, 1199.5, 1172.6, 1056.8, 986.5, 906.4, 862.9, 721.5 cm^{-1}. ^{1}H NMR ($CDCl_3$, 400 MHz): δ = 6.86 (dd, 1 H,

J = 8.0, 15.7 Hz), 5.79 (dd, 1 H *J* = 1.0, 15.7 Hz), 3.72 (s, 3 H), 3.631-3.625 (m, 2 H), 2.33, (septet, 1 H, *J* = 6.8 Hz), 1.59-1.51 (m, 2 H), 1.48-1.41 (m, 2 H), 1.32 (bs, 1 H), 1.06 (d, 3 H, *J* = 6.7 Hz). Minor isomer peaks: δ = 6.0 (dd, 0.07 H, *J* = 10.2, 11.4 Hz), 3.70 (s, 0.21 H), 1.02 (d, 0.26 H, *J* = 6.6 Hz).^{13}C ($CDCl_3$, 75 MHz): δ = 167.4, 154.5, 119.7, 62.9, 51.6, 36.5, 32.2, 30.5, 19.6. HRMS [ESI$^+$] calcd for $C_9H_{17}O_3$ [M+H], 173.1178, found 173.1169. $[\alpha]_D^{24}$= +26.3 (*c* 1.79, $CHCl_3$)

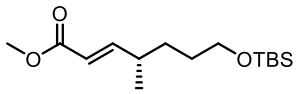

3.5

methyl (*R*,*E*)-7-((*tert*-butyldimethylsilyl)oxy)-4-methylhept-2-enoate (3.5)

To **3.4** (0.420 g, 2.44 mmol), TBSCl (0.441 g, 2.93 mmol), and triethylamine (0.321 g, 3.17 mmol) in CH_2Cl_2 (12 mL) at 0°C was added DMAP and the reaction mixture was allowed to warm to room temperature and stirred for 70 h. Water was added and the reaction mixture was extracted with CH_2Cl_2, dried ($MgSO_4$), and concentrated under reduced pressure. The crude residue was purified by chromatography on SiO_2 (CH_2Cl_2) to give **3.5** as a pale-yellow liquid (0.608 g, 87%).

IR (ATR): 2933.7, 2858.7, 1726.1, 1654.8, 1463.9, 1437.3, 1257.2, 1203.6, 1173.3, 1095.6, 1008.7, 939.6, 833.3, 774.6, 718.2. ^{1}H ($CDCl_3$, 300 MHz): δ = 6.87 (dd, 1 H, *J* = 7.9, 15.7 Hz), 5.78 (dd, 1 H, *J* = 1.3, 15.7 Hz), 3.73 (s, 3 H), 3.58 (t, 2 H, *J* = 6.0 Hz), 2.31 (septet, 1 H, *J* = 6.8 Hz), 1.53-1.37 (m, 4 H), 1.05 (d, 3 H, *J* = 6.7 Hz), 0.89 (s, 9 H), 0.04 (s, 6 H). Minor isomer peaks: δ = 3.70 (s, 0.2 H), 1.01 (d, 0.2 H, *J* = 6.7 Hz). ^{13}C ($CDCl_3$, 100 MHz): δ = 167.5, 154.9, 119.5, 63.2, 51.6, 36.5, 32.3, 30.5, 26.1 (3 C), 19.6, 18.5, -5.16 (2 C).HRMS [ESI$^+$] calcd for $C_{15}H_{31}O_3Si$ [M+H], 287.2042, found 287.2026.

$[\alpha]_D^{24}$= -53.0 (*c* 0.63, $CHCl_3$)

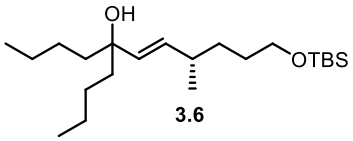

3.6

(*R,E)*-5-butyl-11-((*tert*-butyldimethylsilyl)oxy)-8-methylundec-6-en-5-ol (3.6)

To **3.5** (0.600 g, 2.09 mmol) in THF (6.0 mL) at 0°C was added n-butyllithium (1.6 M in hexanes, 3.0 mL, 4.82 mmol), and the reaction mixture was stirred for 1 h. The mixture was quenched with saturated ammonium chloride and allowed to warm to room temperature. The mixture was extracted with diethyl ether, washed with brine, dried ($MgSO_4$), and concentrated under reduced pressure to give **3.6** as a yellow oil which was used without further purification (0.707 g, 91%).

IR (ATR): 3482.0, 2931.6, 2860.7, 1463.4, 1381.3, 1252.4, 1096.8, 1005.2, 975.8, 939.7, 834.0, 774.6 cm^{-1} ^1H NMR ($CDCl_3$, 300 MHz): δ = 5.47-5.33 (m, 2 H), 3.59 (t, 2 H, J = 6.5 Hz), 2.13 (septet, 1 H, J = 6.7 Hz), 1.56-1.44 (m, 7 H), 1.35-1.25 (m, 11 H), 0.99 (d, 3 H, J = 6.7 Hz), 0.91-0.87 (m, 15 H), 0.04 (s, 6 H). ^{13}C ($CDCl_3$, 100 MHz): δ = 134.5, 134.2, 75.0, 63.5, 41.06, 41.04, 36.6, 33.3, 30.9, 26.1 (3 C), 25.93, 25.87, 23.3 (2 C), 21.2, 18.5, 14.3 (2 C), -5.1 (2 C). HRMS [ESI^+] calcd for $C_{22}H_{47}O_2Si$ [M+H], 371.3340, found 371.3344. $[\alpha]_D^{24}$ = +6.2 (c 1.16, CHCl3)

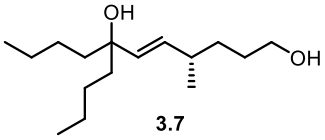

3.7

(*S, E*)-7-butyl-4-methylundec-5-ene-1,7-diol (3.7)

To **3.6** (0.690 g, 1.86 mmol) in THF (9.0 mL) was added tetra-n-butylammonium fluoride (5.6 mL) and the reaction mixture was stirred at room temperature for 19 h. Water was added and

the mixture was extracted with diethyl ether, dried ($MgSO_4$), filtered, and concentrated under reduced pressure to give the crude residue which was purified by chromatography on SiO_2 (5-12% acetone/CH_2Cl_2) to give the product as a yellow oil (0.355 g, 74%).

IR (ATR): 3362.2, 2931.2, 2865.8, 1710.2, 1458.8, 1376.7, 1135.1, 1056.8, 976.3, 903.5, 733.1 cm^{-1}. ^1H NMR ($CDCl_3$, 300 MHz): δ = 5.48-5.34 (m, 2 H), 3.64-3.63 (m, 2 H), 2.15 (septet, 1 H, J = 6.8 Hz), 1.61-1.45 (m, 5 H), 1.38-1.23 (m, 13 H), 1.00 (d, 3 H, J = 6.7 Hz), 0.89 (t, 6 H, J = 6.7 Hz). ^{13}C NMR ($CDCl_3$, 75 MHz): δ = 134.8, 133.9, 75.0, 63.3, 41.1 (2 C), 36.7, 33.3, 30.8, 26.0, 25.9, 23.3 (2 C), 21.2, 14.2 (2 C). HRMS [ESI^+] calcd for $C_{16}H_{33}O_2$ [M+H], 267.2481, found 257.2465. $[\alpha]_D^{24}$ = +7.9 (*c* 1.02, $CHCl_3$)

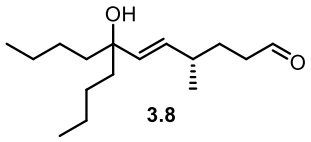

3.8

(*S*,*E*)-7-butyl-7-hydroxy-4-methylundec-5-enal (3.8)

To a solution of **3.7** (0.080 g, 0.312 mmol) and triethylamine (0.126 g, 1.25 mmol) in CH_2Cl_2 (0.6 mL) at 0°C was added sulfur trioxide pyridine complex (0.149 g, 0.936 mmol) in dimethlysulfoxide (1.0 mL), and the reaction mixture was allowed to warm to room temperature and stirred for 4 h. Water was added and the mixture was extracted with CH_2Cl_2, washed with water, saturated ammonium chloride, dried ($MgSO_4$), filtered, and concentrated under reduced pressure to give the crude residue which was purified by chromatography on SiO_2 (0-12% acetone/CH_2Cl_2) to give the product as a yellow oil (0.044 g, 55%).

IR (CH_2Cl_2): 3462.4, 2952.3, 2931.9, 2866.4, 2723.5, 1723.9, 1459.4, 1378.5, 1131.6, 978.1 cm^{-1} ^1H NMR ($CDCl_3$, 400 MHz): δ = 9.76 (t, 1 H, J = 1.6 Hz), 5.39 (m, 2 H), 2.43 (app t, 2 H, J = 7.0, 8.0 Hz), 2.18-2.14 (m, 1 H), 1.72-1.64 (m, 1 H), 1.62-1.55 (m, 2 H), 1.52-1.41 (m, 4 H), 1.34-1.22 (m, 8 H), 1.02 (d, 3 H, J = 6.7 Hz), 0.89 (t, 6 H, J = 7.2 Hz). ^{13}C NMR ($CDCl_3$, 100

MHz): δ = 202.8, 135.8, 132.9, 75.0, 42.1, 41.04, 41.00, 36.5, 29.1, 26.0, 25.9, 23.3 (2 C), 21.1, 14.24, 14.23. HRMS [ESI$^+$] calcd for $C_{16}H_{29}O$ [M-OH], 237.2218, found 237.2232. $[\alpha]_D^{24}$ = +10.0 (*c* 0.70, $CHCl_3$)

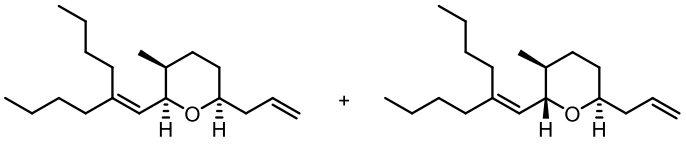

3.9 **3.10**

6-allyl-2-(2-butylhex-1-en-1-yl)-3-methyltetrahydro-2*H*-pyran (3.9 and 3.10)

To a solution of **3.8** (0.045 g, 0.176 mmol) and allyltrimethylsilane (0.072 g, 0.629 mmol) in acetonitrile (5.2 mL) at 0°C was added Re_2O_7 (10 mg/mL, 0.24 µL, 0.005 mmol) and the reaction mixture was stirred at 0°C for 30 minutes. The reaction mixture was quenched with pyridine (~2 drops) and concentrated under reduced pressure to give the crude residue which was purified by chromatography on SiO_2 (0-5% diethyl ether/pentane) to afford the product as a 3:1 mixture of diastereomers (0.0341 g, 69%). The mixture was purified again by chromatography on SiO_2 (1% diethyl ether/pentane) to isolate the two diastereomers (2,6-*cis*: 0.0231 g, 44%, 2,6-*trans*: 0.0086 g, 20%).

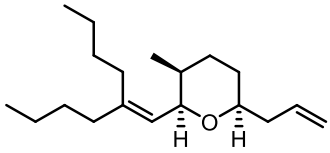

3.9

(2*R*,3*S*,6*S*)-6-allyl-2-(2-butylhex-1-en-1-yl)-3-methyltetrahydro-2*H*-pyran (3.9)

IR (CH_2Cl_2): 3081.2, 2927.8, 2859.7, 1644.1, 1458.8, 1377.5, 1341.4, 1202.9, 1054.4, 980.6, 910.0, 739.4 cm^{-1}.

^{1}H NMR ($CDCl_3$, 300 MHz): δ = 5.85 (ddt, 1 H, *J* = 7.4, 10.1, 17.1 Hz), 5.22 (d, 1 H, 8.0 Hz), 5.08-4.99 (m, 2 H), 4.18 (dd, 1 H, *J* = 2.2, 8.0 Hz), 3.42-3.34 (m, 1 H), 2.40-2.32 (m, 1 H),

2.22-2.13 (m, 1 H), 2.03-1.97 (m, 4 H), 1.80-1.74 (m, 1 H), 1.70-1.59 (m, 2 H), 1.45-1.25 (m, 10 H), 0.98 (d, 3 H, *J* = 6. Hz), 0.93-0.87 (m, 6 H).

^{13}C NMR ($CDCl_3$, 75 MHz): δ = 142.3, 135.4, 124.7, 116.5, 41.2, 36.5, 32.4, 31.1, 31.0, 30.9, 30.4, 25.5, 23.1, 22.7, 14.20 (2 C), 14.18 (2 C), 12.2.

HRMS [ESI$^+$] calcd for $C_{19}H_{35}O$ [M+H], 279.2682, found 279.2683.

$[\alpha]_D^{25}$ = -21.8 (*c* 0.49, $CHCl_3$)

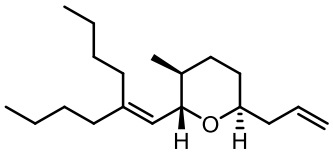

3.10

(2*S*,3*S*,6*S*)-6-allyl-2-(2-butylhex-1-en-1-yl)-3-methyltetrahydro-2*H*-pyran

IR (CH_2Cl_2): 3080.1, 2958.5, 2930.1, 2865.9, 1713.9, 1641.0, 1458.0, 1376.9, 1232.7, 1187.4, 1145.2, 1054.4, 995.5, 913.1, 735.0 cm^{-1}.

^{1}H NMR ($CDCl_3$, 400 MHz): δ = 5.80 (ddt, 1 H, *J* = 7.0, 10.2, 17.1 Hz), 5.16-5.01 (m, 2 H), 3.98-3.91 (m, 2 H), 2.57-2.50 (m, 1 H), 2.33-2.26 (m, 1 H), 2.07-1.99 (m, 4 H), 1.78-1.65 (m, 2 H), 1.55-1.51 (m, 1 H), 1.44-1.25 (m, 11 H), 0.92-0.87 (6 H), 0.84 (d, 3 H, *J* = 6.3 Hz).

^{1}H NMR (C_6D_6, 500 MHz): δ = 5.87 (ddt, 1 H, *J* = 6.7, 10.2, 17.1 Hz), 5.31 (d, 1 H, *J* = 8.3 Hz), 5.10-5.05 (m, 1 H), 5.06-5.03 (m, 1 H), 4.14 (t, 1 H, *J* = 7.7 Hz), 3.92-3.88 (m, 1 H), 2.56-2.50 (m, 1 H), 2.21-2.16 (m, 3 H), 2.04 (t, 2 H, *J* = 7.6 Hz), 1.61-1.54 (m, 2 H), 1.50-1.33 (m, 9 H), 1.32-1.25 (m, 3 H), 0.95-0.92 (m, 6 H), 0.89 (t, 3 H, *J* = 7.3 Hz).

^{13}C NMR ($CDCl_3$, 125 MHz): δ = 145.1, 135.9, 125.0, 116.5, 72.3, 72.0, 36.6, 36.3, 35.4, 31.0, 30.8, 30.5, 27.5, 26.7, 23.2, 22.7, 18.3, 14.20, 14.15.

HRMS [ESI$^+$] calcd for $C_{19}H_{35}O$ [M+H], 279.2682, found 279.2691.

$[\alpha]_D^{26}$ = +26.9 (*c* 0.13, $CHCl_3$)

Appendix B : Spectra

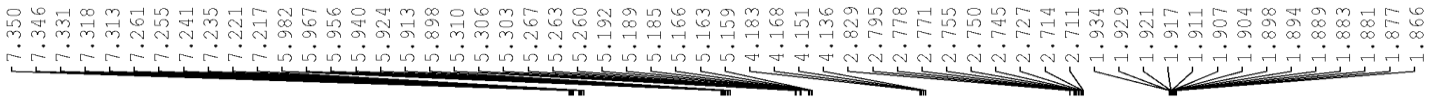

^{1}H NMR
$CDCl_3$, 400 MHz

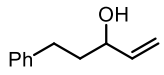

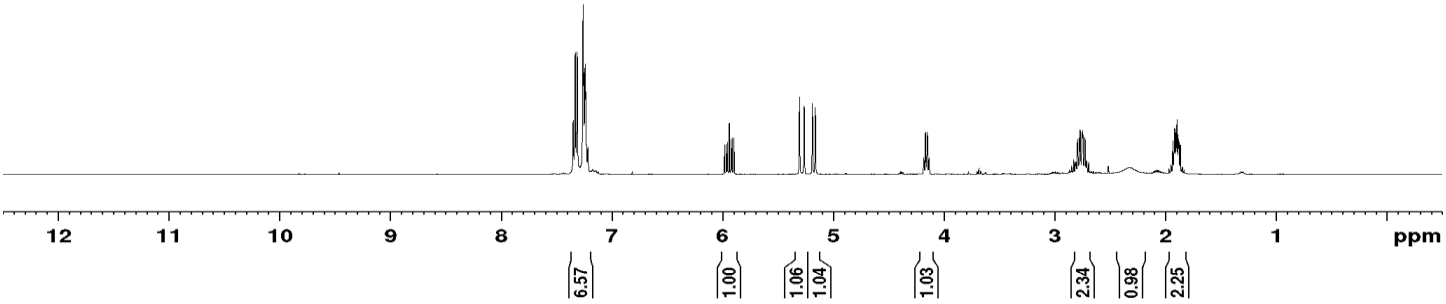

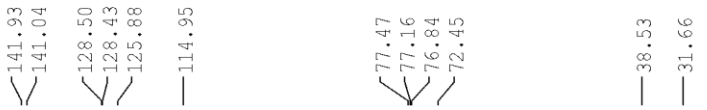

^{13}C NMR
$CDCl_3$, 100 MHz

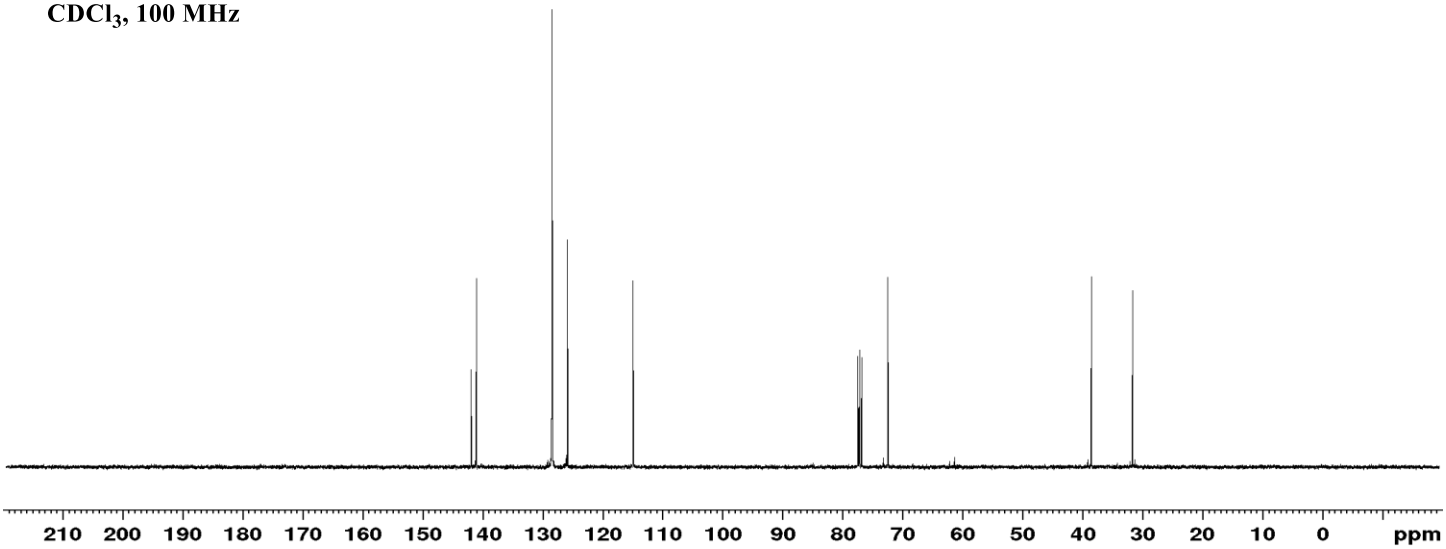

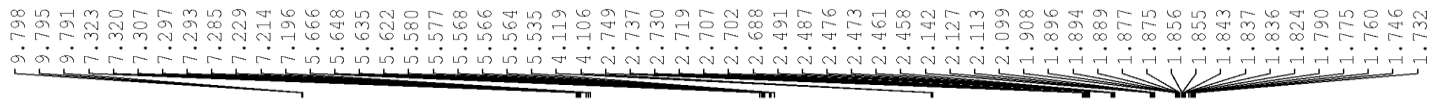

^{1}H NMR

$CDCl_3$, 500 MHz

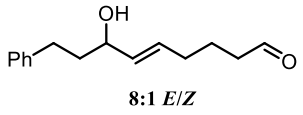

8:1 *E*/*Z*

^{13}C NMR

$CDCl_3$, 125 MHz

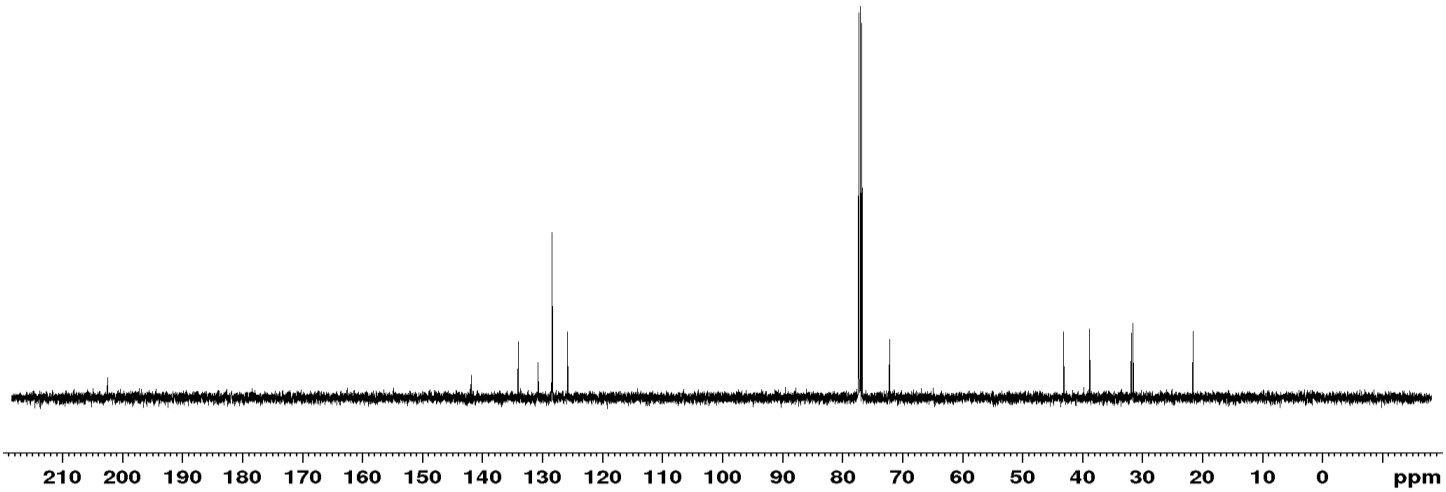

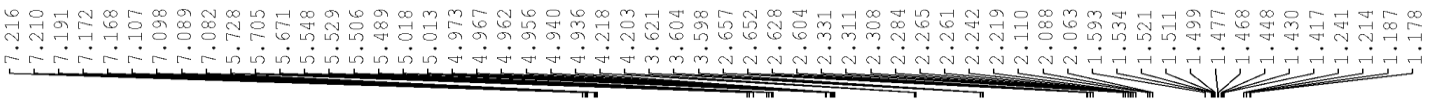

^{1}H NMR

$CDCl_3$, 300 MHz

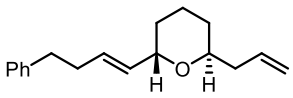

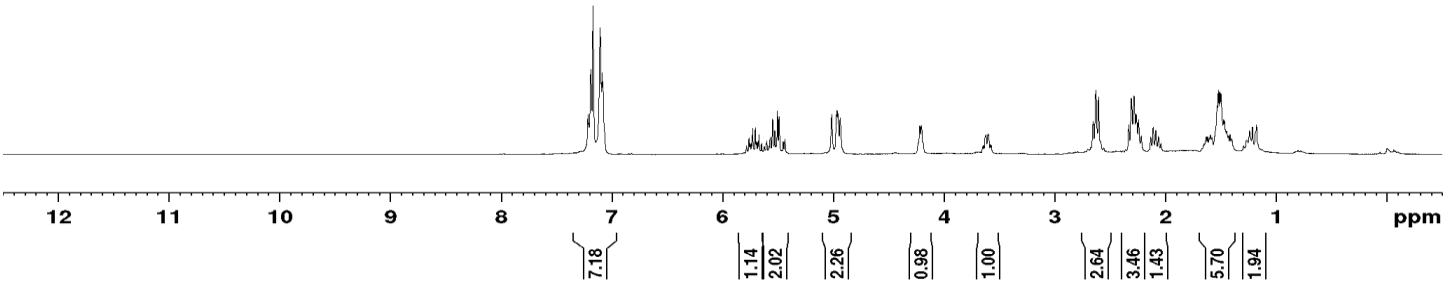

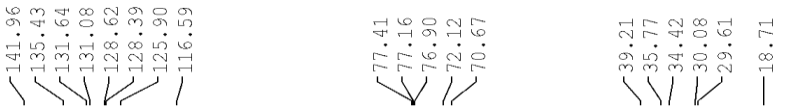

^{13}C NMR

$CDCl_3$, 125 MHz

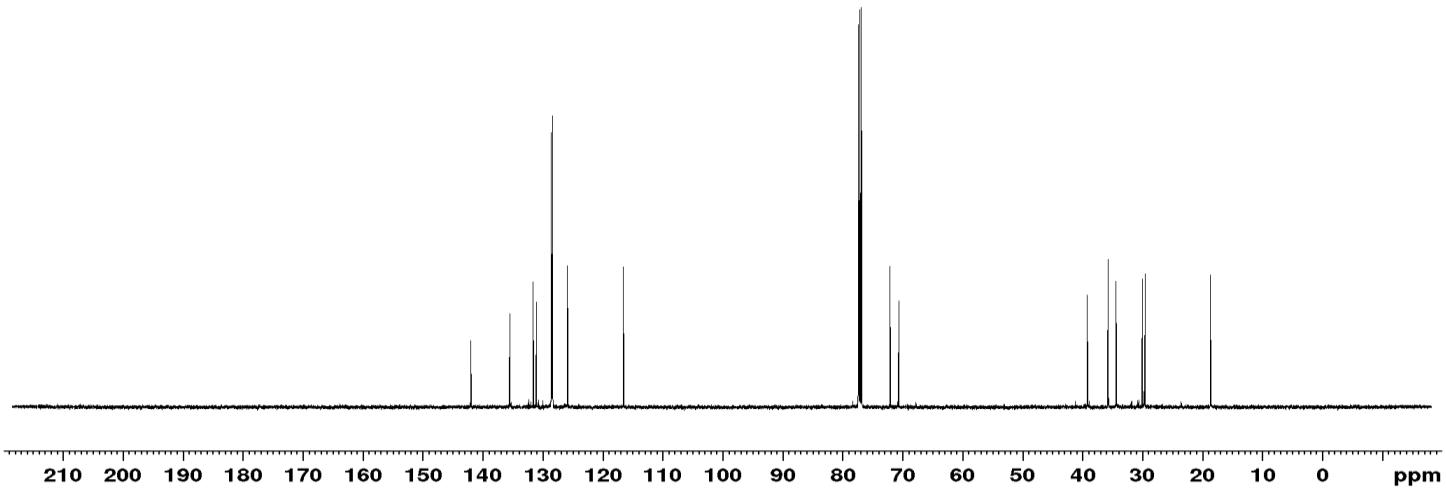

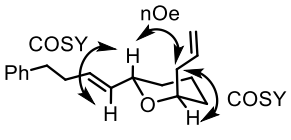

HH COSY
$CDCl_3$, 500 MHz

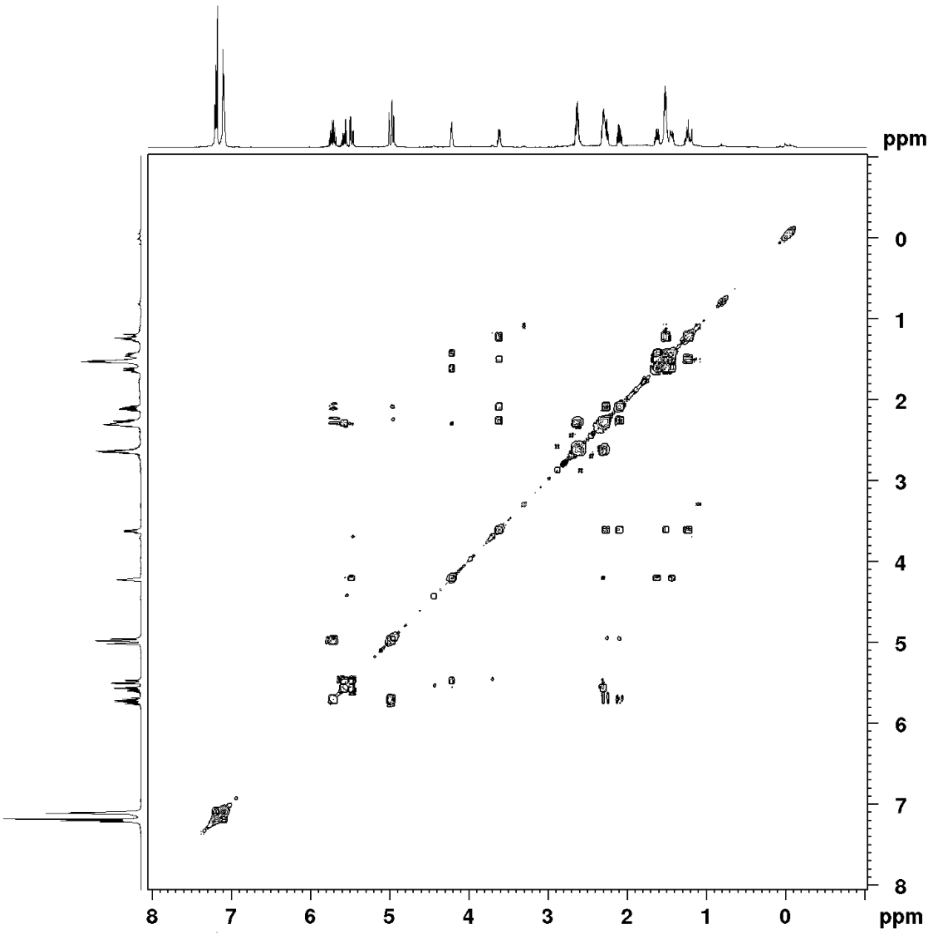

NOESY
$CDCl_3$, 500 MHz

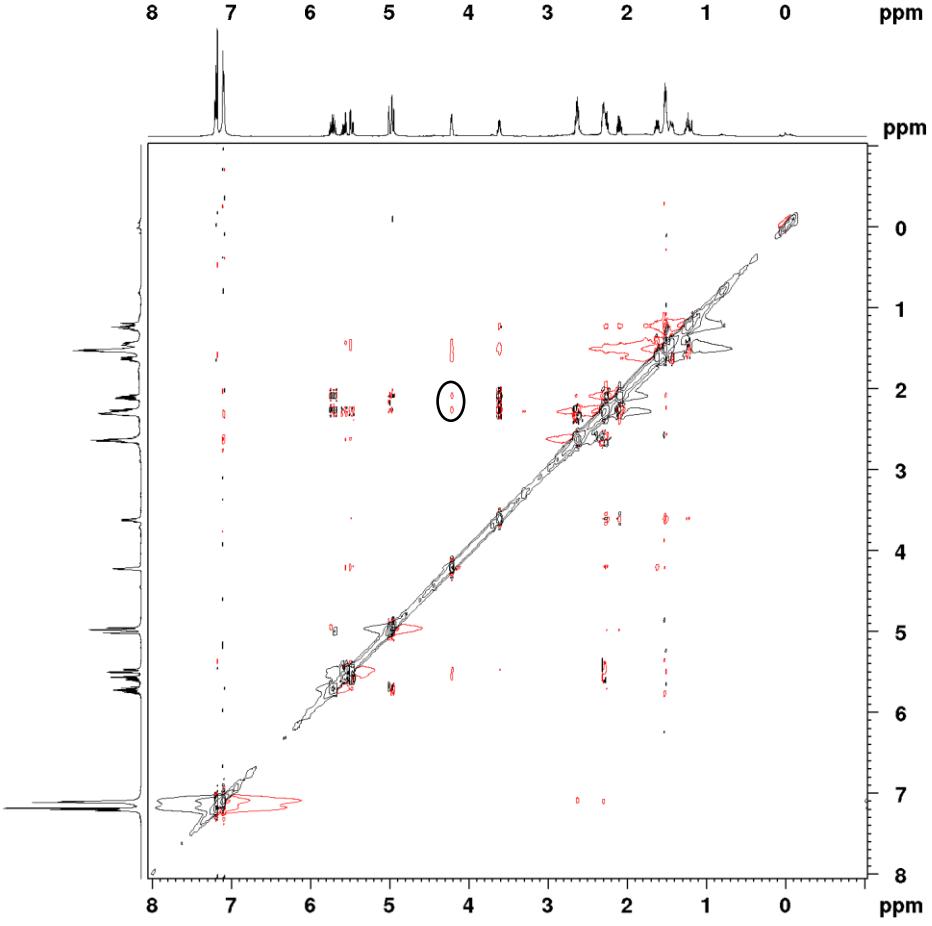

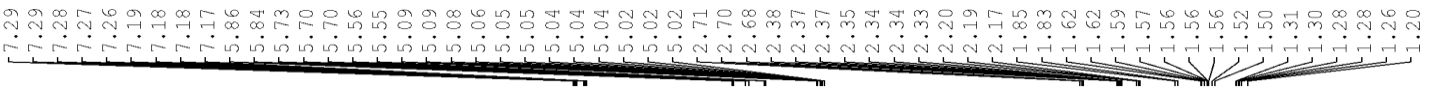

^{1}H NMR
$CDCl_3$, 500 MHz

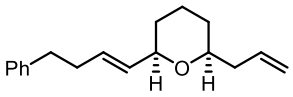

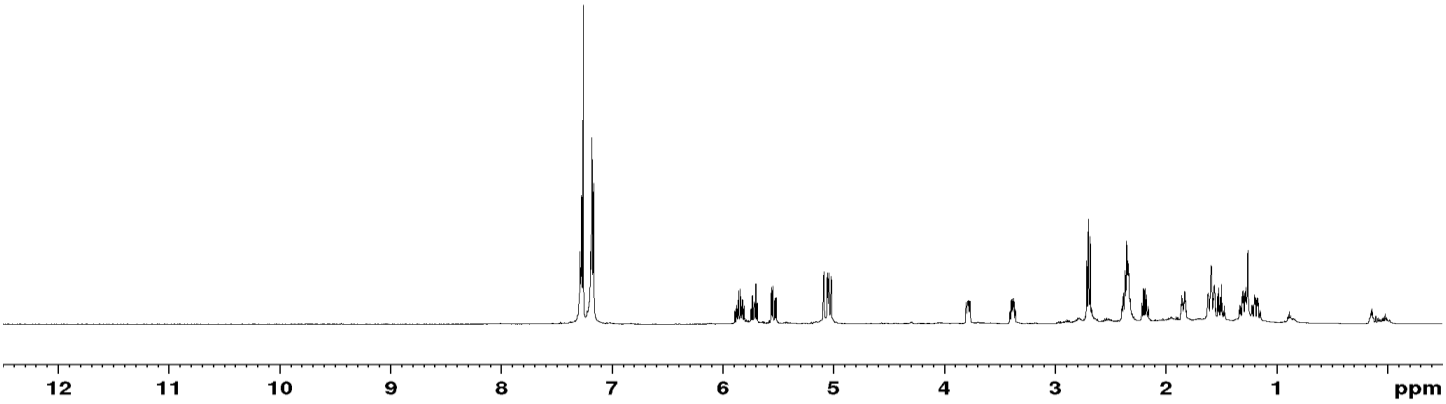

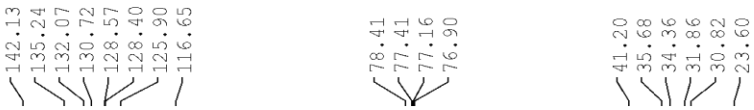

^{13}C NMR
$CDCl_3$, 125 MHz

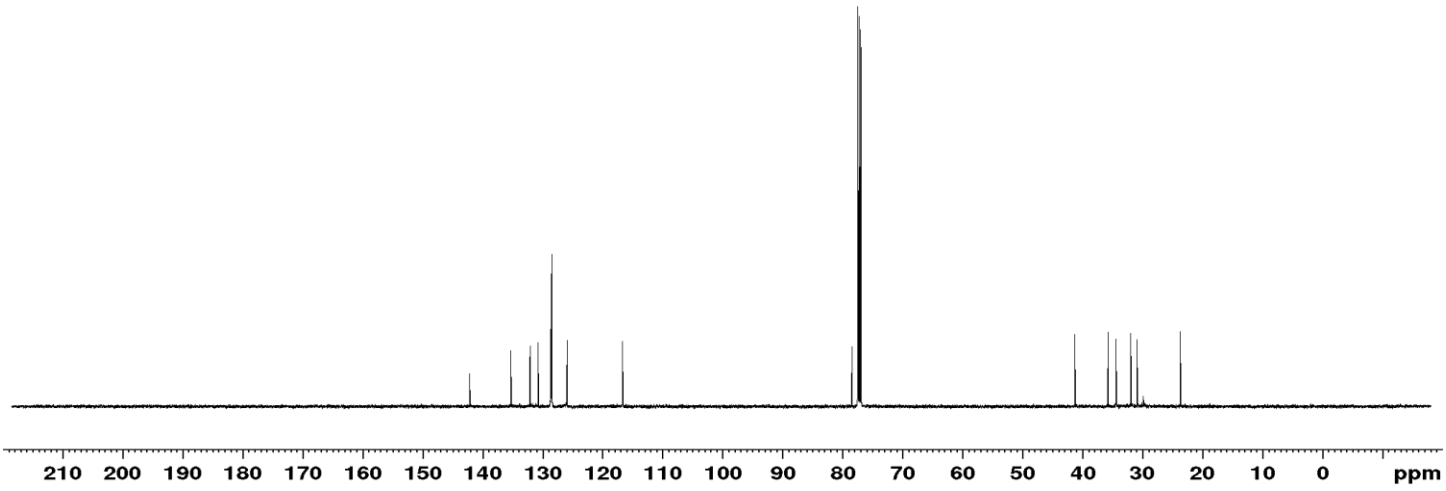

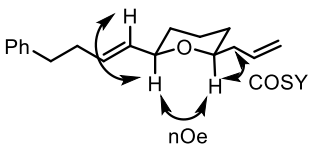

HH COSY
$CDCl_3$, 500 MHz

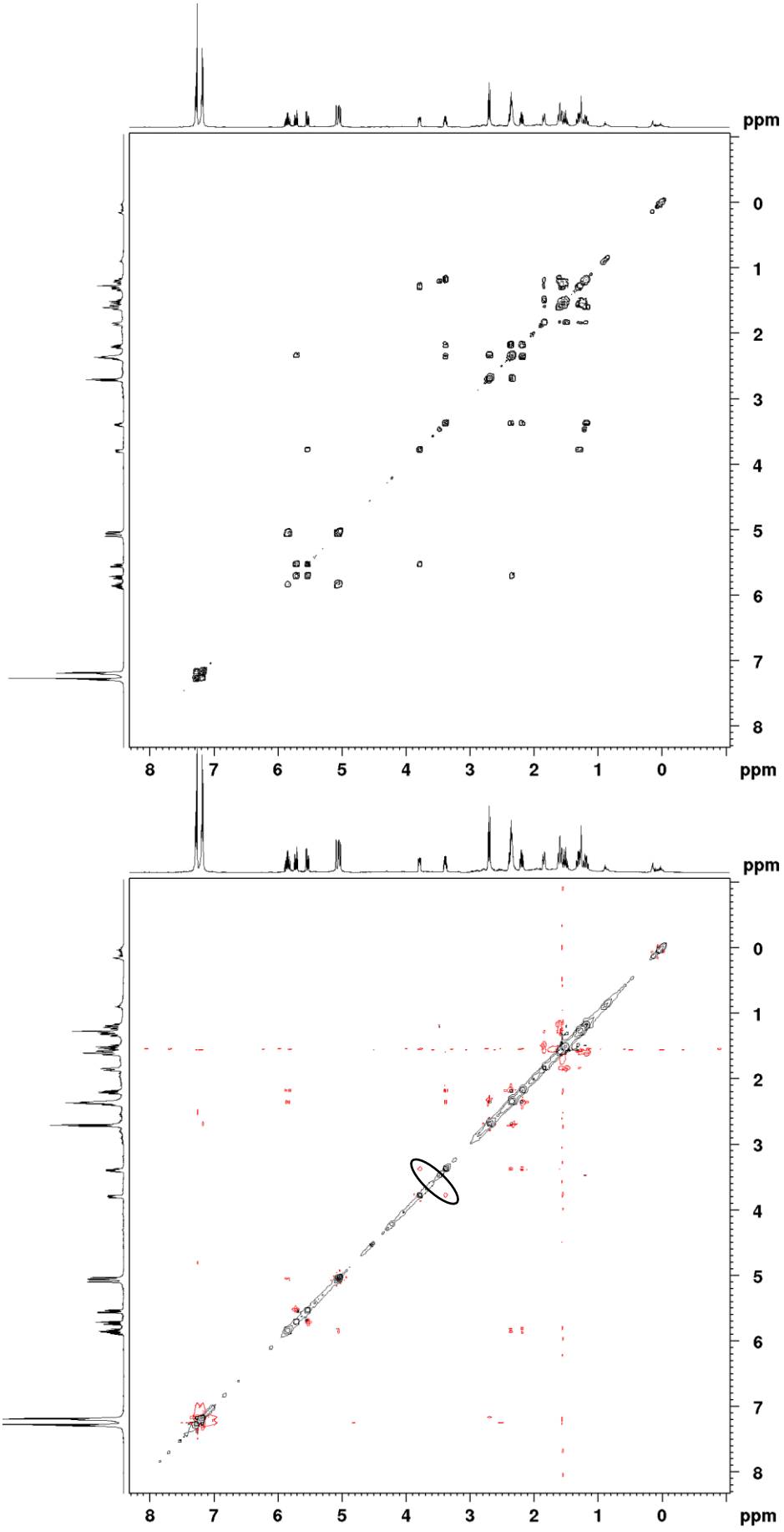

^{1}H NMR·

$CDCl_3$, 300 MHz

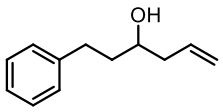

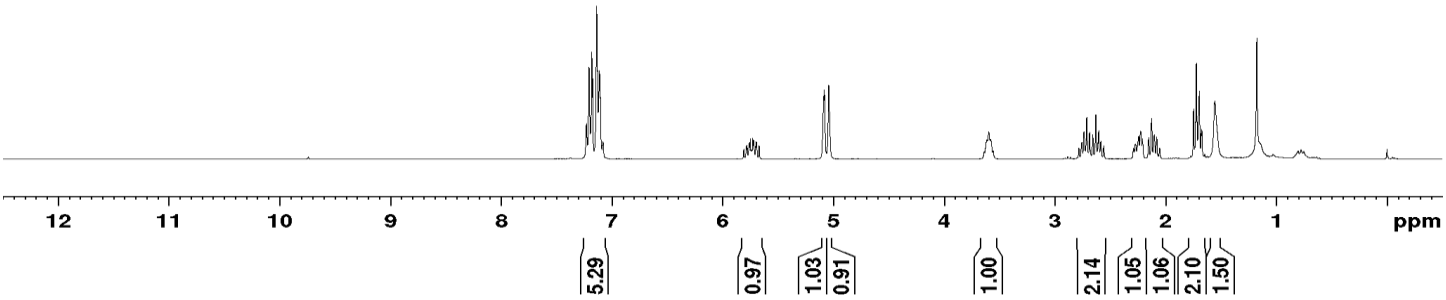

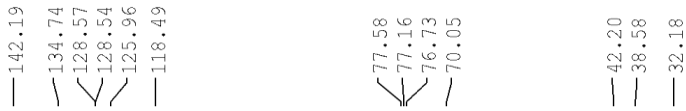

^{13}C NMR

$CDCl_3$, 75 MHz

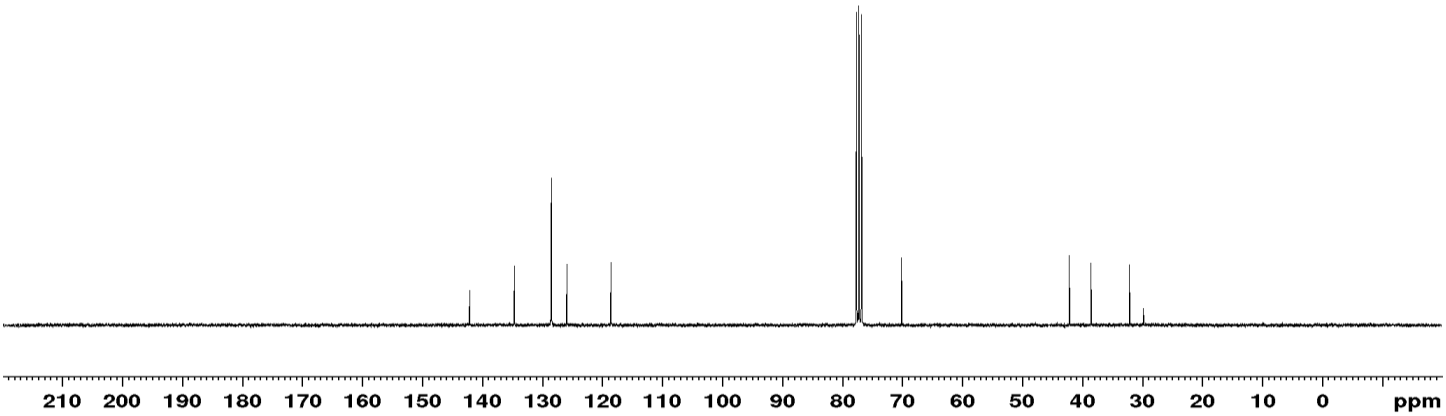

^{1}H NMR
$CDCl_3$, 500 MHz

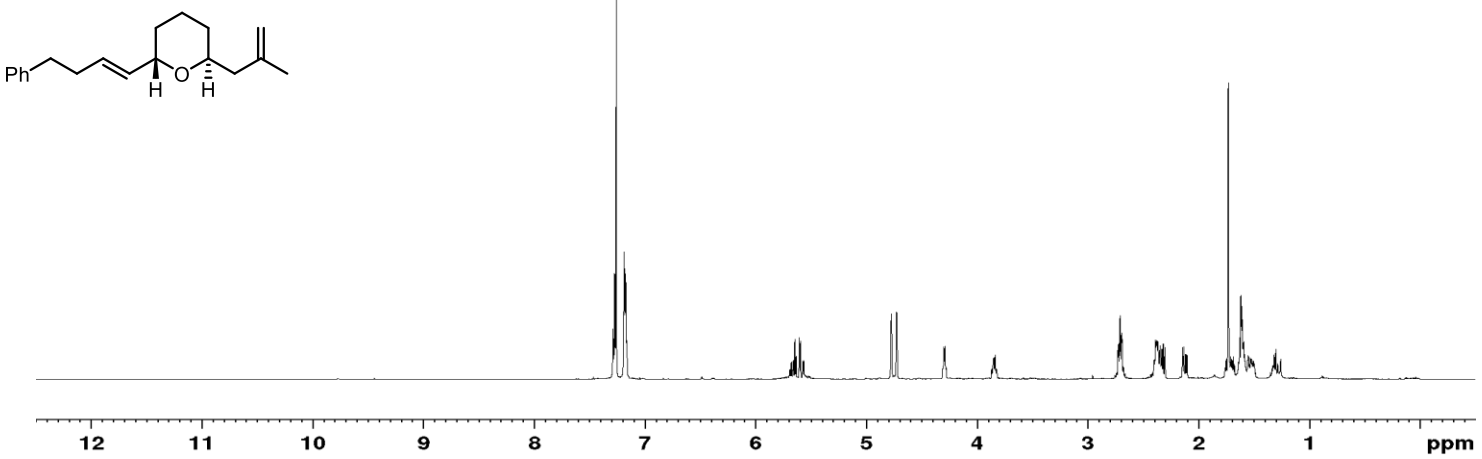

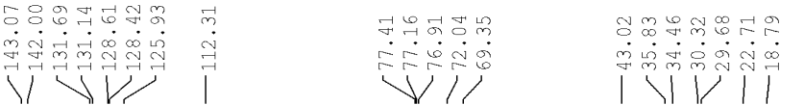

^{13}C NMR
$CDCl_3$, 125 MHz

NOESY
$CDCl_3$, 500 MHz

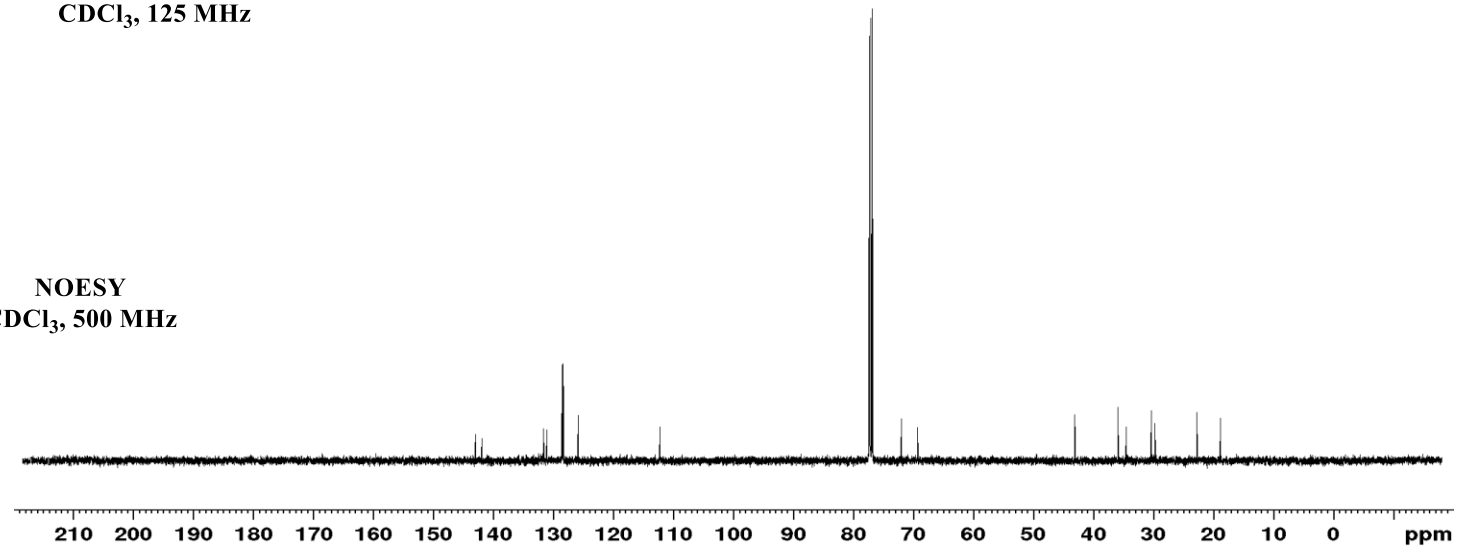

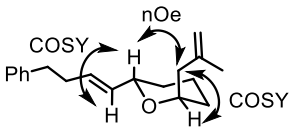

HH COSY
$CDCl_3$, 500 MHz

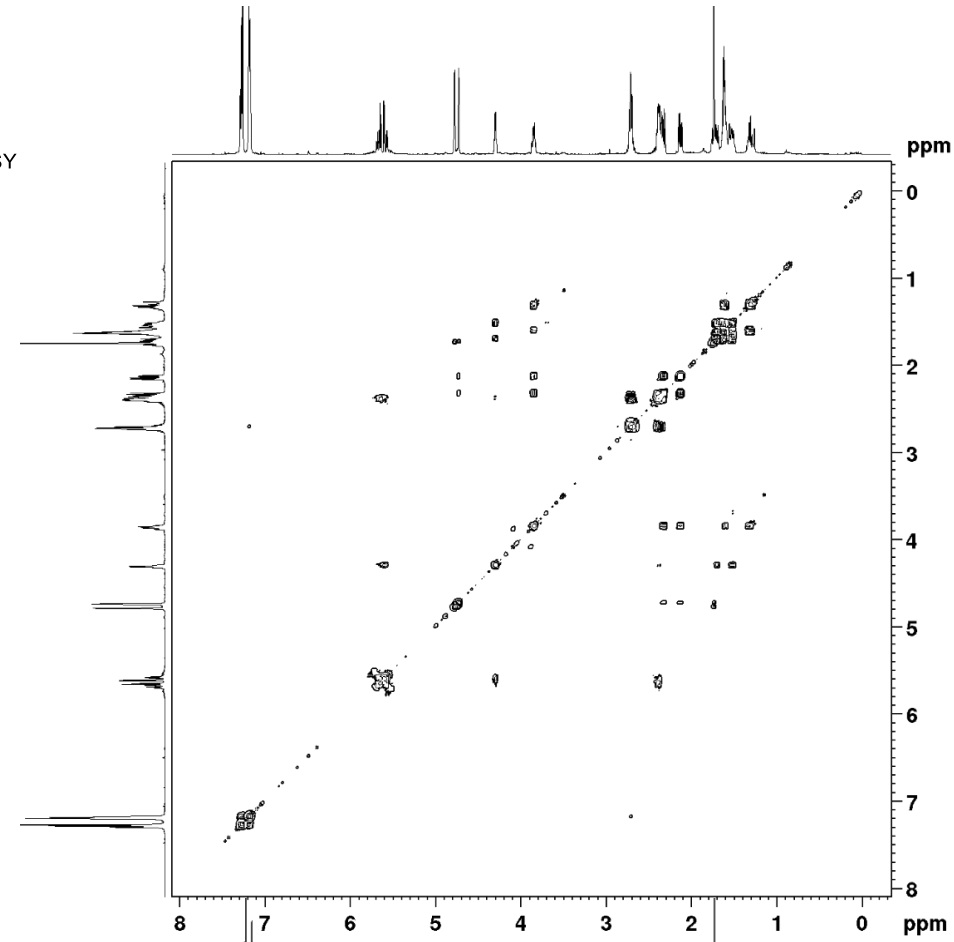

NOESY
$CDCl_3$, 500 MHz

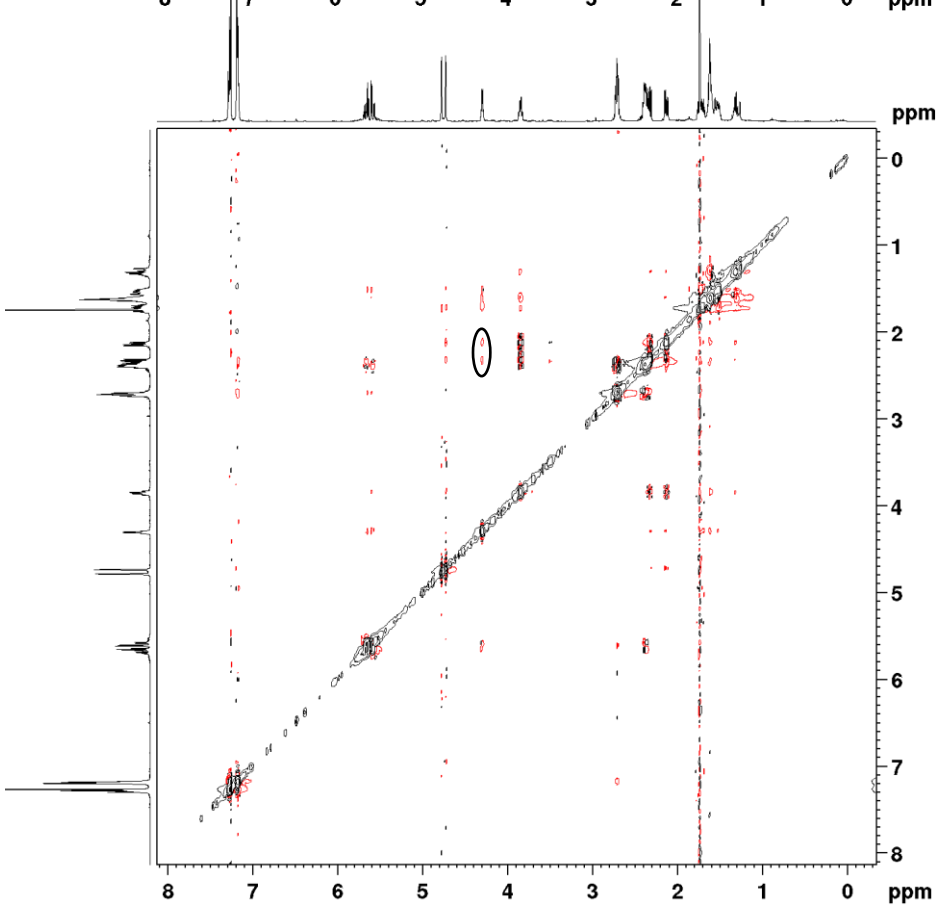

^{1}H NMR
$CDCl_3$, 300 MHz

3.44

^{13}C NMR
$CDCl_3$, 75 MHz

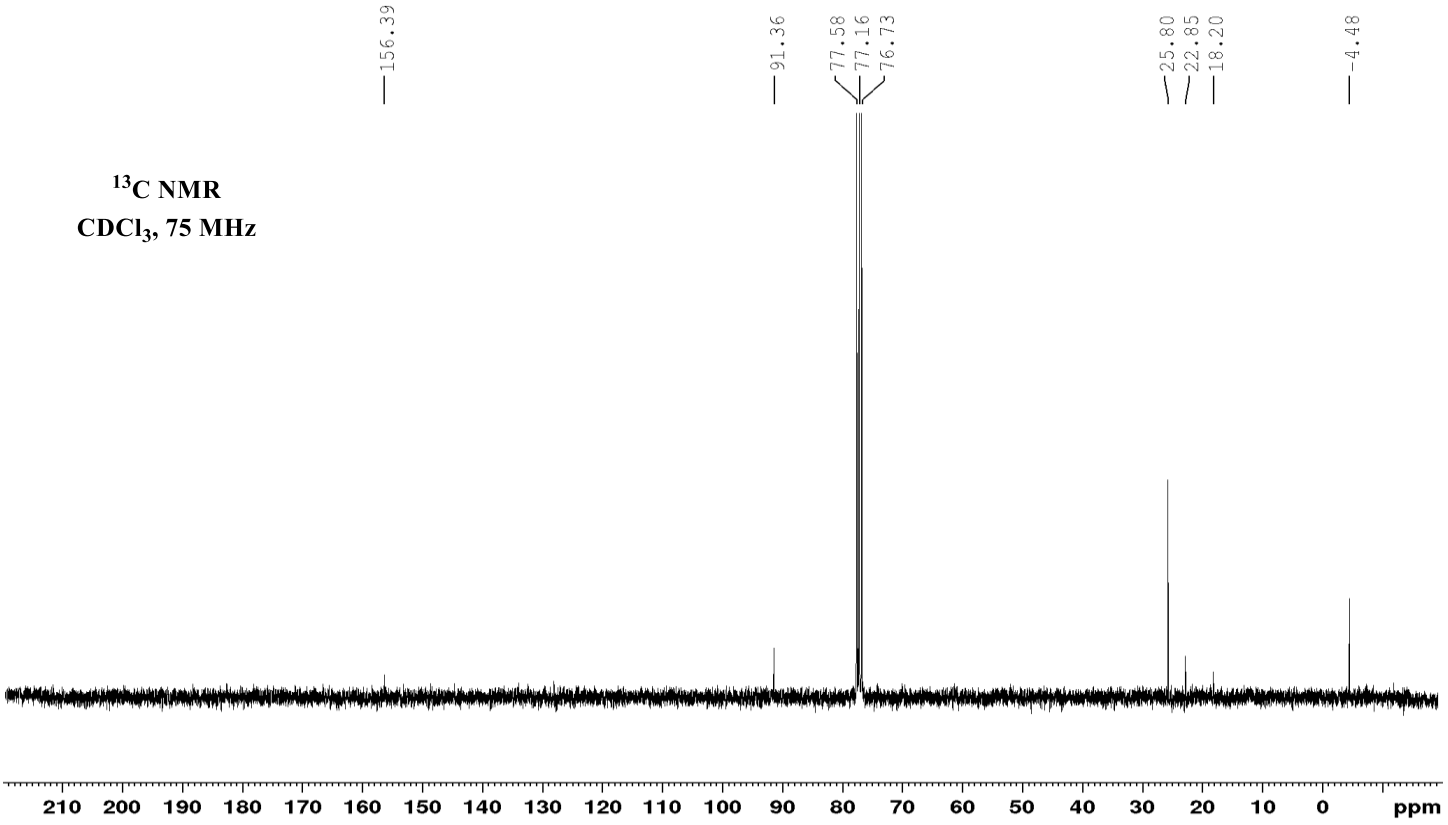

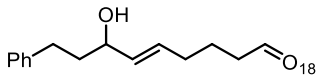
OH
Ph
O18

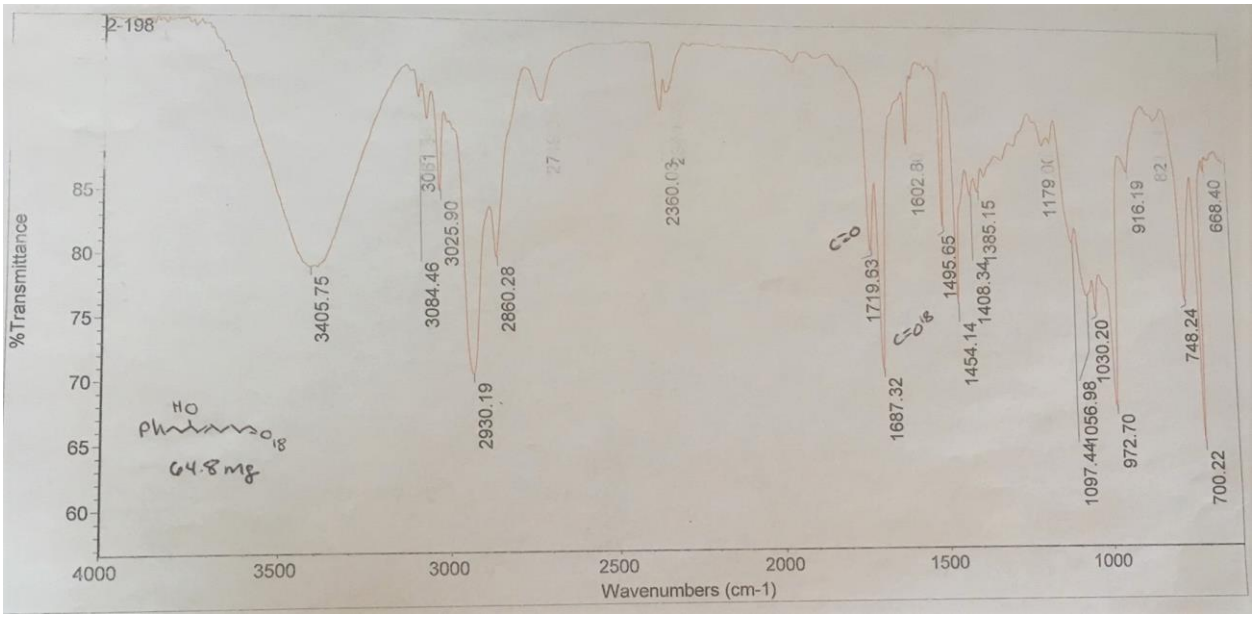
2-198
%Transmittance
85
80
75
70
65
60
4000
3500
3000
2500
2000
1500
1000
Wavenumbers (cm-1)
3405.75
3084.46
3061
3025.90
2930.19
2860.28
2360.03
1719.63
C=O
1687.32
C=O
1602.8
1495.65
1454.14
1408.34
1385.15
1179.0
1097.44
1056.98
1030.20
972.70
916.19
748.24
700.22
668.40
HO
Ph
O18
64.8mg

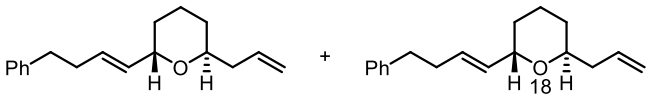

C:\Xcalibur\data\Floreancig\80558ESIPN 09/25/18 15:37:28 SA-2-215

80558ESIPN#19-41 RT: 0.18-0.40 AV: 12
T: FTMS + p ESI Full ms [100.0000-1500.0000]
m/z= 257.00000-258.00000

m/z	Intensity	Relative	Theo. Mass	Delta (ppm)	Composition
257.19041	746163712.0	100.00	257.18999	0.42	$C_{18}H_{25}O$

80558ESIPN#19-41 RT: 0.18-0.40 AV: 12
T: FTMS + p ESI Full ms [100.0000-1500.0000]
m/z= 259.00000-260.00000

m/z	Intensity	Relative	Theo. Mass	Delta (ppm)	Composition
259.19494	217471376.0	100.00	259.19424	0.70	$C_{18}H_{25}{}^{18}O$

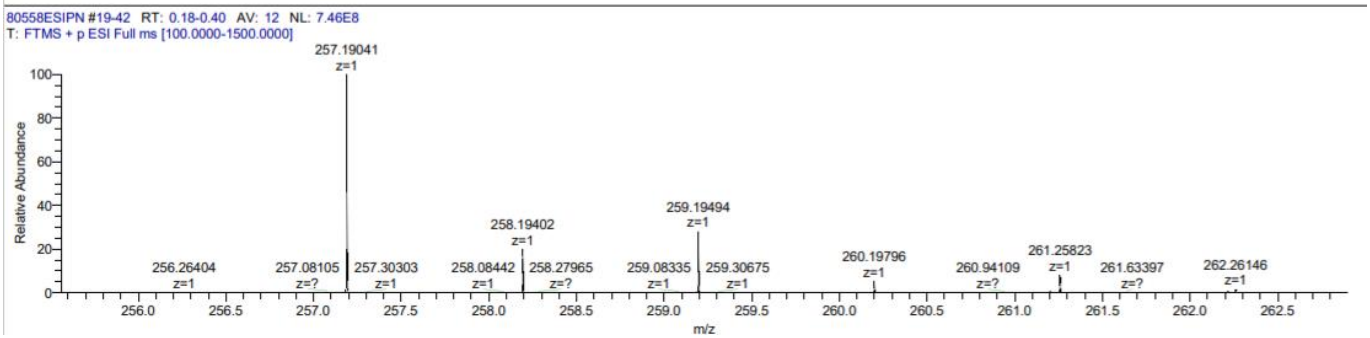

^{1}H NMR
$CDCl_3$, 500 MHz

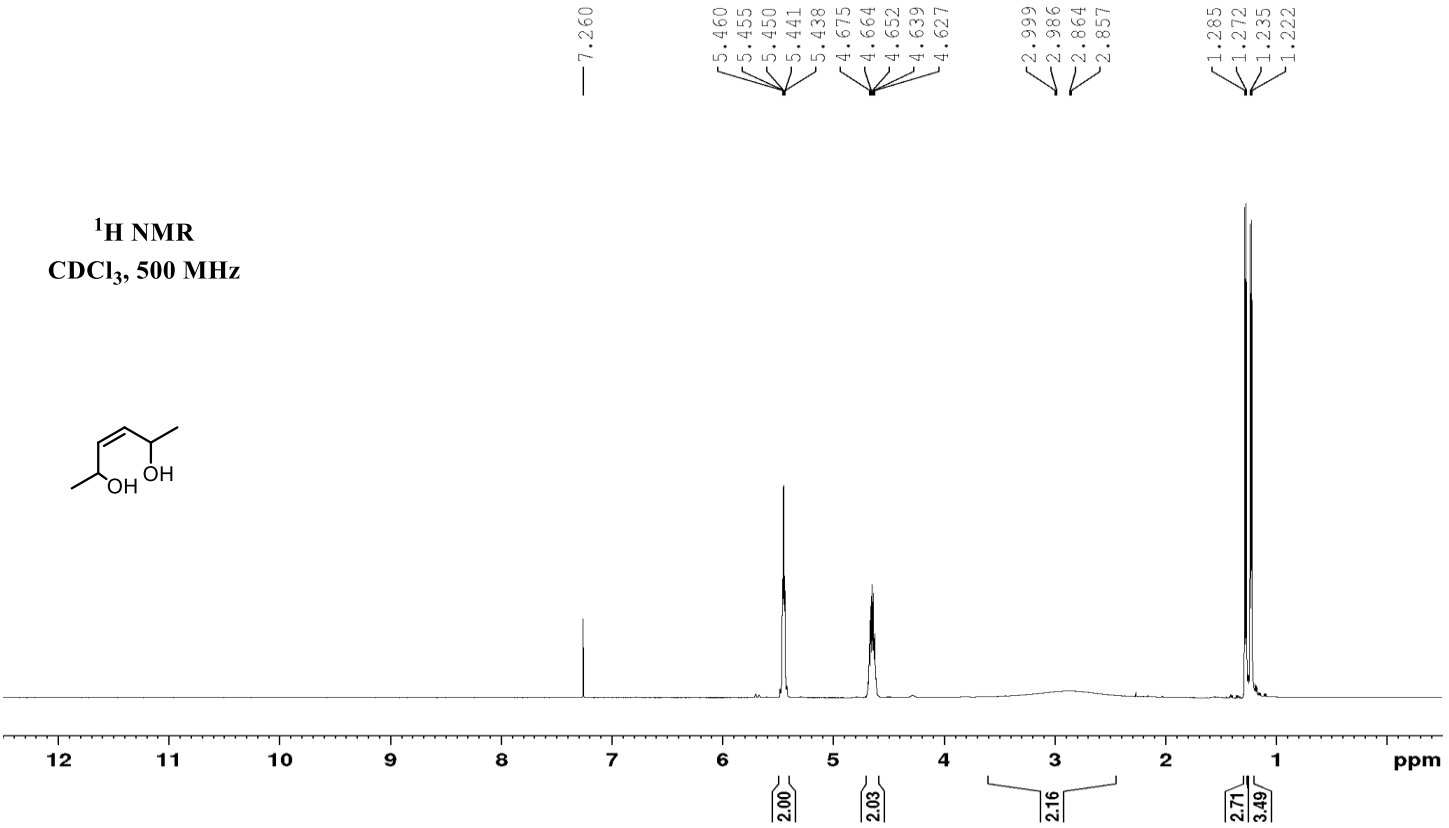

^{13}C NMR
$CDCl_3$, 125 MHz

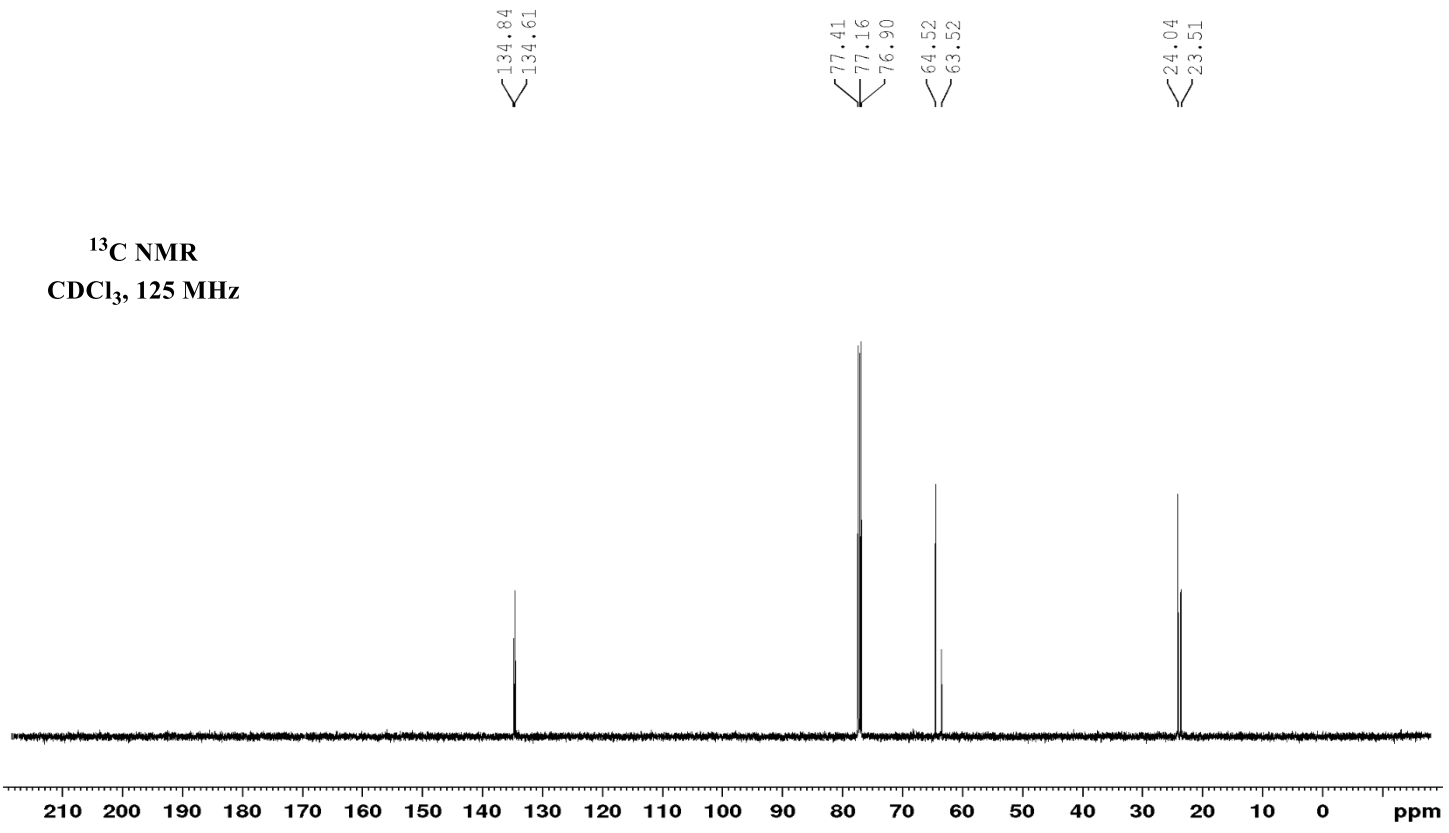

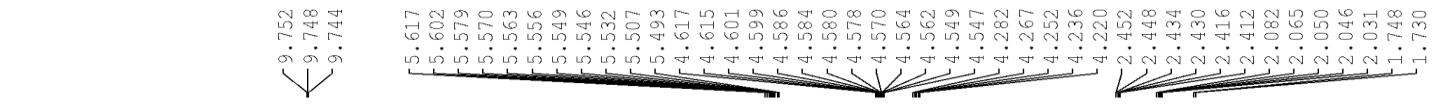

^{1}H NMR
$CDCl_3$, 400 MHz

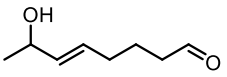

10:1 E/Z

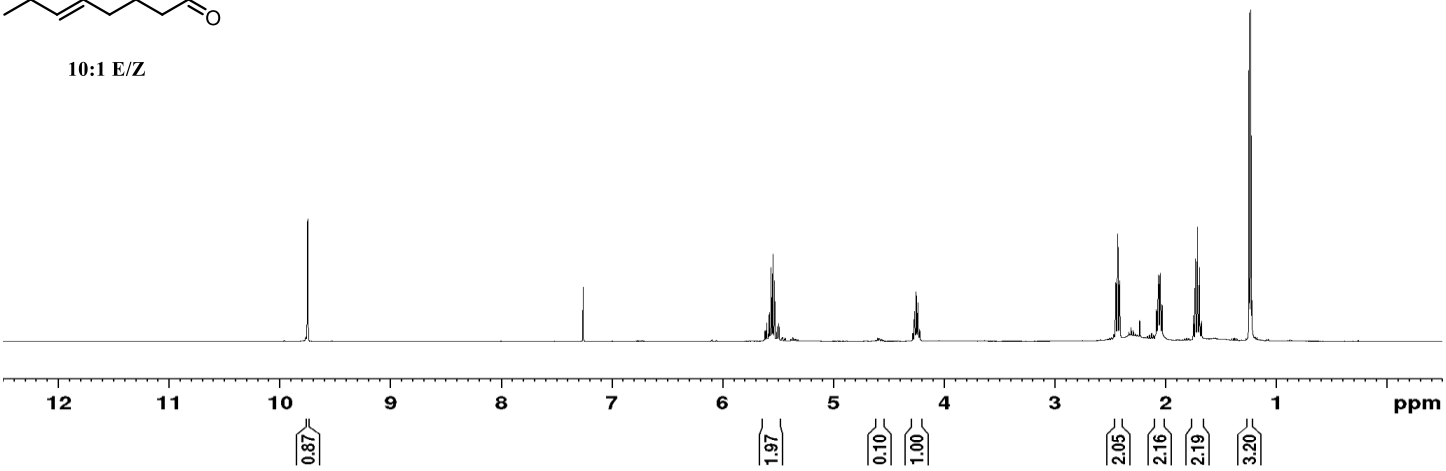

^{13}C NMR
$CDCl_3$, 100 MHz

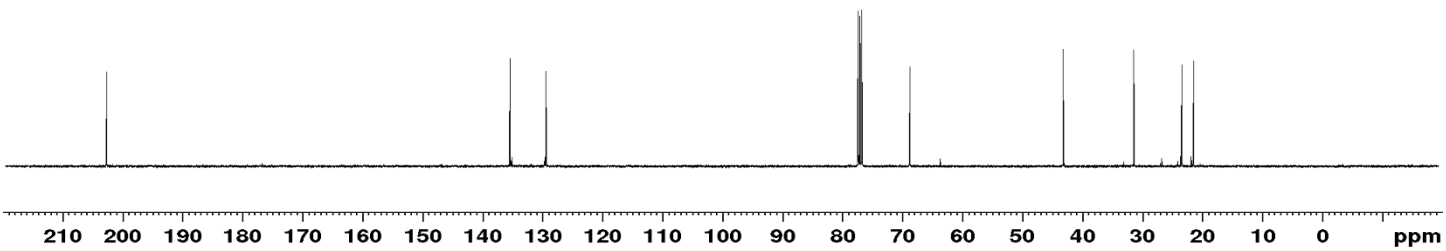

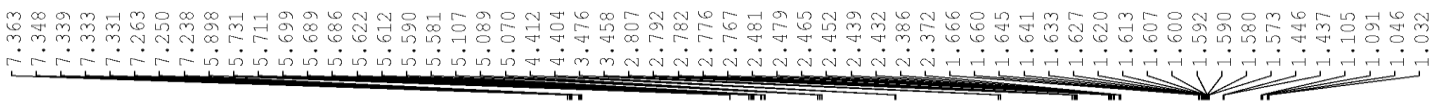

^{1}H NMR
$CDCl_3$, 500 MHz

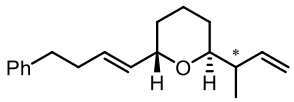

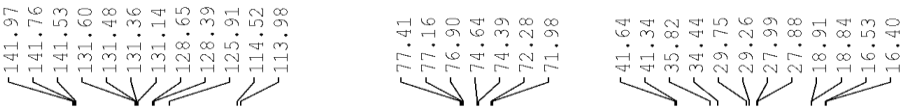

^{13}C NMR
$CDCl_3$, 125 MHz

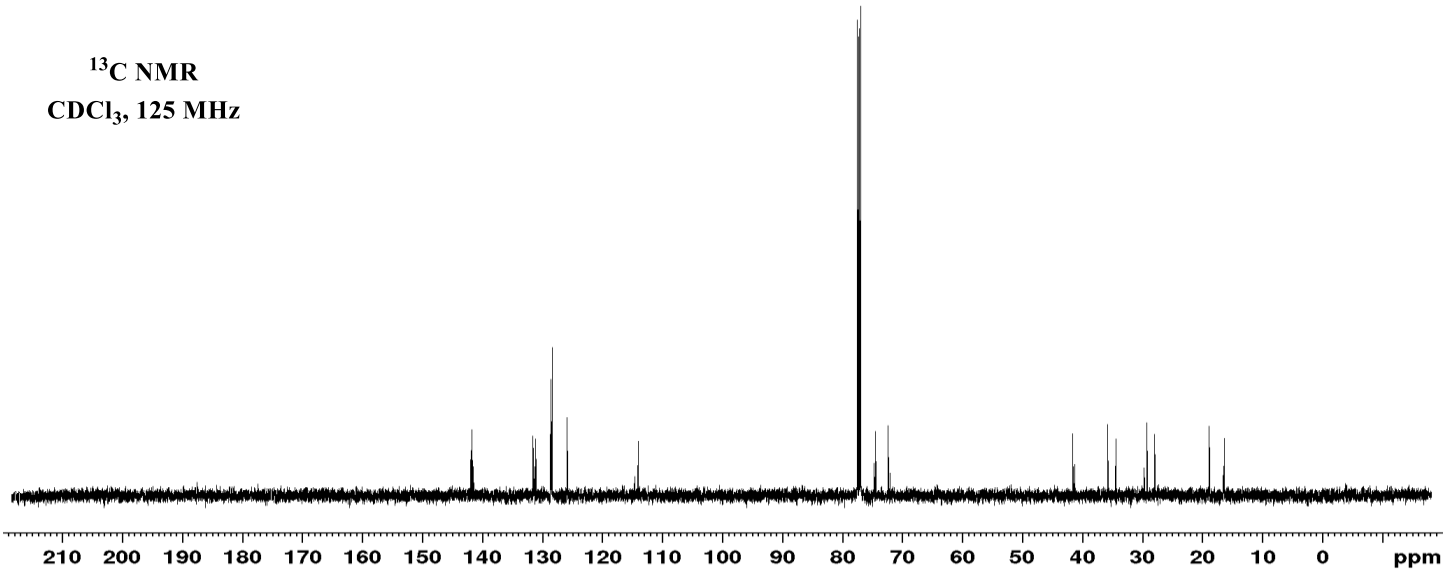

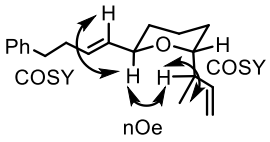

HH COSY
$CDCl_3$, 500 MHz

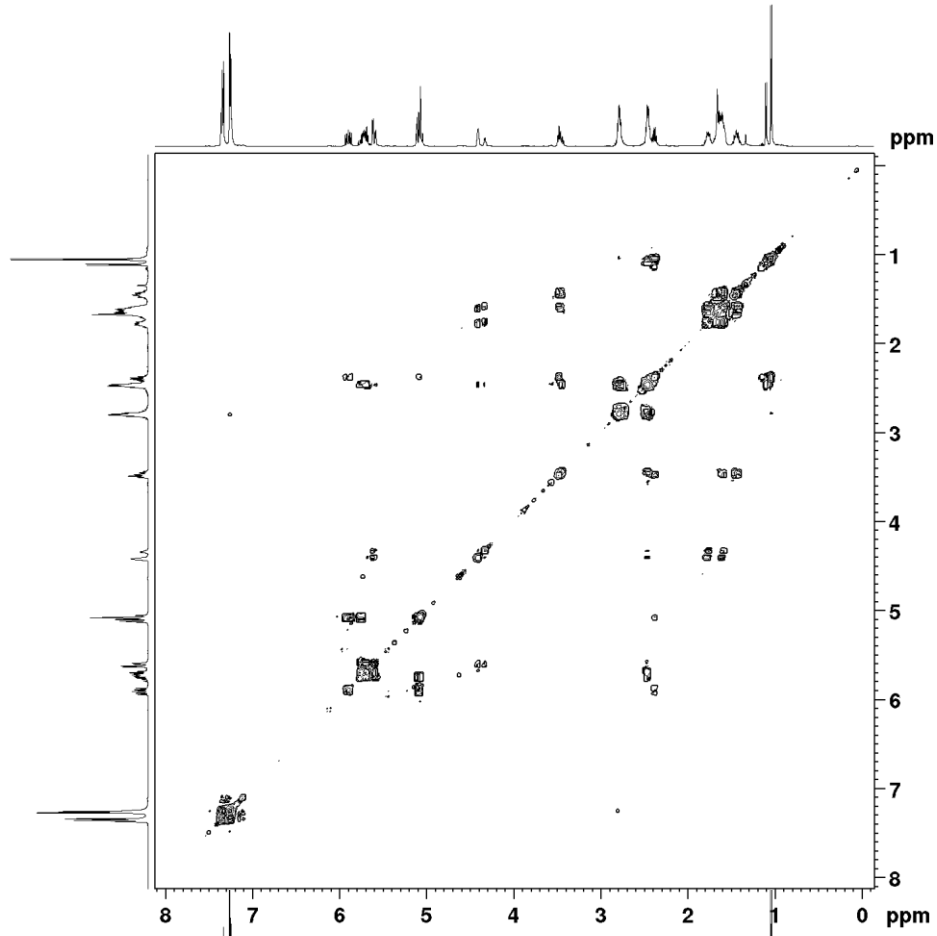

NOESY
$CDCl_3$, 500 MHz

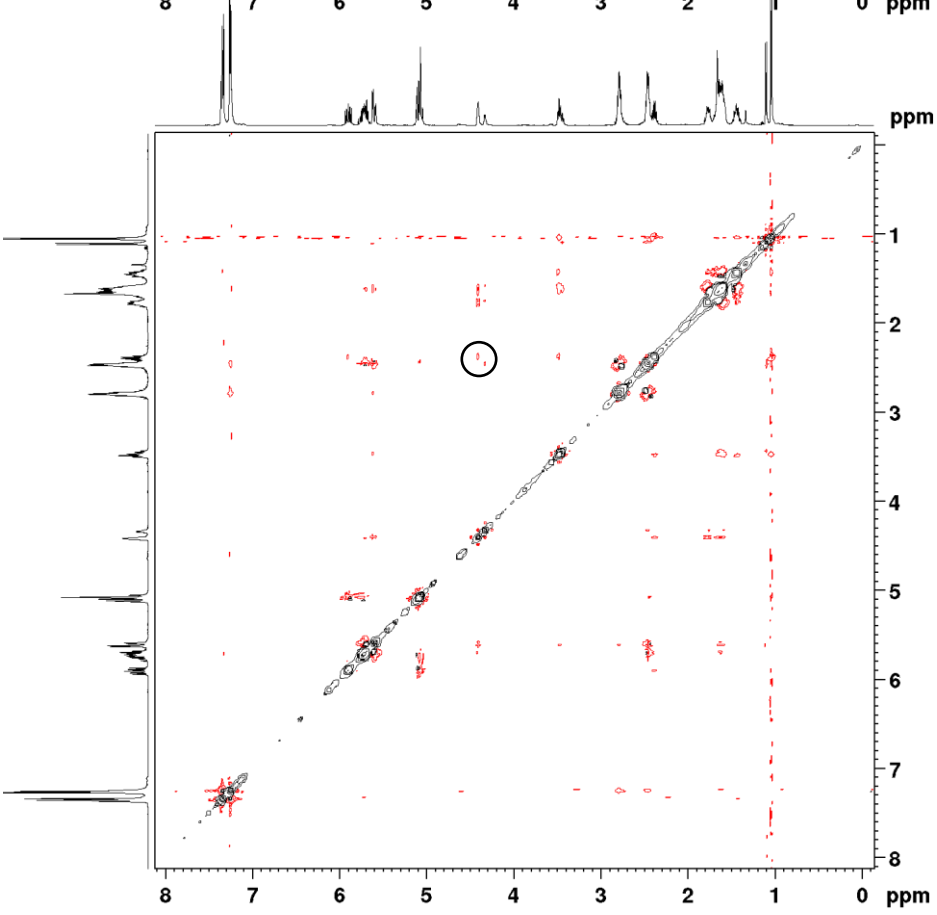

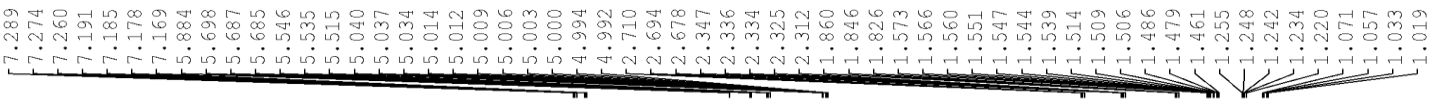

^{1}H NMR

$CDCl_3$, 500 MHz

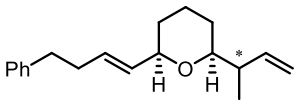

^{13}C NMR

$CDCl_3$, 125 MHz

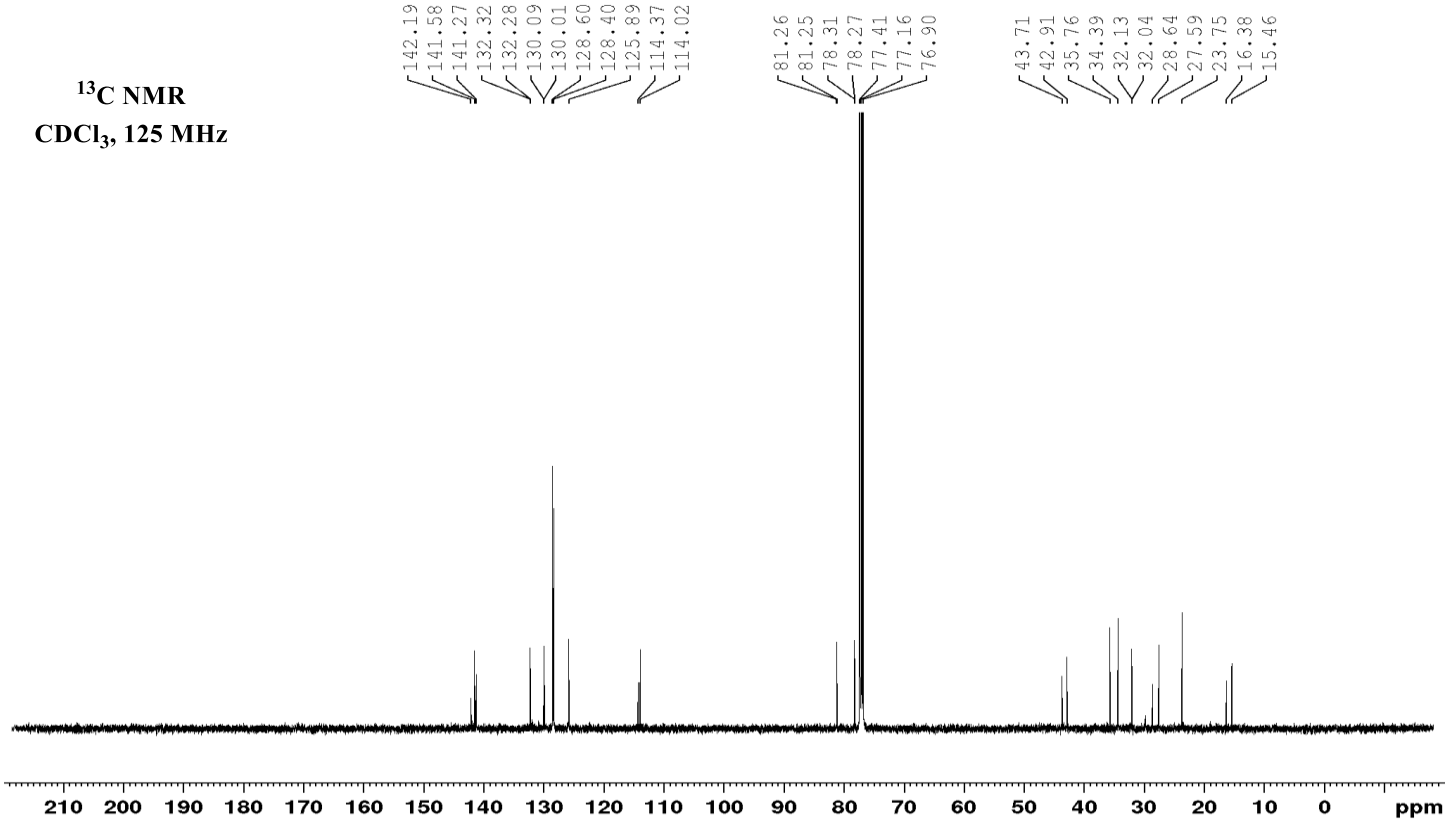

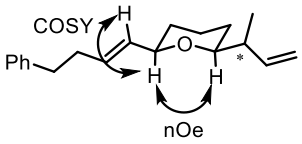

HH COSY
$CDCl_3$, 500 MHz

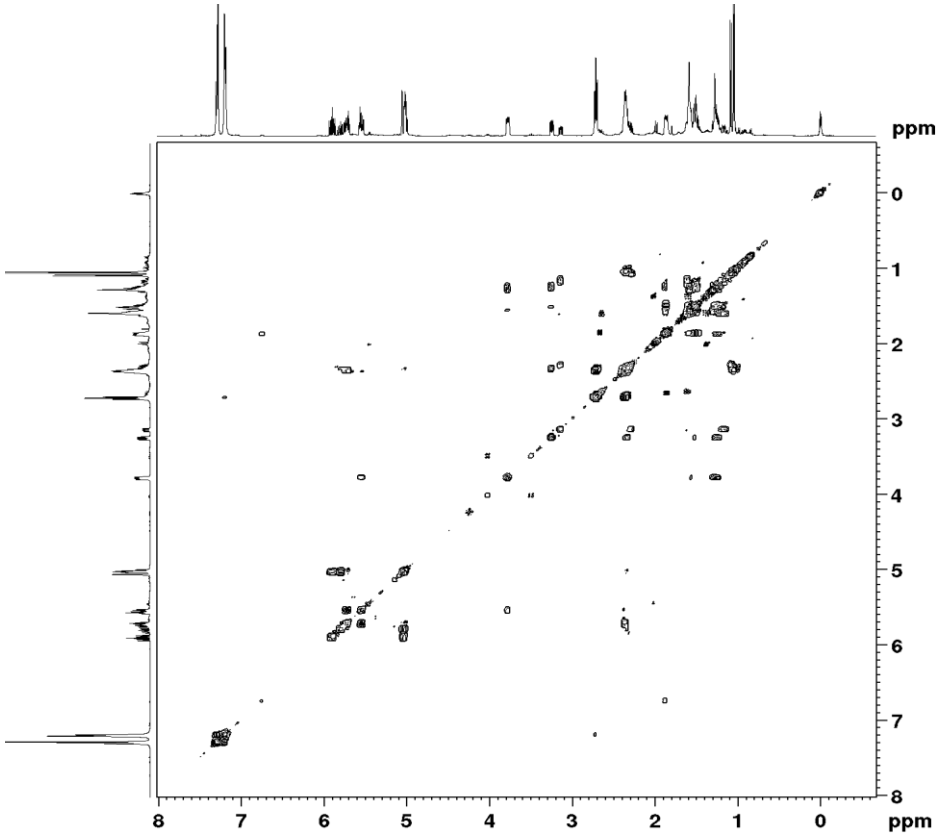

NOESY
$CDCl_3$, 500 MHz

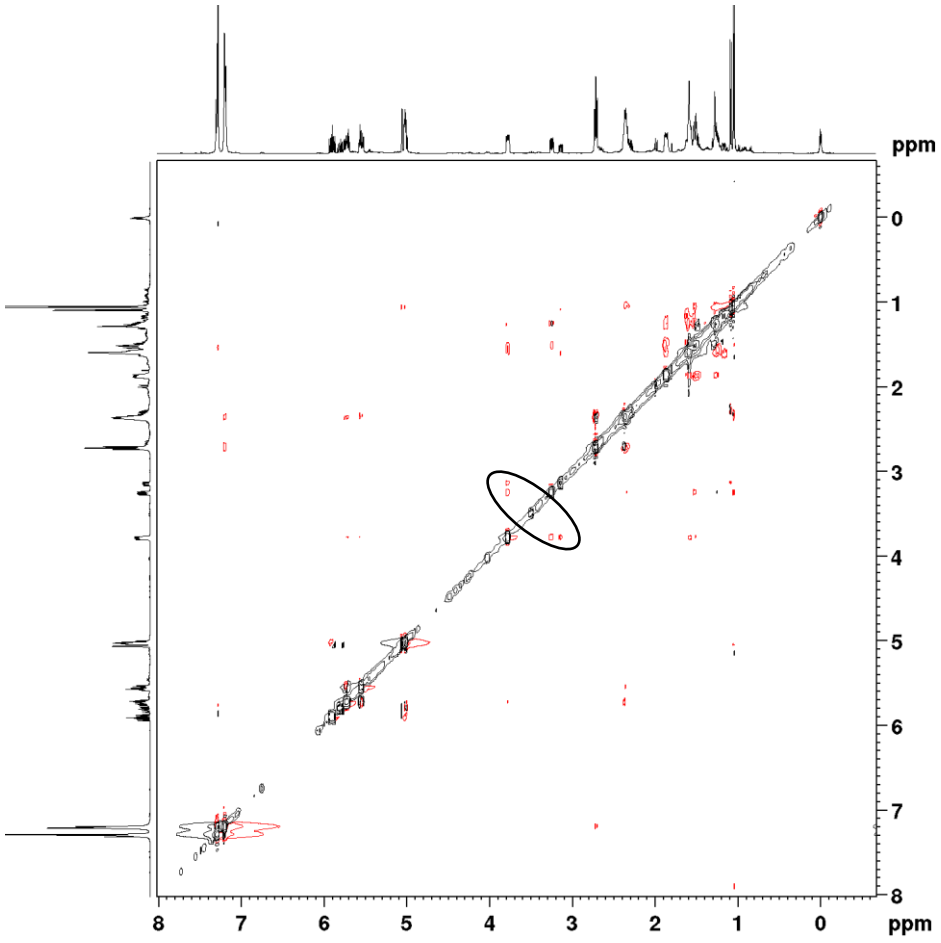

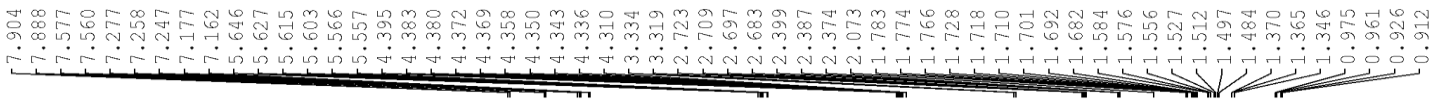

^{1}H NMR
$CDCl_3$, 500 MHz

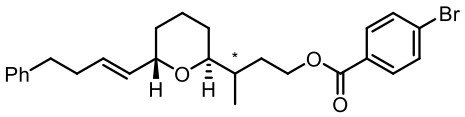

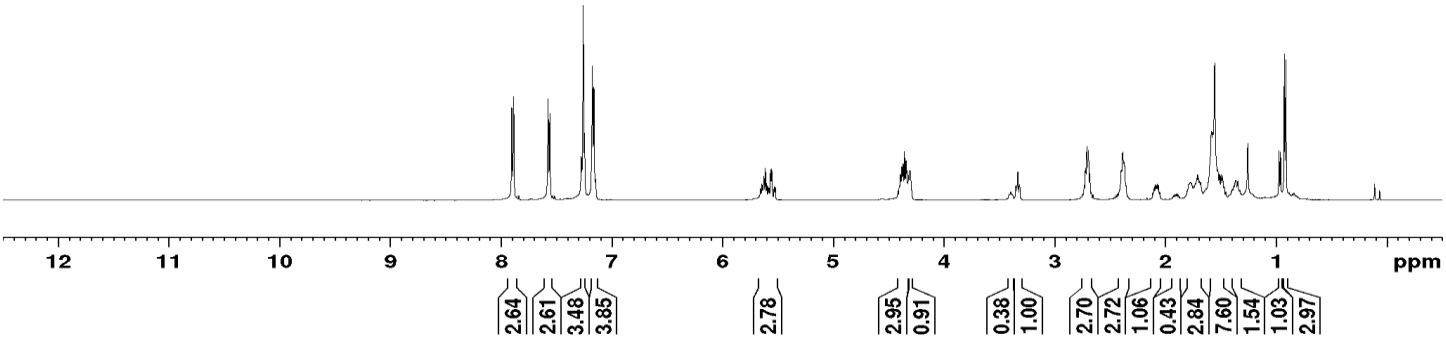

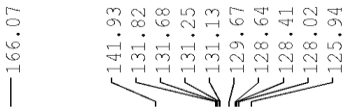

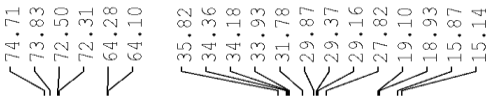

^{13}C NMR
$CDCl_3$, 125 MHz

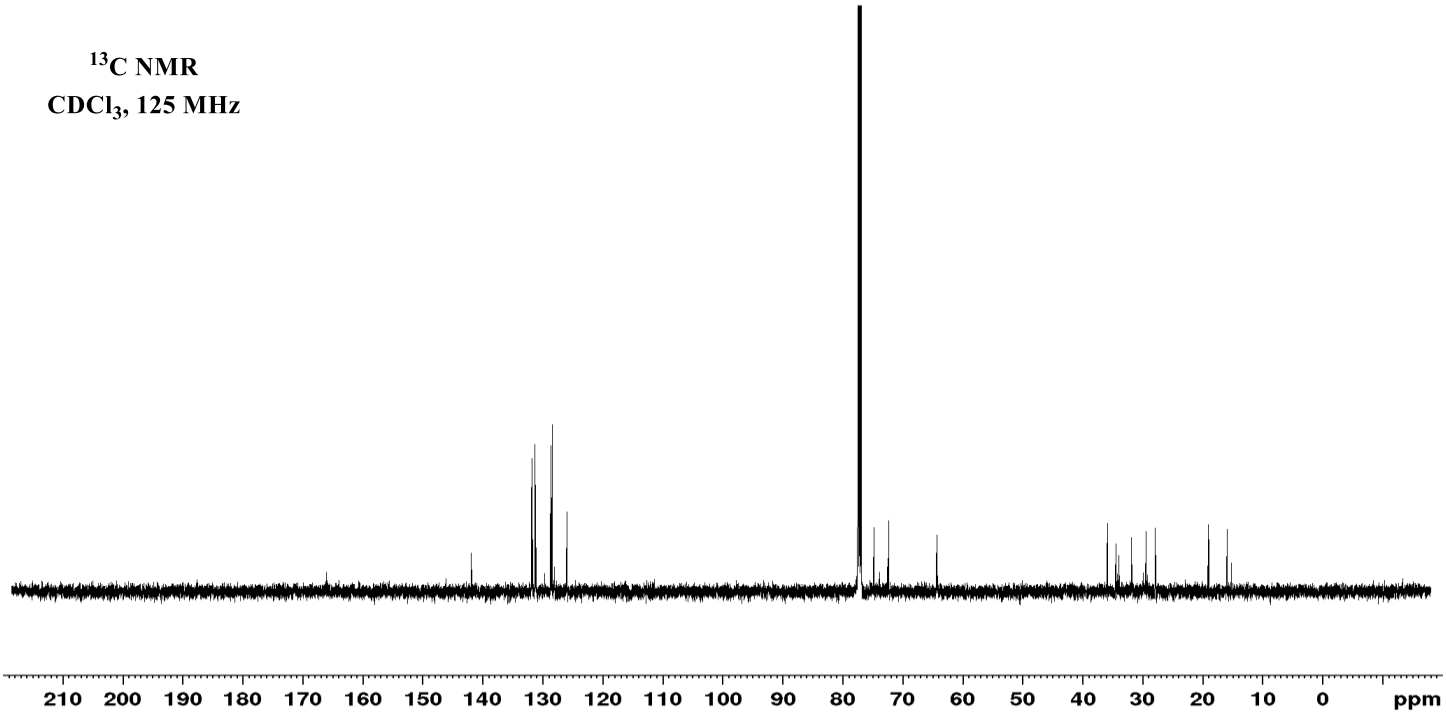

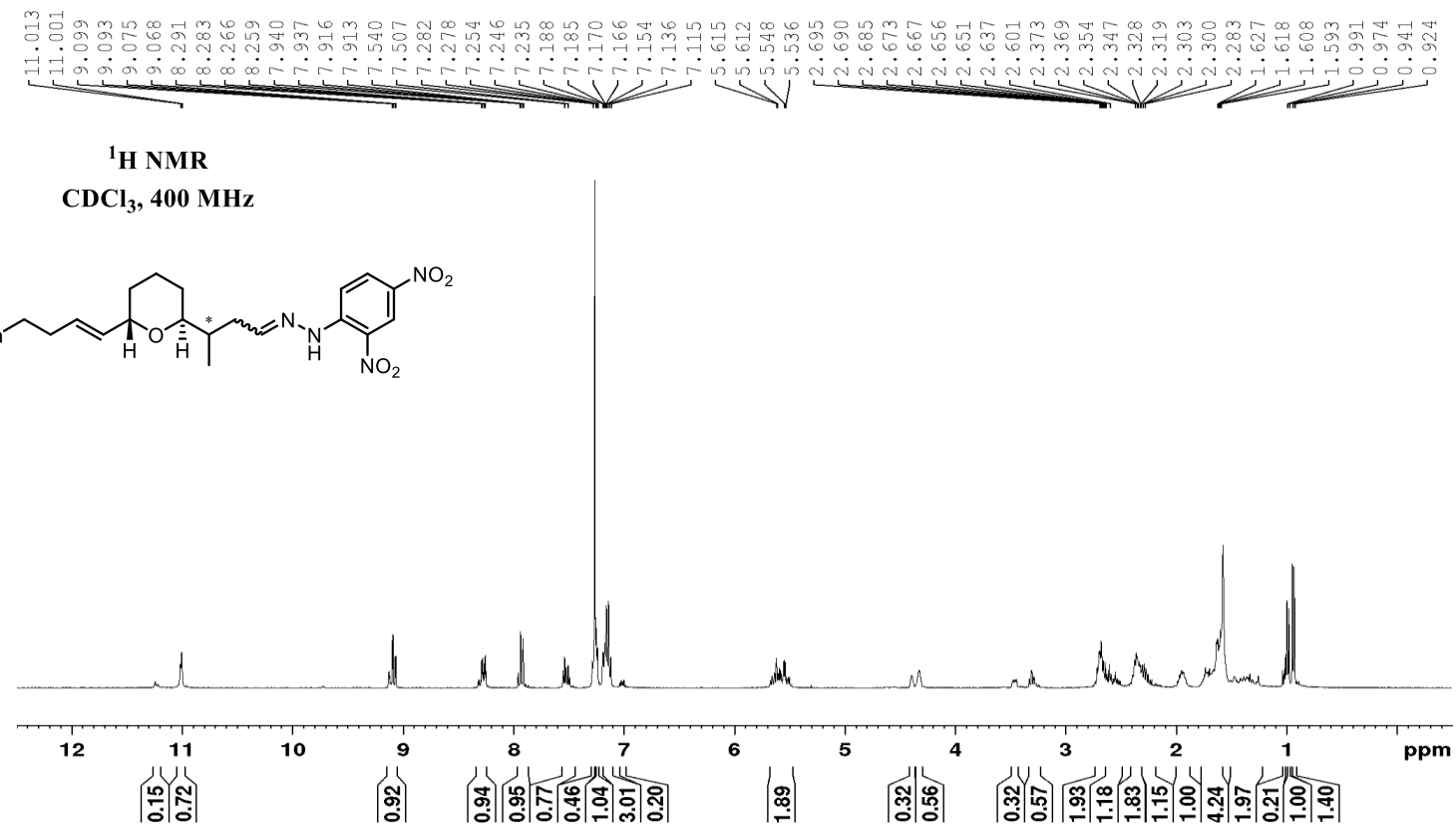
11.013
11.001
9.099
9.093
9.075
9.068
8.291
8.283
8.266
8.259
7.940
7.937
7.916
7.913
7.540
7.507
7.282
7.278
7.254
7.246
7.235
7.188
7.185
7.170
7.166
7.154
7.136
7.115
5.615
5.612
5.548
5.536
2.695
2.690
2.685
2.673
2.667
2.656
2.651
2.637
2.601
2.373
2.369
2.354
2.347
2.328
2.319
2.303
2.300
2.283
1.627
1.618
1.608
1.593
0.991
0.974
0.941
0.924
1H NMR
CDCl3, 400 MHz
Ph
O
H
H
N
N
H
NO2
NO2
12
11
10
9
8
7
6
5
4
3
2
1
ppm
0.15
0.72
0.92
0.94
0.95
0.77
0.46
1.04
3.01
0.20
1.89
0.32
0.56
0.32
0.57
1.93
1.18
1.83
1.15
1.00
4.24
1.97
0.21
1.00
1.40

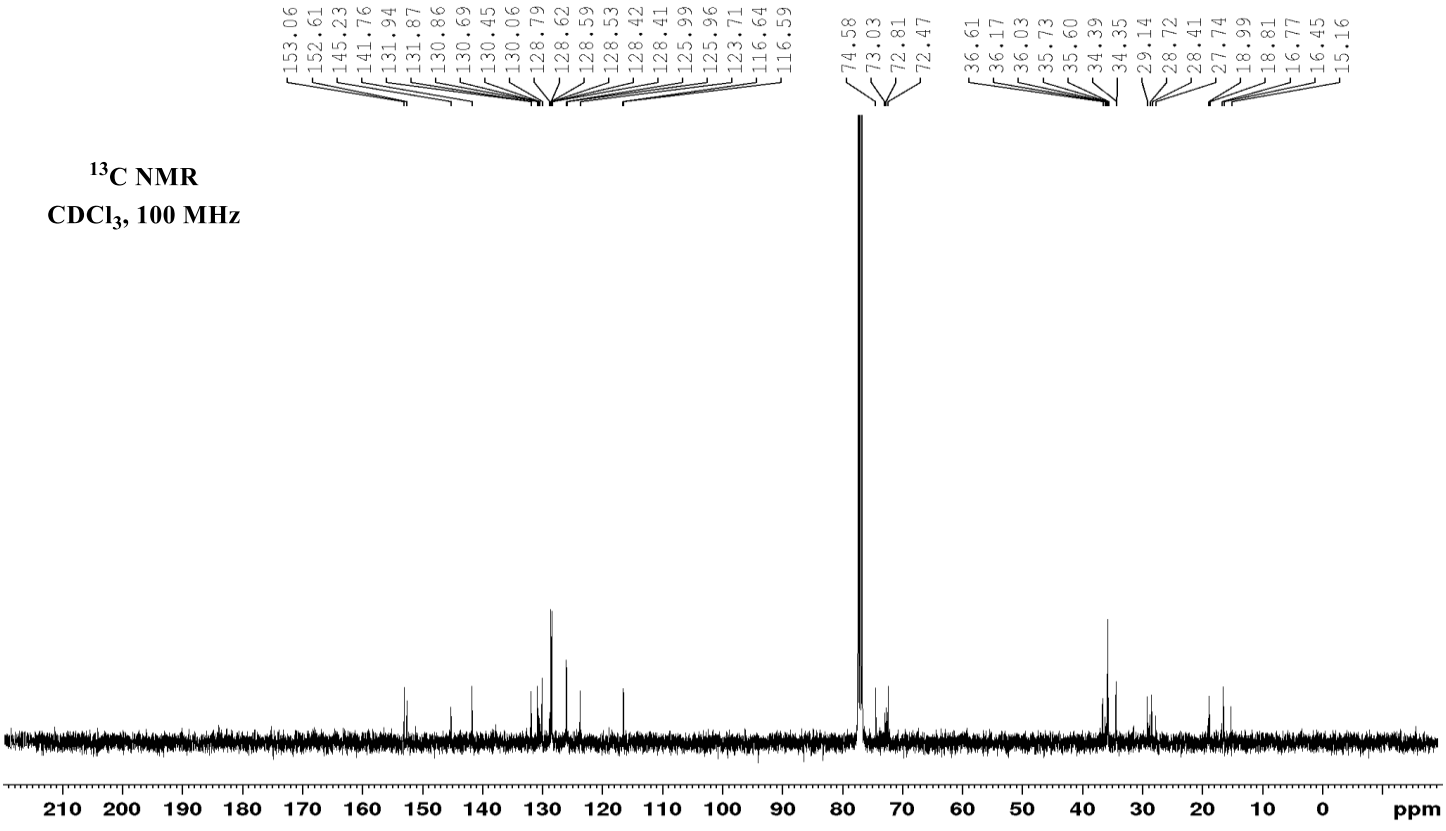
153.06
152.61
145.23
141.76
131.94
131.87
130.86
130.69
130.45
130.06
128.79
128.62
128.59
128.53
128.42
128.41
125.99
125.96
123.71
116.64
116.59
74.58
73.03
72.81
72.47
36.61
36.17
36.03
35.73
35.60
34.39
34.35
29.14
28.72
28.41
27.74
18.99
18.81
16.77
16.45
15.16
13C NMR
CDCl3, 100 MHz
210
200
190
180
170
160
150
140
130
120
110
100
90
80
70
60
50
40
30
20
10
0
ppm

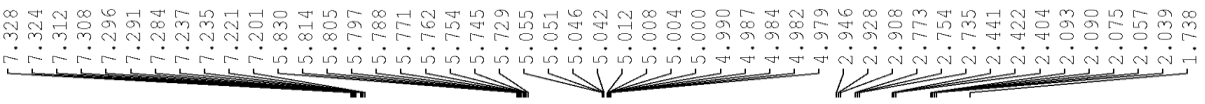

^{1}H NMR
$CDCl_3$, 400 MHz

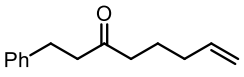

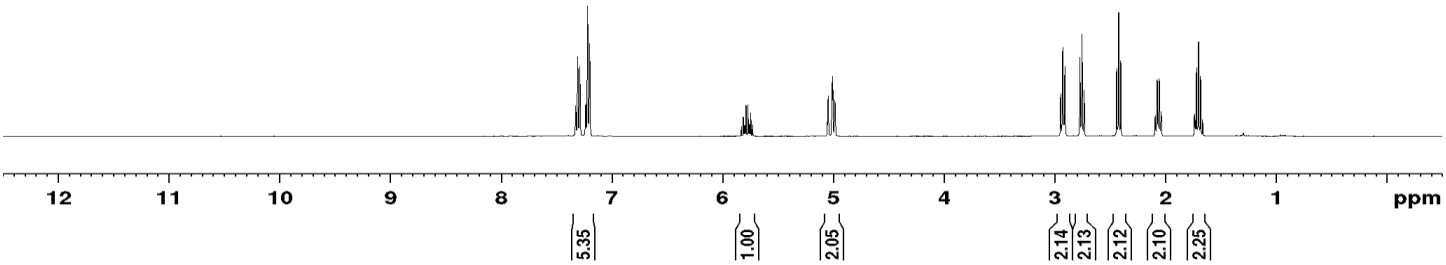

^{13}C NMR
$CDCl_3$, 100 MHz

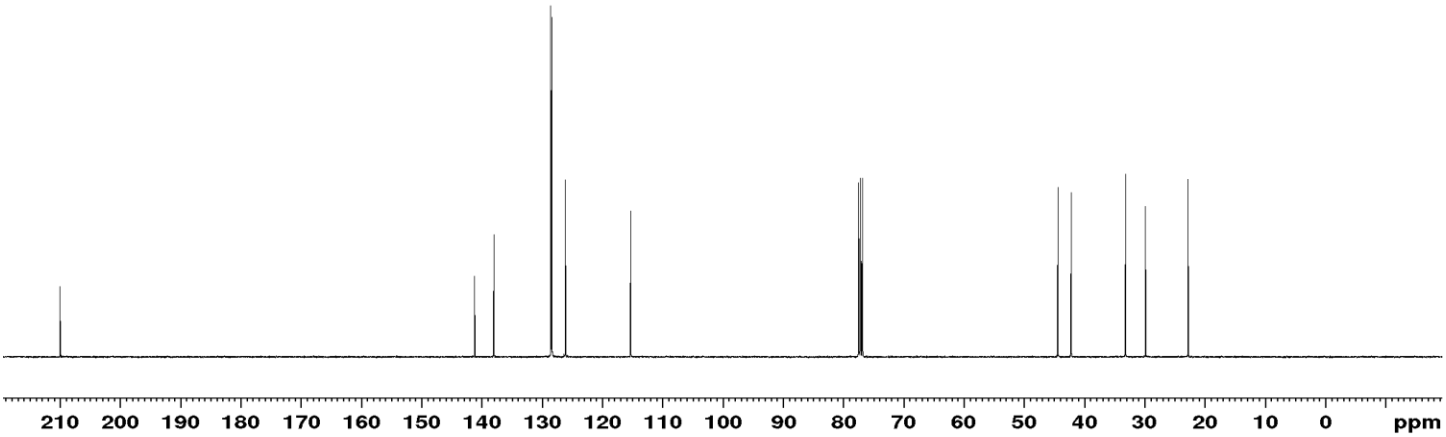

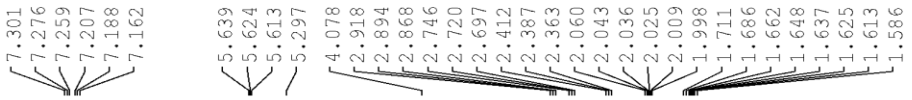

^{1}H NMR
$CDCl_3$, 400 MHz

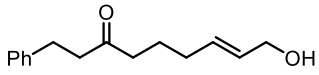

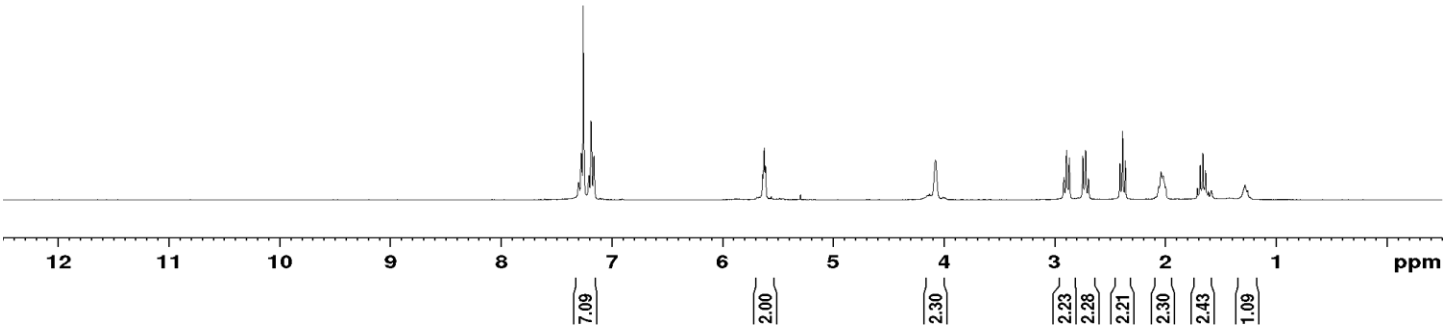

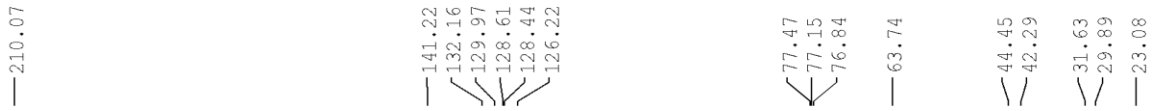

^{13}C NMR
$CDCl_3$, 100 MHz

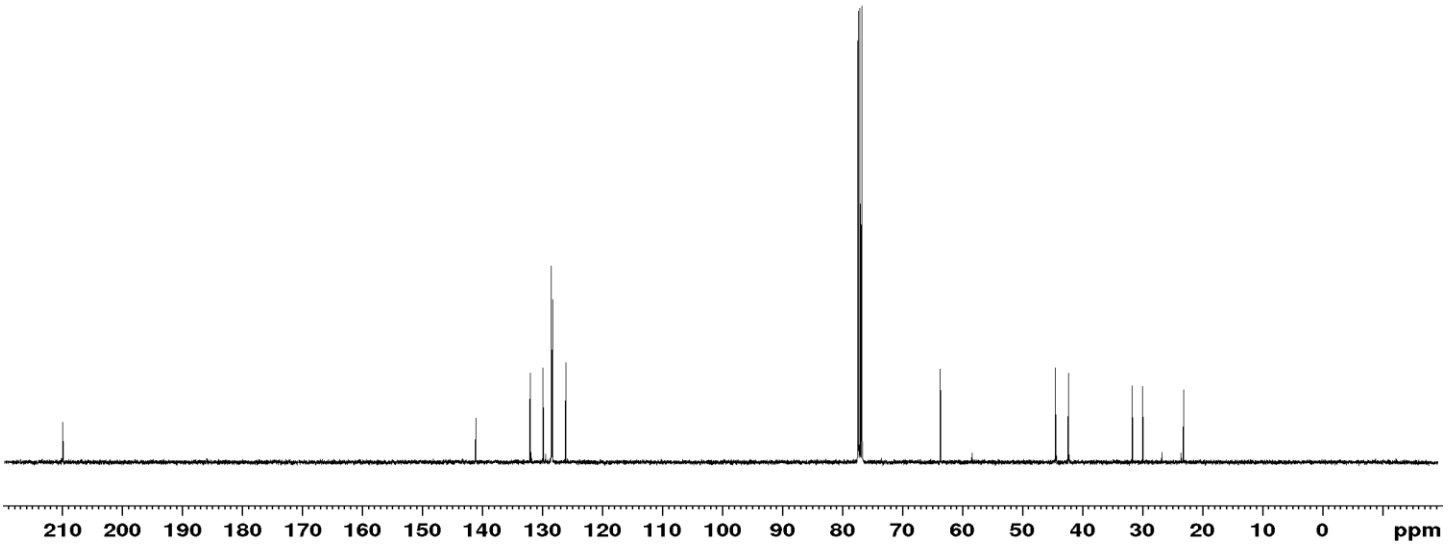

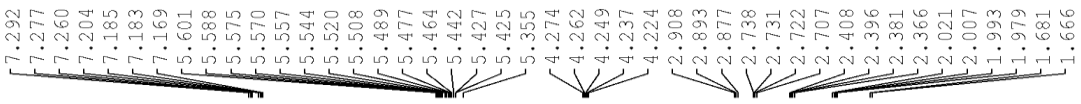

^{1}H NMR
$CDCl_3$, 500 MHz

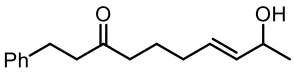

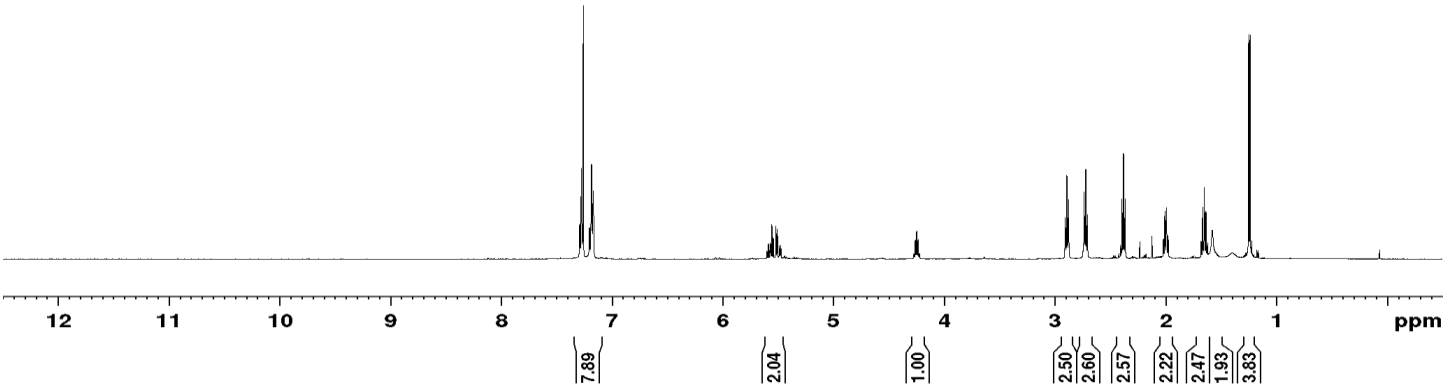

^{13}C NMR
$CDCl_3$, 125 MHz

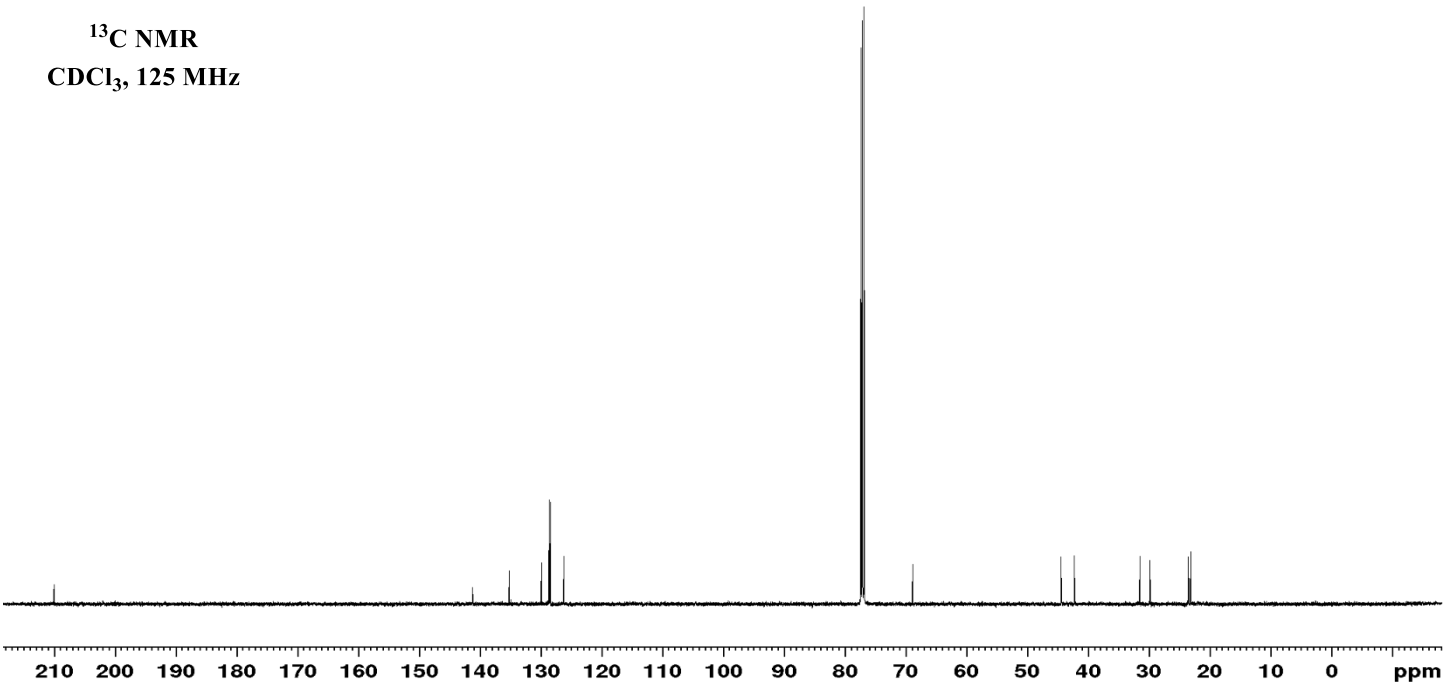

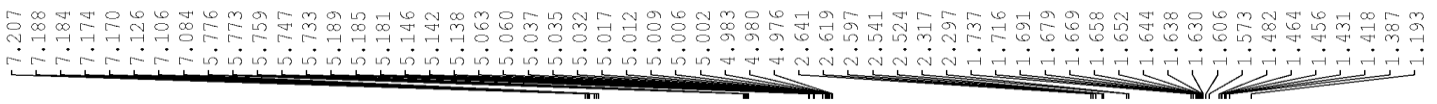

^{1}H NMR

$CDCl_3$, 400 MHz

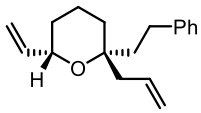

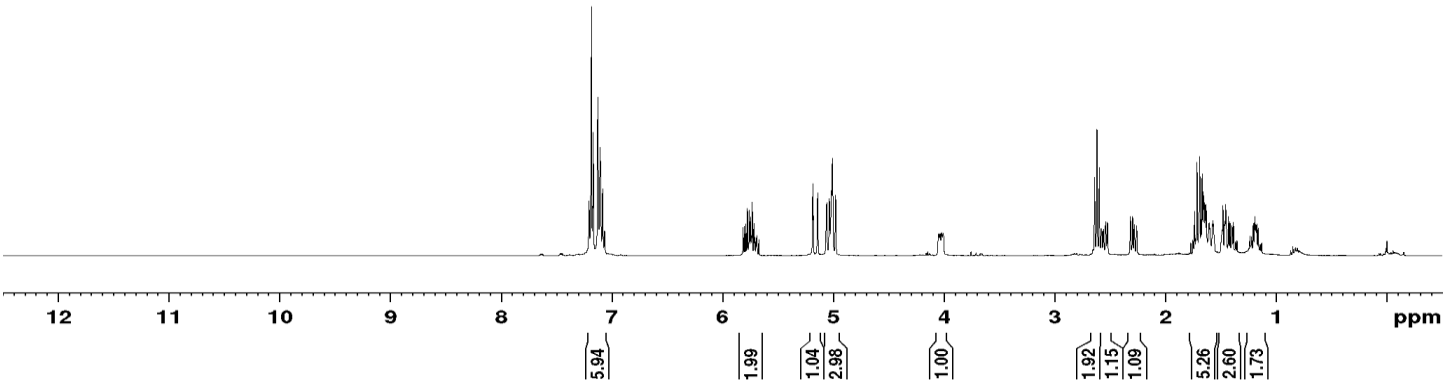

^{13}C NMR

$CDCl_3$, 125 MHz

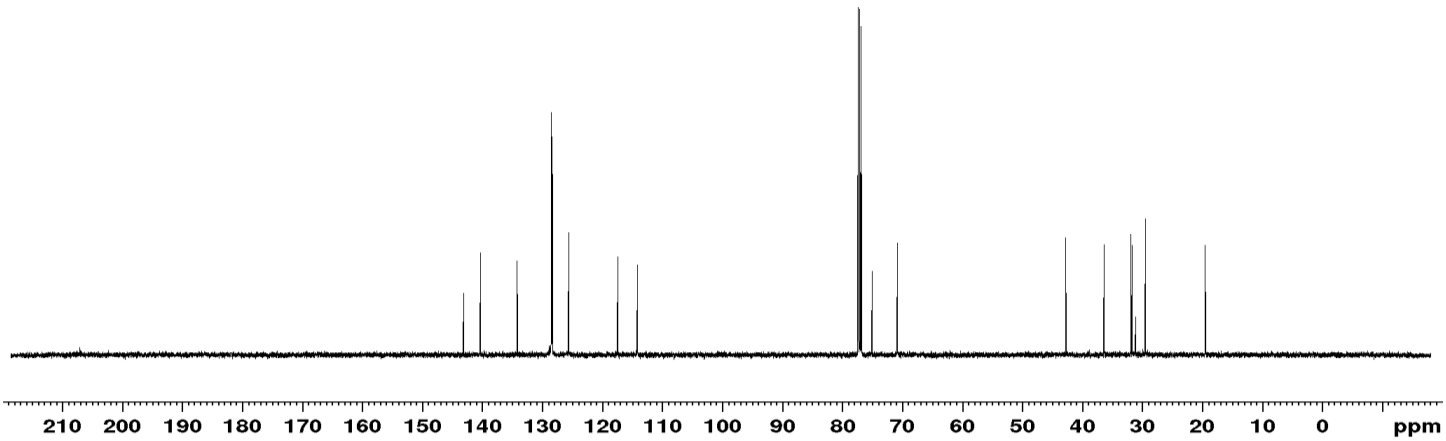

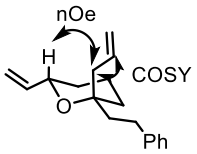

HH COSY
$CDCl_3$, 400 MHz

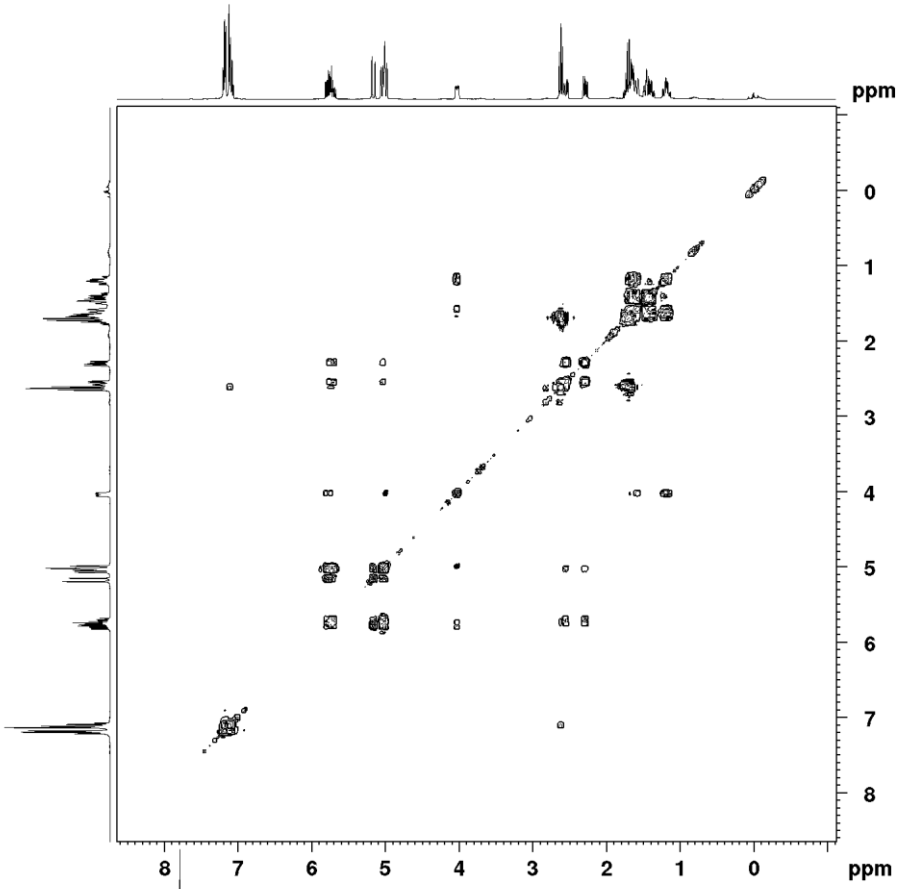

HH NOESY
$CDCl_3$, 400 MHz

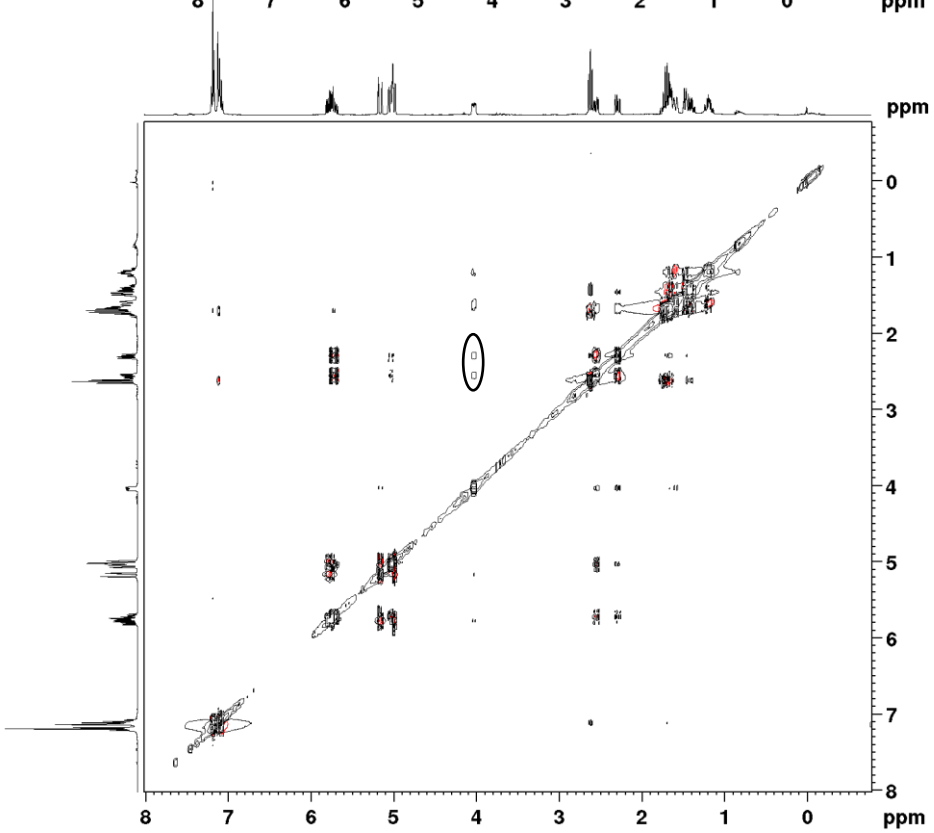

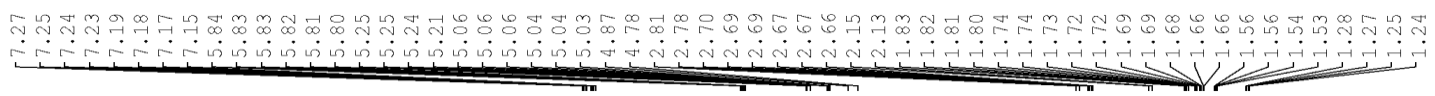

^{1}H NMR
$CDCl_3$, 500 MHz

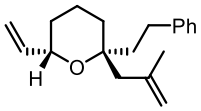

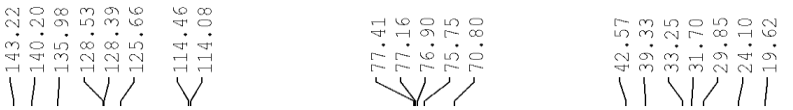

^{13}C NMR
$CDCl_3$, 125 MHz

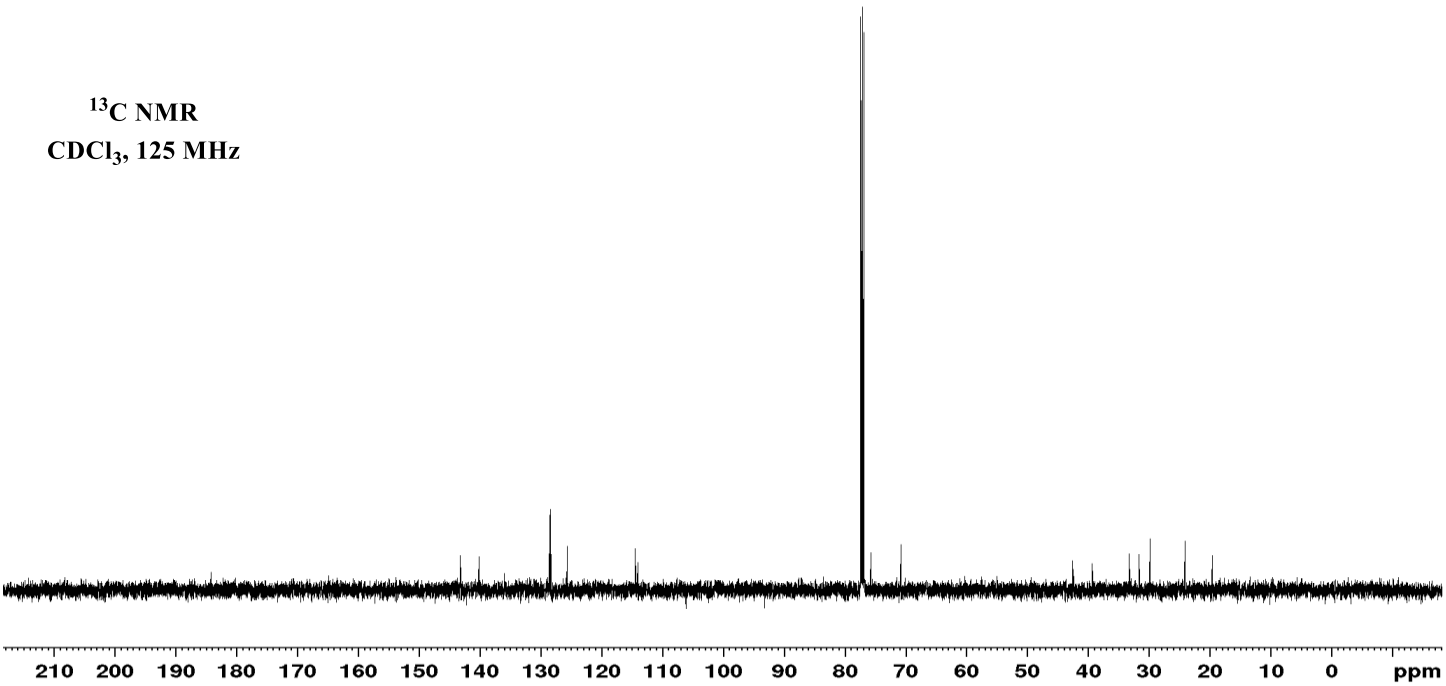

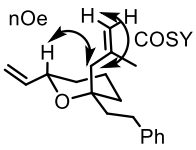
nOe
H
H
COSY
H
O
Ph

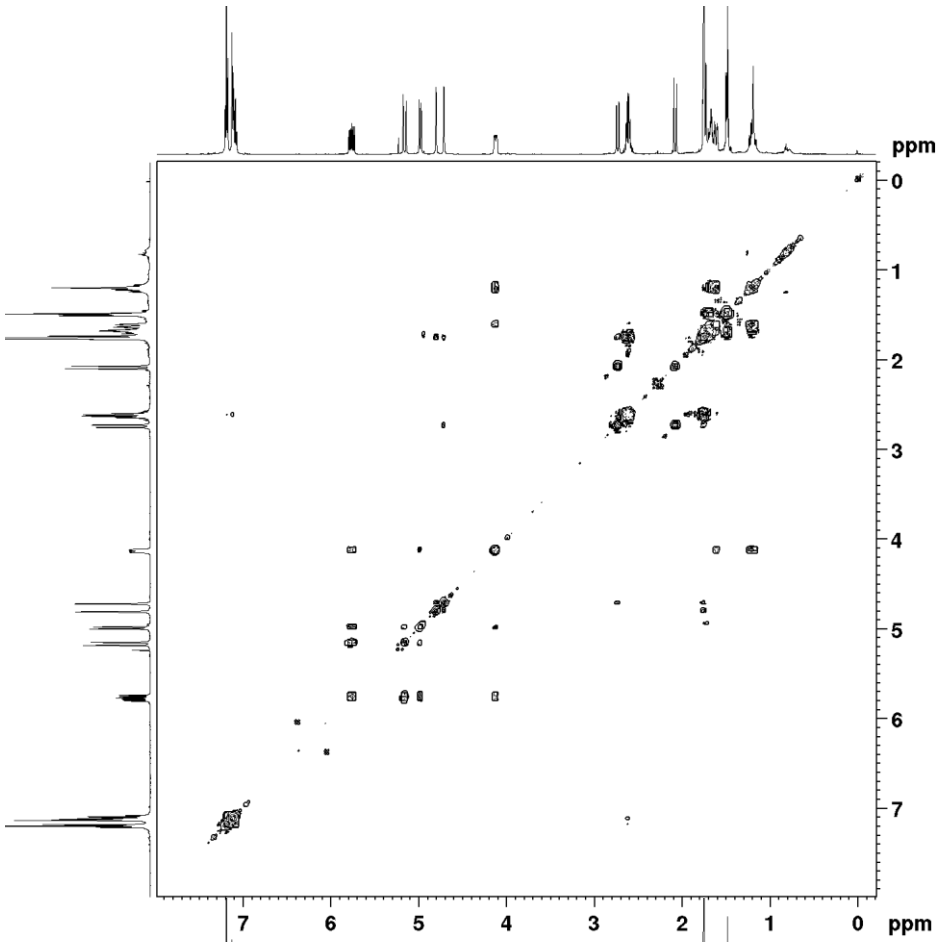
ppm
0
1
2
3
4
5
6
7
7
6
5
4
3
2
1
0
ppm

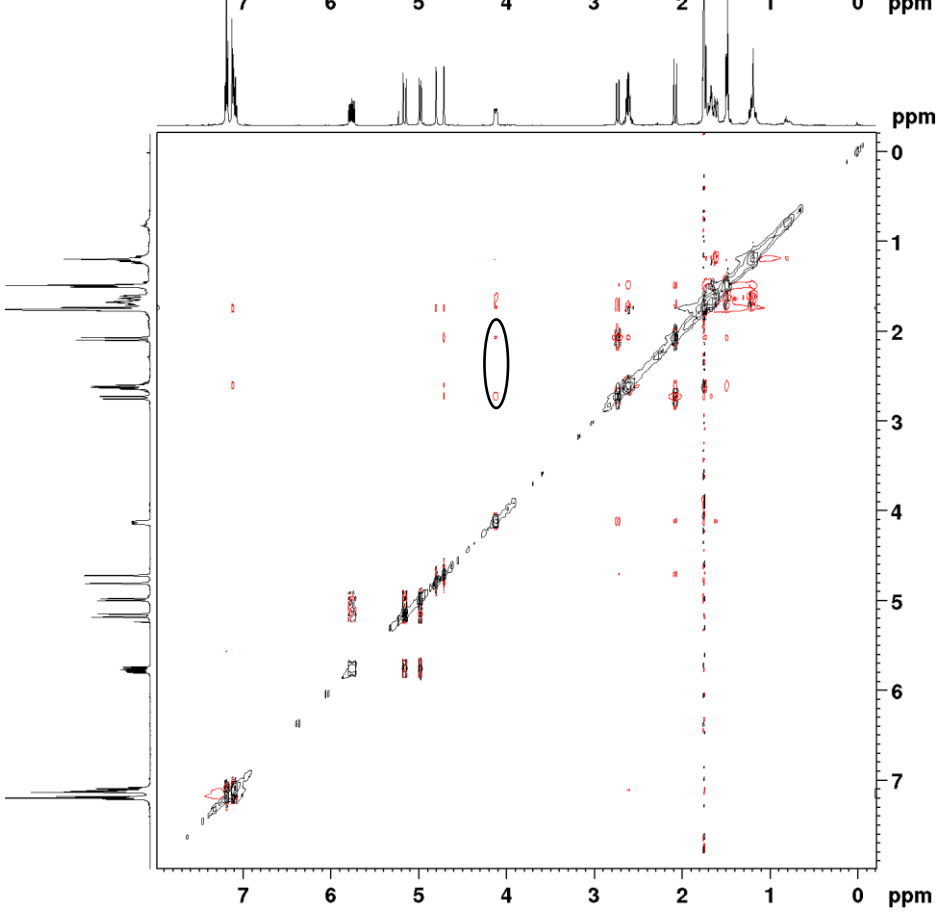
ppm
0
1
2
3
4
5
6
7
7
6
5
4
3
2
1
0
ppm

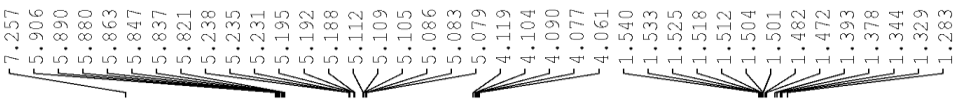

^{1}H NMR

$CDCl_3$, 400 MHz

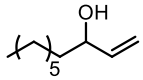

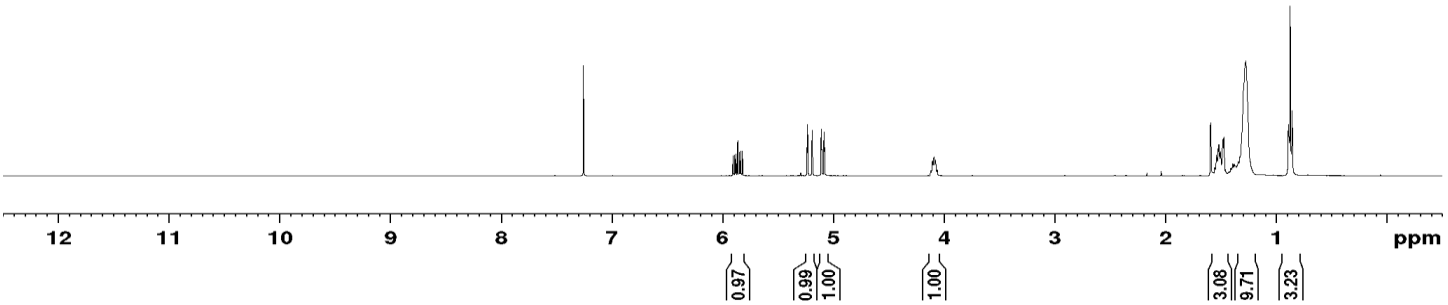

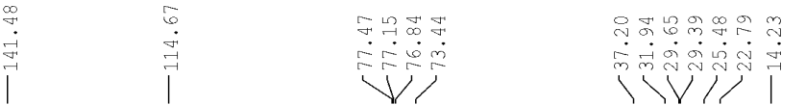

^{13}C NMR

$CDCl_3$, 100 MHz

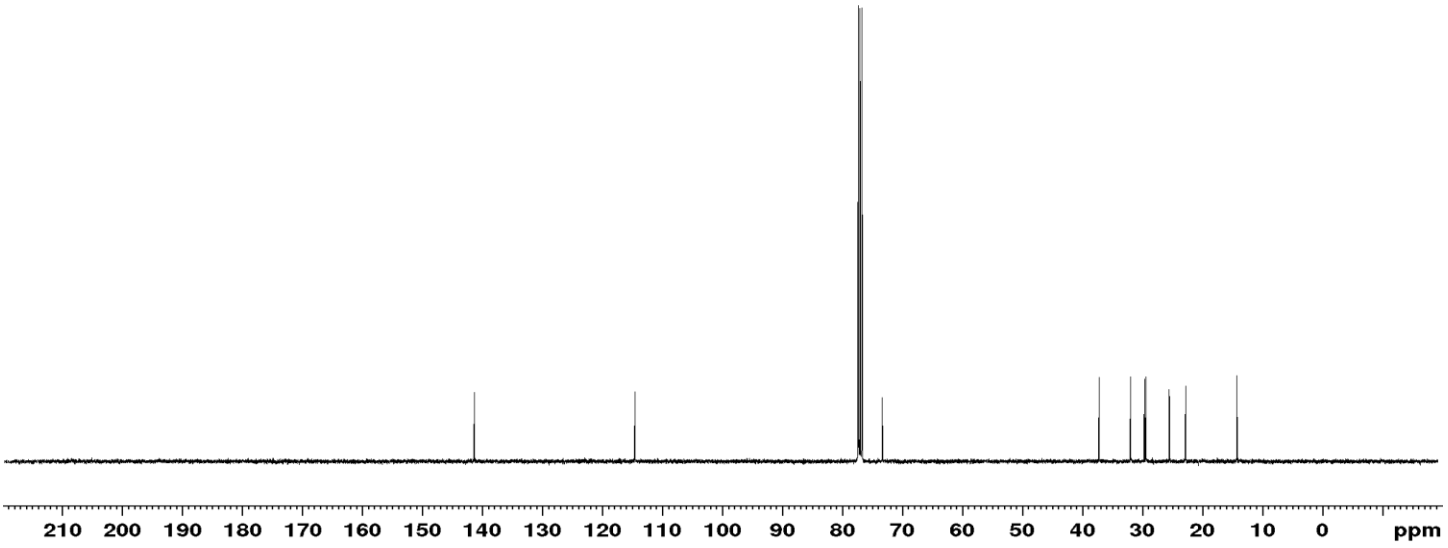

^{1}H NMR
$CDCl_3$, 400 MHz

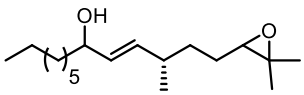

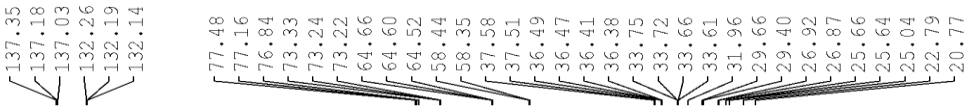

^{13}C NMR
$CDCl_3$, 100 MHz

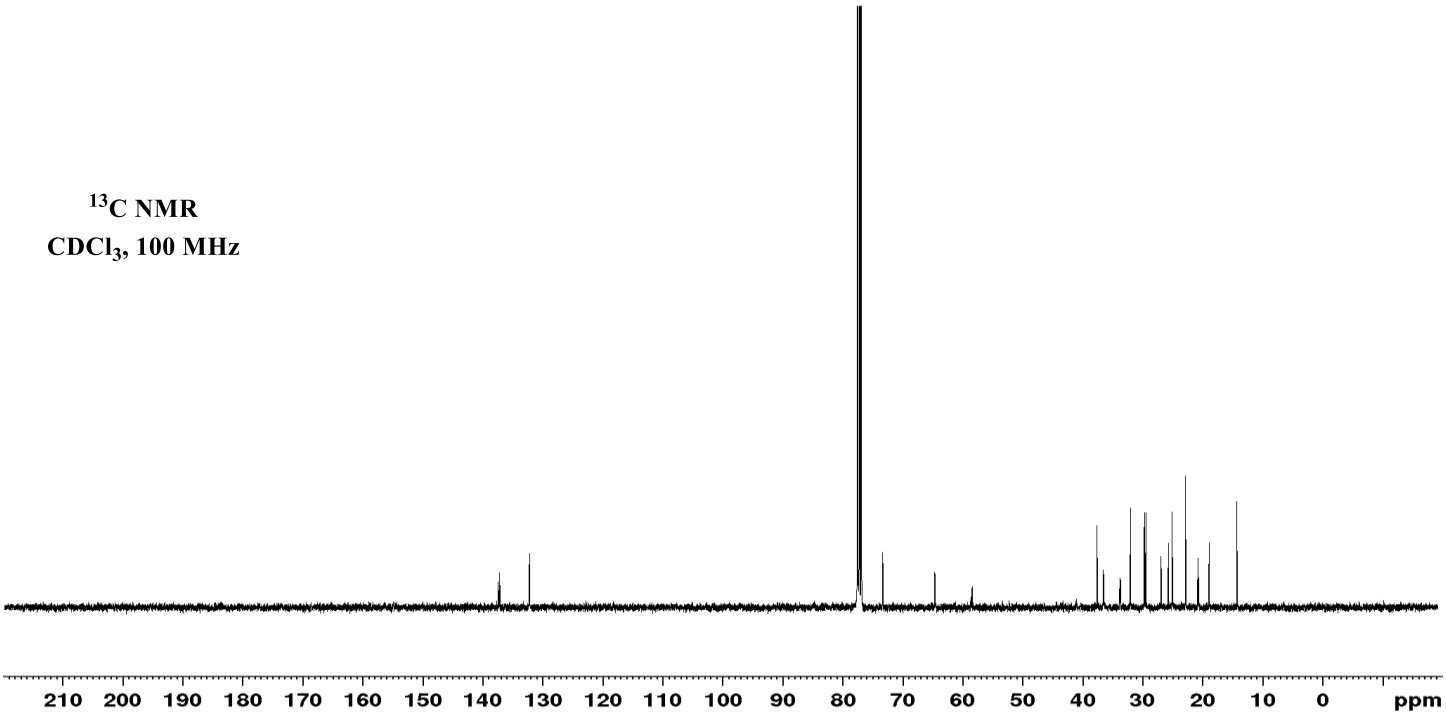

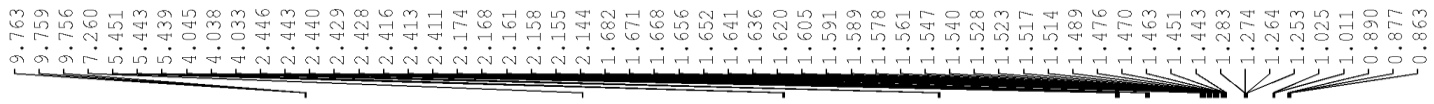

^{1}H NMR
$CDCl_3$, 500 MHz

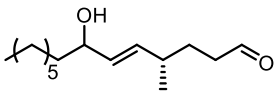

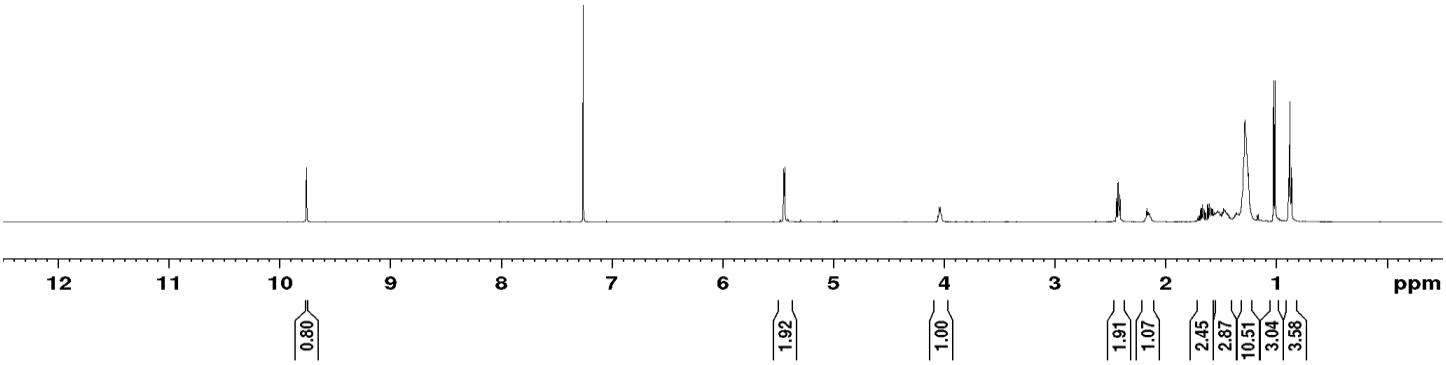

^{13}C NMR
$CDCl_3$, 125 MHz

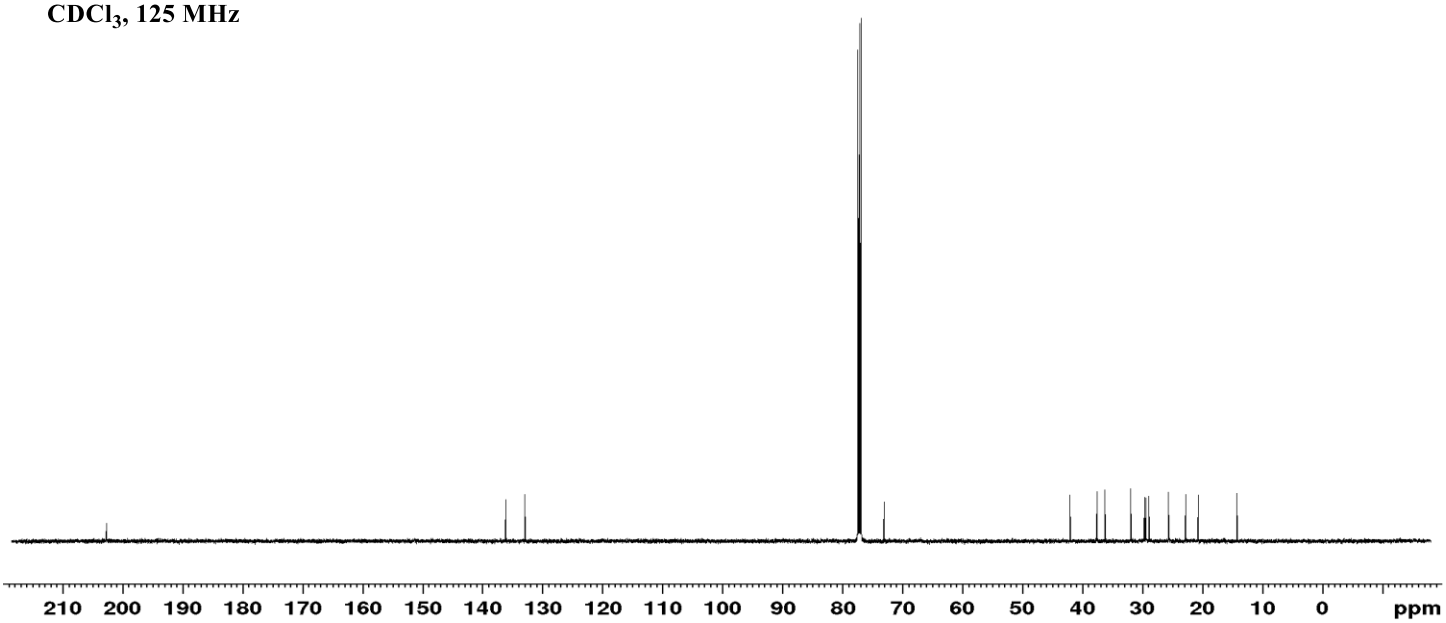

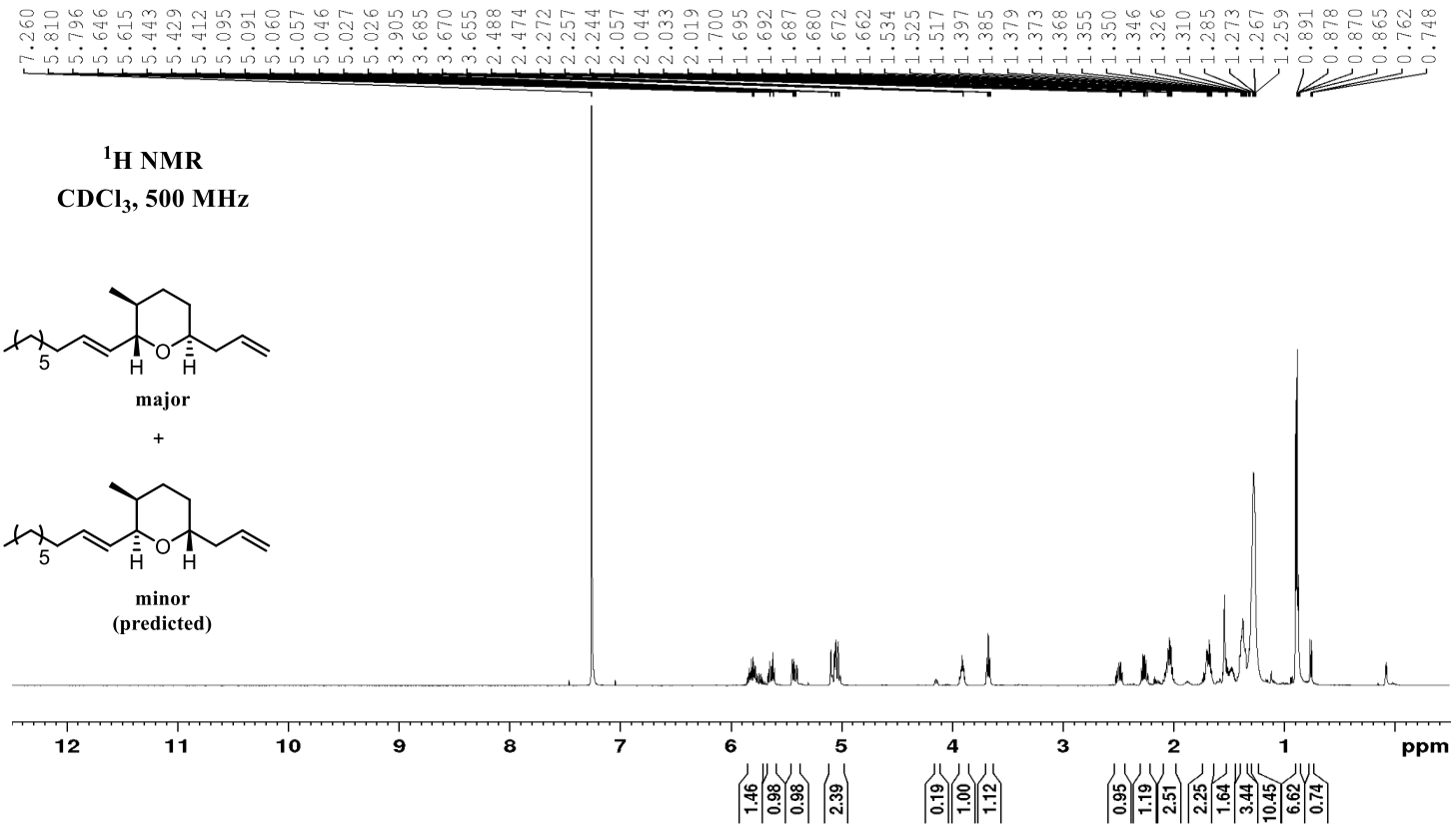
7.260
5.810
5.796
5.646
5.615
5.443
5.429
5.412
5.095
5.091
5.060
5.057
5.046
5.027
5.026
3.905
3.685
3.670
3.655
2.488
2.474
2.272
2.257
2.244
2.057
2.044
2.033
2.019
1.700
1.695
1.692
1.687
1.680
1.672
1.662
1.534
1.525
1.517
1.397
1.385
1.379
1.373
1.368
1.355
1.350
1.346
1.326
1.310
1.285
1.273
1.267
1.259
0.891
0.878
0.870
0.865
0.762
0.748
1H NMR
CDCl3, 500 MHz
5
H
O
H
major
+
5
H
O
H
minor
(predicted)
12
11
10
9
8
7
6
5
4
3
2
1
ppm
1.46
0.98
0.98
2.39
0.19
1.00
1.12
0.95
1.19
2.51
2.25
1.64
3.44
10.45
6.62
0.74

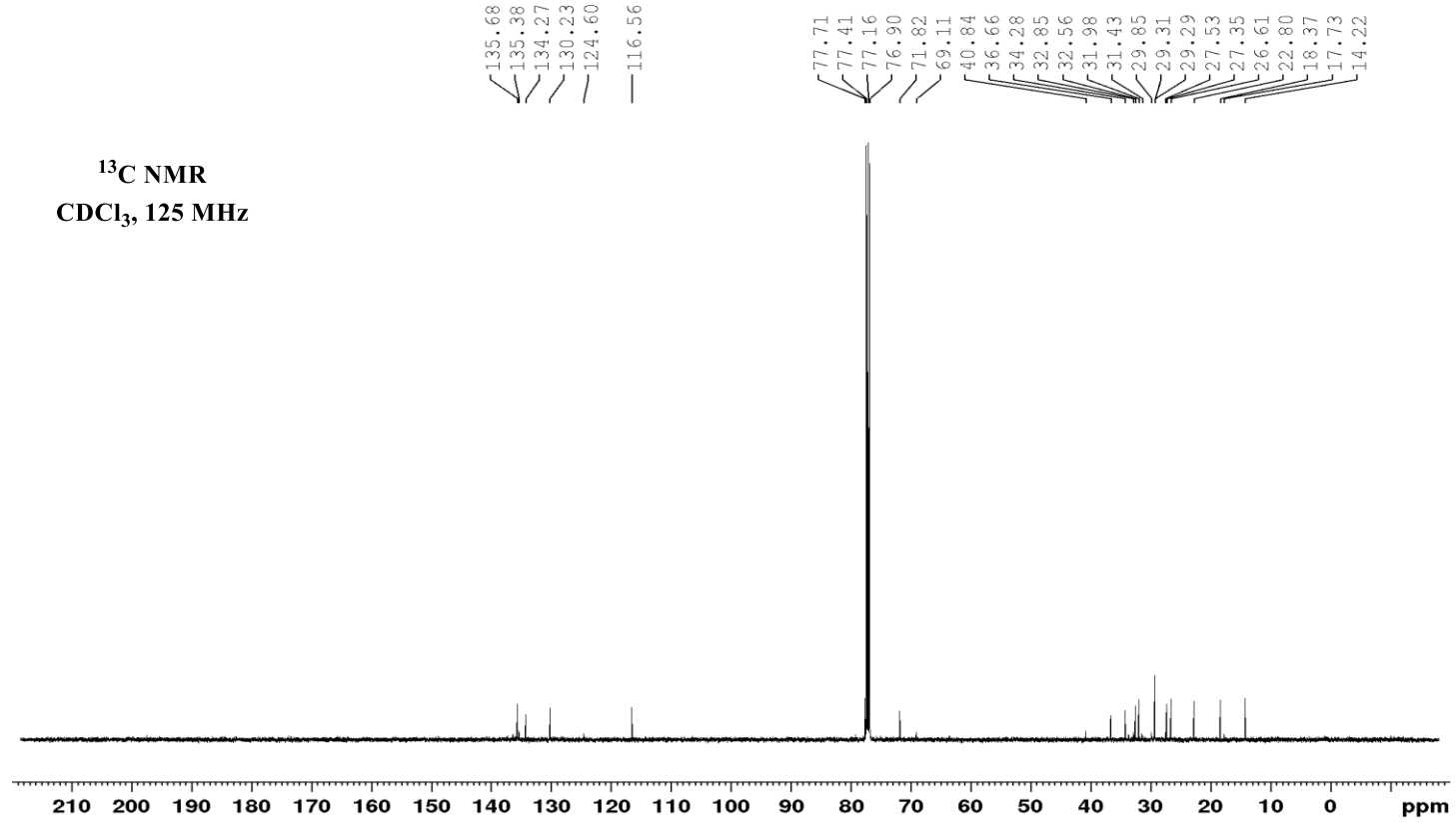
135.68
135.38
134.27
130.23
124.60
116.56
77.71
77.41
77.16
76.90
71.82
69.11
40.84
36.66
34.28
32.85
32.56
31.98
31.43
29.85
29.31
29.29
27.53
27.35
26.61
22.80
18.37
17.73
14.22
13C NMR
CDCl3, 125 MHz
210
200
190
180
170
160
150
140
130
120
110
100
90
80
70
60
50
40
30
20
10
0
ppm

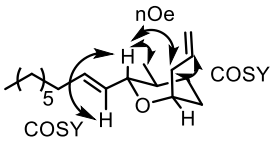

HH COSY
$CDCl_3$, 500 MHz

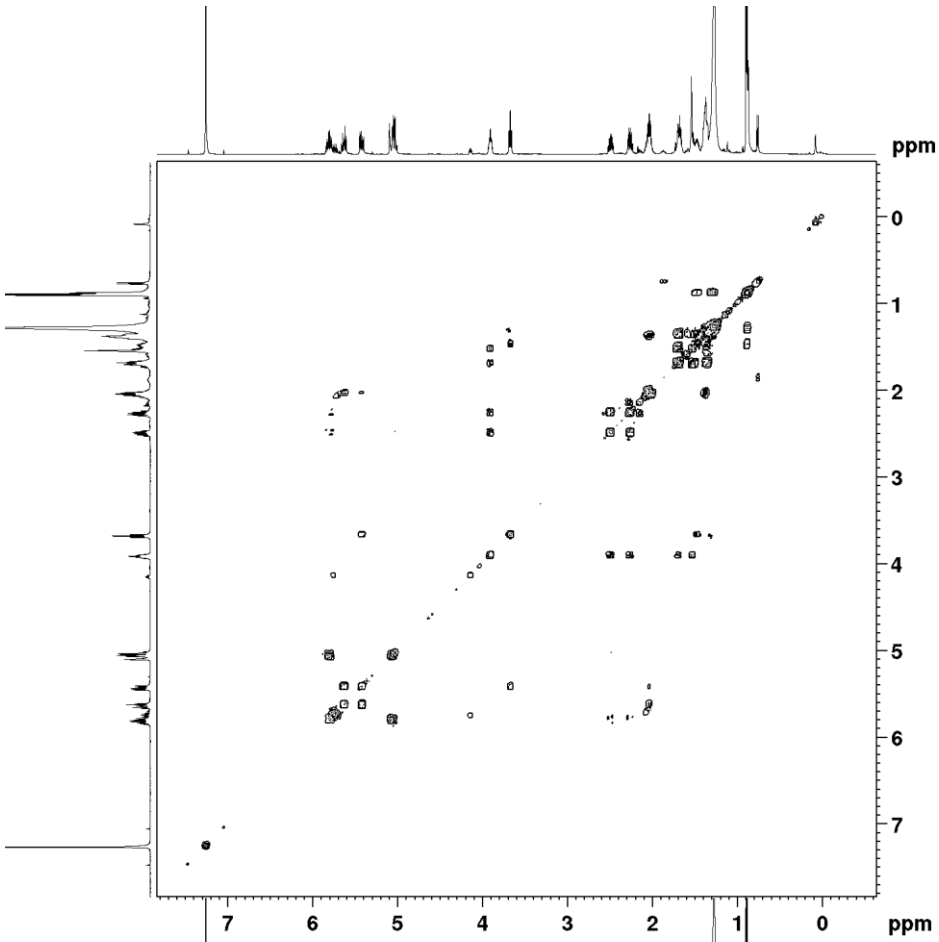

NOESY
$CDCl_3$, 500 MHz

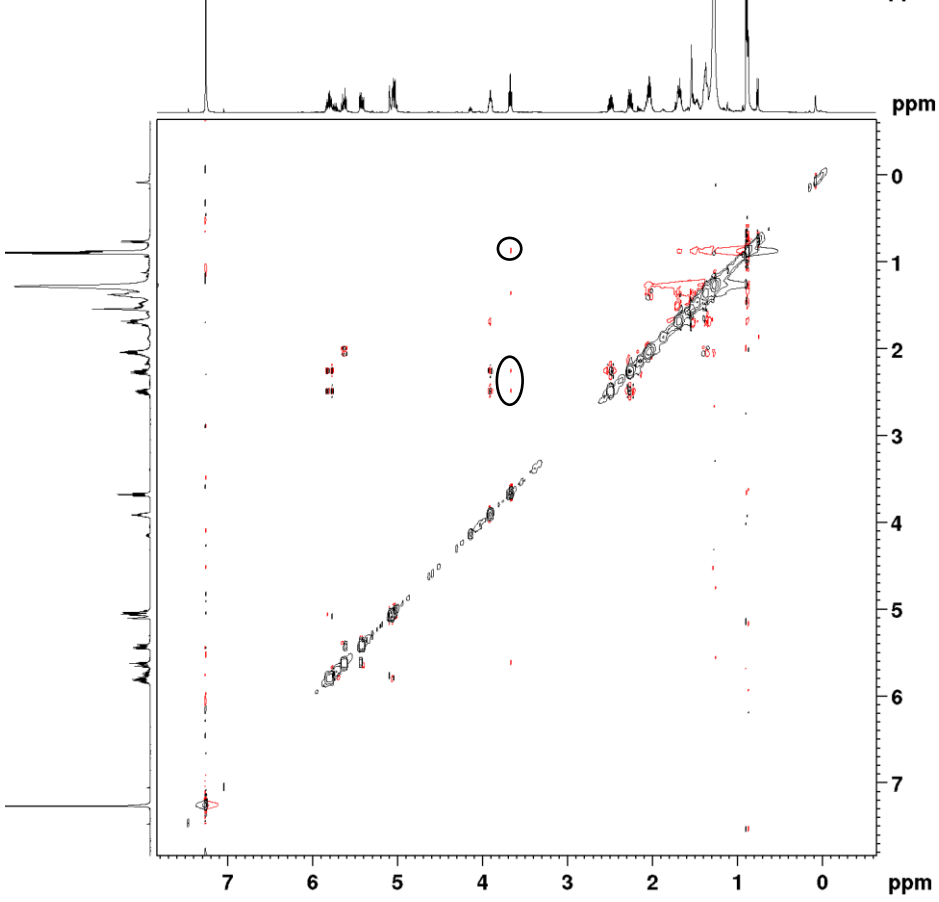

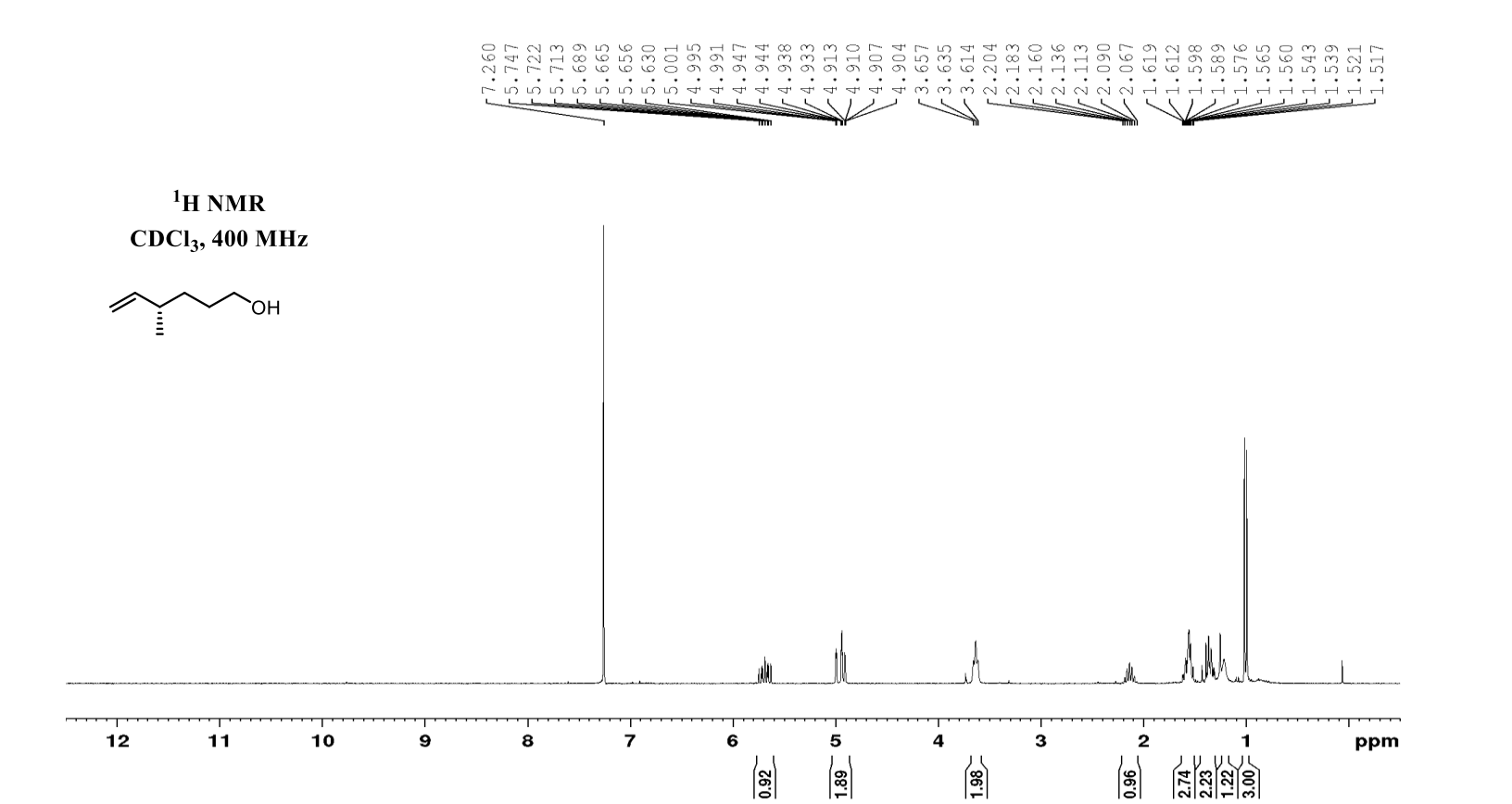

^{1}H NMR
$CDCl_3$, 400 MHz

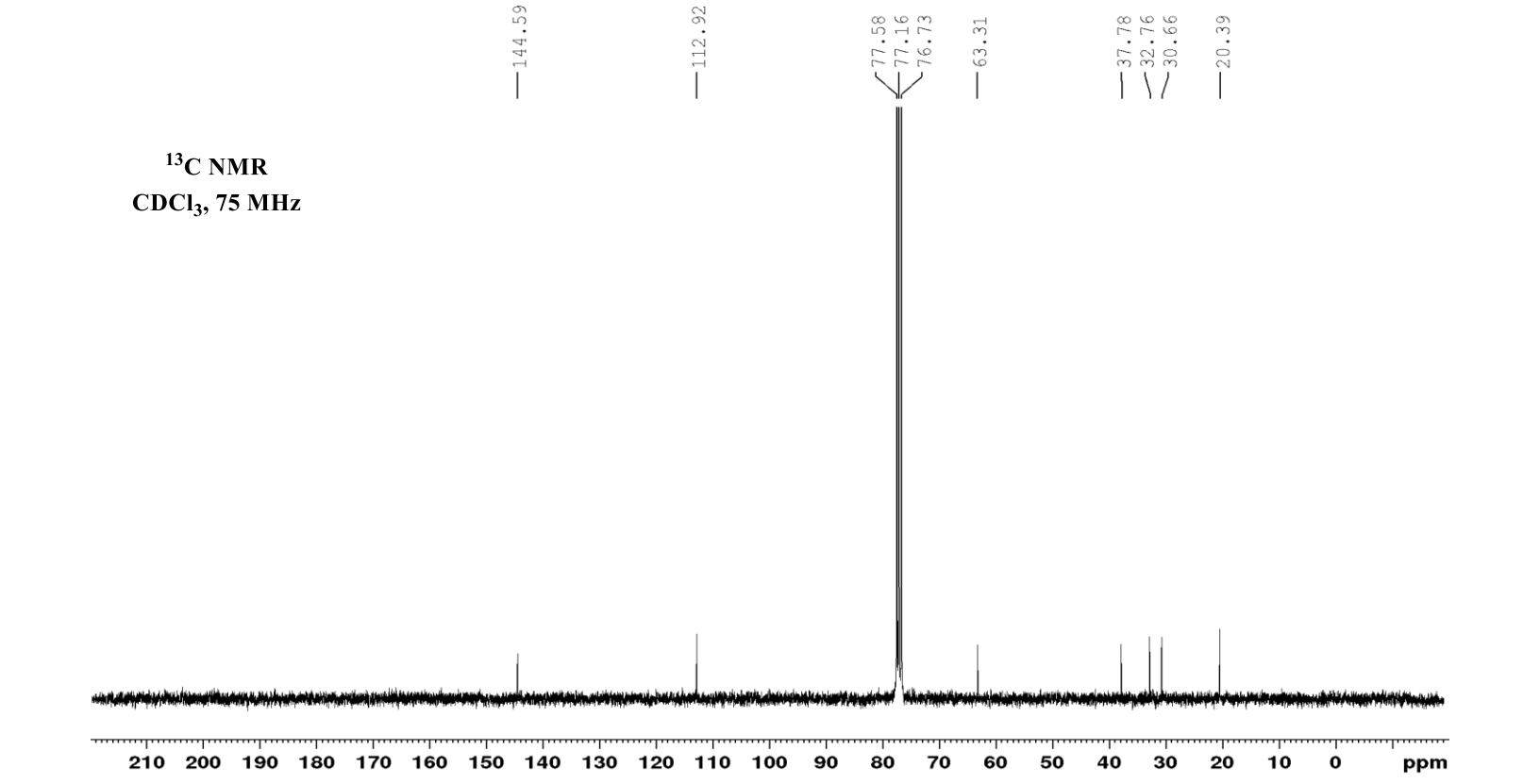

^{13}C NMR
$CDCl_3$, 75 MHz

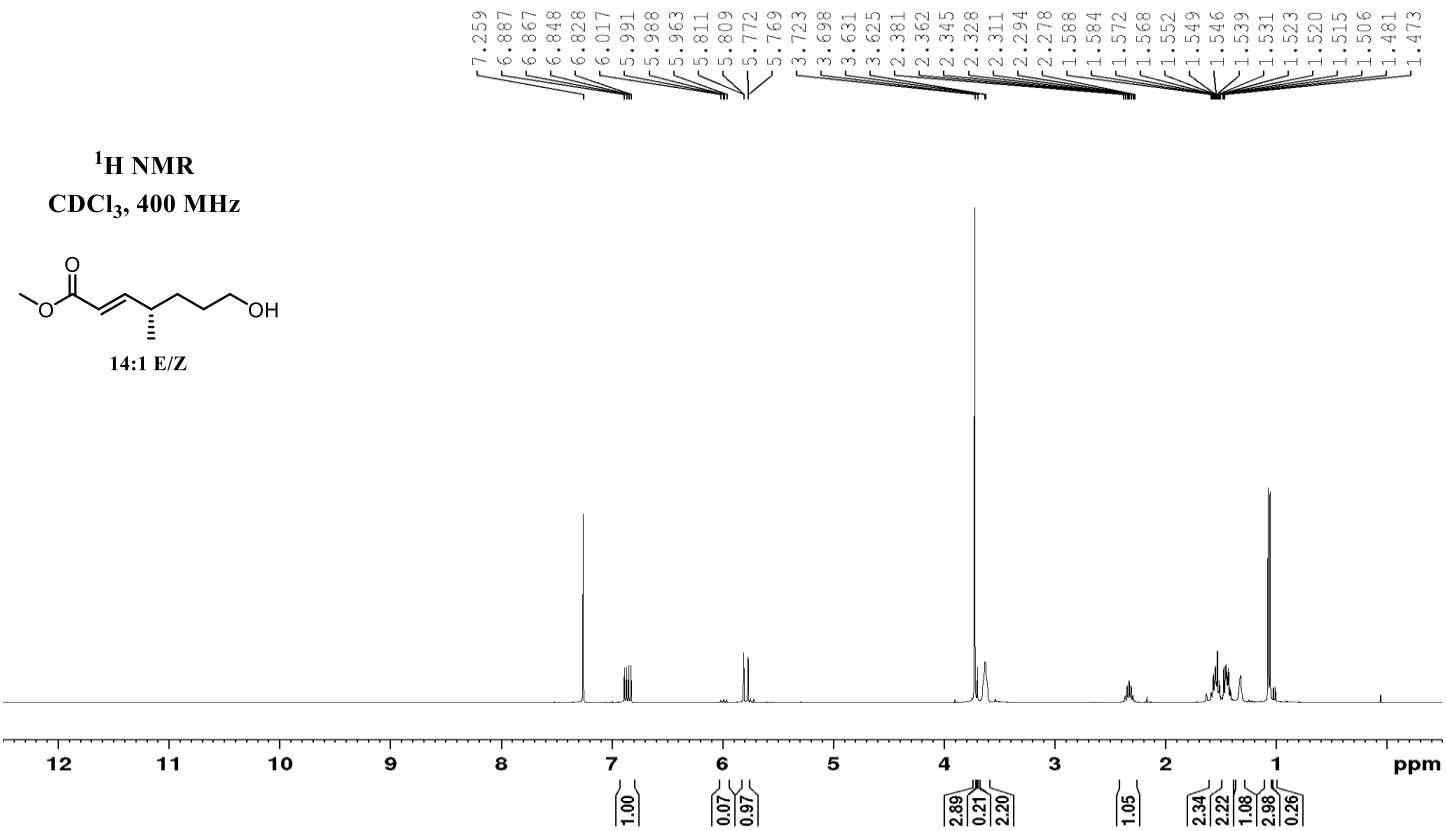
7.259
6.887
6.867
6.848
6.828
6.017
5.991
5.988
5.963
5.811
5.809
5.772
5.769
3.723
3.698
3.631
3.625
2.381
2.362
2.345
2.328
2.311
2.294
2.278
1.588
1.584
1.572
1.568
1.552
1.549
1.546
1.539
1.531
1.523
1.520
1.515
1.506
1.481
1.473
1H NMR
CDCl3, 400 MHz
O
O
OH
14:1 E/Z
12
11
10
9
8
7
6
5
4
3
2
1
ppm
1.00
0.07
0.97
2.89
0.21
2.20
1.05
2.34
2.22
1.08
2.98
0.26

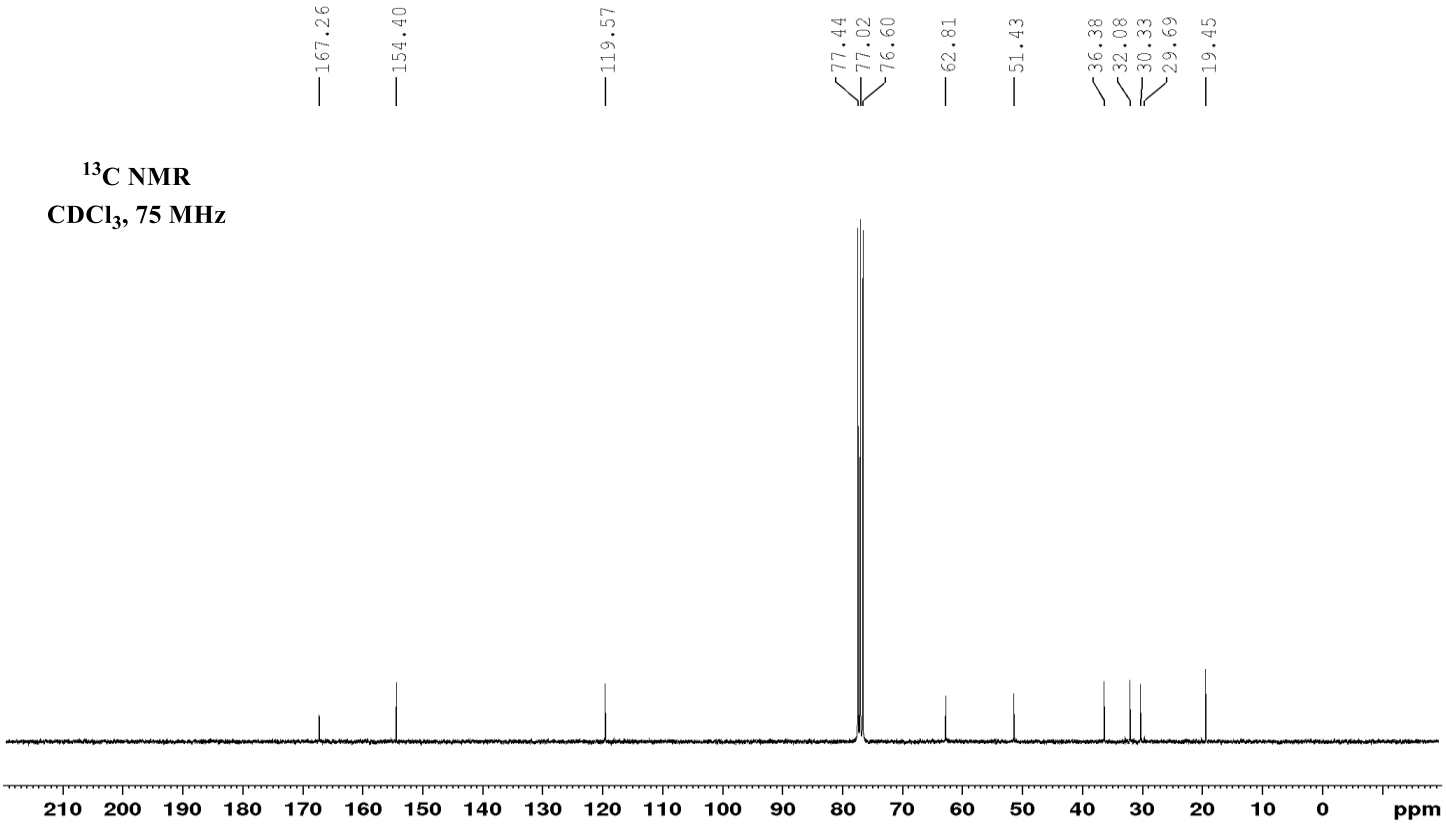
167.26
154.40
119.57
77.44
77.02
76.60
62.81
51.43
36.38
32.08
30.33
29.69
19.45
13C NMR
CDCl3, 75 MHz
210
200
190
180
170
160
150
140
130
120
110
100
90
80
70
60
50
40
30
20
10
0
ppm

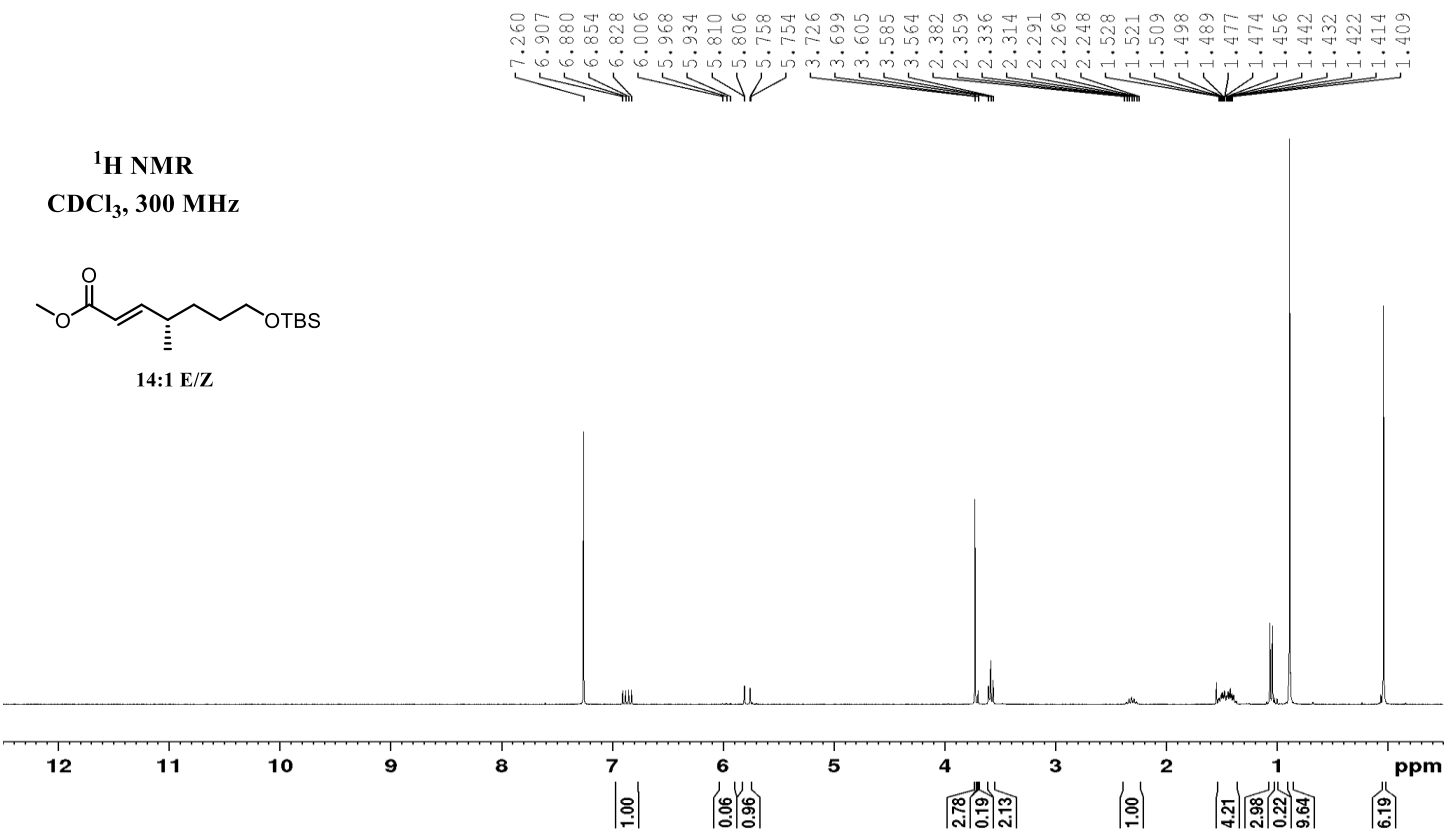

^{1}H NMR
$CDCl_3$, 300 MHz

14:1 E/Z

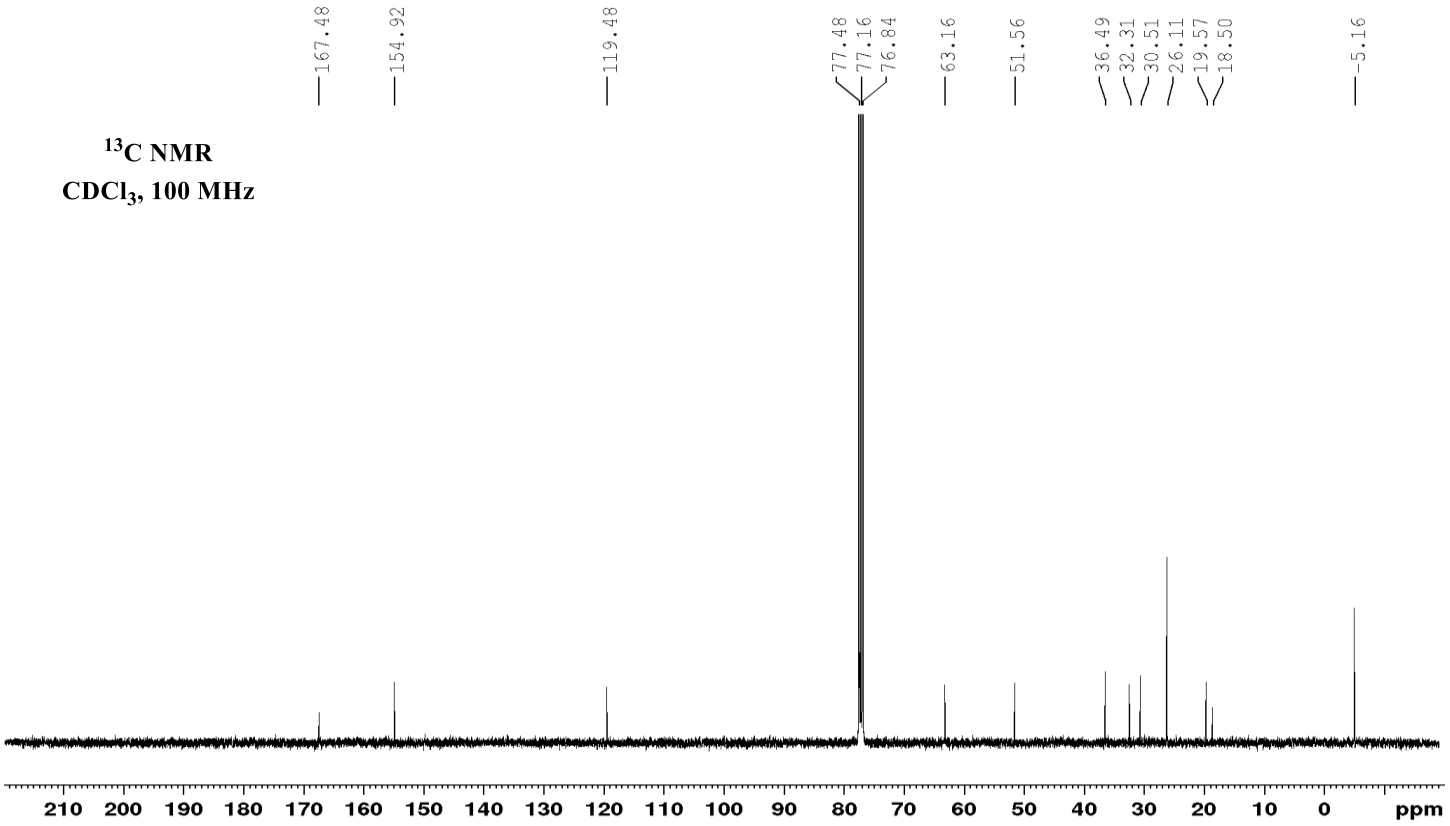

^{13}C NMR
$CDCl_3$, 100 MHz

^{1}H NMR
$CDCl_3$, 300 MHz

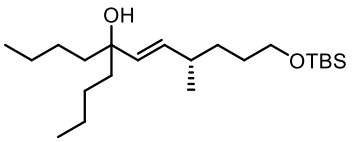

^{13}C NMR
$CDCl_3$, 100 MHz

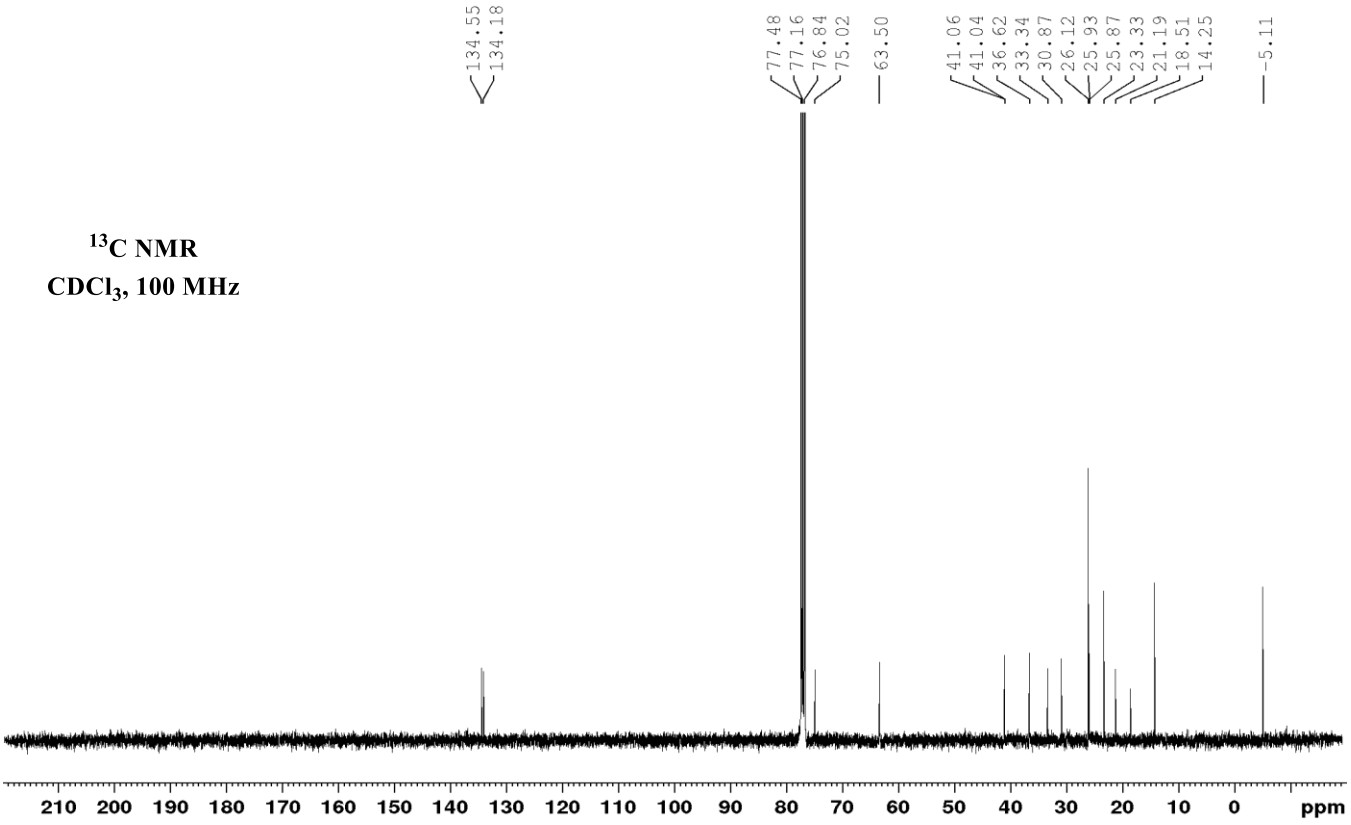

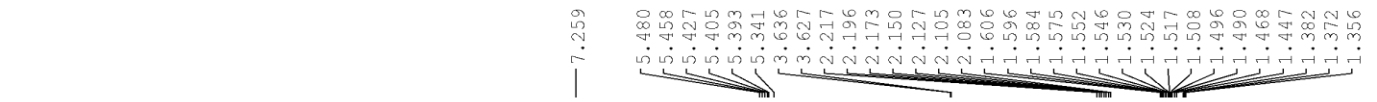

^{1}H NMR
$CDCl_3$, 300 MHz

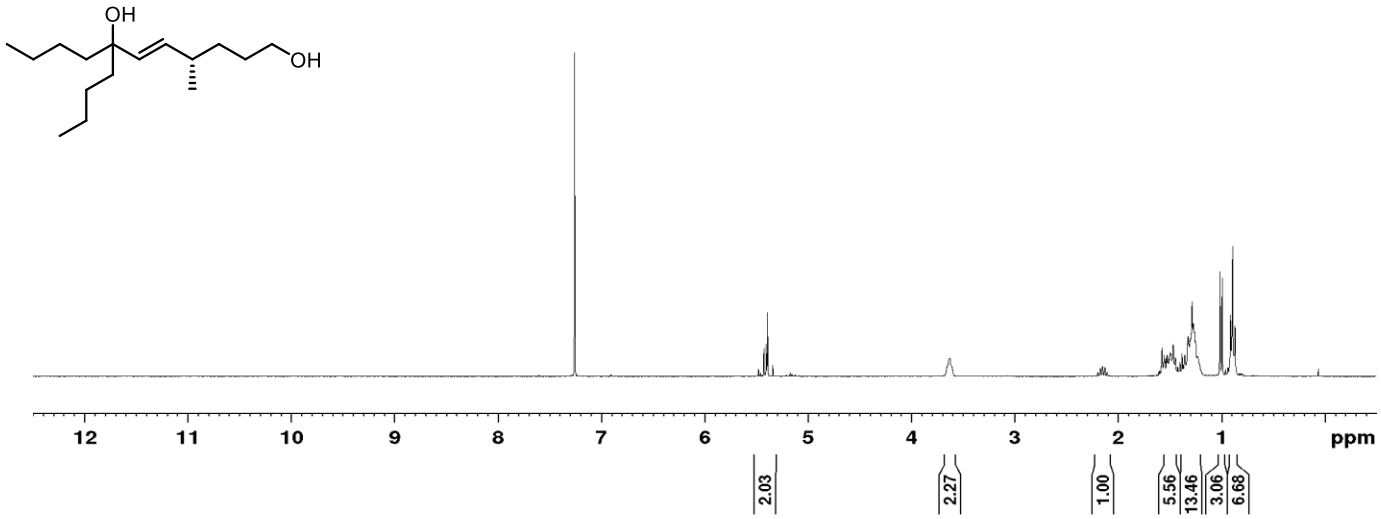

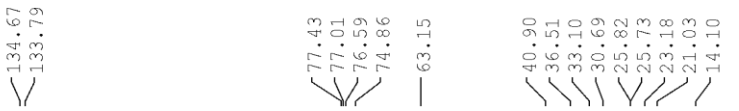

^{13}C NMR
$CDCl_3$, 75 MHz

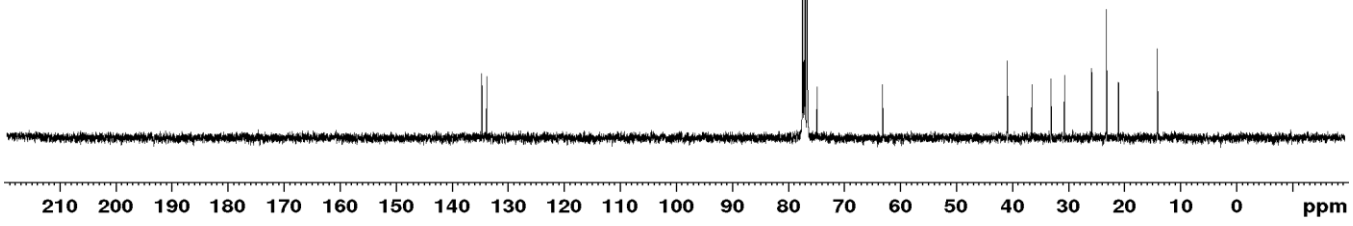

^{1}H NMR
$CDCl_3$, 400 MHz

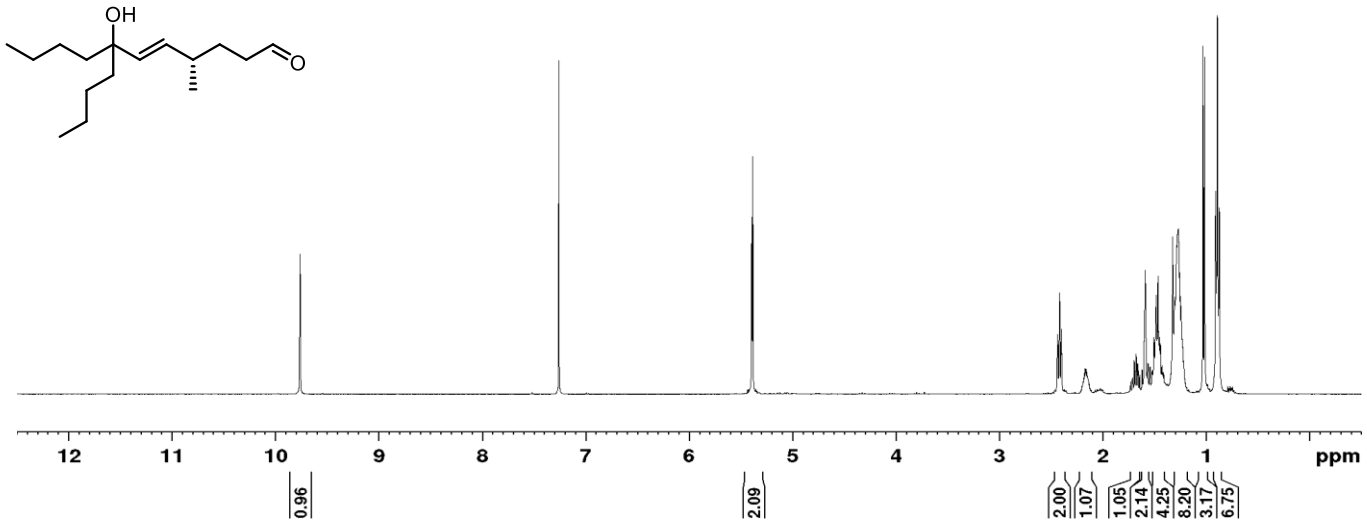

^{13}C NMR
$CDCl_3$, 100 MHz

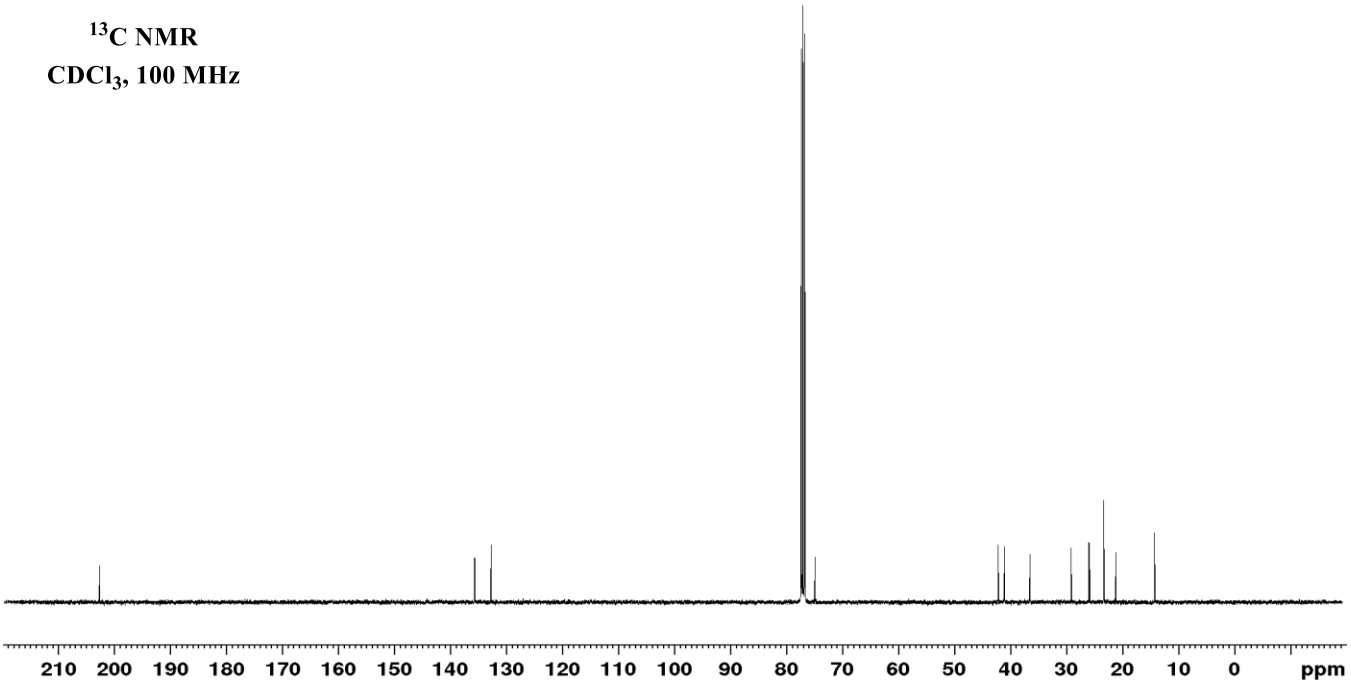

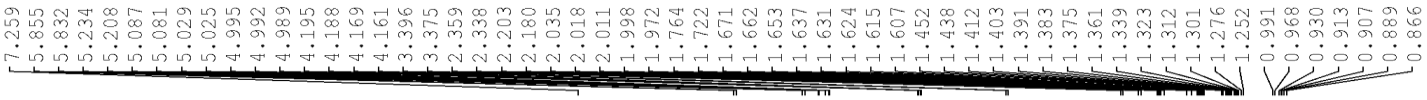

^{1}H NMR
$CDCl_3$, 300 MHz

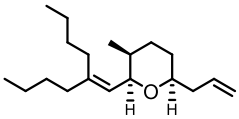

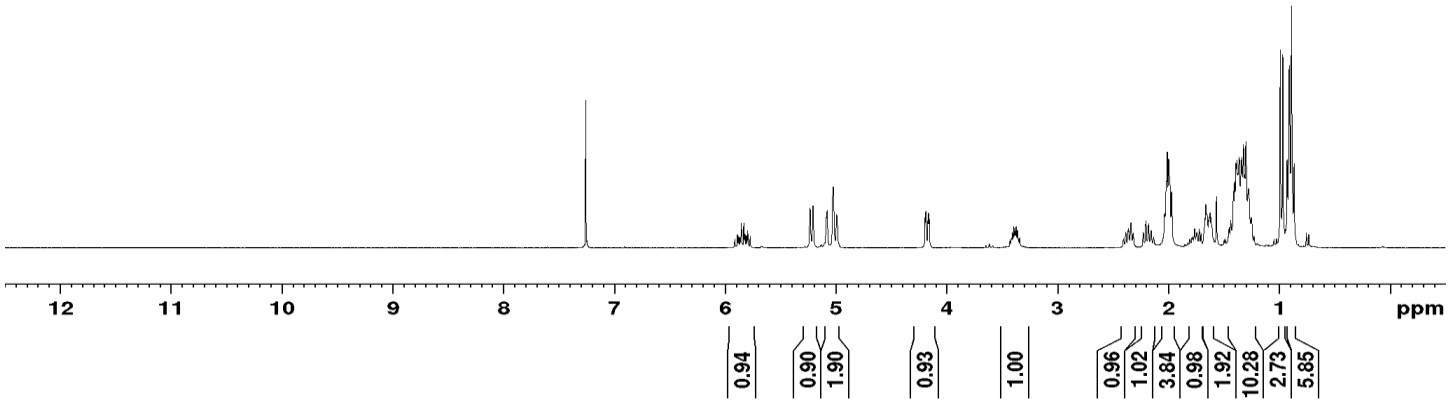

^{13}C NMR
$CDCl_3$, 75 MHz

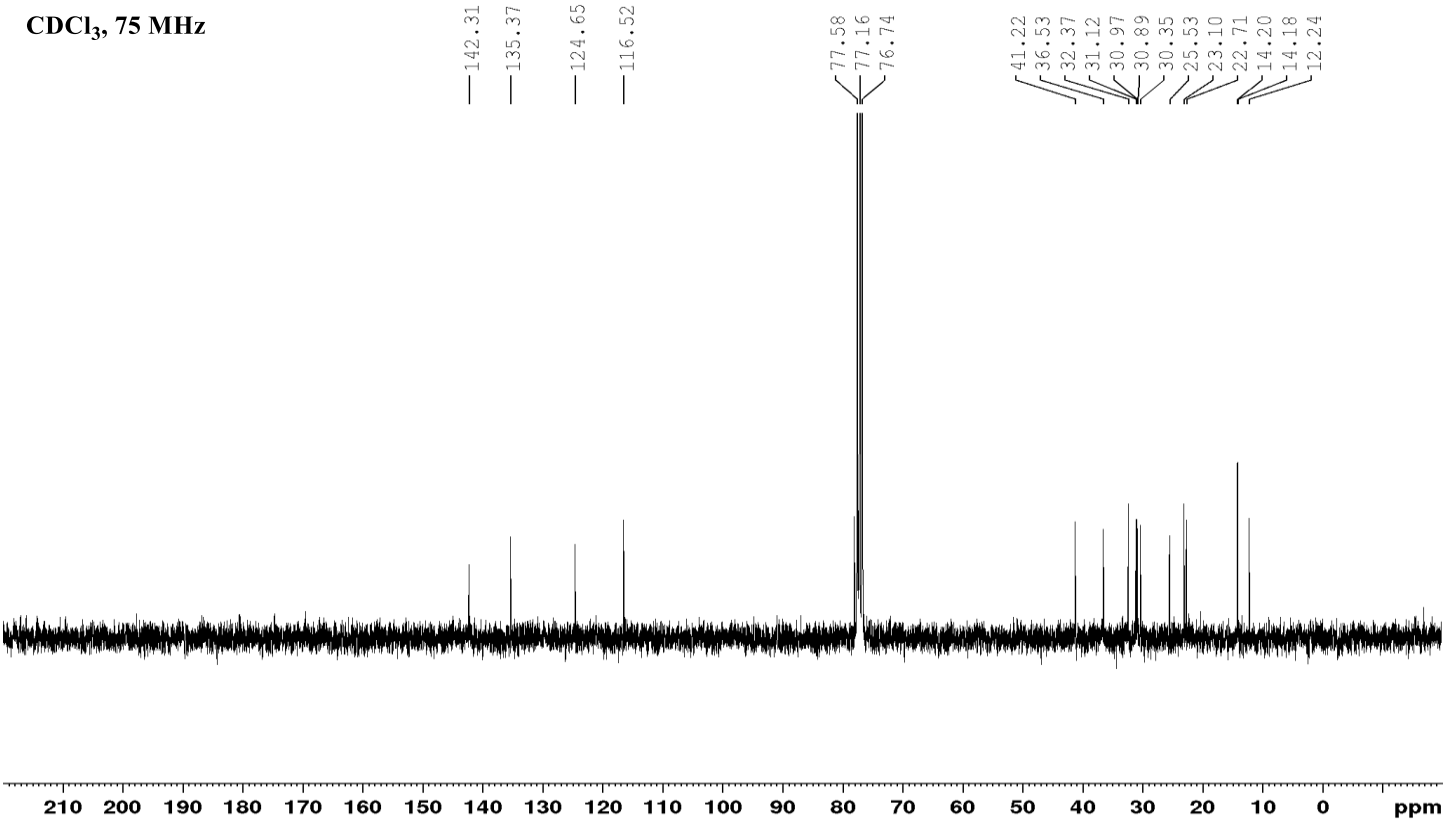

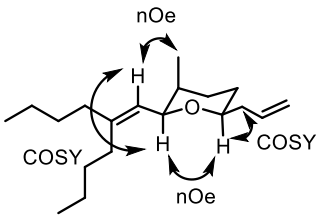

HH COSY
$CDCl_3$, 500 MHz

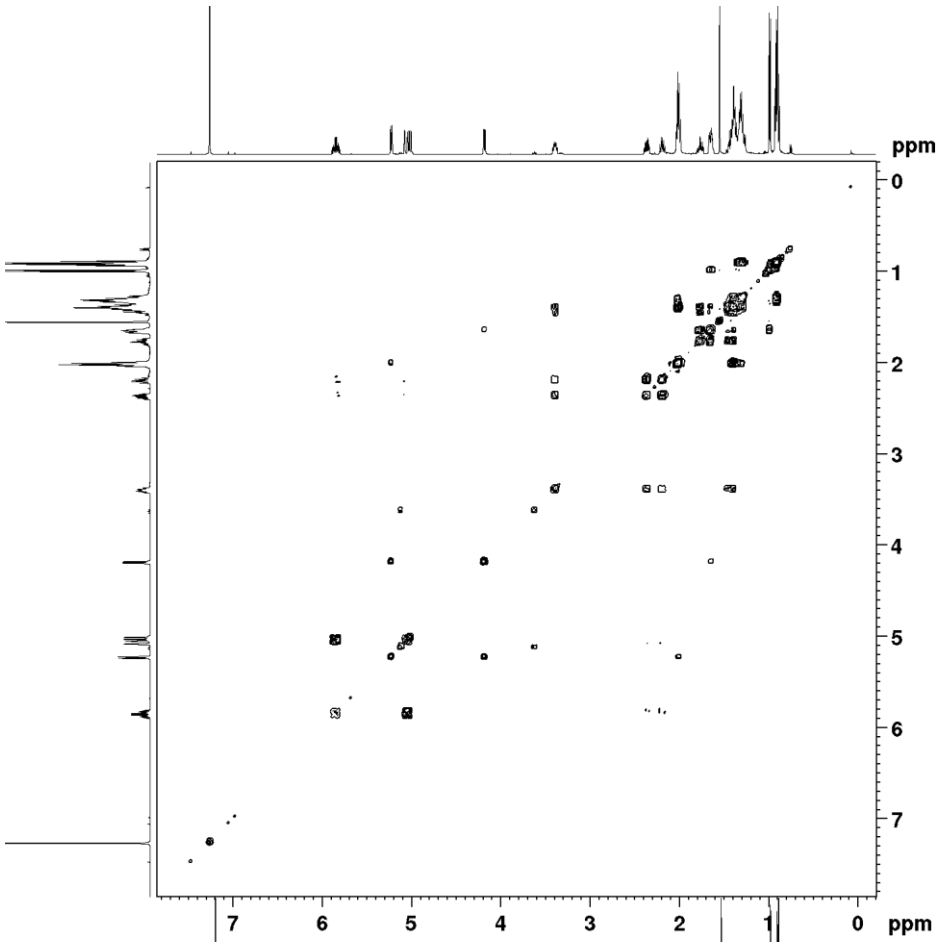

NOESY
$CDCl_3$, 500 MHz

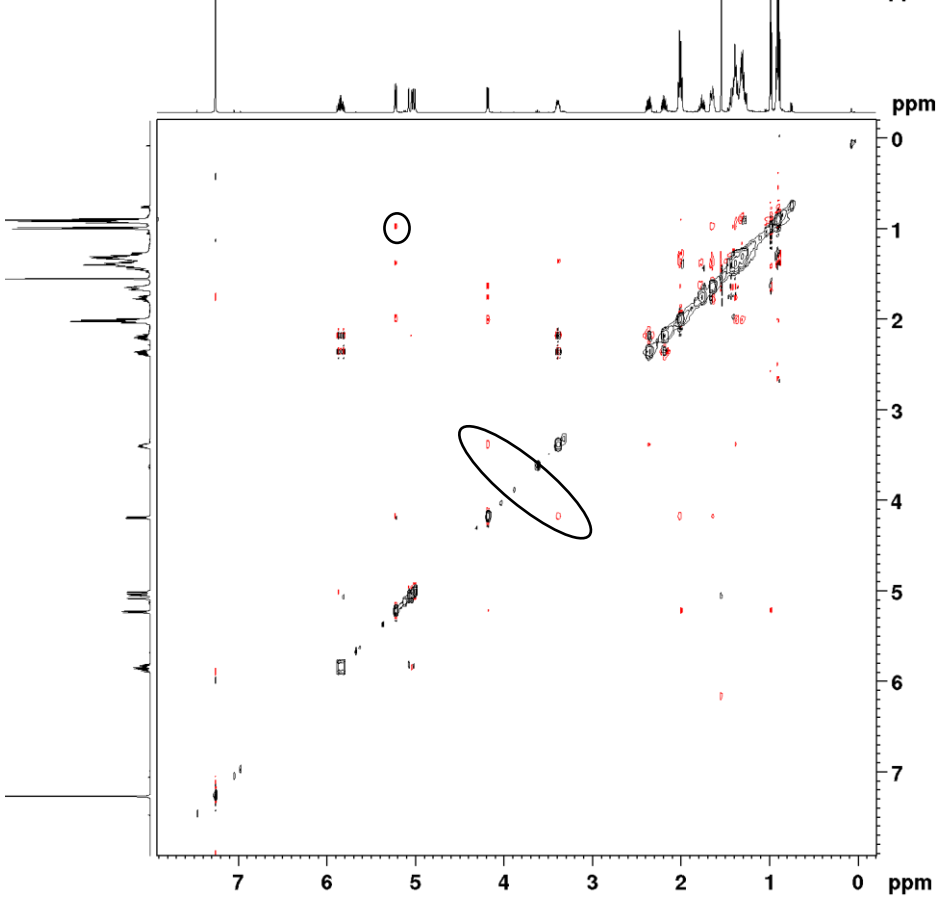

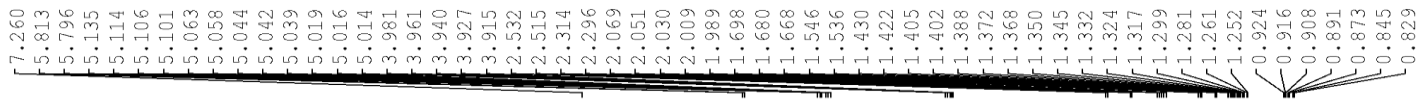

^{1}H NMR
$CDCl_3$, 300 MHz

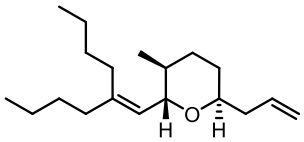

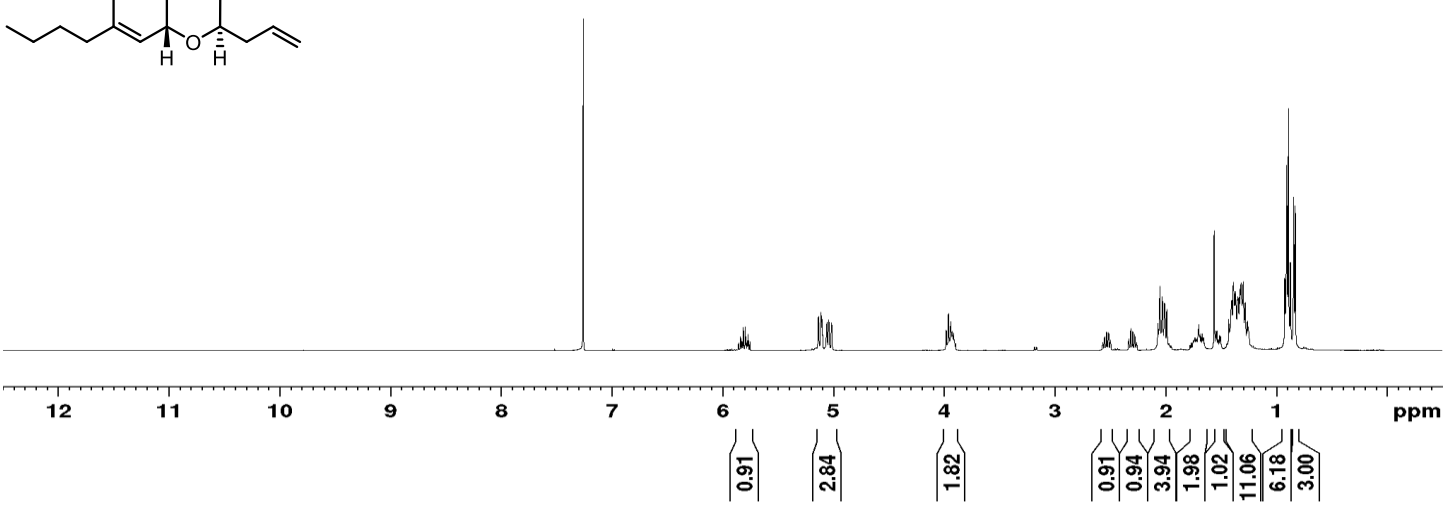

^{1}H NMR
C_6D_6, 500 MHz

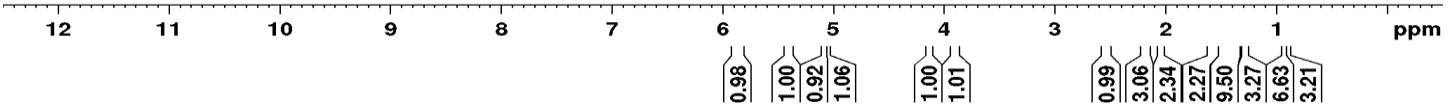

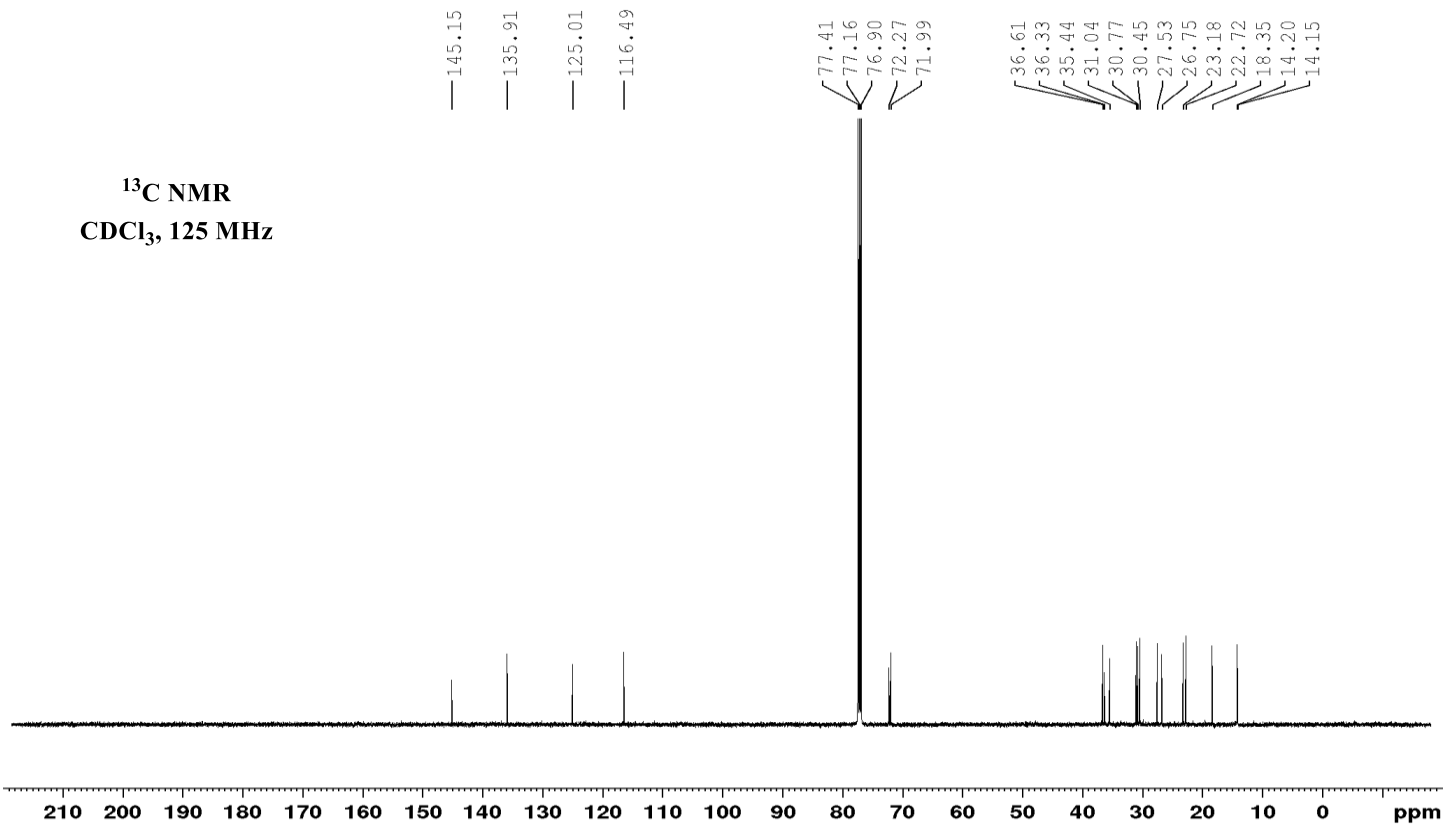

^{13}C NMR
$CDCl_3$, 125 MHz

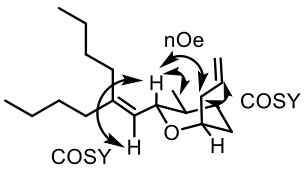

HH COSY
$CDCl_3$, 500 MHz

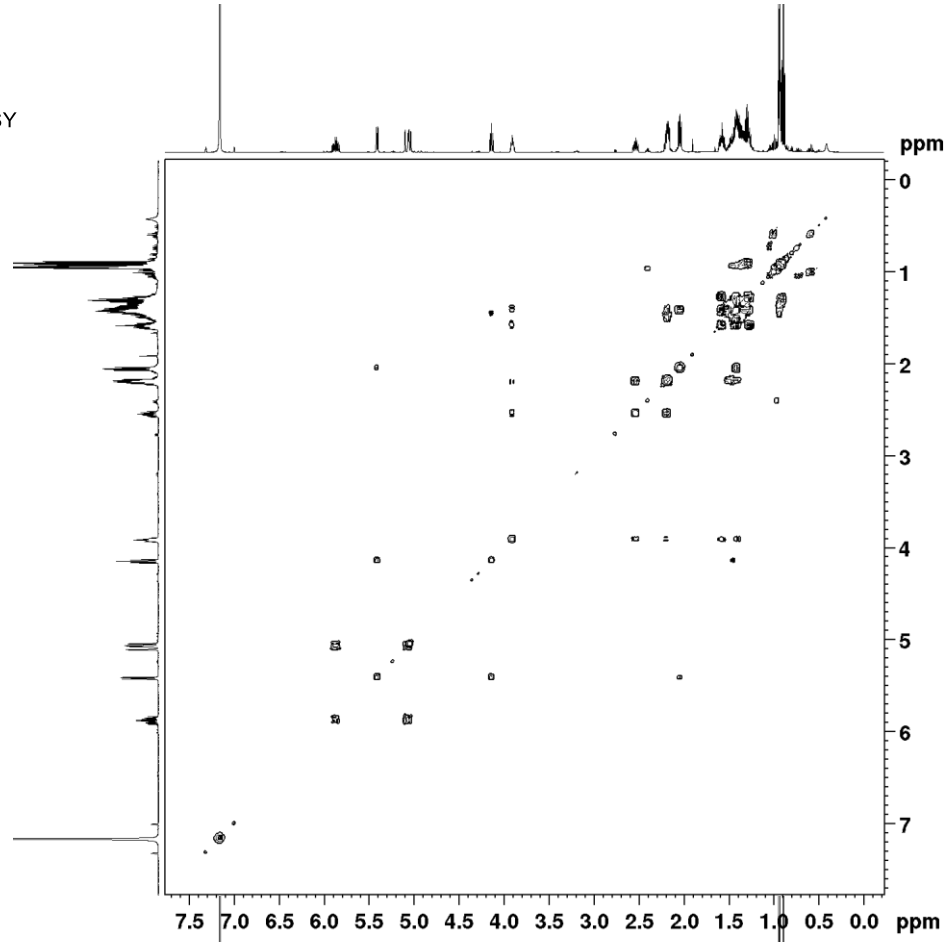

NOESY
C_6D_6, 500 MHz

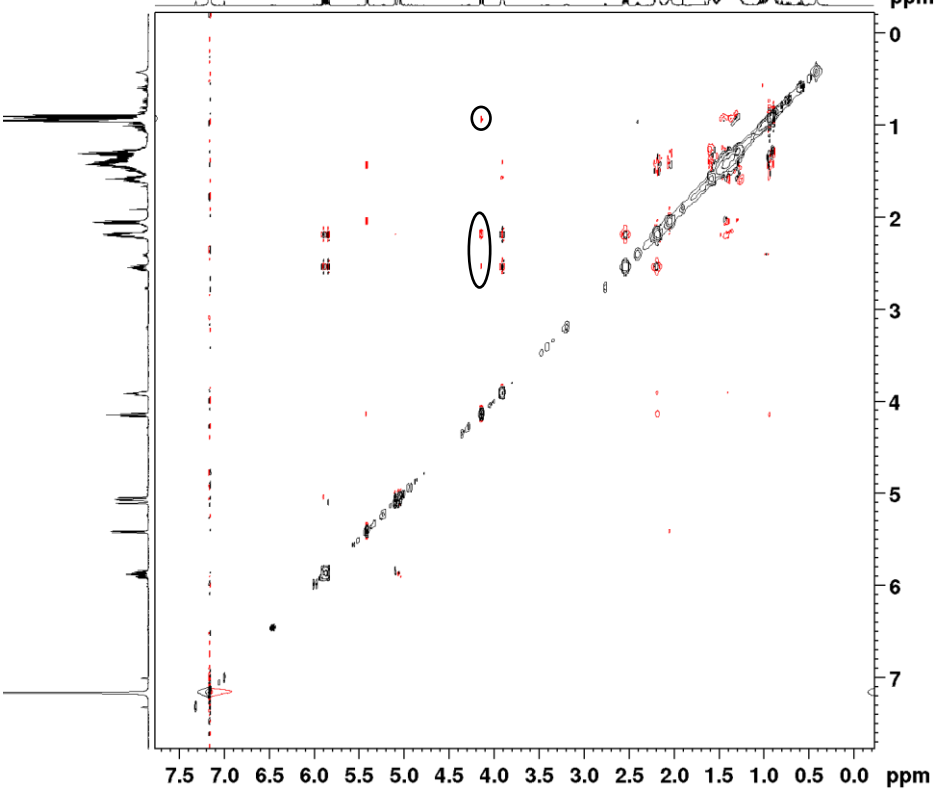

Bibliography

1. Méndez-Lucio,O.; Medina-Franco, J.L. *Drug Discov. Today* **2016,** 1-7.

2. Leach, A.R.; Hann, M.M. *Curr. Opin. Chem. Biol.* **2011**, *15*, 489-496.

3. Lovering, F. *Med Chem Comm.* **2013**, *4*, 515-519.

4. Whitlock, H.W. *J. Org. Chem.* **1998**, *63*, 7982-7989.

5. Bertz, S. H. *J. Am. Chem. Soc.* **1981**, *103*, 3599-3601.

6. Baran, P.S.; Gaich, T. *J. Org. Chem.* **2010**, *75*, 4657-4673.

7. Oehlschlager, A.C.; Mishra, P.; Dhami, S. *Can. J. Chem.* **1984**, *62*, 791-797.

8. Charbardes, P.; Kuntz, E.; Varagnat, J. *Tetrahedron* **1977**, *33*, 1775-1783.

9. Osborn, J.A.; Le Ny, J.P.; Gisie, H.; Bellemin-Laponnaz, S. *Angew. Chem. Int. Ed.* **1997**, *36(9)*, 976-978.

10. Grubbs, R.H.; Beutner, G.L., Morrill, C. *J. Org. Chem.*, **2006**, *71*, 7813-7825.

11. Morrill, C. (2006) *Application of transition metal catalysis to small molecule synthesis.* Dissertation (Ph.D.), California Institute of Technology. doi: 10.7907/QRWG-BM33. **https://resolver.caltech.edu/CaltechETD:etd-08222005-162934**

12. Munday, R.H., Denton, R.M., Anderson, J.C.; *J. Org. Chem.*, **2008**, *73*, 8033-8038.

13. Lee, D.; Hansen, E.C. *J. Am. Chem. Soc.*, **2006**, *128*, 8142-8143.

14. Lee, D.; Lo, Wai Yip; Cho, E.J.; Volchkov, I.; Hansen, E.C.; Yun, S.Y. *Angew. Chem. Int. Ed.* **2010**, *49*, 4261-4263.

15. Seiders, J.R.; Jung, H.H.; Floreancig, P.E. *Angew. Chem. Int. Ed.* **2007**, *46*, 8464.

16. Xie, Y.; Floreancig, P.E. *Angew. Chem. Int. Ed.* **2010,** *49*, 4261-4263.

17. Xie, Y. (2015). *Exploring the Synthetic Application of Allylic Alcohol Isomerization* (Doctoral Dissertation). Retrieved from Pitt ETD Database: **http://d-scholarship.pitt.edu/23770/**.

18. Tadpetch, K.; Rychnovsky, S.D; *Org. Lett.* **2008**, *10(21)*, 4839-4842.

19. Guérinot, A.; Serra-Muns, A.; Gnamm, C.; Bensoussan, C.; Reymond, S.; Cossy, J.; *Org. Lett.* **2010**, *12(8)*, 1808-1811.

20. Trost, B.M.; Li, Chao-Jun.; *J. Am. Chem. Soc.* **1994,** *116*, 10819-10820.

21. Semmelhack, M.F.; Bodurow, C.; *J. Am. Chem. Soc.* **1984**, *106*, 1496-1498.

22. Woerpel, K.A.; Tabacco, S.A., Romero, J.A.C. *J. Am. Chem. Soc.* **2000**, *122*, 168-169.

23. Woods, R.J.; Andrews, C.W.; Bowen, J.P. *J. Am. Chem. Soc.* **1992**, *114*, 859-864.

24. Lewis, M.D.; Cha, J.K.; Kishi, Y. *J. Am. Chem. Soc.* **1982**, *104*, 4976-4978.

25. Yang, M.T.; Woerpel, K.A. *J. Org. Chem.* **2009**, *74*, 545-553.

26. Kendale, J.C.; Valentin, E.M.; Woerpel, K.A. *Org. Lett.* **2014**, *16*, 3684-3687.

27. Kafle, A.; Liu, J.; and Cui, L. *Can. J. Chem.* **2016**, *94*, 894-901.

28. Demchenko, A.V.; *Curr. Org. Chem.* **2003**, *7*, 35-79.

29. Ratcliffe, A.J.; Fraser-Reid, B.; *J. Chem. Soc.* **1990**, 747-750.

30. Xie, Y.; Floreancig, P.E. *Angew. Chem. Int. Ed.* **2014**, *53*, 4926-4929.

31. Sammakia, T.; Smith, R.S. *J. Am. Chem. Soc.* **1994**, *116*, 7915-7916.

32. Matsutani, H.; Ichikawa, S.; Yaruva, J.; Kusumoto, T.; Hiyama T. *J. Am. Chem. Soc.* **1997**, *119*, 4541-4542.

33. Rodriguex, A.A.; Yoo, H.; Ziller, J.W.; Shea, K.J. *Tetrahedron Lett*. **2009**, *50*, 6830.

34. Cranwell, P.B.; Hiscock, J.R.; Haynes, C.J.E.; Light, M.E.; Wells, N.J.; Gale, P.A. *Chem. Commun.* **2013**, *49*, 874.

35. Crich, D.; Sun, S. *J. Am. Chem. Soc.* **1997**, *119*, 11217-11223

36. Crich, D. *Acc. Chem. Res.* **2010**, *43*, 1144-1153.

37. a) Chang, R. Physical Chemistry for the Biosciences. Sausalito: University Science Books, 2005. 368-370. b) Garrett, Reginald H.; Grisham C.M. Biochemistry 4th ed. Boston: Brooks/Cole Cengage Learning, 2010. 389-397. c) Segel, I.H. Biochemical Calculations. 2nd ed. New Jersey: John Wiley and Sons, inc., 1976. 216-218.

38. Atkins, P.; de Paula, J. Physical Chemistry for the Life Sciences. New York, NY: W.H. Freeman and Company, 2006. 275-276.

39. Danishefsky, S. J.; DeNinno, S.; Lartey, P. *J. Am. Chem. Soc.* **1987**, *109*, 2082-2089

40. Westley, J.W., *Ed. Polyether Antibiotics*; Marcel Dekker: New York, 1083; Vol. I and II

41. Brooks, H.A.; Gardner, D.; Poyser, J.P.; King, T.J. *J. Antibiot.* **1984**, *37*, 1501.

42. Danishefsky, S.J.; Selnick, H.G.; DeNinno, M.P.; Zelle, R.E. *J. Am. Chem. Soc.* **1987**, *109*, 1572-1574.

43. Kishi, Y.; Hatakeyama, S.; Lewis, M.D. *Frontiers in Chemistry (28th IUPAC Congress)* **1982**, 287-304.

44. Larsen, E.M.; Wilson, M.R.; Taylor, R.E. *Nat. Prod. Rep.* **2015**, *32*, 1183.

45. Rohrs, T.M.; Qin, Q. Floreancig, P.E. *Angew. Chem. Int. Ed.* **2017**, *56(36)*, 10900-10904.

46. Kruse, C.G.; Poels, E.K.; Jonkers, F.L; Vandergen, A.J. *J. Org. Chem.* **1978**, *43*, 3548.

47. Green, M.E.; Rech, J.C.; Floreancig, P.E. *Angew. Chem. Int. Ed.* **2008**, *47*, 7317.

48. Byrn, M.; Calvin, M. *J. Am. Chem. Soc.* **1966**, 88(9), 1916-1922.

49. Song, Z.; Hsung, R.P. *Org. Lett.* **2007**, *9(11)*, 2199-2202.

50. Boyer, J.; Corrice, R.J.P; Perz, R.; Reye, C. *J. Organomet. Chem.*, **1979**, *172*, 143.

51. Boyer, J.; Corrice, R.J.P; Perze, R.; Reye, C. *Tetrahedron* **1981**, *37*, 2165.

52. Sundararaman, P.; Herz W. *J. Org. Chem.*, **1977**, *42(5)*, 813-819.

53. Molander, G.A.; Jean-Gerard, L. *J. Org. Chem.* **2009**, *74(3)*, 1297-1303.

54. Einhorn, J.; Einhorn, C.; Ratajczak, F.; Pierre, J. *J. Org. Chem.* 1996, 61, 7452-7454.

55. Gualandi, A.; Rodeghiero, G.; Faraone, A.; Patuzzo, F.; Marchini, M.; Calogero, F.; Perciaccante, R.; Jansen, T.P.; Ceroni, P.; Cozzi, P.G. *Chem. Commun.* **2019**, *55*, 6838.

56. Mikami, K.; Kawakami, Y.; Akiyama, K.; Aikawa, K. *J. Am. Chem. Soc.*, **2007**, *129*(*43*), 12950-12951.

57. Hill, R.K. *Synthetic Communications*, **1990**, *20*(*12*), 1877-1884.

58. Xie, Y.; Floreancig, P.E. *Angew. Chem. Int. Ed.* **2011**, *2(12)*, 2423-2427.

59. Satyanararyana, S;. Reddy, B.V. Subbs; Narender, R. *Tett. Lett.* **2014,** *55*, 6027-6029.

60. Magauer T.; Martin H.J.; Mulzer J. *Angew. Chem. Int. Ed.* **2009**, *48(33)*, 6032-6036.